SYNTHESIS, CHARACTERIZATION AND CATALYTIC ACTIVITY OF MOLYBDENUM(VI) DI- AND MONOOXO ARYLOXIDES

by

Mauricio Quiroz-Guzmán

Bachelor of Science, 2002
Universidad de las Américas-Puebla
Puebla, Mexico

Submitted to the Graduate Faculty of the
College of Science and Engineering
Texas Christian University
In partial fulfillment of the requirements
for the degree of

Doctor of Philosophy

August 2008

ACKNOWLEDGEMENTS

Deseo agradecer profundamente a la Doctora Tracy Hanna por haber creído en mí desde el principio. Siempre supo impulsarme y hacerme seguir adelante, aún cuando el camino fuera duro, ella siempre supo infundirme la confianza necesaria para salvar cualquier obstáculo. Gracias Tracy por haber hecho de mi una mejor persona y un científico mas dedicado.

Este trabajo está dedicado especialmente a mis padres Roberto y Evangelina y a mi hermano Carlos. Ellos han estado siempre conmigo, en espíritu y pensamiento. Gracias a ellos hoy soy un hombre de bien. Su amor es mi punto de apoyo para poder impulsarme, sentirme protegido y un aliciente para llegar siempre a las metas deseadas… ¡GRACIAS!

A mi abuelita Soledad, a quien siempre llevo en mi corazón y mi pensamiento. A mis abuelos que han sido llamados al lado de Dios: Isabel, Román y Ángel porque en vida siempre nos apoyaron a mí y a mis padres.

Deseo agradecer a mis padres adoptivos: Cristina, Elvira y Manuel, Catalina e Iván, porque siempre han sabido darme amor y alimentar mis esperanzas dándome fe y certeza en el futuro. A mis hermanos adoptivos: Ismael, Ángel Iván, Gabriela, Diony y Manuel ya que siempre han estado ahí cuando los he necesitado, apoyándome y soportándome en mis momentos de neurosis e histerias.

Al final pero no por eso menos importante a la familia que me adoptó durante estos años de doctorado, mis hermanos de estudio y amigos para toda la vida: Karla, Yamina, Monika, Wendy, Steven, Daniel, Onofrio, Alejandro, Erick, Mario y Jeff porque gracias a ellos este tiempo fue llevadero y pude sentir este lugar como mi casa…

A mis colegas de trabajo: Dr. Liu, Dr. Ghosh, Dr. Wang, Cindy, Kim, Bernat y Joseph, por sus consejos y su continua ayuda.

A la Doctora Cecilia Anaya, por su impulso y su fe en mí. A los distintos profesores del departamento de Quimica de TCU por su apoyo y sus valiosos consejos.

TABLE OF CONTENTS

Acknowledgements…… ii

Table of Contents…….. iii

List of Figures…….. viii

List of Tables……..... x

List of Schemes…….. xi

CHAPTER 1. BACKGROUND AND PURPOSE…….. 1

1.1 Introduction…….. 1

1.2 The element…… 1

1.3 Importance of molybdenum compounds in catalysis…… 4

1.3.1 Molybdenum centers in enzymes……. 5

1.3.2 Oxomolybdenum catalysis……. 8

1.3.2.1 Oxomolybdenum catalysts with industrial applications…… 8

1.3.2.2 Organometallic oxomolybdenum complexes for laboratory catalysis…… 11

1.4 Molybdenum oxo chemistry…….. 12

1.4.1 Compounds containing MoO_4^{2-} …… 13

1.4.2 The MoO_3 core……. 14

1.4.3 Structures containing the *cis*-MoO_2^{2+} core ……. 17

1.4.4 The MoO^{4+} core……... 19

1.5 Motivation of this research……... 20

1.5.1 “Homogenization” of heterogeneous catalysts……... 20

1.5.2 Existing models for α-$[Bi_2MoO_6]$ intermediates…….. 23

1.6 Our model …….. 27

CHAPTER 2. MOLYBDENUM(VI) DIOXO DIARYLOXIDE COMPLEXES ……..… 30

2.1 Introduction……. 30

2.2 Experimental section……. 33

2.2.1 General…….. 33

2.2.2 Preparation of compounds……. 35

2.2.3 Spectrophotometric experiments ……. 44

2.2.3.1 NMR experiments ……. 44

2.2.3.2 Detection of paramagnetic species …… 46

2.2.3.3 UV-vis reaction…….. 47

2.2.4 Concentration effects…….. 47

2.2.5 Reactions with molybdenum adducts…….. 48

2.2.5.1 $MoO_2Cl_2L_2$ adducts as alternatives to MoO_2Cl_2 ……..... 48

2.2.6 Oxygen transfer catalysis……... 49

2.3 Results and discussion ……. 50

2.3.1 Four coordinate molybdenum(VI) dioxo diaryloxides…… 50

2.3.2 Spectrophotometry…….. 51

2.3.3 Side-reactions and paramagnetism…….. 52

2.3.4 Catalytic activity……... 58

2.4 5- and 6-coordinate Mo(VI) dioxo diaryloxides…… 59

2.4.1 $MoO_2Cl_2(DMF)_2$ as precursor for molybdenum dioxo aryloxides……. 59

2.4.2 Steric substituent effects in reactions with $MoO_2Cl_2(DMF)_2$……. 61

2.5 Crystal structure and three-dimensional geometry…….. 62

2.5.1 Coordination number and structural features …… 62

2.5.2 Electronic unsaturation and structural consequences …….. 69

2.6 Conclusions …… 70

CHAPTER 3. MOLYBDENUM(VI) MONOXO ARYLOXIDES……. 71

3.1 Introduction …… 71

3.2 Experimental section……. 75

3.2.1 General…….. 75

3.2.2 Preparation of compounds……. 77

3.2.2.1 Synthesis of lithium aryloxides ……..... 77

3.2.2.2 Reactions between MoO_2Cl_2 and aryl alcohols …… 79

3.2.2.3 Reactions between MoO_2Cl_2 and bidentate phenols

(biphenol and catechol) …… 84

3.2.2.4 Reactions between MoO_2Cl_2 and lithium aryloxides …… 86

3.2.2.4.1 Reactions in a 1:2 MoO_2Cl_2:LiOAr ratio …….. 86

3.2.2.4.2 Reactions in a 1:4 MoO_2Cl_2:LiOAr ratio in “wet hexane” ……. 87

3.2.2.4.3 Reactions between LiOAr and $MoOCl_4$ …….. 89

3.2.2.5 Reactions between LiOAr and $MoO_2Cl_2(DMF)_2$ …….. 90

3.3 Results and discussion ……. 91

3.3.1 Synthesis of products and reaction mechanisms …….. 94

3.3.1.1 Products from addition of mono and bidentate aryl alcohols to MoO_2Cl_2 . 94

3.3.1.2 Products from addition of LiOAr to MoO_2Cl_2 (2:1) …… 101

3.3.1.3 Products from addition of LiOAr to MoO_2Cl_2 (4:1) in “wet hexane”……. 101

3.3.1.4 Products from addition of LiOAr to $MoO_2Cl_2(DMF)_2$ (1:1) …… 103

3.3.2 Spectroscopic characterization …… 104

3.3.2.1 Products from addition of monodentate aryl alcohols to MoO_2Cl_2 …… 104

3.3.2.2 Products from addition of bidentate aryl alcohols to MoO_2Cl_2 …… 106

3.3.2.3 Products from addition of LiOAr and MoO_2Cl_2 (4:1) in “wet hexane” …… 107

3.3.2.4 Products from addition of LiOAr to $MoOCl_4$ …….. 108

3.3.2.5 Products from addition of LiOAr and $MoO_2Cl_2(DMF)_2$ ……. 110

3.3.3 Crystal structure and three-dimensional geometry ……... 111

3.4 Conclusions …… 121

CHAPTER 4. MOLYBDENUM(VI) MONOOXO BISPHENOXIDES …….. 122

4.1 Introduction …….. 122

4.2 Experimental section ……..... 125

4.2.1 General …….. 125

4.2.2 Preparation of compounds …… 127

4.2.2.1 Synthesis of bisphenols …… 127

4.2.2.2 Synthesis of lithium bisphenoxides …….. 129

4.2.2.3 Synthesis of Mo(VI) monooxo *cis* chloro *cis* bisphenoxides …….. 131

4.3 Results and discussion …….. 135

4.3.1 Spectroscopy …….. 138

4.3.2 Electronic and Structural Effects…….. 140

4.3.3. Crystal structure and three-dimensional geometry …….. 142

4.4 Conclusion …….. 146

CHAPTER 5. RING-OPENING METATHESIS POLYMERIZATION OF NORBORNENE USING MOLYBDENUM(VI) MONOOXO ARYLOXO- AND BISPHENOXO COMPLEXES.. 147

5.1 Introduction…….. 147

5.2 Experimental section …… 151

5.2.1 General …….. 151

5.2.2 Polymerization reactions …….. 152

5.2.2.1 Polymerization trials using $MoO(OAr)_{4-n}Cl_{n = 0-2}$ complexes…….. 152

5.2.2.2 Polymerization trials using $MoO(O\text{-}2,6\text{-}Me_2C_6H_3)_2Cl_2$ (**3.2a**) as pro-catalyst and ^{n}BuLi co-catalyst in different ratios …… 154

5.2.2.3 Persistence of the molybdenum active intermediate …….. 155

5.2.2.4 Polymerization trials using $MoOCl_2$(bisphenoxides) …… 156

5.2.2.5 Reactions with Cyclohexene 162
5.3 Results and discussion 162
5.3.1 The procatalysts 163
5.3.2 The mechanism 166
5.3.3 The monomer and the stereochemistry of the polymer 167
5.3.4 Polymerization trials 169
5.4 Conclusions 176
APPENDIX FOR CHAPTER 2 178
APPENDIX FOR CHAPTER 3 200
APPENDIX FOR CHAPTER 4 219
References 227
VITA
ABSTRACT

LIST OF FIGURES

Figure 1.1 Ground state configuration of molybdenum ……. 2

Figure 1.2 The major families of mononuclear oxomolybdenum enzymes …… 6

Figure 1.3 Useful oxomolybdenum complexes in olefin polymerization and epoxidation…. 11

Figure 1.4 Possible coordination environments of the MoO_4^{2-} core …… 14

Figure 1.5 Elements of MoO_3 structure …… 15

Figure 1.6 Structure of $MoO_3 \bullet H_2O$ projected almost parallel to [001] ……. 16

Figure 1.7 Molybdenum(VI) trioxo complexes …… 16

Figure 1.8 Structure postulated by Shustorovich for solid MoO_2Cl_2 …… 17

Figure 1.9 The principal molybdenum-oxo dπ-pπ bonding interactions in an octahedral coordination environment …… 18

Figure 1.10 ORTEP diagram of 4-coordinate MoO_2(O-2,6-^{t}Bu$_2$C$_6$H$_3$)•HO-2,6-^{t}Bu$_2$C$_6$H$_3$ …. 18

Figure 1.11 MoO^{4+} complexes…… 20

Figure 1.12. $Mo_4(\mu\text{-}OH)_3(\mu\text{-}O)$ moiety …….. 23

Figure 1.13 Mo(VI) oxo complex with dangling allyl groups and molybdenum(IV) allyl complex …….. 24

Figure 1.14 [CpMo^{IV}(=NR)(π-allyl)], and [(^{t}BuN=)$_2$Mo^{VI}(metallyl)$_2$] …… 25

Figure 1.15 Mo-O-Bi alkoxide complexes …… 26

Figure 1.16 Models for Mo-O-Bi sites …….. 27

Figure 1.17 Model clusters …… 28

Figure 1.18 Our model approach …… 28

Figure 2.1 ORTEP view of MoO_2(O-2,6-^{t}Bu$_2$-4-EtC$_6$H$_2$)$_2$ (**2.2c**) ……..…… 63

Figure 2.2 ORTEP view of compound MoO_2(O-2,6-^{t}Bu$_2$-4-(OMe)C$_6$H$_2$)$_2$ (**2.2e**) ……... 63

Figure 2.3 ORTEP view of Li{MoO_2Cl[2,2'-CH_2(O-6-^{t}Bu-4-MeC$_6$H$_2$)$_2$]}·3DME (**4**) ……. 64

Figure 2.4 ORTEP view of MoO_2(O-2,6-^{t}Bu$_2$-4-EtC$_6$H$_2$)$_2$(DMF) (**2.5c**) …… 67

Figure 2.5 ORTEP view of MoO_2(O-2,6-$Me_2C_6H_3)_2(DMF)_2$ (**5l**) ……..…… 68

Figure 3.1 ORTEP view of MoO(O-2,4-$Me_2C_6H_3)_4$ (**3.4a**) ……. 113

Figure 3.2 ORTEP view of MoO(O-2,4-$Me_2C_6H_3)_2Cl_2$·(THF) (**3.2b**) …… 114

Figure 3.3 ORTEP view of MoO(O-2-(allyl)$C_6H_4)_4$(DMF) (**3.5f**) ……... 114

Figure 3.4 ORTEP view of MoO(O-2,6-^{i}Pr$_2C_6H_3)_3$Cl(DMF) (**3.5h**) …….. 115

Figure 3.5 ORTEP view of [Mo(O)Cl]$_2${[μ-rac-BIPHEN(O_2)-κ^2*O:O'*]$_2$-(μ-O)} (**3.7**) ……. 118

Figure 3.6 ORTEP view of Mo(O)Cl($C_6H_4O_2$-κ^2*O,O'*)(C_6H_4O(OH)-κ^2*O,O'*)·Et_2O (**3.8**) …….. 120

Figure 4.1 Possible interactions between ligand and metal orbitals that might account for the observed LMCT bands ……. 140

Figure 4.2 ORTEP view of Mo(O)Cl_2{2,2'-CH_2(O-6-^{t}Bu-4-Me$C_6H_2)_2$-κ^2*O,O'*} (**4.3a**) ……. 144

Figure 4.3 ORTEP view of Mo(O)Cl_2{2,2'-CH(^{i}Pr)(O-4,6-^{t}Bu$_2C_6H_2)_2$-κ^2*O,O'*} (**4.3b**) …… 144

Figure 5.1 Molybdenum(VI) monooxo complexes used as procatalysts for polymerization of NBE …… 164

Figure 5.2 ^{1}H NMR spectrum in C_6D_6 (expansion) of a polyNBE …… 169

Figure 5.3 ^{1}H NMR spectrum in C_6D_6 of polyNBE generated from the precursor **4.3a** and 0.5 equiv. of Et_3Al in THF at room temperature …….. 175

LIST OF TABLES

Table 1.1 Some Properties of Molybdenum …… 2

Table 1.2 Reaction Catalyzed by Molybdenum Oxides …… 9

Table 2.1 List of Compounds Presented in Chapter 2 ……... 31

Table 2.2 Reactions Between $MoO_2Cl_2(DMF)_2$ and Various LiO-2,6-^{t}Bu$_2$-4-RC_6H_2 ……. 60

Table 2.3 Crystallographic Data for Molecules **2.2c**, **2.2e** and **2.4** …….. 62

Table 2.4 Selected Bond Lengths (Å) of Molecules **2.2a**, **2.2c**, **2.5c**, **2.5l** ……. 65

Table 2.5 Selected Bond Angles (deg) of Molecules **2.2a**, **2.2c**, **2.5c**, **2.5l** ……... 66

Table 2.6 Crystallographic Data for Molecules **2.5c** and **2.5l** …….. 67

Table 3.1 List of Compounds Presented in Chapter 3 …….. 73

Table 3.2 Crystallographic Data for Molecules **3.2b**, **3.4a**, **3.5f** and **3.5h** …….. 111

Table 3.3 Selected Bond Lengths (Å) of Molecules **3.2a**, **3.3a**, **3.4a**, **3.2b**, **3.5h** and **3.5f**... 112

Table 3.4 Selected Bond Angles (deg) of Molecules **3.2a**, **3.3a**, **3.4a**, **3.2b**, **3.5h** and **3.5f** 113

Table 3.5 Crystallographic Data for Molecules **3.7** and **3.8** …….. 117

Table 4.1 List of Compounds Presented in Chapter 4 ……... 124

Table 4.2 Crystallographic Data for Molecules **4.3a** and **4.3b** ……. 142

Table 4.3 Selected Bond Lengths (Å) of Molecules **3.2a**, **3.3a**, **3.4a**, **4.3a**, **4.3b** ……. 143

Table 4.4 Selected Bond Angles (deg) of Molecules **3.2a**, **3.3a**, **3.4a**, **4.3a**, **4.3b** ……..... 143

Table 5.1 Yields of polyNBE Using a Stock Solution of Complex **3.2a** as Precursor and 0.5 equiv. of ^{n}BuLi …… 172

LIST OF SCHEMES

Scheme 1.1 DMSO reductase active site …… 8

Scheme 1.2 Chiral $MoO_2(acac)(L^*)$ complexes tethered via a bidentate O,O-ligand on zeolite …….. 12

Scheme 1.3. Proposed active site of bismuth molybdate …….. 22

Scheme 1.4 Mo^{VI} oxo bridged allyl complex …… 24

Scheme 1.5 Mo^{VI} imido complex designed for HCl elimination in order to anchor the allyl ligand …….. 25

Scheme 1.6 The different research lines that will be covered in this doctoral dissertation.. 29

Scheme 2.1 Reaction of MoO_2Cl_2 with various LiO-2,6-^{t}Bu$_2$-4-RC_6H_2 …… 51

Scheme 2.2 Proposed reaction pathway for formation of the observed phenoxy radicals.. 56

Scheme 2.3 Steric control of coordination number by variation of the steric bulk of the aryloxy ligand in reactions with $MoO_2Cl_2(DMF)_2$ …….. 61

Scheme 3.1 Reaction of MoO_2Cl_2 with various aryl alcohols ……... 95

Scheme 3.2 Concerted aryl alcohol addition across the Mo=O bond …….. 96

Scheme 3.3 Proposed reaction pathway for the formation of Mo(O)(OH)[rac-BIPHEN(OH)]Cl_2 (**3.6**) and [Mo(O)Cl]$_2${[μ-rac-BIPHEN(O_2)-κ^2*O:O'*]$_2$(μ-O)} (**3.7**) …… 98

Scheme 3.4 Proposed reaction mechanisms for the formation of Mo(O)Cl($C_6H_4O_2$-κ^2*O,O'*)(C_6H_4O(OH)-κ^2*O,O'*) (**3.8**) …….. 99

Scheme 3.5 Proposed reaction mechanism for the formation of $MoO(OAr)_4$ complexes … 102

Scheme 3.6 Alternative synthesis of $MoOCl_2(OAr)_2$ complexes for ligands with sterically congested or highly electron-withdrawing substituents …….. 109

Scheme 4.1 Reaction conditions for the synthesis of different bisphenols …… 136

Scheme 4.2 Synthetic routes for the syntheses of Mo(VI) monooxo bisphenoxides …… 137

Scheme 5.1 Most studied olefin metathesis reactions …….. 148

Scheme 5.2 The “pairwise” exchange of alkylidene fragments between two olefins …….. 149

Scheme 5.3 Olefin metathesis reaction mechanism …….. 149

Scheme 5.4 Generation of the proposed active Mo(VI) monooxo catalysts. Complexes **3.2a** and **4.3a** are used as models …… 166

Scheme 5.5 Ring opening metathesis polymerization of NBE ……. 167

Scheme 5.6 Different possible combinations of dyad tacticity and double bond stereochemistry in polyNBE …… 168

Scheme 5.7 Polymerization of NBE using Mo(VI) monooxo di-, tri-, and tetraaryloxo complexes ……. 169

Scheme 5.8 Polymerization of NBE using $MoO(O\text{-}2,6\text{-}Me_2C_6H_3)_2Cl_2$ (**3.2a**) and ^{n}BuLi in different ratios ……... 171

Scheme 5.9 Polymerization of NBE using a stock solution of **4.3a** and ^{n}BuLi in different ratios …….. 173

Scheme 5.10 Polymerization trials with **4.3a** using 0.5 and 1.0 equiv. of Et_3Al and $PhCH_2MgCl$ as co-catalysts …… 174

Scheme 5.11 Polymerization of NBE with complex **4.3b** as initiator and 1.0 equiv. of ^{n}BuLi ……... 176

CHAPTER 1

BACKGROUND AND PURPOSE

1.1 Introduction

The chemistry of molybdenum is immensely rich and diverse. Molybdenum is essential for life, the element has many applications in industry, and molybdenum chemistry has often been involved in the understanding of fundamental principles of the theory and practice of the chemical sciences.[1] The purpose of this chapter is to identify those important physical and chemical properties of molybdenum and its compounds that cause its versatile chemistry and reactivity.

I will present essential properties of molybdenum (Section 1.2), outline the importance of molybdenum compounds as catalysts in natural and industrial processes (Section 1.3), and introduce some molybdenum complexes that have relevance in this doctoral dissertation (Section 1.4). I will then explain the scientific motivation that stimulated this research (section 1.5), describe the different research projects described in this dissertation, and explain how they impact current research in the field of oxomolybdenum(VI) organometallic chemistry (Section 1.6).

1.2 The element

Molybdenum is a lustrous, silvery metal and a member of group 6 of the periodic table of the elements. The metal is fairly soft when pure, and is attacked slowly by acids.[2] Fundamental properties of molybdenum are given in Table 2.1.

Table 1.1 Some Properties of Molybdenum.[3]

Atomic number	42	Melting point (Kelvin)	2890
Number of naturally occurring isotopes	7	Boiling point (Kelvin)	4885
Atomic weight ($g \cdot mol^{-1}$)	95.94(2)[4]	Atomic Radii (pm)	145,[a] 190,[b] 139[c]
Electronic configuration	$[Kr]4d^5 5s^1$		Mo^{6+} 59[d]
Valence orbitals	4d 5s 5p		Mo^{5+} 61[d]
Pauling electronegativity	1.8		Mo^{4+} 65[d]
Young's Modulus (GPa)	329		Mo^{3+} 69[d]

[a] Covalent/Empirical radius.[5, 6] [b] Calculated.[7] [c] Metallic radius (12-coordinate).[8, 9] [d] Ionic radius (6-coordinate).[9]

The chemical properties of molybdenum (as of any other atom) are largely determined by the arrangement of the electrons in its outermost valence shell. Molybdenum has six valence electrons and nine atomic orbitals of energy suitable for use in chemical bonding, namely 5 x 4d, 1 x 5s and 3 x 5p = 9 orbitals. Its ground-state electron configuration is [Kr] $5s^1 4d^5$, shown in Figure 1.1.[10] This configuration does not follow the aufbau principle, which would give [Kr] $5s^2$ $4d^4$. The reason for this exception is a lower total energy obtained by forming a half filled d subshell (5 electrons), even though that forces an s electron into the d subshell.

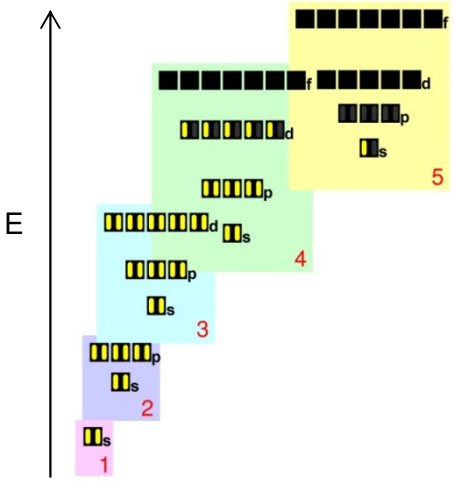

Figure 1.1 Ground state electron configuration of molybdenum.[10]

Electronegativity (together with the atomic number, mass and valency) is an important atomic parameter. This parameter strongly impacts the nature of the bonds formed by a given atom.[11] The electronegativity of a given element is not an invariable atomic property and, in particular, increases with the oxidation state of the element.[12] Molybdenum has a moderate Pauling electronegativity of 1.8 in its ground state,[11] a value that rises up to 2.35 in Mo(VI).[12] This increase is expected as the atom has lost electron density and holds on to its remaining electrons more tightly. Like its early transition metal neighbors, molybdenum can readily lose all of its valence electrons, and it is often found in its highest permissible oxidation state of d^0 Mo(VI). The more electronegative later d-block transition metals, in contrast, normally use up to two electrons, rarely four and only very exceptionally six.[13] Molybdenum thus displays a rich chemistry and a variety of accessible oxidation states (one representative example of each is given): d^8 Mo^{2-} (rare), $[Mo(CO)_5]^{2-}$; d^6 Mo^0, $[Mo(CO)_6]$; d^5 Mo^{1+} (rare), $[Mo(\eta\text{-}C_6H_6)_2]^+$; d^4 Mo^{2+}, Mo_6Cl_{12}; d^3 Mo^{3+}, $MoCl_3$; d^2 Mo^{4+}, MoO_2; d^1 Mo^{5+}, $MoCl_5$; d^0 Mo^{6+} (common), MoO_3.[3]

Molybdenum is a refractory metal (extraordinarily resistant to heat, wear and corrosion) typically used in high temperature applications.[14] Significant properties include:

1. High melting point (Table 1.1), exceeded only by that of W and Ta.[14]
2. Good strength and ductility at room temperature.[14]
3. Stiffness (Table 1.1), greater than that of steel (Young's Modulus 210 GPa).[1]
4. Resistance to most chemical reagents, but it is attacked by oxidizing acids and molten oxidizing salts, such as potassium nitrate and potassium carbonate.[14, 15]
5. It oxidizes slowly in air at 350 ^oC and rapidly at temperatures above 650 ^oC, a weakness for some of its high temperature uses.[14]

These properties reflect the high strength of interatomic bonding resulting from the efficient overlap of the half filled 4d orbitals.[16]

The electronic structure of molybdenum is characterized, as in the case for 3d, 4d and 5d metals in general, by the overlap and hybridization of a wide nearly electron free s-p band.

Molybdenum has a relatively narrow d-band in comparison with chromium (the opposite is expected: d bands in 3d elements are usually narrower than those of 4d elements).[17] In the case of molybdenum the Fermi energy falls in a range of energies in which the d-electron density of states is not large, leading to a low electron specific heat (electrons contribute to electrical conduction and heat conduction and not to specific heat).[1] As a consequence, molybdenum exhibits a relatively good thermal conductivity (138 W m^{-1} K^{-1} at 300 K)[3] together with a low specific heat,[14] and a low coefficient of thermal expansion (4.8 $\mu m \cdot m^{-1} \cdot K^{-1}$ at 25 °C) that is about half that of most steels.[18] These characteristics enable molybdenum to be thermally treated to produce a structure with lower thermal stresses than most other materials.[14] The relatively high electrical conductivity permits it to be used for many electrical applications.[16]

1.3 Importance of molybdenum compounds in catalysis.

Molybdenum is an extraordinarily versatile element: it forms compounds with most inorganic and organic ligands, has oxidation states from (–2) to (+6), and has coordination numbers from 4 to 8.[19] This dissertation will focus on compounds that bear molybdenum in its higher oxidation states (mainly 6+) because of their applications in catalysis or as models for active catalytic sites.[20-23]

The chemistry of molybdenum in high oxidation states is dominated by oxo species: molybdates $[Mo^{VI}O_4]^{2-}$; poly- and heteropolymolybdates; and, in complexes, $Mo^{VI}O_2^{2+}$, $Mo^{V}O^{3+}$, $Mo^{V}_2O_3^{4+}$, $Mo^{V}_2O_4^{2+}$, $Mo^{IV}O^{4+}$, and $Mo^{IV}O_2$ as central units.[24, 25] The oxide MoO_3, the molybdenum blues,[26] the polymolybdates,[27] and the remarkable molybdenum wheels of Achim Muller[28] are built from linked $[MoO_x]$ polyhedra.[19, 29]

Oxomolybdenum redox chemistry is exploited in selective oxidation catalysis.[23] In the oxidase enzymes and the heterogeneous catalysts bismuth molybdate and iron molybdate, molybdenum shuttles between oxidation states (VI) and (IV) while transferring O or HO to substrate molecules.[29, 30]

Oxomolybdenum chemistry is versatile and important not only for enzymatic catalysis, but also for industrial and laboratory purposes in both homogeneous and heterogeneous phases.

Sections 1.3.1 and 1.3.2 are intended to explain the important role of oxomolybdenum catalysis in chemistry.

1.3.1 Molybdenum centers in enzymes.

Molybdenum is essential to all species. As with any other trace metals, though, what is essential in tiny amounts can be highly toxic in large doses. Animal experiments have shown that too much molybdenum causes fetal deformities. The parts of the body with most molybdenum are the bones, skin, liver and kidney.[2]

In living beings, molybdenum is associated with a diverse range of redox active enzymes that catalyze fundamental reactions in the metabolism of nitrogen, sulfur and carbon.[2] With the exception of nitrogenases that contain an iron-molybdenum-sulfur cluster, molybdenum is incorporated into proteins as a monometallic molybdenum cofactor.[31] The molybdenum cofactor contains a mononuclear Mo atom coordinated via a dithiolate sidechain to an organic cofactor named pterin (Figure 1.2).[32] In eukaryotes, the pterin cofactor (termed either molybdopterin or pyranopterin) has a terminal phosphate group on the pterin sidechain. In prokaryotes, however, the cofactor usually occurs as the dinucleotide of cytosine, guanosine, adenosine or inosine.[33]

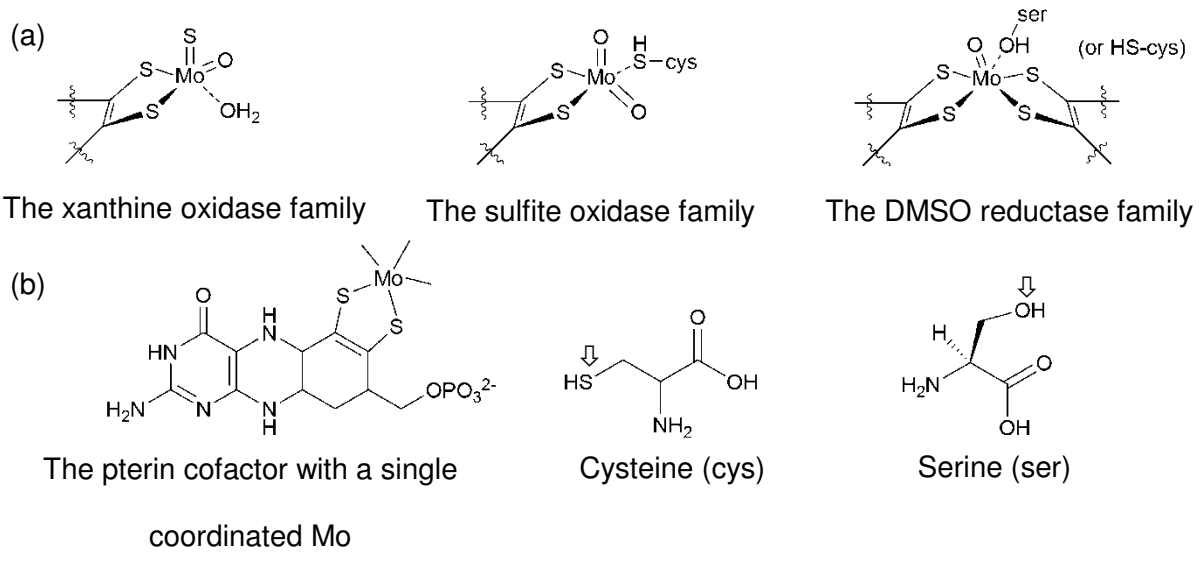

Figure 1.2 The major families of mononuclear oxomolybenum enzymes. (a) Active site structures of the three families of molybdenum cofactors. (b) The structure of the pterin cofactor that is common to molybdenum containing enzymes, and the structures of the cysteine and serine sidechains. The symbol "⇨" indicates the point of connectivity between the amino acid residue from the protein and the molybdenum center.[33]

The vast majority of these enzymes possess a Mo=O unit in their active sites and are often referred to as oxomolybdenum enzymes.[34] This term is not strictly applicable to the entire class of enzymes, however, as some (polysulfide reductase, for example, and possibly formate dehydrogenase) do not catalyze oxygen atom transfer, and others do not possess a Mo=O unit.[31]

The mononuclear molybdenum enzymes are usually categorized on the basis of the structures of their molybdenum centers (Figure 1.2).[31, 33] Molybdenum containing enzymes are divided into three families, each with a distinct active site structure and type of reaction catalyzed. The first, the xanthine oxidase family (named after the enzyme of the same name isolated from cow's milk), has an $LMo^{VI}(O)(S)(OH_2)$ core in the oxidized state,[31] with one equivalent of the pterin cofactor (designated L) coordinated to the metal (Figure 1.2). These enzymes typically catalyze the hydroxylation of carbon centers, although the carbon monoxide (CO) dehydrogenase from Oligotropha carboxidovorans, which oxidizes CO to CO_2, is an exception.[33, 35] The second family includes sulfite oxidase (typically isolated from avian or

mammalian liver) and nitrate reductase (from plants that assimilate nitrate from the soil). Again, the (oxidized) metal center has a single equivalent of the pterin cofactor, but as part of an $LMo^{VI}(O)_2$(HS–cys) core, with a cysteine ligand provided by the polypeptide (Figure 1.2a).[32, 33] Members of this second family catalyze the transfer of an oxygen atom either to or from a lone pair of electrons on the substrate.[32] The third family is diverse in both structure and function, but all members have two equivalents of the pterin cofactor bound to the metal. The molybdenum coordination sphere usually contains a single Mo=O group and a sixth ligand in an $L_2Mo^{VI}(O)(HX)$ core. The sixth ligand, (HX), can be (HS-cys) or (HO-ser).[33]

In general, molybdenum enzymes catalyze the transfer of an oxygen atom, ultimately derived from or incorporated into water, to or from a substrate in a two-electron redox reaction.[29, 30, 32] Enzymes from the DMSO reductase and sulfite oxidase families catalyze oxygen transfer to or from a substrate. Members of the xanthine oxidase family catalyze oxidative hydroxylation reactions of aldehydes and aromatic heterocyclic compounds. The reactions are summarized in Equations 1.1-1.3:[32]

DMSO reductase $(CH_3)_2S{=}O + 2H^+ + 2e^- \leftrightarrow (CH_3)_2S + H_2O$ (1.1)

Sulfite oxidase $SO_3^{2-} + H_2O \leftrightarrow SO_4^{2-} + 2H^+ + 2e^-$ (1.2)

Xanthine oxidase $R\text{-}CHO + H_2O \leftrightarrow R\text{-}COOH + 2H^+ + 2e^-$ (1.3)

The cycling between the oxidized Mo(VI) and the reduced Mo(IV) states of the enzyme is common to all these reactions.[36] It is convenient to consider the overall reaction mechanism as consisting of a coupled pair of reductive and oxidative half-reactions, characterized by the reduction of Mo(VI) and the oxidation of Mo(IV), respectively. The active site and mechanism of operation of DMSO reductase is shown in Scheme 1.1.[33]

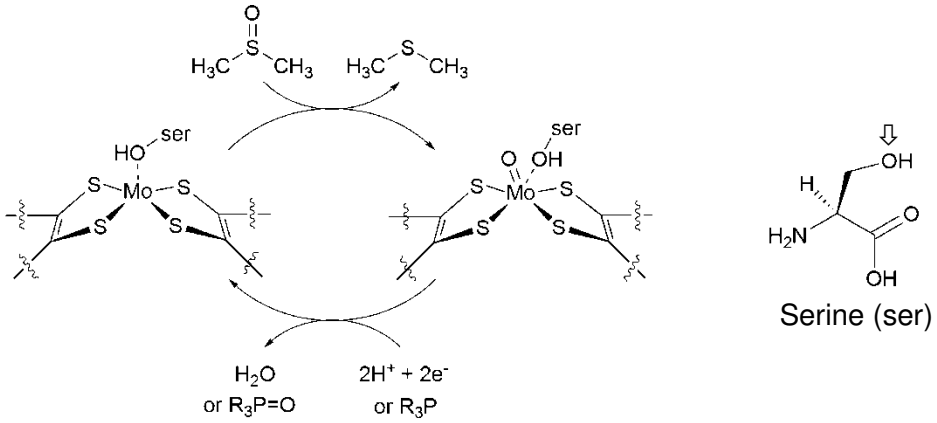

Scheme 1.1 DMSO reductase active site. The active site contains molybdopterin that supports molybdenum in its highest oxidation state (VI). The proposed mechanism of DMSO reductase cycles molybdenum between the +4 and +6 oxidation states.[36] The oxidized enzyme is subsequently reduced by reaction with either the DorC cytochrome (c-type cytochrome protein)[37] or a water-soluble phosphine (R_3P) to give the phosphine oxide $R_3P{=}O$.[33] The symbol "⇨" indicates the point of connectivity between the residual amino acid from the protein and the molybdenum center.

1.3.2 Oxomolybdenum catalysis.

1.3.2.1 Oxomolybdenum catalysts with industrial applications.

Molybdenum oxides have been used as corrosion inhibitors for steel (MoO_4^{2-}), industrial lubricants (MoO_3); in lithium-based high density batteries (MoO_3), as dye precursors (reds, violets and blues), in formulation of pigments and inks (molybdate oranges are widely used in thermoplastics), and as fire retardant and smoke suppressors in plastics (MoO_3);[14] but undoubtedly their major application is found in the catalysis of industrial processes.

Reactions catalyzed by molybdenum compounds constitute a large part of the heterogeneous processes in the world industry.[14] The introduction of molybdates (mainly MoO_3) as catalysts for selective oxidation of olefins to unsaturated aldehydes and acids, and the development of the synthesis of acrylonitrile by ammoxidation of propene on bismuth molybdate, are considered to be turning points in the history of modern petrochemistry.[38, 39] Table 1.2 lists some of the important industrial transformations that are catalyzed by oxomolybdenum compounds.

Table 1.2 Reactions Catalyzed by Molybdenum Oxides (modified from ref.[40])

Type of reaction	Example	Catalyst	T (°C)	Conv.
REACTIONS WITH MOLECULAR HYDROGEN				
Isotopic exchange	$H_2 + D_2 \rightarrow 2HD$	MoO_3/Al_2O_3-SiO_2	80	High
Hydrogenation	Benzene → Cyclohexane	MoO_3	420-450	60
	Acetylene → Ethylene	MoO_3CoCl_2/SiO_2	260-300	100
Hydrogenolysis	α and β methylnaphthalene → naphthalene + methane	CoO-MoO_3/Al_2O_3		40
	Ethylcyclohexane → products	MoO_3/Al_2O_3	510	
Reduction	Organosulfur → hydrocarbons + H_2S	CoO-MoO_3/Al_2O_3	225-425	
REACTIONS WITH MOLECULAR OXYGEN				
Selective oxidation	Propylene → Acrolein	Bi_2O_3-MoO_3	450	95
	Butene → Maleic anhydride	CoO-MoO_3-P_2O_5/Al_2O_3	450	76
	Benzene → Maleic anhydride	$V_2O_5MoO_3$-P_2O_5/Al_2O_3	425-450	85
	Acrolein → Acrylic acid	CoO-MoO_3-TeO_2	383	85
Oxidative condensation	Propylene + NH_3 → acrylonitrile	Bi_2O_3-MoO_3	400-500	80
	Toluene + NH_3 → benzonitrile	V_2O_5-MoO_3/Al_2O_3	415	94
Oxidative dehydrogenation	Butene → Butadiene	Bi_2O_3-MoO_3	370-550	90
	Ethylbenzene → styrene	MoO_3-MgO	420-450	84
Oxyhydration	Propylene → Acetone	SnO_2-MoO_3	135	
Oxidative dehydro-condensation	n-butane + H_2S → Thiophene	CoO-MoO_3/Al_2O_3	570	37

Type of reaction	Example	Catalyst	T (°C)	Conv.
OXYGEN TRANSFER REACTIONS				
Epoxidation	Propylene + H_2O_2 → Propylene oxide	MoO_3 in H_2O_2	60	80
ISOMERIZATION				
Structural isomerization	n-pentane → isopentanes	MoO_3/Al_2O_3	455-495	50
Ring contraction	Cyclohexane → Me-C_5H_9	MoO_3/Al_2O_3	455-495	37
DISPROPORTIONATION				
Olefin metathesis	Propylene → C_4H_8 + Ethylene	MoO_3/Al_2O_3	66-288	43
POLYMERIZATION				
Polymerization	Ethylene → Polyethylene	MoO_3/Al_2O_3	200-260	50
	Acetylene → Benzene	$CoO\text{-}MoO_3/Al_2O_3$	62	98
ADDITION				
Addition to C=C	Allyl-OH + H_2O_2 → Glycerol	MoO_3 in acetic acid	70-100	
DECOMPOSITION				
Dehydration	Isopropanol → Propylene	MoO_3	191-224	100
Dehydrogenation	Cyclohexane → Benzene	MoO_3/Al_2O_3	500	63

Heterogeneous catalysts, such as those described above, are able to endure harsh conditions and treat large amounts of substrate; on the other hand homogeneous catalysts generally have higher selectivities and reactivities but need milder reaction conditions.[40] Molybdenum oxo complexes have an important position as homogeneous catalysts (mainly at laboratory scale), but their true strength resides in their capabilities as models for a better mechanistic understanding of heterogeneous catalysts.[20, 21, 41]

1.3.2.2 Organometallic oxomolybdenum complexes for laboratory catalysis.

Organometallic molybdenum oxo complexes find their applications primarily in the catalysis of olefin polymerization and in oxidation reactions (although some molybdenum oxo complexes have been claimed to be active as hydroformylating catalysts).[42] Well-defined, relatively stable, Lewis acid free catalysts,[43] such as the Schrock catalyst shown in Figure 1.3a,[44] can provide living polymers with very narrow molecular weight distributions. Molybdenum oxo complexes such as $MoO_2(CH_3)_2$(bpy), shown in Figure 1.3b, catalyze the ring-opening metathesis polymerization (ROMP) of norbornene in combination with the Grignard reagent MeMgBr as cocatalyst.[45] Organomolybdenum oxo complexes, especially those containing MoO_2 moieties, can be efficient and selective oxidizing agents in the presence of organic hydroperoxides.[23] $MoO_2R_2L_2$ (R= CH_3, C_2H_5; L= bidentate Lewis ligand such as substituted 1,4-diazobutadienes, phenanthroline, and substituted bipyridines) (Figure 1.3b and c) are also active for the epoxidation of olefins using *tert*-butylhydroperoxide (TBHP) as oxidant.[20, 46, 47]

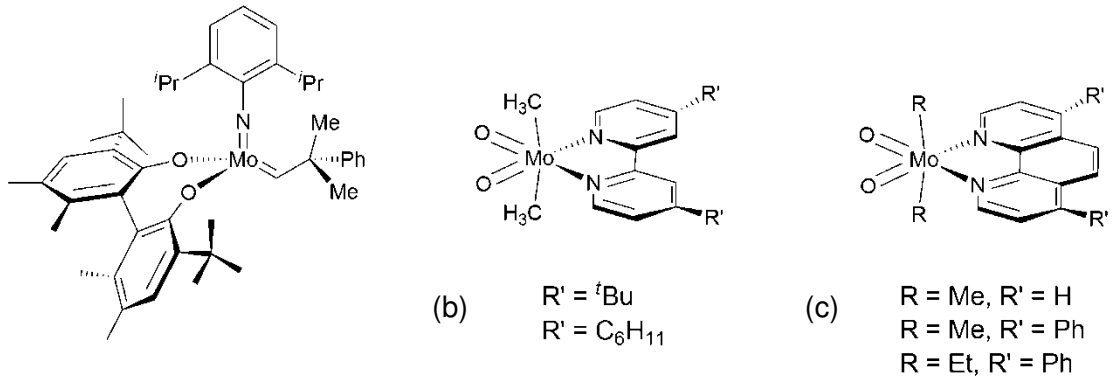

Figure 1.3 Useful oxomolybdenum complexes in olefin polymerization and epoxidation. (a) Schrock catalyst,[44] (b), (c) $MoO_2R_2L_2$ (L = bidentate Lewis base ligand).[20, 46, 47]

Alcon and Atlantic Richfield Company developed a process for the production of epoxides using alkyl hydroperoxide in the presence of a homogeneous catalyst based on molybdenum[48] (presumably a molybdenum oxide). In general, complexes with the formulation MoO_2X_2 and MoO_2(L-L), such as MoO_2(acac), are well known in olefin epoxidation reactions.[49] Heterogenization (immobilization of homogeneous catalyst on carrier materials or ionic liquids)

of such MoO_2X_2 complexes, with good performance in olefin epoxidation, has attracted increasing interest in recent years.[41] Chiral MoO_2(acac)(L*) complexes, where L* is a chiral bidentate *O*,*O*-ligand derived from (L)-*trans*-4-hydroxyproline, have been successfully heterogenized on zeolite Y and tested for epoxidation of allyl alcohols with TBHP (Scheme 1.2).[50]

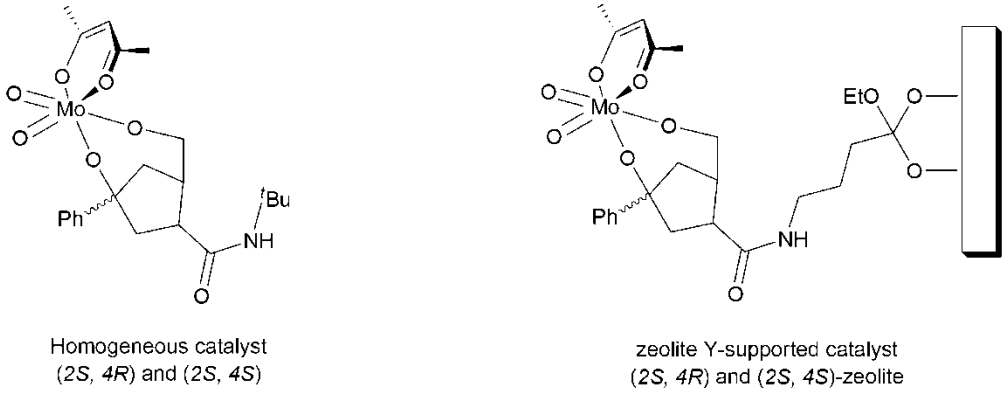

Scheme 1.2 Chiral MoO_2(acac)(L*) complexes tethered via a bidentate O,O-ligand on zeolite.[50]

1.4 Molybdenum oxo chemistry.

Molybdenum has a diverse chemistry partly because of its capacity to adopt different oxidation states, but even within this diversity it is possible to mark some general features. The energies of the molybdenum valence orbitals are suitable for the formation of bonds, and there is a marked tendency for molybdenum to fill these orbitals to result in a 2 x 9 = 18 electron environment. For most molybdenum coordination compounds the coordination number is six (granted that the six ligands are neither bulky nor really small). Lower coordination numbers might impose transformations to the geometry of the ligands (from bent to linear or vice versa) to satisfy the 18-electron rule, e. g. $Mo(NO)_4$.[51-53] This specific feature will be covered in the Chapter 2 of this dissertation.

We will focus on molybdenum in its highest oxidation states, especially in the oxidation state 6+. The chemistry of hexavalent molybdenum is dominated by the oxo ligand and its analogs. This highest of molybdenum oxidation states requires for its stabilization the presence

of ligands that are not only good σ donors but also good π donors. Sufficient charge density can then be placed on the molybdenum to avoid violating the Pauling Electroneutrality Principle.[11] The ligands need filled p orbitals that are not otherwise engaged in bonding with other atoms. Formally this yields a situation in which a multiple bond is formed between the Mo and its donor ligand. Different ligands meet these criteria, and form stable Mo(VI) complexes: the oxo ligand (O^{2-}), and by analogy sulfido (S^{2-}), selenido (Se^{2-}), peroxide (O_2^{2-}), persulfido (S_2^{2-}), imido (NR^{2-}), nitrido (N^{3-}), alkylcarbido (RC^{3-}, equivalent to alkylidyne), hydrazido (R_2NN^{2-}) and hydroxylamido (R_2NO^-). Amongst this ligand diversity, the oxo chemistry stands as a guidepost from which one can extrapolate to make predictions of the structural chemistry of complexes with analogous ligands.[25]

Mononuclear compounds dominate the coordination chemistry of Mo^{VI}. This is due in part to the absence of d electrons in Mo^{VI} complexes, which precludes the formation of Mo^{VI}-Mo^{VI} metal-metal bonds. Despite this predisposition, a very large class of homo- and hetero-polymolybdates that contain polynuclear Mo^{VI}, and a substantial number of dinuclear complexes of Mo^{VI}, are well known.

Our attention at this point will be restricted to molybdenum(VI) oxo complexes. In presenting the chemistry of Mo^{VI} we first will introduce complexes in which oxo groups provide the only source of π donation. Later, within the mononuclear class we will make distinctions between compounds with four, three, two, and one oxo ligands.

1.4.1 Compounds containing MoO_4^{2-}.

The oxoanion MoO_4^{2-} is isolated in the form of salts of monovalent, divalent and trivalent cations. The salts of the monovalent cations are usually water soluble[22] while salts with larger cations (e.g. ^{t}BuN$^+$) may also have solubility in nonaqueous solvents.[25] The salts of di- and tri-valent cations are generally insoluble and form three-dimensional structures in the solid state.

One example of the MoO_4^{2-} unit can be found in K_2MoO_4. In K_2MoO_4 the Mo-O distance is 1.76 Å, among the longest for terminal oxo linkages. The $(NH_4)_2MoO_4$ salt is isomorphous to K_2MoO_4.[54] MoO_4^{2-} usually displays a tetrahedral four-coordinate environment, but a six coordinate Mo^{VI} geometry is observed in polymeric structures where it acts as ligand of a metal ion, e.g. $NiMoO_4$ (Figure 1.4).[55]

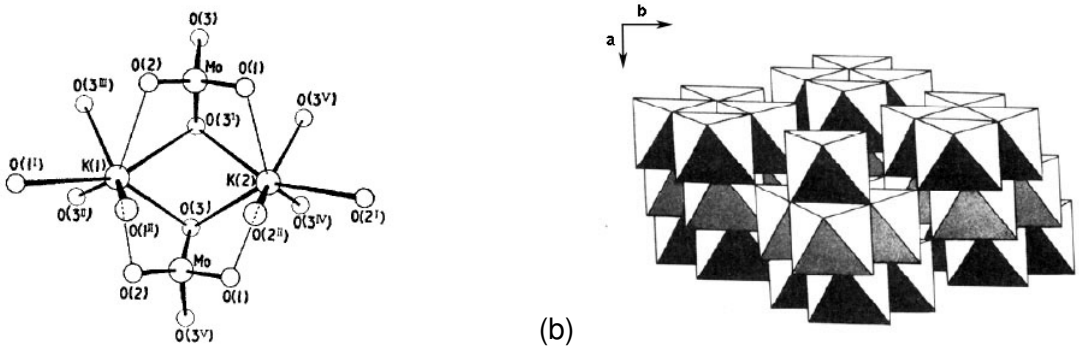

(a) (b)

Figure 1.4 Possible coordination environments of the MoO_4^{2-} core. (a) X-ray crystal structure of K_2MoO_4. MoO_4^{2-} units display a tetrahedral symmetry.[54] (b) Structure showing packing of NiO_6 octahedra in NiO_{16} units. Unshared octahedra are MoO_6.[55]

1.4.2 The MoO_3 core.

MoO_3 is an important material and the ultimate oxidation product of all molybdenum compounds. It is a pale yellow solid that readily sublimes at temperatures above 700 ^oC to form plate-like crystals. The vapor contains cyclic Mo_3O_9, Mo_4O_{12} and Mo_5O_{15} molecules based on corner-shared MoO_4 tetrahedra.[9] These molybdenum oxides have been trapped in argon matrices, together with the pyramidal MoO_3 molecule that has a bond angle of 61.5^o. The size of Mo^{VI} is such that, in oxide materials, it is commonly found in either tetrahedral or octahedral coordination (refer to section 1.3.2.1). In α-MoO_3, though, the molybdenum environment is square pyramidal within each layer of the structure (Figure 1.5). The coordination environment of the metal atom in MoO_3 can be considered as that of a distorted octahedron, but since the two longest bonds correspond to bond orders of less than one, it is alternatively described as a Mo-O tetrahedron[22] featuring a *cis* dioxo unit (oxide distances: terminal oxo with d(Mo-O) = 1.67 Å, bridging oxo between individual species to form infinite chains with d(Mo-O) = 1.95 Å and

2.33 Å, and bridging oxo that joins chains into a network with d(Mo-O) = 2.25 Å and 1.33 Å). Figure 1.5a shows an infinite chain of corner-sharing tetrahedra. When such chains are linked together to increase the coordination of molybdenum to 5 (Figure 1.5b), and other chains are brought from beneath to complete this coordination to 6 (Figure 1.5c), sheets are formed. These sheets are composed of ribbons of octahedral-sharing edges with two adjacent octahedra, and corners with octahedra of parallel ribbons on both sides (Figure 1.5d).[40]

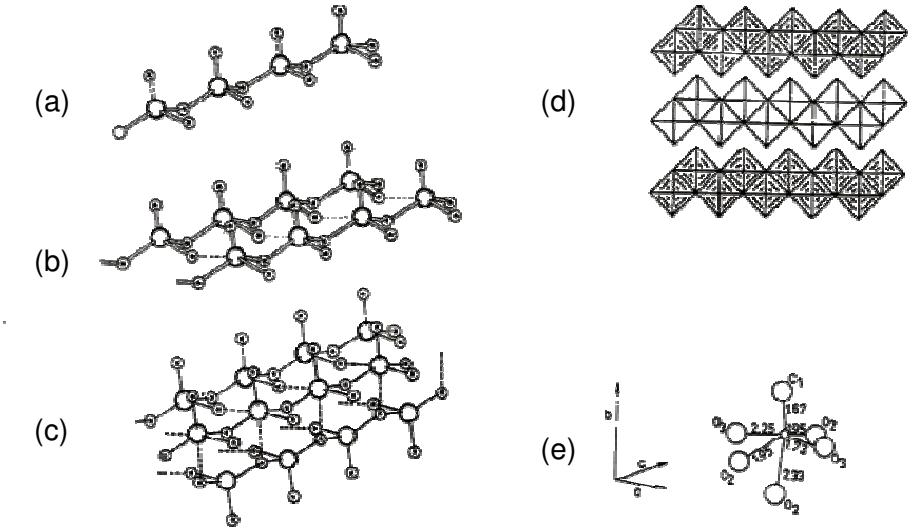

Figure 1.5 Elements of MoO_3 structure. (a) chain of tetrahedra, (b) linking of the chains, (c) formation of the sheet, (d) projection of the structure, (e) Mo-O lengths.[40]

A striking feature of α-MoO_3 is its ability to accommodate both neutral species, such as water, alcohols and amines, and simple ions such as H^+ and Li^+, between its layers; this theme is taken up in a following section. MoO_3 is a very important component of many catalysts and can itself be used for partial oxidation of methanol to formaldehyde. Modifications to the α-form of MoO_3 yield β-MoO_3 and β'-MoO_3, which have their own intercalation chemistry.[56]

The layering capacity of MoO_3 is illustrated in Figure 1.6. The structure of white α-$MoO_3 \bullet H_2O$ is based on the ubiquitous *cis* dioxo moiety and consists of isolated zigzag chains of edge-shared $MoO_5(OH_2)$ octahedra.

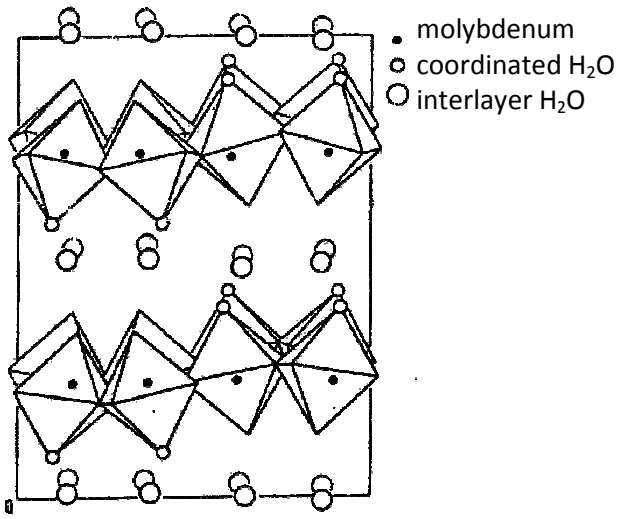

Figure 1.6 Structure of $MoO_3 \cdot H_2O$ projected almost parallel to [001].[22]

The MoO_3 structural unit is found in only a few monomeric oxo Mo^{VI} complexes; some examples are shown in Figure 1.7. *fac*-Trioxo molybdenum(VI) complexes are generated under strongly oxidizing conditions in the presence of chelating ligands.[57] The complex MoO_3(dien) (Figure 1.5a) has a six-coordinate octahedral structure with a *cis* trioxo arrangement. Its X-ray structure[58] reveals Mo-O distances averaging 1.74 Å, O-Mo-O angles averaging 106°, and Mo-N distances averaging 2.32 Å. MoO_3(dien) shows little stability in solution.[59] The triazacyclononane ligand (Me_3tcn) is a useful reagent in the preparation of MoO_3 core complexes (Figure 1.5b) by oxidative decarbonylation of *fac*-(Me_3tcn)$Mo(CO)_3$.[60] The triazacyclohexane (^{t}Bu$_3$tach) ligand has also proven to support a wealth of MoO_3 chemistry.[57] Oxidative decarbonylation of (^{t}Bu$_3$tach)$Mo(CO)_3$ by 30% H_2O_2, produces (^{t}Bu$_3$tach)MoO_3 (Figure 1.7c).[61]

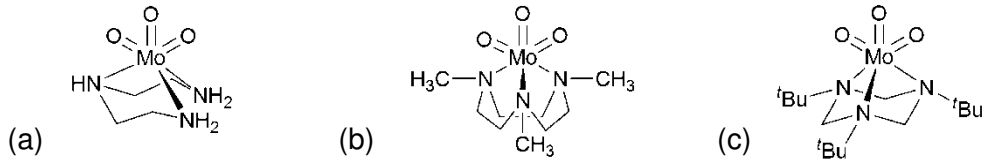

Figure 1.7 Molybdenum(VI) trioxo complexes. (a) MoO_3(dien),[58] (b) MoO_3(Me_3tcn),[60] and (c) MoO_3(^{t}Bu$_3$tach).[61]

1.4.3 Structures containing *cis*-MoO_2^{2+} cores.

The *cis*-MoO_2^{2+} core is particularly widespread in oxomolybdenum chemistry. This unit forms primarily mononuclear complexes, but also dimers, oligomers, and polyoxomolybdates. The common orthorhombic modification of MoO_3 and the triclinic α-$MoO_3 \cdot H_2O$ are formed of *cis*-MoO_2^{2+} units.[22] Oxohalides such as MoO_2Cl_2 form part of this family; in the solid state MoO_2Cl_2 is suggested to consist of infinite chains of MoO_2Cl_4 octahedra with bridging chlorine atoms (Figure 1.8),[62] and in the gas phase to feature *cis* dioxo Mo units with tetrahedral configuration.[5, 63]

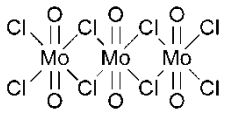

Figure 1.8 Structure postulated by Shustorovich for solid MoO_2Cl_2.[62]

Organometallic complexes containing the MoO_2^{2+} unit are by far the most common in Mo^{VI} chemistry, and an important part of this doctoral dissertation. These compounds are usually six-coordinate although some 5- and 4-coordinate compounds are known,[64-67] among them some previously reported by our research group[68, 69] and those presented in Chapter 2 of this dissertation.

The vast majority of MoO_2^{2+} complexes are six-coordinate and mostly of distorted octahedral structure. In the octahedral structure (as in pretty much any other geometry) the two Mo=O bonds are invariably *cis* to each other.[70] One π-symmetry p orbital of each oxygen atom interacts with a separate d orbital, and the third d orbital mixes with the remaining two oxygen π-symmetry orbitals (Figure 1.9a).[70] The strong σ and π donor nature of the oxo ligands makes it favorable for them to avoid competing for the same p and d orbitals. If the oxo groups were trans (Figure 1.9b), they would be forced to share two d orbitals. By residing in adjacent coordination sites they share only a single d orbital. Repulsion between the short Mo=O bonds and the other bonds determines the remaining details of geometry.[25]

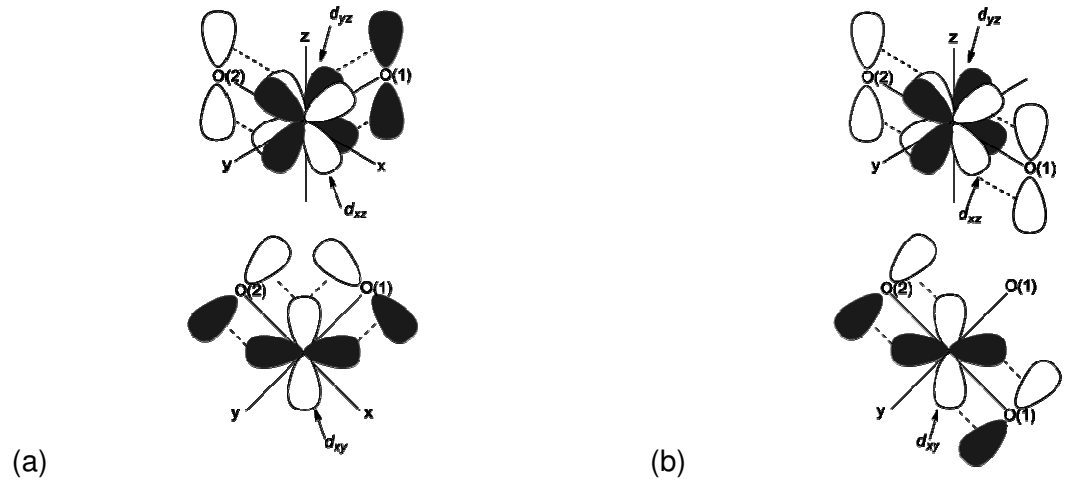

Figure 1.9 The principal molybdenum-oxo dπ-pπ bonding interactions in an octahedral coordination environment. (a) In the *cis* oxo arrangement, each of the oxygen atoms can form one strong π bond unencumbered by competition, O(1) with the metal d_{yz} orbital (shaded), and O(2) with d_{xz} (unshaded). The π interactions in the xy plane, though, result in a competition between the p orbitals on O(1) and O(2) for the only suitably oriented metal dπ orbital, d_{xy}. (b) The *trans* oxo conformation is disfavored due to the competition between the p orbitals on O(1) and O(2) for the orbitals d_{xz} (unshaded) and d_{xy} of the metal. Adapted from ref.[70, 71]

The reactivity of the MoO_2^{2+} unit has been thoroughly studied not only for fundamental reasons, but also because of its capacity for important oxygen atom transfer reactions.

Several complexes are known to possess a *cis* dioxo structure and to be non-octahedral in nature. Figure 1.10 shows a four-coordinate complex MoO_2(O-2,6-^{t}Bu$_2$C$_6$H$_3$)$_2$·ArOH bearing the MoO_2^{2+} core.[68]

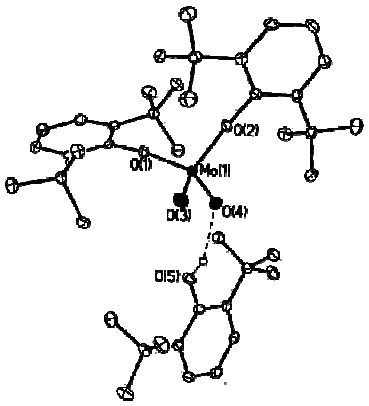

Figure 1.10 ORTEP diagram of 4-coordinate MoO_2(O-2,6-^{t}Bu$_2$C$_6$H$_3$)•HO-2,6-^{t}Bu$_2$C$_6$H$_3$.[68]

The MoO_2^{2+} group manifests itself in the infrared and/or Raman spectrum in the form of an intense two-band pattern corresponding to the symmetric and asymmetric Mo-O stretching vibrations, most commonly at 900-950 and 880-910 cm^{-1}. EXAFS studies[72] have shown that the MoO_2^{2+} core is readily identifiable in a variety of known compounds. These have been used to calibrate the EXAFS technique, which was subsequently used to identify this core in sulfite oxidase and in desulfo xanthine oxidase.[25, 32]

The MoO_2^{2+} core is prone to undergo redox reactions, which yield the formation of a reduced Mo center with the removal of an oxo group (Equation 1.4). This feature has been exploited by nature, by incorporating MoO_2^{2+} centers in several oxygen transfer enzymes, and industrially, in heterogeneous and homogeneous catalysis (Section 1.3.2).

$$Mo^{VI}O_2^{2+} \underset{[O]}{\overset{-[O]}{\rightleftharpoons}} Mo^{IV}O^{2+} \qquad (1.4)$$

1.4.4 The MoO^{4+} core

The MoO^{4+} unit is found in Mo^{VI} chemistry in a relatively small number of authenticated structures. The simplest set of complexes with the MoO^{4+} unit is $MoOX_4$ (X = F, Cl, Br). While a square pyramidal structure seems probable for the chloro and bromo complexes, the fluoro complex is polymeric in both the solid state and in solution.[25, 63]

The synthesis of complexes bearing the MoO^{4+} moiety is motivated mainly by two reasons: their resemblance to active sites in oxomolybdenum enzymes,[73-76] and their possible activity as procatalysts for olefin metathesis reactions (tungsten complexes containing a single oxo ligand are excellent procatalysts).[77, 78]

Polydentate ligands are commonly used to stabilize MoO^{4+} core complexes. Hayano et al. reported several MoO^{4+} aryloxides obtained by reacting $MoOCl_4$ (notoriously difficult to handle) with several mono- and multidentate aryloxy anions at low temperatures (Figure 1.11a).[79] A bidentate catecholate and a tridentate Schiff base ligand are used to bind a MoO^{4+} unit thought to be the Mo(VI) center of DMSO-reductase (Figure 1.11b).[80] Our research group

has reported the synthesis of Mo(VI) monoxo aryloxides (Figure 1.11c)[81] and bisphenoxides; these topics will be discussed in chapters 3 and 4 of this dissertation.

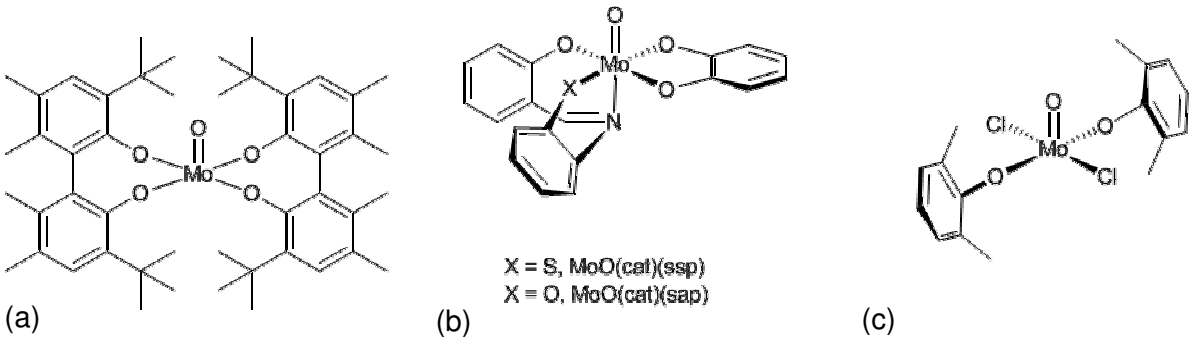

(a) (b) (c)

Figure 1.11 MoO^{4+} complexes. (a)[79] and (c)[81] molybdenum(VI) monooxo aryloxide complexes, (b) molybdenum(VI) monooxo catecholate with an NOS donor Schiff base ligand: N-salicylidene-2-aminobenzenethiolate (ssp) or N-salicylidene-2-aminophenolate (sap).[80]

1.5 Motivation of this research.

1.5.1 "Homogenization" of heterogeneous catalysts

Despite the importance of molybdenum oxo compounds (mainly metal oxides) as industrial and natural catalysts, there is comparatively little information on the mechanisms governing their activity. Models of these metal oxide catalysts could help to explain how such oxides interact with substrates. Research has focused on the downsizing of metal oxides to small molecular fragments, because smaller metal oxide assemblies can be better understood in terms of structure and reactivity. Addition of organic molecules to a metal center of a metal oxide has proven to be an effective way to synthesize the desired models for metal oxides.[20]

Our research group has been extensively interested in the operating mechanism behind the SOHIO process. The SOHIO process is the selective oxidation and ammoxidation of propylene to make acrolein (Equation 1.5) and acrylonitrile (Equation 1.6), used in industry in large scales.

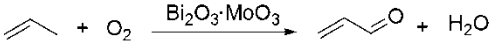

(1.5)

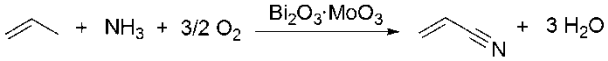

(1.6)

The predominant commercial process for acrylonitrile and acrolein production uses a multicomponent catalyst based on the Bi_2O_3•MoO_3 catalyst developed by SOHIO (Standard Oil of Ohio Company) workers in 1959-1962.[82, 83] In the ensuing decades, catalyst performance has been significantly improved. The current multicomponent catalysts are still based on bismuth molybdate but also contain metal oxide additives. Today the SOHIO acrylonitrile process is used in over 90% of the world's acrylonitrile production, representing plants in sixteen countries worldwide. In 2005 the annual worldwide production of acrylonitrile was estimated at more than 5 million tons per year.[21, 39] While the ammoxidation of propene is highly selective, at present the maximum acrolein yield at high propene conversion (90-95%) using commercial catalyst is approximately 80%.[21] Hence, despite the long history of the process, an improvement in the selectivity is still desirable. However, it is difficult to rationally design a catalyst capable of higher selectivities, because neither the exact functioning of the mixed metal oxide catalysts employed nor their uniqueness are well understood.[21] Mechanistic proposals based on isotopic labeling, spectroscopic measurements, and organometallic modeling have been postulated for the formation of acrolein and acrylontrile.[84-86] For acrolein, the overall process is assumed to occur as follows:[84]

1. Coordination/chemisorption of propene to a molybdenum site of the catalyst's surface
2. H atom abstraction from the propene at a bismuth site to form a π-allylic species
3. C-O bond formation at a molybdenum site
4. a second hydrogen abstraction, probably by the Mo=O moiety
5. reoxidation of the active site by oxygen (either coming from the bulk catalysts or from an external gas stream) accompanied by water elimination.

For acrylonitrile, the process is believed to be similar, but with initial NH_3 substitution for a terminal Mo=O moiety, and subsequent C-N bond formation rather than C-O bond formation.[84] The preeminent mechanistic theory is shown in Scheme 1.3.[38, 85]

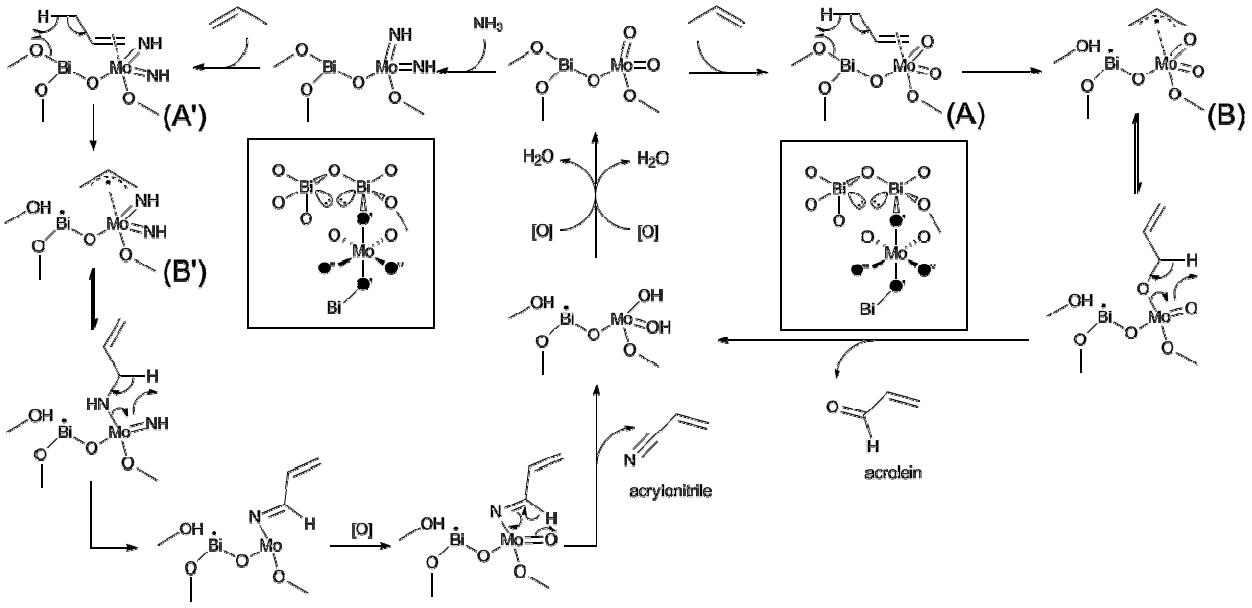

Scheme 1.3. Proposed active site of bismuth molybdate (in square) and reaction mechanism of selective propylene oxidation (right) and ammoxidation (left). In the active site, ●' denotes the lattice oxygen responsible for the α-hydrogen abstraction from the adsorbed olefin and ●'' the lattice oxygen (or NH moiety) that inserts into the chemisorbed surface π-allylic intermediate. π-O, α-O, π-N, and σ-N denote respectively the allylic species associated with Mo–O or M–NH sites, π- or σ-bonded.[84, 85]

Our main motivation is to produce organometallic molecules that resemble the catalytic active site of Bi_2O_3/MoO_3, and to use them to gain fundamental knowledge about the inherent chemical and physical properties of bismuth and molybdenum oxides and their interaction with substrates. The present work will focus specifically on the MoO_3 component of the SOHIO process.

In the ambitious task of modeling of the SOHIO catalyst active site we are not alone, and a great deal of research on this topic has been conducted within the last decade. Limberg offers an extensive summary of the research that has been done in this field.[21] A short summary of it will be given here with some modifications and additions, in order to provide a better idea of where our research is located in the context of homogeneous molybdenum oxo chemistry.

1.5.2 Existing models for α-[Bi_2MoO_6] intermediates

Species **A** (in Scheme 1.3) is proposed to consist of a high oxidation state Mo center, embedded in a hard oxo environment. Binding of olefins to $O=Mo^{VI}$ units has been demonstrated.[87] Models for surface intermediate **B**, which according to Scheme 1.3 decompose to give allyloxymolybdenum, are not yet known. This does not seem surprising, as **B** is often described as a "radical-like π-allyl-molybdenum complex". Complexes designed to model these intermediates should contain a π-allylmolybdenum group covalently bound to an oxo ligand. Figure 1.12 shows a complex with the $Mo_4(\mu\text{-}OH)_3(\mu\text{-}O)$-moiety.[88] It shows an interesting fluxional behavior in solution; the allyl$(CO)_2$ ligand set rotates with respect to the oxygen donor set. This fluxionality could give an idea of how mobile the allymolybdenum unit could be on the surface of α-[Bi_2MoO_6]. In this species Mo is found in oxidation state II, lower than its oxidation state in the heterogeneous metal oxide.

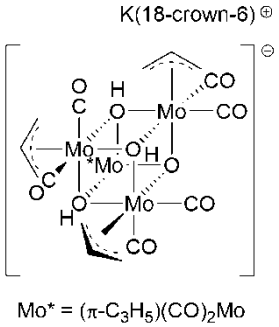

Figure 1.12. $Mo_4(\mu\text{-}OH)_3(\mu\text{-}O)$ moiety; possible model for **B**.[88]

Further attempts to mimic **B** include the Mo(VI) aryloxide, shown in Figure 1.13a, which was expected to bind the metallic center through two places as a chelating aryloxo/olefin ligand, but the olefin functions remained dangling and did not coordinate to the molybdenum.[89] A Mo(IV) complex where two chloride ligands are bound to the metal center instead of the expected oxo functionality successfully bound the allyl moiety, constituting one of the few Mo(IV) allyl compounds known to date (Figure 1.13b).[90]

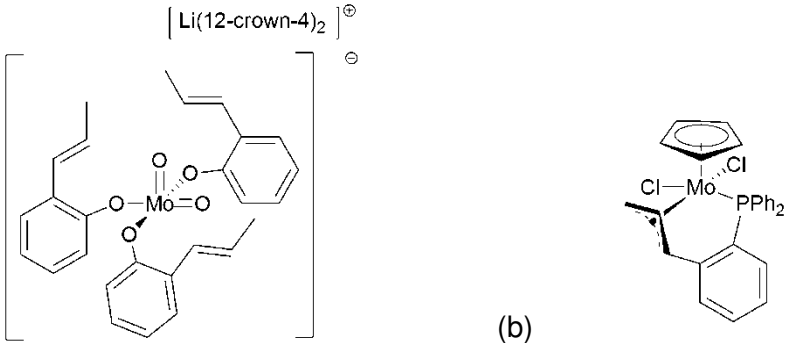

Figure 1.13 Possible model complexes of **B**. (a) Mo(VI) oxo complex with dangling allyl groups,[89] (b) molybdenum(IV) allyl complex.[90]

A better model for **B** is shown in Scheme 1.4. This molecule features oxo bridges between allyl molybdenum units and a Mo^{VI} unit. When this complex is warmed, it generates allyl radicals that are not trapped by the oxo ligands, but rather abstract hydrogen atoms to yield propene. Thermolysis of this complex in the presence of O_2 yielded as volatile products allyl alcohol and acrolein.[91]

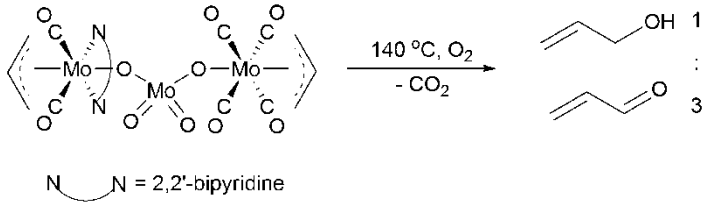

Scheme 1.4 Mo^{VI} oxo bridged allyl complex. Upon heating in the presence of O_2, allyl alcohol and acrolein are released.[91]

Compounds meant to model the intermediate **B'**, shown in Scheme 1.3, should contain a π-allyl-molybdenum group covalently bound to an imido ligand. Two fine examples are the low valent $[CpMo^{IV}(=NR)(\pi\text{-allyl})]$ complex[92] (Figure 1.14a) and the $[(^{t}BuN=)_2Mo^{VI}(methylallyl)_2]$ (Figure 1.14b). The latter complex could not be characterized structurally, but spectroscopic evidence pointed to the π-coordination of one of the allyl ligands.[93]

Figure 1.14 Models for intermediate **B'**. (a) [$CpMo^{IV}(=NR)(\pi\text{-allyl})$],[92] (b) [$(^tBuN=)_2Mo^{VI}(metallyl)_2$].[93]

Complexes containing O=Mo=NR units that bind olefin or allyl ligands are of special interest since the bismuth molybdate surface during the SOHIO process might contain neighboring oxo and imido ligands at Mo^{VI} sites. A complex containing these units was synthesized and is shown in Scheme 1.5, but the allyl ligand did not bind to the Mo^{VI} center. All attempts so far to produce interaction with the metallic center have been unsuccessful.[94]

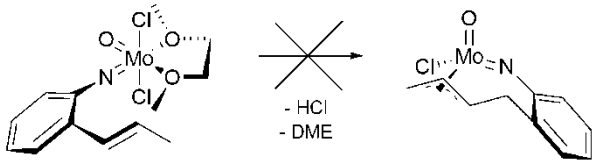

Scheme 1.5 Mo^{VI} imido complex designed for HCl elimination in order to anchor the allyl ligand.[94]

The first steps in the SOHIO process not only include the binding of the olefin on the molybdenum site, but also the hydrogen abstraction by the bismuth moiety. A homometallic molybdenum complex might not completely describe the first steps of this process, so a heterometallic model is needed. There have been several attempts to produce such a model, and Mo/Bi alkoxides have played an important role. Examples are shown in Figure 1.15.

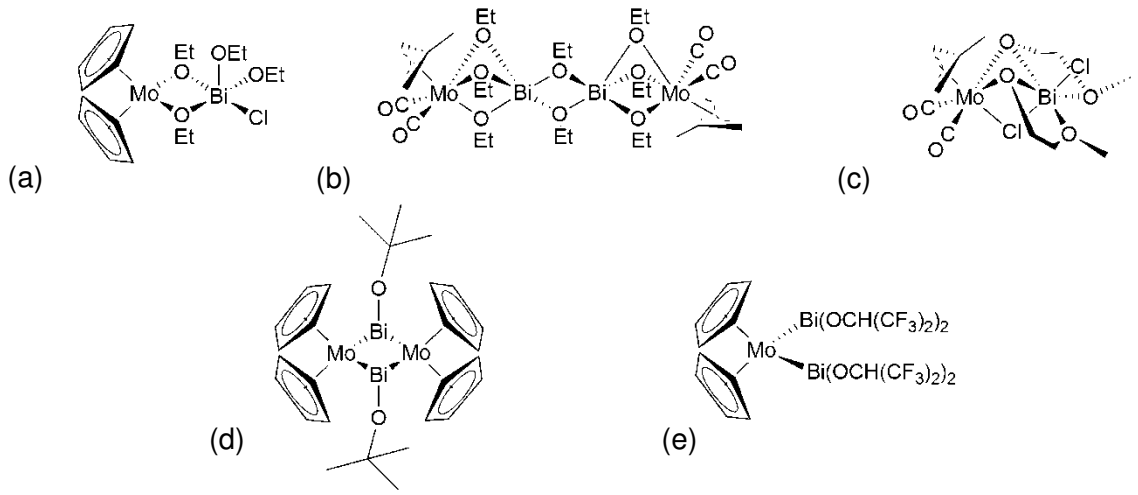

Figure 1.15 Mo-O-Bi alkoxide complexes. (a) $[Cp_2Mo(\mu\text{-}OEt)_2Bi(OEt)_2Cl]$,[95] (b) $[((CH_3)C_3H_4)Mo(CO)_2(\mu\text{-}OEt)_3Bi(\mu\text{-}OEt)_2Bi(\mu\text{-}OEt)_3Mo(CO)_2((CH_3)C_3H_4)]$,[96] (c) $[((CH_3)C_3H_4)Mo(CO)_2(\mu\text{-}\kappa O,2\kappa O'\text{-}OCH_2CH_2OCH_3)_2(\mu\text{-}Cl)BiCl]$,[96] (d) $[\{Cp_2Mo\}_2\{\mu\text{-}Bi(O^tBu)\}_2]$,[97] (e) $[Cp_2Mo(Bi\{OCH(CF_3)_2\}_2)_2]$.[98]

The examples shown in Figure 1.15 do not include what could be called a true Mo-O-Bi moiety. Within the last years, complexes providing structurally authenticated Mo-O-Bi linkages have appeared; the synthetic details are outside the scope of this manuscript, but the structures are displayed in Figure 1.16. It is important to remark that Figure 1.16a shows a complex with oxo bridges between Mo^{VI} and Bi^{V}; Figures 1.16b-d are complexes with oxo bridges between Mo^{VI} and Bi^{III}.

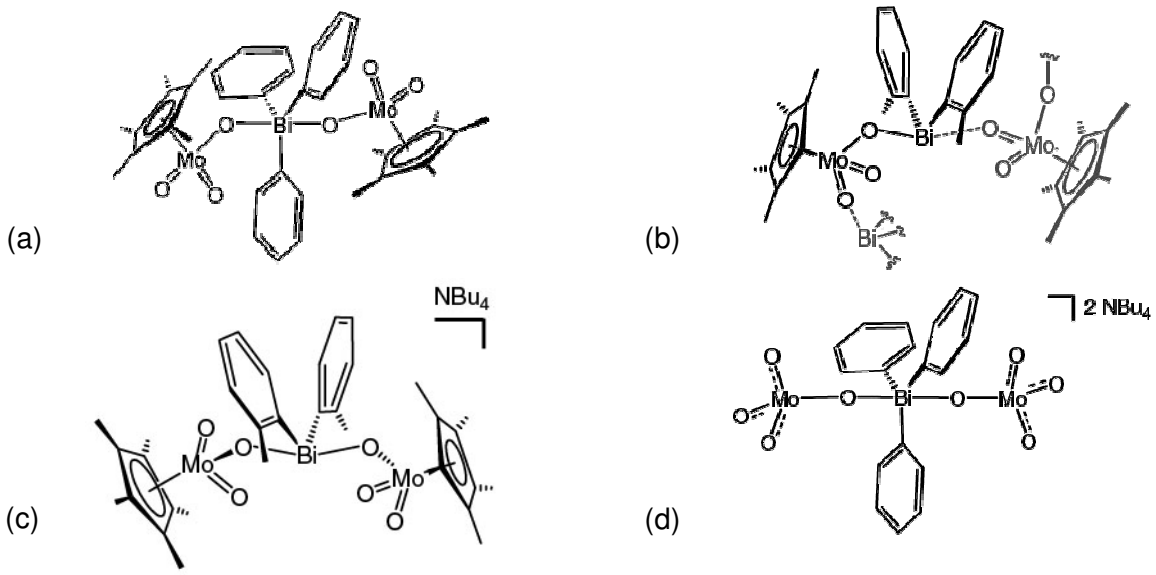

Figure 1.16 Models for Mo-O-Bi sites. (a) $[(Cp^*Mo(O)_2\text{-}(\mu\text{-}O)_2BiPh_3]$,[99] (b) polymeric $[(Cp^*Mo(O)_2)\text{-}(\mu\text{-}O)\text{-}(Bi(o\text{-}tolyl)_2)]_n$,[99] (c) $NBu_4[\{Cp^*Mo(O)_2\text{-}(\mu\text{-}O)\text{-}\}_2(Bi(o\text{-}tolyl)_2)]$,[100] and (d) $[NBu_4]_2[BiPh_3(MoO_4)_2]$.[100]

1.6 Our model

The structure and properties of MoO_3 were discussed in section 1.4.2. It is possible to regard the electronic structure of Mo in MoO_3 as equivalent to that of a *cis* dioxo complex based on the structural characteristics mentioned above.[22] In the gas phase the most abundant molybdenum oxide cluster species observed from the evaporation of MoO_3 is the Mo_3O_9 cluster (Figure 1.17b).[86] *Ab initio* calculations have found that systems such as the MoO_2Cl_2 cluster (Figure 1.17a) could mimic the energetics for several key processes with the Mo_3O_9 cluster.[86] *cis* Dioxo Mo^{VI} complexes can therefore be considered desirable systems to mimic and study the reactions carried out by heterogeneous metal oxides.

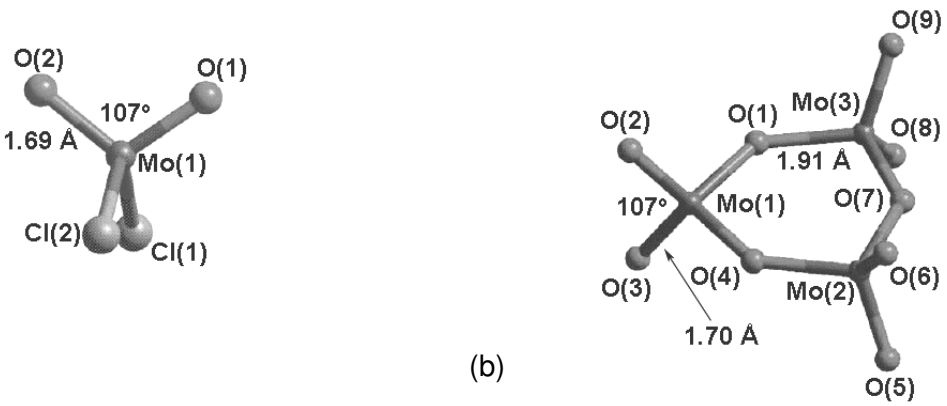

(a) (b)

Figure 1.17 Model clusters. (a) Model cluster of MoO_2Cl_2, (b) MoO_3 site in gas phase.[86]

Early work assigned terminal oxo ligands (or imido ligands in the ammoxidation case) the role of the trapping site, and this theory is still discussed.[85] The results of more recent work, however, put forward the alternative idea that bridging oxo ligands might be the ultimate oxygenation sites.[21, 84] In this sense our target model shown in Figure 1.18b might be able to explore the proposed coordination to bridging oxo ligands. Our approach to the MoO_3 active site uses bulky aryloxy ligands because they provide a platform where electronics and sterics can be tuned. The information on stability, reactivity and structural geometry that we obtained by adjusting these parameters will be presented in the next chapters.

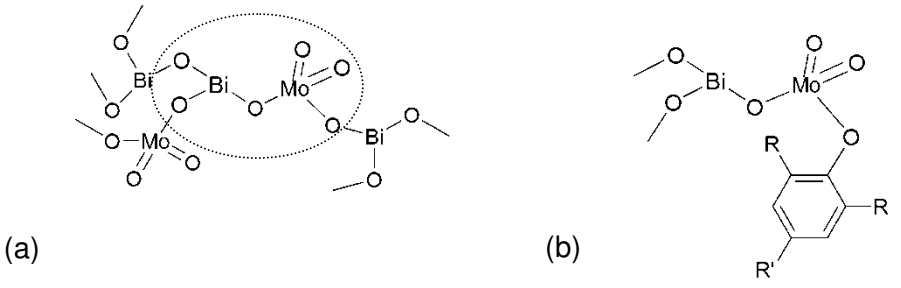

(a) (b)

Figure 1.18 Our model approach. (a) The proposed SOHIO active site,[85] (b) our molybdenum dioxo aryloxide target.

As mentioned in section 1.5.2, it is evident that any complex that aims to model the active site of the SOHIO process should contain the heterobimetallic Bi-O-Mo core. At this stage of our research, our efforts are directed towards the construction of building blocks that can later be joined. This effort includes the synthesis of Mo^{VI} and Bi^{III} aryloxide complexes (importance of

alkoxides as models was discussed in section 1.5.2) that provide us with understanding of their reactivity and synthesis, and can then be used for the generation of our own heterometallic complex models of the SOHIO catalyst active site.

In our quest for the understanding of the electronic and steric factors that govern the formation of Mo^{VI} dioxo aryloxides (Chapter 2) we also discovered the interesting chemistry of the MoO^{4+} aryloxide complexes (Chapter 3). These complexes and their cousins, the molybdenum(VI) monoxo bisphenoxides (Chapter 4), constituted a challenging chapter of this doctoral research from a synthetic point of view. At the same time, they gave us knowledge on how shape and reactivity of molecules are intimately related. Scheme 1.6 shows the different stages of the research that will be presented in the following chapters.

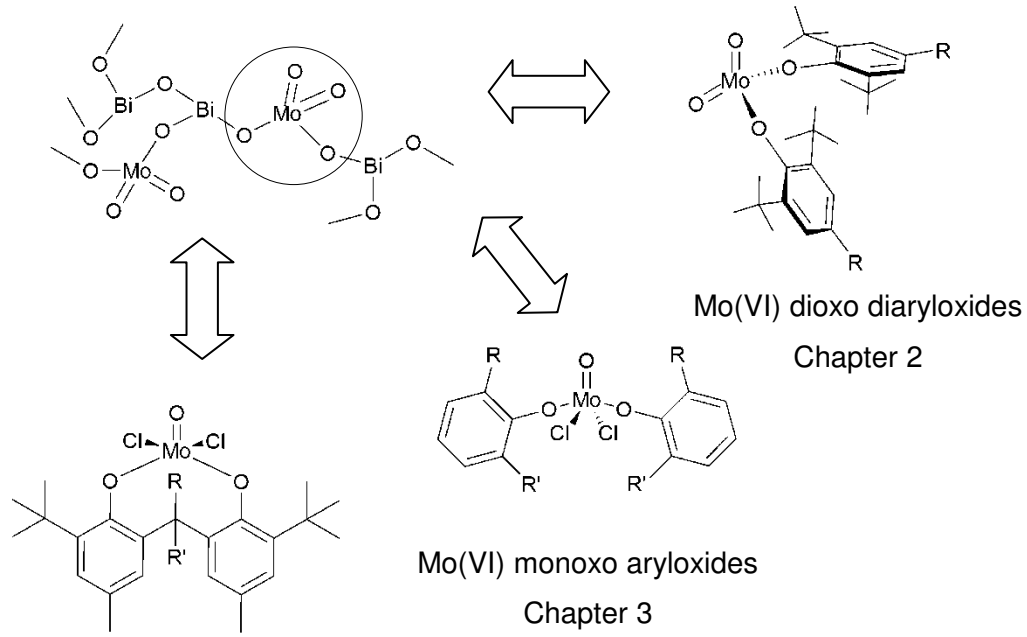

Scheme 1.6 The different research lines that will be covered in this doctoral dissertation.

The ultimate goal pursued with this research is the acquisition of fundamental knowledge that will help to build up the body of the oxomolybdenum organometallic chemistry.

CHAPTER 2

MOLYBDENUM(VI) DIOXO DIARYLOXIDE COMPLEXES

2.1 Introduction

Metal oxides are important in numerous industrial processes; among them molybdenum stands out as a versatile element possessing a large number of stable and accessible oxidation states. Several important chemical reactions are catalyzed by molybdenum oxides: ammoxidation of propene to acrylonitrile,[38, 84] hydrodesulfurization,[101] oxygen transfer reactions[102] and olefin metathesis,[103] to name a few. The important role of molybdenum is not restricted to industrial catalysis: nature has incorporated molybdenum in over 20 enzymes, such as xanthine oxidase, aldehyde oxidase, and sulfite oxidase, where oxygen transfer is crucial.[104]

Small-molecule model systems are frequently used to virtually break down the complicated metal oxide network into smaller molecular fragments that can be better understood in terms of structure and reactivity, to then better understand the catalytic activity of the corresponding metal oxides. Organometallic oxo complexes have attracted the attention of researchers as tangible model systems. Metal oxo aryloxide complexes, for example, are both soluble analogues and precursors for metal oxides. We have been interested in molybdenum dioxo aryloxides that can model heterogeneous active sites in oxidation catalysis.

We have reported the synthesis of the first four-coordinate molybdenum(VI) aryloxide $MoO_2(OAr)_2$[68] and more recently the formation of the four, five and six-coordinate analogues by manipulation of the steric environment of the aryloxide ligand, using pyridine to fill empty coordination sites.[69] Herein we will describe reactions leading to $MoO_2(OAr)_2$ molecules with different electronic properties, the synthesis of 4-, 5- and 6-coordinate Mo dioxo aryloxides starting from the air and moisture stable $MoO_2Cl_2(DMF)_2$ adduct, and the complete characterization of the monomeric Li{MoO_2Cl[2,2'-CH_2(O-6-^{t}Bu-4-MeC_6H_2)$_2$]}·3DME. We will also suggest a possible intermediate during the synthesis of $MoO_2(OAr)_2$ that could account for the observation of a radical side product detected by EPR spectroscopy.

Table 2.1 introduces the series of the different lithium and ammonium aryloxides, and the 4-, 5- and 6-coordinate molybenum dioxo diaryloxides that will be discussed in this chapter. The labeling identifies each compound from this chapter.

Table 2.1 List of Compounds Presented in This Chapter.

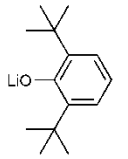

(**2.1a**)

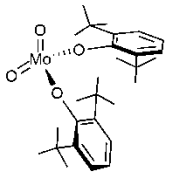

(**2.2a**)

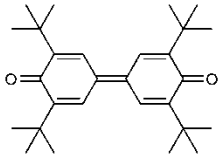

(**2.3a**)

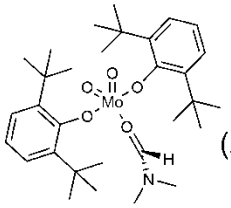

(**2.5a**)

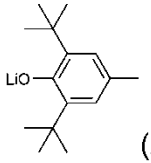

(**2.1b**)

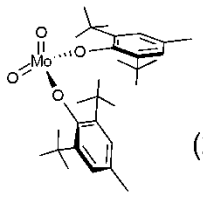

(**2.2b**)

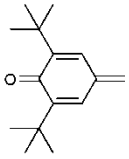

(**2.3b**)

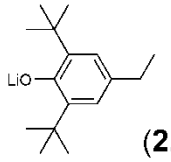

(**2.1c**)

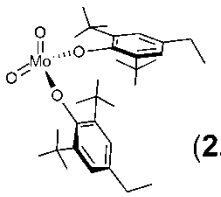

(**2.2c**)

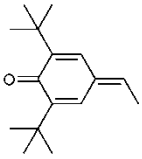

(**2.3c**)

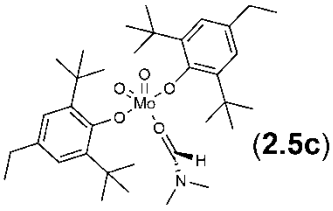

(**2.5c**)

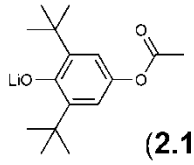

(**2.1d**)

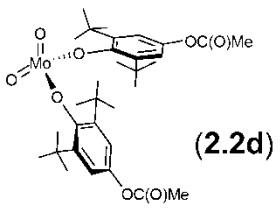

(**2.2d**)

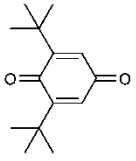

(**2.3d**)

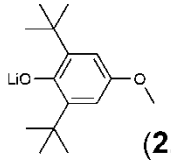

(**2.1e**)

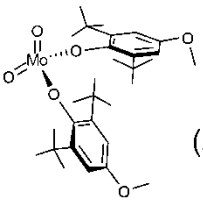

(**2.2e**)

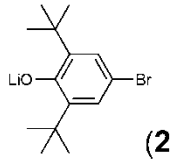

(**2.1f**)

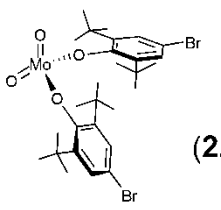

(**2.2f**)

Table 2.1 (Continuation)

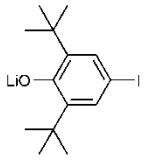

(**2.1g**)

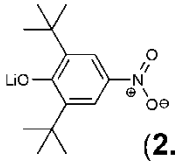

(**2.1h**)

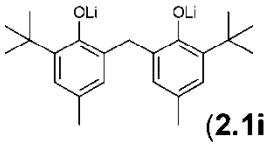

(**2.1i**)

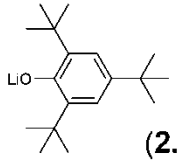

(**2.1j**)

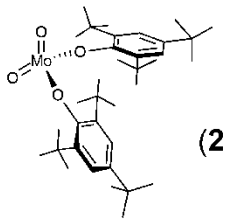

(**2.2j**)

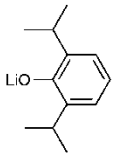

(**2.1k**)

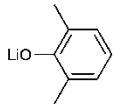

(**2.1l**)

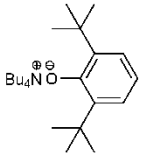

(**2.1m**)

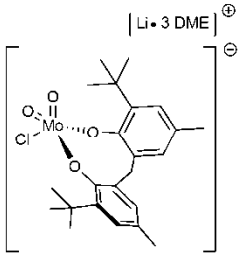

(**2.4**)

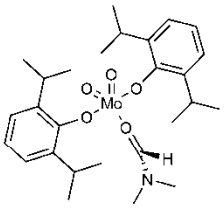

(**2.5k**)

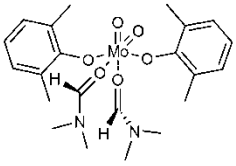

(**2.5l**)

2.2 Experimental section

2.2.1 General

All manipulations were performed under nitrogen or argon using standard Schlenk techniques or in a NEXUS 1 VAC Atmospheres glovebox. Molybdenum(VI) dichloride dioxide, *n*-butyllithium (2.0 M solution in *n*-pentane), 2,6-dimethylphenol, 2,6-di-*tert*-butyl-4-methylphenol, 2,6-di-*tert*-butyl-4-ethylphenol, 2,6-di-*tert*-butyl-4-methoxyphenol, 2,6-di-*tert*-butyl-4-bromophenol, 2,2'-methylenebis(6-*tert*-butyl-4-methylphenol), MoO_3, HCl, HBr, DMF, DMSO, $OPPh_3$, 2,2'-bipyridyl and N,N,N',N''-tetramethylethylenediamine were obtained from Aldrich and were used as received. PPh_3 was recrystallized from anhydrous hot ethanol. Bu_4NOH (1.0 M in methanol) was purchased from Aldrich and stored over molecular sieves for 2 days prior to use. 2,6-di-*tert*-butyl-4-nitrophenol and 2,6-di-*tert*-butyl-4-iodophenol were prepared from 2,6-di-*tert*-butylphenol (Aldrich) and HNO_3/CH_3COOH or HIO_4/Al_2O_3, respectively, as reported.[105, 106] 2,6-di-*tert*-butyl-4-acetoxyphenol was made from 2,6-di-*tert*-butyl-*p*-benzoquinone, Zn^0, $(CH_3CO)_2O$, and pyridine as previously described.[105] LiO-2,6-^{t}Bu$_2$C$_6$H$_3$ (**2.1a**),[68] LiO-2,6-Me$_2$C$_6$H$_3$ (**2.1l**),[69] LiO-2,6-^{i}Pr$_2$C$_6$H$_3$ (**2.1k**),[69] LiO-2,4,6-^{t}Bu$_3$C$_6$H$_2$ (**2.1j**),[69] MoO$_2$(O-2,4,6-^{t}Bu$_3$C$_6$H$_2$)$_2$ (**2.2j**),[69] ·O-2,4,6-^{t}Bu$_3$C$_6$H$_2$,[107] $MoO_2Cl_2(CH_3CN)_2$,[108] $MoO_2Cl_2(THF)_2$,[108] $MoO_2Cl_2(DMF)_2$,[109] $MoO_2Cl_2(DMSO)_2$,[110] $MoO_2Br_2(DMF)_2$,[111] $MoO_2Cl_2(OPPh_3)_2$,[112] MoO_2Cl_2(bipy),[113] and MoO_2Cl_2(tmen)[114] were synthesized as described in the literature. 1,2-dimethoxyethane (DME), hexanes, diethyl ether (Et_2O) and tetrahydrofuran (THF) were freshly distilled under argon from Na/benzophenone; toluene was filtered through activated alumina and Cu-based oxygen absorbent as described by Grubbs et al.[115] *n*-Pentane, dimethyl sulfoxide (DMSO), ethanol and acetonitrile (anhydrous grade) were purchased from Aldrich and stored over molecular sieves. Carbon disulphide (HPLC grade, Aldrich) was distilled from CaH_2 and further refluxed and distilled from P_2O_5, both times under argon.[116] Methanol (HPLC grade, Aldrich) was pre-dried over molecular sieves for 48 h and further refluxed and distilled from CaO under nitrogen. 1,3,5-triisopropylbenzene (Aldrich) was distilled from CaH_2 under argon atmosphere. NMR solvents (benzene-d_6,

dimethylsulfoxide-d_6 and chloroform-d) were degassed and vacuum distilled from CaH_2. Benzene-d_6 was additionally vacuum transferred from Na/benzophenone. All solvents (including NMR solvents) were stored inside the glovebox over 4 Å molecular sieves (previously activated) for 48 h before use.

The melting points of the products were observed in sealed capillary tubes on a Mel-temp apparatus (Laboratory Devices, Cambridge, MA). ^1H and ^{13}C NMR spectra were recorded on a Mercury Varian Plus 300 MHz spectrometer. The ^1H NMR spectrum of compound **2.1i** was recorded in a Varian NOVA 400 MHz spectrometer. We will use the notation *ipso*, *ortho*, *meta* and *para* to refer to carbons C_1 through C_4 on the aryl ring, where C_1 is bonded as C_1-O-Mo. IR spectra were obtained with a MIDAC Corporation M-Series FTIR spectrometer. UV/vis spectra were recorded on an Agilent 8543 UV-visible spectrophotometer. Elemental analyses were performed at the University of Illinois (Urbana-Champaign) but the results were not satisfactory. FAB mass spectrometric analyses were conducted at the National Center for Research Resources (St. Louis, MO). Satisfactory HRMS were obtained, except for compounds **2.4**, **2.5a**, **2.5k** and **2.5l**.

All single crystals were coated with paratone-N oil (Hampton Research), and mounted onto thin glass fibres. Diffraction data were collected using graphite monochromated MoK_α radiation (λ = 0.71073 Å) on a Bruker SMART 1000 CCD area detector diffractometer via ϕ and ω scans. All data were collected at 223 K. The structures were solved using SHELXS-97[117] by direct methods. All structures were refined by least-squares full matrix refinement against F^2 using SHELXL-97 and all fully-occupied non-hydrogen atoms were refined with anisotropic atomic displacement parameters (adps). Hydrogen atoms were geometrically placed and refined as part of a rigid model. Geometric restraints were applied, and partially occupied atom sites were refined with isotropic adps.

Additional details, including solution NMR (^1H and ^{13}C) data, UV-vis information and EPR spectra can be found in the appendix of this chapter.

2.2.2 Preparation of compounds

LiO-2,6-^{t}Bu$_2$-4-MeC$_6$H$_2$ (2.1b): A 15 mL solution of 2,6-^{t}Bu$_2$-4-MeC$_6$H$_2$OH (1.0000 g, 4.5382 mmol) in Et_2O was prepared and cooled in an ice bath. ^{n}BuLi (2.26 mL of 2.0 M in pentane, 4.5 mmol) was mixed with Et_2O (7 mL); the resulting mixture was added dropwise (via addition funnel) to the phenol solution with strong stirring over a period of 30 min at 0 °C (the reaction is highly exothermic). The reaction mixture was allowed to reach room temperature over 2 h, stirring constantly. The solvent was concentrated in vacuo to *ca.* 7 mL and the mixture stored at -35 ˚C. After 1 day a white crystalline precipitate formed. The yellowish supernatant was removed with a pipette, and the precipitate was crystallized from Et_2O (7 mL) a second time. The supernatant was pipetted out and the white powder was dried under vacuum. Yield 0.7605 g (74%). ^{1}H NMR (C_6D_6): δ (ppm) 7.30 (s, 2H, aromatic *H*), 2.40 (s, 3H, C*H*$_3$), 1.68 (s, 18H, C(C*H*$_3$)$_3$).

LiO-2,6-^{t}Bu$_2$-4-EtC$_6$H$_2$ (2.1c): was prepared following the same procedure as for **1a** but using 2,6-^{t}Bu$_2$-4-EtC$_6$H$_2$OH (1.000 g, 4.266 mmol) and ^{n}BuLi solution (2.13 mL, 4.3 mmol). Yield 0.8410 g (82%). ^{1}H NMR (C_6D_6): δ (ppm) 7.33 (s, 2H, aromatic *H*), 2.70 (q, 2H, *J* = 7.5 Hz, C*H*$_2$CH$_3$), 1.69 (s, 18H, C(C*H*$_3$)$_3$), 1.31 (t, 3H, *J* = 7.5 Hz, CH$_2$C*H*$_3$).

LiO-2,6-^{t}Bu$_2$-4-[OC(O)Me]C$_6$H$_2$ (2.1d): was prepared following the same procedure as for **1a** but using 2,6-^{t}Bu$_2$-4-[OC(O)Me]C$_6$H$_2$OH (1.0000 g, 3.7827 mmol) and ^{n}BuLi solution (1.89 mL, 3.8 mmol). Yield 0.8709 g (85%). ^{1}H NMR (DMSO-d_6): δ (ppm) 6.28 (s, 2H, aromatic *H*), 2.07 (s, 3H, OC(O)C*H*$_3$), 1.29 (s, 18H, C(C*H*$_3$)$_3$).

LiO-2,6-^{t}Bu$_2$-4-(OMe)C$_6$H$_2$ (2.1e): was prepared following the same procedure as for **1a** but using 2,6-^{t}Bu$_2$-4-(OMe)C$_6$H$_2$OH (1.0000 g, 4.2310 mmol) and ^{n}BuLi solution (2.11 mL, 4.22 mol). Yield 0.7124 g (69%). ^{1}H NMR (C_6D_6): δ (ppm) 7.21 (s, 2H, aromatic *H*), 3.42 (s, 3H, OC*H*$_3$), 1.40 (s, 18H, C(C*H*$_3$)$_3$).

LiO-2,6-^{t}Bu$_2$-4-BrC$_6$H$_2$ (2.1f): was prepared following the same procedure as for **1a** but using 2,6-^{t}Bu$_2$-4-BrC$_6$H$_2$OH (1.0000 g, 3.5060 mmol) and ^{n}BuLi solution (1.75 mL, 3.5 mmol). Yield 0.5478 g (71%). ^{1}H NMR (C_6D_6): δ (ppm) 7.66 (s, 2H, aromatic *H*), 1.48 (s, 18H, C(C*H*$_3$)$_3$).

LiO-2,6-^{t}Bu$_2$-4-IC$_6$H$_2$ (2.1g): was attempted following the same procedure as for **1a** but using 2,6-^{t}Bu$_2$-4-IC$_6$H$_2$OH (1.0000 g, 3.0100 mmol) and ^{n}BuLi solution (1.50 mL, 3.0 mmol). Product **1g** was formed along with several side-products. Purification via recrystallization was unsuccessful.

LiO-2,6-^{t}Bu$_2$-4-(NO$_2$)C$_6$H$_2$ (2.1h): was prepared following the procedure for **1a** but using 2,6-^{t}Bu$_2$-4-(NO$_2$)C$_6$H$_2$OH (1.000 g, 3.9790 mmol) and *n*-BuLi solution (1.99 mL, 4.0 mmol). The resulting ethereal fine orange dispersion did not precipitate or form any solid aggregate at -35 ^{o}C, making its purification difficult; but ^{1}H NMR showed only product. Solvent was removed under vacuum. Crude yield 0.9215 (90%). ^{1}H NMR (DMSO-d_6): δ (ppm) 7.67 (s, 2H, aromatic *H*), 1.26 (s, 18H, C(C*H*$_3$)$_3$).

2,2'-CH$_2$(LiO-6-^{t}Bu-4-MeC$_6$H$_2$)$_2$ (2.1i): was prepared following the procedure for **1a** but using 2,2'-CH$_2$(6-^{t}Bu-4-MeC$_6$H$_2$OH)$_2$ (1.0000 g, 2.9368 mmol) and ^{n}BuLi solution (2.93 mL, 5.87 mmol). Yield 0.7884 g (75 %). ^{1}H NMR (CD_3CN): δ (ppm) 6.85 (d, 2H, *J* = 2.0 Hz, aromatic *H*), 6.66 (d, 2H, *J* = 2.0 Hz, aromatic *H*), 3.71 (s, 2H, methylene C*H*$_2$), 2.12 (s, 6H, C*H*$_3$), 1.33 (s, 18H, C(C*H*$_3$)$_3$).

(Bu$_4$N)(O-2,6-^{t}Bu$_2$C$_6$H$_3$) (2.1m): was prepared by a modification in the procedure reported for the synthesis of the analogous (Et$_4$N)(OC$_6$H$_5$).[118] A solution of HO-2,6-^{t}Bu$_2$C$_6$H$_3$ (1.0000 g, 4.8468 mmol) in 20 mL of anhydrous methanol was added to Bu$_4$NOH (1.0 M in methanol, 4.9 mL, 4.9 mmol) contained in a 50-mL Schlenk flask with a stirbar. The reaction flask was then connected to a mild nitrogen flow, fitted with a reflux graham condenser, and a teflon valve in the top of the condenser connected to a bubbler filled with mineral oil. With stirring the reaction mixture was heated at 50 ^{o}C for 2 h. Volatiles were removed under vacuum leaving behind a dark purple solid which was recrystallized 4 times from THF:CH_3CN (7 mL:1

mL). The purple needles were dried under vacuum with heating at 79 °C for 3 days, yielding 1.4010 g (64%) of product. ^{1}H NMR ($CDCl_3$): anion δ (ppm) 7.14 (d, 2H, *J* = 9 Hz, aromatic *H*), 6.78 (t, 1H, *J* = 9 Hz, aromatic *H*), 1.41 (s, 18H, $C(CH_3)_3$); cation δ (ppm) 3.34 (broad m, 8H, $^{\oplus}N(CH_2CH_2CH_2CH_3)_4$), 1.64 (broad m, 8H, $^{\oplus}N(CH_2CH_2CH_2CH_3)_4$), 1.37 (broad m, 8H, $^{\oplus}N(CH_2CH_2CH_2CH_3)_4$), 0.97 (t, 12H, *J* = 9 Hz, $^{\oplus}N(CH_2CH_2CH_2CH_3)_4$). The structure of **1m** was corroborated by single crystal X-ray diffraction (see appendix).

MoO_2(O-2,6-^{t}$Bu_2C_6H_3$)$_2$ (2.2a): LiO-2,6-^{t}$Bu_2C_6H_3$ (0.2136 g, 1.006 mmol) and MoO_2Cl_2 (0.10000 g, 0.5029 mmol) were dissolved, each in 10 mL of DME. The lithium salt solution was added dropwise to the blue MoO_2Cl_2 solution with rapid stirring at room temperature. After 12 h, the reaction mixture was filtered through a medium pore sintered glass frit and the volatiles were removed under vacuum. A ^{1}H NMR spectrum of the crude reaction mixture (after the first filtration) revealed three major components; MoO_2(O-2,6-^{t}$Bu_2C_6H_3$)$_2$ (**2a**), HO-2,6-^{t}$Bu_2C_6H_3$, and 3,3',5,5'-tetra-*tert*-butyl-4-4'-diphenoquinone (**3a**). ^{n}Pentane (15 mL) was added to the dry dark mass and the mixture was stirred for 6 h. The resulting mixture was filtered, concentrated under vacuum to *ca*. 5 mL and stored at -35 °C for 2 days affording orange crystals. The supernatant was withdrawn and recrystallization in pentane was performed twice more. The crystals were dried under vacuum. Yield 0.1006 g (40%), m.p. 124-125 °C. IR (C_6H_6) and ^{1}H NMR data matched those reported in the literature.[68]

MoO_2(O-2,6-^{t}Bu_2-4-MeC_6H_2)$_2$ (2.2b): was prepared following the procedure used for **2a** but using LiO-2,6-^{t}Bu_2-4-MeC_6H_2 (0.2275 g, 1.005 mmol) and MoO_2Cl_2 (0.1000 g, 0.5029 mmol). The ^{1}H NMR spectrum of the crude reaction mixture (after the first filtration) revealed two major components; MoO_2(O-2,6-^{t}Bu_2-4-MeC_6H_2)$_2$ (**2b**) and HO-2,6-^{t}Bu_2-4-MeC_6H_2, and traces of 2,6-di-*tert*-butyl-4-methylenecyclohexa-2,5-dienone[119] (**3b**). ^{n}Pentane (15 mL) was added to the dry dark mass and the mixture was stirred for 6 h. The resulting mixture was filtered, concentrated under vacuum to *ca*. 5 mL, kept in an oil bath for 10 min at 45 °C to maximize the solubility of the desired complex, and then stored at -35 °C. After 1 day a green crystalline precipitate was

observed and the supernatant was withdrawn with a pipette. Reprecipitation from *n*-pentane (including heating and cooling) was repeated two times. Yield: 0.1002 g (35%). ^{1}H NMR ($CDCl_3$): δ 7.07 (s, 4H, aromatic *H*), 2.30 (s, 6H, C*H*$_3$), 1.45 (s, 36H, C(C*H*$_3$)$_3$). ^{13}C{^{1}H} NMR ($CDCl_3$): δ 162.2 (*ipso C*), 139.4 (*ortho C*), 133.0 (*para* C), 126.2 (*meta C*), 35.2 (*C*(CH$_3$)$_3$), 31.6 (C(*C*H$_3$)$_3$), 21.4 (*C*H$_3$). m.p. 150-152 °C. IR (cm^{-1}, KBr): 1635w, 1434s, 1409m, 1394m, 1363w, 1313w, 1263w, 1230w, 1204s, 1186m, 1159m, 1113s, 1026sh, 962m (Mo=O), 939s (Mo=O), 897s, 860w. UV-vis (C_6H_6) λ_{max}/nm (ε/dm^{3}mol^{-1}cm^{-1}): 278 (6355), 354 (5340). HRMS (FAB) Calc. 1st isotopic mass 562.2464 (M^+). Found 562.2484 (M^+). Calc 2nd isotopic mass 563.2498 (M^+). Found 563.2500 (M^+).

MoO_2(O-2,6-^{t}Bu$_2$-4-EtC_6H_2)$_2$ (2.2c): was prepared like **2a** but using LiO-2,6-^{t}Bu$_2$-4-EtC_6H_2 (0.2417 g, 1.006 mmol) and MoO_2Cl_2 (0.1000 g, 0.5029 mmol). A ^{1}H NMR spectrum of the crude reaction mixture (after the first filtration) revealed two major components; MoO_2(O-2,6-^{t}Bu$_2$-4-EtC_6H_2)$_2$ (**2c**) and HO-2,6-^{t}Bu$_2$-4-EtC_6H_2, and traces of 2,6-di-*tert*-butyl-4-ethylidenecyclohexa-2,5-dienone[119] (**3c**). Extraction, filtration and recrystallization were carried out in *n*-pentane as described for **2b**. After 3 recrystallizations, the resulting crystalline product was dried under vacuum. X-ray quality crystals were obtained from a concentrated solution of **2c** in toluene:acetonitrile in a 3:1 ratio. Yield 0.1217 g (40%). ^{1}H NMR ($CDCl_3$): δ 7.10 (s, 4H, aromatic *H*), 2.60 (q, 4H, *J* = 7.5 Hz, C*H*$_2$CH$_3$), 1.47 (s, 36H, C(C*H*$_3$)$_3$), 1.22 (t, 6H, *J* = 7.5 Hz, CH$_2$C*H*$_3$). ^{13}C{^{1}H} NMR ($CDCl_3$): δ 162.4 (*ipso C*), 139.4 (*para C*), 139.3 (*ortho C*), 125.0 (*meta C*), 35.3 (*C*(CH$_3$)$_3$), 31.6 (C(*C*H$_3$)$_3$), 28.8 (*C*H$_2$CH$_3$), 15.6 (CH$_2$*C*H$_3$). m.p. 168-169 °C. IR (cm^{-1}, KBr): 1760w, 1600m, 1458s, 1411vs, 1394s, 1363s, 1327w, 1265m, 1202vs, 1184vs, 111vs, 1065w, 960vs (Mo=O), 937vs (Mo=O), 926s, 877s, 761m, 643w, 583w. UV-vis (C_6H_6) λ_{max}/nm (ε/dm^{3}mol^{-1}cm^{-1}): 362 (28530). HRMS (FAB) Calc. 1st isotopic mass 590.2777 (M^+). Found 590.2786 (M^+). Calc 2nd isotopic mass 591.2811 (M^+). Found 591.2795 (M^+).

MoO_2(O-2,6-^{t}Bu$_2$-4-[OC(O)Me]C_6H_2)$_2$ (2.2d): was prepared like **2a**, but using LiO-2,6-^{t}Bu$_2$-4-[OC(O)Me]C_6H_2 (0.2718 g, 1.006 mmol) and MoO_2Cl_2 (0.1000 g, 0.5029 mmol). Addition

was performed dropwise at -78 °C. The reaction mixture was allowed to warm to room temperature and stirred for 12 h. The ^{1}H NMR spectrum of the crude reaction mixture (after the first filtration) showed three major components (along with some other unknown side products); MoO_2(O-2,6-^{t}Bu$_2$-4-[OC(O)Me]C_6H_2)$_2$ (**2d**), HO-2,6-^{t}Bu$_2$-4-[OC(O)Me]C_6H_2, and 2,6-di-*tert*-butyl-1,4-benzoquinone (**3d**). Isolation of **2d** was attempted via recrystallization from the concentrated mother liquor at -35 °C, but decomposition into phenol and benzoquinone was observed. ^{1}H NMR (C_6D_6): δ 7.25 (s, 4H, aromatic *H*), 1.44 (s, 6H, OC(O)C*H*$_3$), 1.34 (s, 36H,C(C*H*$_3$)$_3$).

MoO_2(O-2,6-^{t}Bu$_2$-4-(OMe)C_6H_2)$_2$ (2.2e): was prepared like **2a**, but using LiO-2,6-^{t}Bu$_2$-4-(OCH_3)C_6H_2 (0.2435 g, 1.005 mmol) and MoO_2Cl_2 (0.1000 g, 0.5029 mmol). Addition was performed dropwise at -78 °C. The reaction mixture was allowed to warm to room temperature and stirred for 12 h. The ^{1}H NMR spectrum of the crude reaction mixture (after the first filtration) showed three major components; MoO_2(O-2,6-^{t}Bu$_2$-4-(OMe)C_6H_2)$_2$ (**2e**), HO-2,6-^{t}Bu$_2$-4-(OMe)C_6H_2 and benzoquinone **3d**. Extraction and filtration were carried out with *n*-pentane as described for **2b**. Volatiles were evaporated under reduced pressure, 5 mL DME were added, and the resulting red solution was stored at -35 °C. After 1 day blocky orange crystals were observed, the supernatant was decanted and the crystals were recrystallized from Et_2O two more times. X-ray quality crystals were selected from the last recrystallization; the remaining crystals were dried under vacuum. Yield 0.123 g (41%). ^{1}H NMR ($CDCl_3$): δ 6.81 (s, 4H, aromatic *H*), 3.79 (s, 6H, OC*H*$_3$), 1.47 (s, 36H,C(C*H*$_3$)$_3$). ^{13}C{^{1}H} NMR ($CDCl_3$): δ 158.9 (*ipso C*), 154.8 (*para* C), 141.0 (*ortho C*), 110.6 (*meta C*), 55.3 (O*C*H$_3$), 35.5 (*C*(CH$_3$)$_3$), 31.4 (C(*C*H$_3$)$_3$). m.p. 156-158 °C. IR (cm^{-1}, KBr): 2961s, 1594vs 1469w, 1445w, 1431w, 1407vs, 1300s, 1257s, 1185vs,1107s, 1058vs, 961s (Mo=O), 936vs (Mo=O), 887vs, 753w. UV-vis (C_6H_6) λ_{max}/nm (ε/dm^{3}mol^{-1}cm^{-1}): 278 (8975), 383 (10391). HRMS (FAB) Calc. 1st isotopic mass 594.2362 (M^+). Found 594.2344 (M^+). Calc 2nd isotopic mass 595.2397 (M^+). Found 595.2405 (M^+).

MoO_2(O-2,6-^{t}Bu$_2$-4-BrC_6H_2)$_2$ (2.2f): was prepared like **2a**, but using LiO-2,6-^{t}Bu$_2$-4-BrC_6H_2 (0.2928 g, 1.006 mmol) and MoO_2Cl_2 (0.1000 g, 0.5029 mmol). Addition was performed

dropwise at -78 °C. The reaction mixture was allowed to warm to room temperature and stirred for 12 h. The ^{1}H NMR spectrum of the crude reaction mixture (after the first filtration) showed three major components; MoO_2(O-2,6-^{t}Bu$_2$-4-BrC_6H_2)$_2$ (**2f**), HO-2,6-^{t}Bu$_2$-4-BrC_6H_2, and diphenoquinone **3a**. Isolation of **2f** was attempted via recrystallization from the concentrated mother liquor at -35 °C, but decomposition into phenol and diphenoquinone was observed (scaled up reactions, shorter reaction times, reaction in the dark, different $MoO_2Cl_2L_2$ adducts and other solvents such as CH_3CN, THF, DMF, Et_2O, benzene and *n*-pentane were used as reaction solvents/recrystallization systems, with no success). ^{1}H NMR ($CDCl_3$): δ 7.47 (s, 4H, aromatic *H*), 1.31 (s, 36H,C(C*H*$_3$)$_3$).

MoO_2(O-2,6-^{t}Bu$_2$-4-(NO_2)C_6H_2)$_2$ (2.2h): was attempted like **2a**, but using LiO-2,6-^{t}Bu$_2$-4-(NO_2)C_6H_2 (0.2587 g, 1.006 mmol) and MoO_2Cl_2 (0.1000 g, 0.5029 mmol). Addition was performed dropwise at -78 °C. The reaction mixture was allowed to warm to room temperature and stirred for 12 h. The ^{1}H NMR spectrum of the crude reaction mixture (after the first filtration) showed HO-2,6-^{t}Bu$_2$-4-(NO_2)C_6H_2, and traces of diphenoquinone **3a**; **2h** was not observed. Presence of **3a** increased when DME was used as recrystallization solvent. Different reaction conditions were tried: scaled up reactions, shorter reaction times, reaction in the dark and other solvents such as CH_3CN, THF, DMF, Et_2O, benzene and *n*-pentane with no success.

Li{MoO_2Cl[2,2'-CH_2(O-6-^{t}Bu-4-MeC_6H_2)$_2$]}·3DME (2.4): was prepared like **2a**, but using 2,2'-CH_2(LiO-6-^{t}Bu-4-MeC_6H_2)$_2$ (0.050 g, 0.142 mmol) and MoO_2Cl_2 (0.028 g, 0.140 mmol) with stirring for 48 h. The ^{1}H NMR spectrum of the crude reaction mixture (after the first filtration) revealed two major components; Li{MoO_2Cl[2,2'-CH_2(O-6-^{t}Bu-4-MeC_6H_2)$_2$]}·3DME (**4**) and 2,2'-CH_2(6-^{t}Bu-4-MeC_6H_2OH)$_2$. The solvent was concentrated to 7 mL in vacuo and the solution was stored at -35 °C for 2 days to yield a dark red crystalline product. The product was recrystallized from DME two times more. Yield 0.041 g (37%). ^{1}H NMR (CD_3CN): δ 6.95 (s, 1H, aromatic *H*), 6.83 (s, 1H, aromatic *H*), 6.81 (s, 1H, aromatic *H*), 6.75 (s, 1H, aromatic *H*), 4.72 (d, 1H, *J* = 14.7 Hz, methylene C*H*$_2$), 3.53 (d, 1H, *J* = 14.7 Hz , methylene C*H*$_2$), 3.44 (s, 12H, C*H*$_2$ of

DME), 3.28 (s, 18H, C*H*$_3$ of DME), 2.22 (s, 3H, C*H*$_3$), 2.15 (s, 3H, C*H*$_3$), 1.47 (s, 9H, C(C*H*$_3$)$_3$), 1.18 (s, 9H, C(C*H*$_3$)$_3$). ^{13}C{^{1}H} NMR (C_6D_6): δ 164.3 (*ipso C*), 162.5 (*ipso C*),137.9 (*ortho C*-^{t}Bu), 136.7 (*ortho C*-^{t}Bu), 131.9 (*para C*), 130.4 (*para C*), 129.9 (*ortho C*-CH_2), 129.3 (*ortho C*-CH_2), 128.8 (*meta C* next to methylene), 128.5 (*meta C* next to methylene), 125.5 (*meta C* next to C$(CH_3)_3$), 125.4 (*meta C* next to C$(CH_3)_3$), 72.2 (*C*H_2 of DME), 58.8 (*C*H_3 of DME), 36.0 (*C*H_2 of bridge), 35.4 (*C*$(CH_3)_3$), 35.0 (*C*$(CH_3)_3$), 30.3 (C(*C*$H_3)_3$), 30.2 (C(*C*$H_3)_3$), 20.8 (*C*H_3). IR (cm^{-1}, KBr): 3436vs, 2953vs, 2919sh, 2875sh, 2358w, 2329w, 1633w, 1444m, 1362w, 1233m, 1083m, 941w, 901w (Mo=O), 865m (Mo=O), 574 m. λ_{max}/nm (ε/dm^{3}mol^{-1}cm^{-1}): 278 (28301) 522 (30464), 627 (14067).

MoO_2(O-2,6-^{t}$Bu_2C_6H_3)_2$(DMF) (2.5a): A solution of LiO-2,6-^{t}$Bu_2C_6H_3$ (0.1841, 0.8673 mmol) in 10 mL of Et_2O was added dropwise to a stirring suspension of $MoO_2Cl_2(DMF)_2$ (0.3000 g, 0.8695 mmol) in 10 mL of Et_2O at room temperature. After 24 h stirring was stopped and the reaction was filtered through a medium pore frit to separate the insoluble and unreacted $MoO_2Cl_2(DMF)_2$ from the reaction products. Volatiles were evaporated from the filtrate and hexanes (10 mL) were added and the mixture was kept in an oil bath at 45 °C for 5 minutes. A hot filtration through a medium pore frit was performed and the orange solution was concentrated to *ca*. 3 mL under vacuum. The solution was kept at -35 °C for 1 day, and orange blocky crystals were observed. The supernatant was decanted and the crystals were dried under vacuum. Yield 0.1223 g (23%). ^{1}H NMR ($CDCl_3$): δ 8.00 (s, 1H, aldehyde *H* of DMF), 7.29 (d, 4H, *J* = 7.8 Hz, aromatic *H*), 6.98 (t, 2H, *J* = 7.8 Hz, aromatic *H*), 2.94 (s, 3H, C*H*$_3$ of DMF), 2.86 (s, 3H, C*H*$_3$ of DMF), 1.47 (s, 36H, C(C*H*$_3$)$_3$). ^{13}C{^{1}H} ($CDCl_3$): δ 163.9 (*ipso C*), 162.7 (*C*=O of DMF), 139.7 (*ortho* C), 125.7 (*meta C*), 124.0 (*para C*), 36.6 (*C*$(CH_3)_3$), 35.3 (*C*H_3 of DMF), 31.6 (*C*H_3 of DMF), 30.26 (C(*C*$H_3)_3$). m.p. 112-114 °C. IR (cm^{-1}, KBr) 3606m, 3078w, 3021m, 2957vs, 2870s (C-H of CHO), 1935w, 1645vs (C=O), 1580w, 1481m, 1424m, 1401vs (C-N), 1389s, 1362s, 1355s, 1262m, 1218vs, 1197s, 961w, 942vs, 914vs (Mo=O), 877vs (Mo=O), 824m, 802m, 760m, 751m, 695m, 674m, 566w, 456m. λ_{max}/nm (ε/dm^{3}mol^{-1}cm^{-1}): 347 (8426).

MoO_2(O-2,6-^{t}Bu_2-4-EtC_6H_2)$_2$(DMF) (2.5c): was prepared in a similar fashion to **5a** but using LiO-2,6-^{t}Bu_2-4-EtC_6H_2 (0.2089 g, 0.8693 mmol) and $MoO_2Cl_2(DMF)_2$ (0.3000 g, 0.8695 mmol). The resulting ethereal reaction mixture was filtered and volatiles evaporated, leaving behind a dark solid. Hexanes (15 mL) were added to this solid, the solution was heated in an oil bath at 45 °C for 5 min, then the hot orange solution was filtered through a medium pore frit. The resulting orange solution was stored at -35 °C. After 1 day orange crystals were collected and recrystallized in hexane (the solution was heated to 45 °C and stored at -35 °C). Note: If heating is performed either for too long, at a higher temperature, or multiple times at 45 °C, loss of DMF is observed yielding product **2c**. Yield 0.1919 g (33%). ^{1}H NMR ($CDCl_3$): δ 8.00 (s, 1H, aldehyde *H* of DMF), 7.10 (s, 4H, aromatic *H*), 2.94 (s, 3H, C*H*$_3$ of DMF), 2.87 (s, 3H, C*H*$_3$ of DMF), 2.59 (q, 4H, *J* = 7.5 Hz, C*H*$_2$CH$_3$), 1.47 (s, 36H, C(C*H*$_3$)$_3$), 1.21 (t, 6H, *J* = 7.5 *Hz*, CH_2C*H*$_3$). ^{13}C{^{1}H} ($CDCl_3$): δ 162.6 (*C*=O of DMF), 162.4 (*ipso C*), 139.4 (*para C*), 139.3 (*ortho C*), 125.0 (*meta* C), 36.5 (*C*H$_3$ of DMF) 35.2 (*C*(CH$_3$)$_3$), 31.6 (C(*C*H$_3$)$_3$), 30.3 (*C*H$_3$ of DMF), 28.8 (*C*H$_2$CH$_3$), 15.6 (CH_2*C*H$_3$). m.p. 112-114 °C. IR (cm^{-1}, KBr): 3064w, 3009w, 2957s, 2868m, 2360m, 2342m, 1649vs (C=O), 1597w, 1432m, 1413s, 1391m, 1364s, 1257m, 1223vs, 1117m, 1060w, 958w, 937s (Mo=O), 907vs (Mo=O), 873m, 843s, 802m, 772m, 697m, 638w, 565m. λ_{max}/nm (ε/dm^{3}mol^{-1}cm^{-1}): 278 (19029), 362 (28342). HRMS (FAB) Calc. 1st isotopic mass 590.2777 (M-DMF+·). Found 590.2784 (M-DMF+·). Calc 2nd isotopic mass 591.2811 (M-DMF+·). Found 591.2805 (M-DMF+·).

MoO_2(O-2,6-^{i}$Pr_2C_6H_3$)$_2$(DMF) (2.5k): was prepared similarly to **5a** but using LiO-2,6-^{i}$Pr_2C_6H_3$ (0.1602 g, 0.8697 mmol) and $MoO_2Cl_2(DMF)_2$ (0.3000 g, 0.8695 mmol). The resulting ethereal reaction mixture was filtered and concentrated under vacuum to ca. 15 mL and stored at -35 °C. After 3 days dark blue crystals were observed (small amount, sideproduct). The X-ray structure of these crystals showed a complex with a MoO^{4+} core (see chapter 3). The supernatant was withdrawn, deposited in a vial and stored at -35 °C. After 2 weeks a greenish precipitate was observed. The supernatant was removed and the solid dried under vacuum. The

solid was identified as MoO_2(O-2,6-^{i}Pr$_2$C$_6$H$_3$)$_2$(DMF) by ^{1}H NMR. Yield 0.198 g (36%). ^{1}H NMR ($CDCl_3$): δ 7.86 (s, 1H, aldehyde *H* of DMF), 7.06 (d, 4H, *J* = 6.0 Hz, aromatic *H*), 6.93 (t, 2H, *J* = 6.0 Hz, aromatic *H*), 3.51 (q, 4H, *J* = 6.0 Hz, C*H* of ^{i}Pr), 2.90 (s, 3H, CH_3 of DMF), 2.38 (s, 3H, CH_3 of DMF), 1.25 (d, 24H, *J* = 9.0 Hz, CH_3 of ^{i}Pr). ^{13}C{^{1}H} ($CDCl_3$): δ 165.0 (*C*=O of DMF), 160.2 (*ipso C*), 137.5 (*ortho C*), 123.0 (*meta* C), 122.9 (*para C*), 37.8 (*C*H_3 of DMF), 32.4 (*C*H_3 of DMF) 27.1 (C*H* of ^{i}Pr), 23.4 (CH_3 of ^{i}Pr). m.p. 95-97 °C. IR (cm^{-1}, KBr): 1650vs, 1433s, 1361m, 1327w, 1257m, 1196s, 1120w, 939s (Mo=O), 916s (Mo=O), 891m, 868m, 793w, 757m, 698m. λ_{max}/nm (ε/dm^{3}mol^{-1}cm^{-1}): 278 (19029), 362 (28342).

MoO_2(O-2,6-$Me_2C_6H_3$)$_2$(DMF)$_2$ (2.5l): was prepared following a similar procedure as for **5a** but using LiO-2,6-$Me_2C_6H_3$ (0.1114 g, 0.8696 mmol) and $MoO_2Cl_2(DMF)_2$ (0.3000 g, 0.8695 mmol). After 24 h, the stirring was stopped and the resulting ethereal reaction mixture was filtered. The ^{1}H NMR spectrum of the filtrate revealed two major components; MoO_2(O-2,6-$Me_2C_6H_3$)$_2$(DMF)$_2$ (**5l**) and HO-2,6-$Me_2C_6H_3$. The filtrate was concentrated to about 3 mL and stored at -35 °C. After 2 days a greenish solid precipitated. The blue supernatant was withdrawn and the solid was recrystallized twice more from Et_2O. X-ray quality crystals were recovered from the last crop. The remaining dark greenish crystals were dried under vacuum. Yield 0.095 g (21%). ^{1}H NMR ($CDCl_3$): δ 7.93 (s, 2H, aldehyde *H* of DMF), 6.95 (d, 4H, *J* = 7.2 Hz, aromatic *H*), 6.74 (t, 2H, *J* = 7.2 Hz, aromatic *H*), 2.92 (s, 6H, CH_3 of DMF), 2.68 (s, 6H, CH_3 of DMF), 2.35 (s, 12H, CH_3). ^{13}C{^{1}H} NMR ($CDCl_3$): δ 164.0 (*ipso C*), 162.9 (*C*=*O* of DMF), 128.0 (*meta C*), 127.0 (*ortho C*), 122.0 (*para C*), 37.2 (*C*H_3 of DMF), 32.0 (*C*H_3 of DMF), 17.0 (*C*H_3). m.p. 142-145 °C. IR (cm^{-1}, KBr) 3436w, 2942s (aliphatic C-H, overlapping C-H of CHO), 1653vs (C=O), 1588w, 1477m, 1433m, 1367m (C-N), 1262s, 1208vs, 1108w, 1029m, 1034w, 937s (Mo=O), 903m (Mo=O), 864m, 802m, 768m, 743w, 707w, 681m, 574m, 540m, 432m. λ_{max}/nm (ε/dm^{3}mol^{-1}cm^{-1}): 278 (6355), 326 (4385), 619 (3293).

2.2.3 Spectrophotometric experiments

2.2.3.1 NMR experiments

Stability of complex in solution. MoO_2(O-2,4,6-^{t}Bu$_3$C$_6$H$_3$)$_2$ (**2.2j**) (0.0651 g, 0.1000 mmol) was dissolved in benzene-d_6 to prepare a 5.00 mL, 0.0200 M stock solution (in a 5.00 mL Pyrex® Class A volumetric flask, tolerance ± 0.02). The greenish solution (0.70 mL) was poured into an 8'' NMR tube. The NMR tube was frozen with liquid nitrogen, evacuated, and sealed with a gas torch. A daily ^{1}H NMR spectrum was recorded, while the sample was allowed to settle outside the glove-box for 7 days (^{1}H NMR spectra were recorded with fixed scales, both vertical and horizontal, and integral locations to maximize consistency in results). No changes in the product peak intensities were observed after this time. A small amount of phenol was observed on day 1, but it was then constant during the whole experiment and did not affect the stability of the complex. This same sample was heated at 45, 80 and 175 ^{o}C for 24 h in each case with no visible changes in the ^{1}H NMR spectra .

Side-product formation. A 0.0200 M stock solution of MoO_2(O-2,4,6-^{t}Bu$_3$C$_6$H$_2$)$_2$ (**2.2j**) (0.70 mL, 0.014 mmol) was mixed with LiO-2,4,6-^{t}Bu$_3$C$_6$H$_2$ (0.0038 g, 0.014 mmol) (**2.1j**) and stirred for 1 h. The resulting orange solution was transferred to an NMR tube. The ^{1}H NMR spectra showed peaks for a small amount of unreacted lithium phenoxide, MoO_2(O-2,4,6-^{t}Bu$_3$C$_6$H$_2$)$_2$, and phenol. The intensity of the alkyl peaks for the three species combined, was qualitatively 2 times smaller than the intensity of the alkyl peaks observed in the control experiment with the same amount and concentration of MoO_2(O-2,4,6-^{t}Bu$_3$C$_6$H$_2$)$_2$. The residual benzene peak was used as internal reference.

Cation dependence for side-product formation. (Bu_4N)(O-2,6-^{t}Bu$_2$C$_6$H$_3$) (0.0088 g, 0.020 mmol) (**1m**) was dissolved in 0.50 mL of CD_3CN and added to a stirring solution of MoO_2Cl_2 (0.0020 g, 0.010 mmol) in 0.50 mL of CD_3CN. After 12 h, stirring was stopped, and the resulting red solution was inspected by ^{1}H NMR. The spectrum showed the expected formation of phenol and diphenoquinone as side-products, along with unidentified peaks.

Correlation between weighed complex and its ^{1}H NMR signal. A 10.00 mL solution of 0.4000 M of 1,3,5-triisopropylbenzene (0.8713 g, 4.000 mmol), as internal standard, was prepared in C_6D_6 (in a 10.00 mL Pyrex® Class A volumetric flask, tolerance ± 0.02). A 1.00 mL aliquot of the 0.4000 M solution was diluted to 10.00 mL in C_6D_6 to afford 10.00 mL of 0.04000 M solution. MoO_2(O-2,4,6-^{t}Bu$_3$C$_6$H$_2$)$_2$ (**2.2j**), (0.0096 g) was added to 0.7 mL of 0.04000 M 1,3,5-triisopropylbenzene solution in an NMR tube and a ^{1}H NMR was taken. The amount of **2.2j** was calculated based on the ratio between the peaks of the internal standard and those of **2.2j** and phenol present in the sample. Calculated weight: 0.0094 g; actual weight: 0.0096 g.

Solvent effects. LiO-2,6-^{t}Bu$_2$-4-RC$_6$H$_2$ (R= H, **2.1a**; OMe, **2.1e**; NO_2, **2.1h**; 1.000 mmol) was stirred in 10 mL of CS_2. After 12 h, stirring was stopped and volatiles were removed under vacuum. A sample was taken for ^{1}H NMR analysis. The ^{1}H NMR spectrum showed just LiO-2,6-^{t}Bu$_2$-4-RC$_6$H$_2$; no HO-2,6-^{t}Bu$_2$-4-RC$_6$H$_2$ was observed.

MoO_2Cl_2 (0.1000 g, 0.5029 mmol) and LiO-2,6-^{t}Bu$_2$-4-RC$_6$H$_2$ (R= H, **2.1a**; OMe, **2.1d**; NO_2, **2.1f**; 1.006 mmol) were each dissolved in CS_2 (10 mL). Each LiOAr solution was added to a MoO_2Cl_2 solution while stirring. After 12 h, stirring was stopped, and aliquots were taken and dried for ^{1}H NMR.

^{1}H NMR (C_6D_6, R = H): Three products were present; MoO_2(O-2,6-^{t}Bu$_2$C$_6$H$_3$)$_2$ (**2.2a**), HO-2,6-^{t}Bu$_2$C$_6$H$_3$, and diphenoquinone (**2.3a**), in an approximate 1:4:3 ratio. The approximate ratio for this same reaction in DME was 2:1:2.

^{1}H NMR (C_6D_6, R = OMe): Three products were present; MoO_2(O-2,6-^{t}Bu$_2$-4-(OMe)C$_6$H$_2$)$_2$ (**2.2e**), HO-2,6-^{t}Bu$_2$-4-(OMe)C$_6$H$_2$, and benzoquinone (**2.3b**) in an approximate 1.0:1.5:0.2 ratio. The ratio for this same reaction in DME was 1.0:1.5:0.8.

^{1}H NMR (C_6D_6, R = NO_2): Two products were present; HO-2,6-^{t}Bu$_2$-4-(NO_2)C$_6$H$_2$ and diphenoquinone (**2.3a**). The ratio was ca. 9:1, whereas diphenoquinone (**2.3a**) is almost absent when DME is used as solvent.

2.2.3.2 Detection of paramagnetic species

LiO-2,6-^{t}Bu$_2$-4-RC$_6$H$_2$ (R= ^{t}Bu, **2.1l**; OMe, **2.1e**; NO$_2$, **2.1h**; 0.2500 mmol) was transferred into a quartz EPR tube and room temperature acquisitions were performed in the solid state. The three samples showed minimal to negligible paramagnetic activity.

EPR (R= ^{t}Bu, solid) g = 2.0040; intensity: ±18.1 x 10^3.

EPR (R= OMe, solid) g = 2.0046; intensity: ±91.7 x 10^3.

EPR (R = NO$_2$, solid) g = 2.0050; intensities: +36.6 x 10^3, -41.0 x 10^3.

MoO_2Cl_2 (0.1000 g, 0.5028 mmol) (three samples) and LiO-2,6-^{t}Bu$_2$-4-RC$_6$H$_2$ (R= ^{t}Bu, **2.1l**; OMe, **2.1e**; NO$_2$, **2.1h**; 1.006 mmol) were each dissolved in 10.0 mL benzene. Each LiOAr solution was added to one MoO_2Cl_2 solution while stirring. After 1 min stirring was stopped, a 1.00 mL aliquot was taken from the reaction mixture, and it was transferred to an EPR tube for analysis (at room temperature).

EPR (R= ^{t}Bu, C_6H_6) g = 2.0048, intensities: +12.7 x 10^6, -12.6 x 10^6.

EPR (R= OMe, C_6H_6) g = 2.0050; intensity: ±1.74 x 10^6.

EPR (R= NO$_2$, C_6H_6) shows coupling to one N atom, and three ^{t}Bu protons with g = 2.0039, a_N= 7.57, and a_H = 2.78; intensities +2.86 x 10^6, -2.14 x 10^6.

Solid ·O-2,4,6-^{t}Bu$_3$C$_6$H$_2$ (0.0313 g, 0.1197 mmol) and MoO_2(O-2,4,6-^{t}Bu$_3$C$_6$H$_2$)$_2$ **2.2j** (0.0780 g, 0.1198 mmol) were placed into EPR tubes, and room temperature ESR experiments were recorded.

EPR (·O-2,4,6-^{t}Bu$_3$C$_6$H$_2$), g = 2.0043; intensity ±5.0 x 10^6.

EPR (MoO_2(O-2,4,6-^{t}Bu$_3$C$_6$H$_2$)$_2$), g = 2.0050; intensities +800.00 x 10^3, -968 x 10^3.

Benzene (0.50 mL) was added to the EPR tubes containing the phenoxy radical and **2.2j**; a second ESR spectrum was recorded.

EPR (·O-2,4,6-^{t}Bu$_3$C$_6$H$_2$) g = 2.0050.[120]

EPR (MoO_2(O-2,4,6-^{t}Bu$_3$C$_6$H$_2$)$_2$) g = 2.0054; intensities + 3.84 x 10^6, -3.25 x 10^6.

All EPR spectra are shown in the appendix of this chapter.

2.2.3.3. UV-vis reaction

Stock 10.00 mL solutions of 0.010 M MoO_2Cl_2 (0.020 g, 0.10 mmol) and LiO-2,4,6-$^tBu_3C_6H_2$ (0.027 g, 0.10 mmol) in benzene were prepared. The appropriate amount of 0.010 M solution was measured and diluted to 10.00 mL to prepare a 1.5 x 10^{-4} M solution of MoO_2Cl_2 and a 3.0 x 10^{-4} M LiO-2,4,6-$^tBu_3C_6H_2$ solution. LiO-2,4,6-$^tBu_3C_6H_2$ solution (5.00 mL of 3.0 x 10^{-4} M, 1.5 x 10^{-3} mmol) was added via syringe to a stirring solution of MoO_2Cl_2 (5.00 mL of 1.5 x 10^{-4} M, 7.5 x 10^{-4} mmol) in a 10 mL UV-vis cell equipped with a septum. When the addition was completed, a UV-vis run was set up for 43 200 s spectra with 300 s lapses. Absorbance at specific wavelengths was recorded: 401 nm for ·O-2,4,6-$^tBu_3$-C_6H_2 (weak) and 357 nm for MoO_2(O-2,4,6-$^tBu_3C_6H_2)_2$) (**2.2j**) (strong). Both wavelengths showed a sudden increase in their absorbance after addition of reagents was completed (within the first 300 s). As the run proceeded, both wavelengths displayed a steady decrease in their absorbance values (*ca*. an overall 10% of the original value). The formation of **2.2j** and ·O-2,4,6-$^tBu_3C_6H_2$ took place at about the same time.

UV-vis spectra are available in the appendix of this chapter.

2.2.4 Concentration effects

MoO_2(O-2,4,6-^{t}Bu$_3$C$_6$H$_2$)$_2$ (**2.2j**)[69] was prepared like **2a**, but using LiO-2,4,6-$^tBu_3C_6H_2$ (0.2698 g, 1.006 mmol) dissolved in 5 mL (case A) and 10 mL (case B) of DME, and MoO_2Cl_2 (0.1000 g, 0.5029 mmol) dissolved in 5 and 10 mL of DME. The 5 and 10 mL lithium salt solutions were added dropwise to the 5 and 10 mL blue MoO_2Cl_2 solutions respectively, with rapid stirring at room temperature. After 12 h, the reaction mixtures were filtered through a medium pore sintered glass frit and 0.50 mL aliquots were taken from each batch for ^{1}H NMR analysis. ^{1}H NMR spectra of case A and B showed approximately the same HOAr:$MoO_2(OAr)_2$ ratio (1.0:5.6). The volatiles were removed under vacuum. ^{n}Pentane (15 mL) was added to the dry dark masses and the mixtures were stirred for 6 h. The resulting mixtures were filtered,

concentrated under vacuum to *ca*. 5 mL each and stored at -35 ^{o}C for 2 days affording dark green crystalline solid. The supernatant was withdrawn and recrystallization in pentane was performed twice more for both batches. The crystals were dried under vacuum. Yield case A: 0.1418 g (43%). Yield case B: 0.1430 g (43%).

2.2.5 Reactions with molybdenum adducts

2.2.5.1 $MoO_2Cl_2L_2$ adducts as alternatives to MoO_2Cl_2.

$MoO_2Cl_2L_2$ where L = CH_3CN, THF, DMF, DMSO, $OPPh_3$, bipy, or tmen, $MoO_2Br_2(DMF)_2$ (0.503 mmol), and LiO-2,6-$^{t}Bu_2$-4-RC_6H_2 (R= H, **2.1a**; OMe, **2.1d**; NO_2, **2.1f**; 0.500 mmol) were each dissolved in 10 mL of Et_2O. Each LiOAr solution was added to a $MoO_2Cl_2L_2$ solution while stirring. After 12 h stirring was stopped, and an aliquot was taken and dried for ^{1}H NMR. The observed products were:

^{1}H NMR (C_6D_6, R = H): 2,6-di-*tert*-butylphenol, $MoO_2(OAr)_2$ **2.2a**, diphenoquinone **2.3a**, and free σ donor ligand (except when L = DMF and halogen = Cl, then **2.5a** is observed).

^{1}H NMR (C_6D_6, R = OMe): $MoO_2(OAr)_2$ **2.2e**, benzoquinone **2.3b** and free σ donor ligand.

^{1}H NMR (C_6D_6, R = NO_2): 2,6-di-*tert*-butyl-4-nitrophenol, diphenoquinone **3a** and free σ donor ligand.

It was observed that **2.2a** and **2.2e** (almost pure) are favored (over phenol and **2.3a** or **2.3b**) when L is DMF; in contrast **2.2a** and **2.2e** are less favored when L = DMSO, $OPPh_3$ CH_3CN, THF or the adduct $MoO_2Br_2(DMF)_2$ is used.

$MoO_2Cl_2(DMF)_2$ as best alternative; solvent and stoichiometric effects.

$MoO_2Cl_2(DMF)_2$ (0.173 g, 0.503 mmol) and LiO-2,6-$^{t}Bu_2$-4-RC_6H_2 (0.212 g, **1a**; 0.242 g, **1d**; 0.257 g, **1f**; 1.00 mmol) were each dissolved in 10 mL of Et_2O. Each LiOAr solution was added to a $MoO_2Cl_2(DMF)_2$ solution while stirring. After 12 h stirring was stopped, and an aliquot was taken and dried for ^{1}H NMR. The reaction products were:

^{1}H NMR (C_6D_6, R = H): 2,6-di-*tert*-butylphenol, $MoO_2(OAr)_2DMF$ **2.5a**, diphenoquinone **2.3a**.

^{1}H NMR (C_6D_6, R = OMe): 2,6-di-*tert*-butyl-4-methoxyphenol, $MoO_2(OAr)_2$ **2.2e**, benzoquinone **2.3b**.

^{1}H NMR (C_6D_6, R = NO_2): 2,6-di-*tert*-butyl-4-nitrophenol, diphenoquinone **2.3a**.

It was observed that **2.2a** and **2.2e** were major products, and almost no phenol or benzoquinone were seen when R = OMe.

$MoO_2Cl_2(DMF)_2$ (0.173 g, 0.503 mmol) and LiO-2,6-^{t}Bu$_2$-4-RC_6H_2 (0.106 g, **2.1a**; 0.121 g, **2.1d**; 0.138 g, **2.1f**; 0.500 mmol) were each dissolved in 10 mL of DME. Each LiOAr solution was added to a $MoO_2Cl_2(DMF)_2$ solution while stirring. After 12 h stirring was stopped, and an aliquot was taken and dried for ^{1}H NMR. The reaction products were:

^{1}H NMR (C_6D_6, R = H): 2,6-di-*tert*-butylphenol, $MoO_2(OAr)_2$ **2.2a** and diphenoquinone **2.3a**.

^{1}H NMR (C_6D_6, R = OMe): 2,6-di-*tert*-butyl-4-methoxyphenol, $MoO_2(OAr)_2$ **2.2e** and benzoquinone **3b**.

^{1}H NMR (C_6D_6, R = NO_2): 2,6-di-*tert*-butyl-4-nitrophenol and diphenoquinone **2.3a**.

The molybdenum product **2.2a** was present but not as main product. When R = OMe, little formation of **2.2e** was observed; 2,6-di-*tert*-butyl-4-methoxyphenol and benzoquinone **2.3b** dominated.

For the reaction between $MoO_2Cl_2(DMF)_2$ (0.173 g, 0.503 mmol) and LiO-2,6-^{t}Bu$_2$-4-RC_6H_2 (0.212 g, **2.1a**; 0.242 g, **2.1d**; 0.257 g, **2.1f**; 1.00 mmol) in DME, we observed similar results to the 1:1 reaction in the same solvent (above). **2a** and **2e** were favored compared to their respective side products.

2.2.6 Oxygen transfer catalysis

A 25.0 mL solution of 0.076 M of triphenylphosphine (0.500 g, 1.90 mmol) was prepared in DMSO. Solid **2.2e**, **2.2j**, **2.4** (0.015 mmol) and nothing, respectively, were added to 5 mL aliquots of the PPh_3 solution while stirring. The samples were heated at 120 ^{o}C for 2 h. A ^{31}P NMR spectrum of each aliquot was taken. One hundred percent conversion of PPh_3 into

$O{=}PPh_3$ was observed when **2.2e** and **2.2j** were used as catalysts; an 81% conversion was observed with **2.4**, and 0% when catalyst was not added.

2.3 Results and discussion

Compounds **2** through **5** were made by simple substitution reactions; the challenge lay in the isolation and characterization of the monomeric species. The difficulty of preparing tractable compounds of this class has been noted in the literature.[121-123]

In order to have a better understanding of molybdenum(VI) dioxo diaryloxides (as prospective building blocks for homo- and heterometallic catalysts or catalysis models), two variables were investigated: electronics and sterics. First, sterics were kept constant (by using 2,6-^{t}Bu$_2$-substituted ligands) and the electronic effect tuned by variation of the *para* substituent R (going from electron-donating (OMe) through electron-withdrawing groups (NO_2)). The electronic effect was then held constant and less bulky ligands were reacted with molybdenum(VI) dioxo dichloride.

The bonding between Mo and ligand atoms can be described as a dπ-pπ interaction.[124] $MoO_2(OAr)_2$ is formally d^0, so π-donor ligands such as ArO^- and O^{2-} with electrons in π symmetry orbitals can interact with the appropriate empty dπ orbitals of the metal atom.

2.3.1 Four coordinate molybdenum(VI) dioxo diaryloxides

MoO_2Cl_2 reacts with 2 equiv of LiO-2,6-^{t}Bu$_2$-4-RC$_6$H$_2$ (R = H (**2.1a**), Me (**2.1b**), Et (**2.1c**), or OMe (**2.1e**)) in DME (Scheme 2.1) to form the isolable compounds **2.2a**, **2.2b**, **2.2c** and **2.2e,** respectively. When R = OC(O)Me (**2.1d**) or Br (**2.1f**) the corresponding molybdenum complex (**2.2d** or **2.2f**) was observed by ^{1}H NMR, but decomposed into phenol and **2.3d** or **2.3a** during isolation. In the case of R = NO_2 (**2.1h**) only phenol and **2.3a** were visible by ^{1}H NMR. Side-product **2.3a** was observed when R = H, Br or NO_2; **2.3d** was seen when R = OC(O)Me and OMe. We obtained our best isolated yields when using electron-donating substituents.

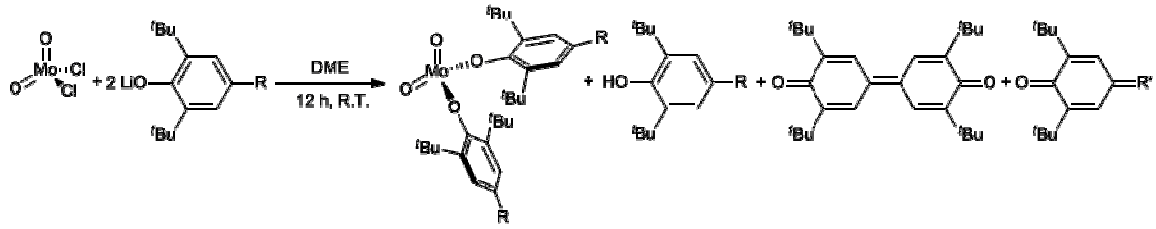

2.1a-f **2.2a-f** **2.3a** **2.3b-d**

Label	R	Products		
		2 (yield)	phenol	quinone
a	H	31%	yes	**2.3a**
b	Me	35%	yes	**2.3b**; R'=CH_2
c	Et	40%	yes	**2.3c**; R' = $CHCH_3$
d	OC(O)Me	NMR only	yes	**2.3d**; R' = O
e	OMe	41%	yes	**2.3d**; R' = O
f	Br	NMR only	yes	**2.3a**
h	NO_2	not observed	yes	**2.3a**

Scheme 2.1 Reaction of MoO_2Cl_2 with various LiO-2,6-^{t}Bu$_2$-4-RC_6H_2 (R = H (**2.1a**), Me (**2.1b**), Et (**2.1c**), or OMe (**2.1e**)) in DME.

All the reactions were fast at room temperature (instant change of color), but they were stirred for 12 h to ensure total consumption of reactants. In all cases DME produced better yields than THF, C_6H_6 or CH_3CN. X-ray quality crystals were obtained for **2c** and **2e** at -35 ^oC. **2b** tends to precipitate (as an amorphous powder) rather than crystallize, and products with electron-withdrawing groups were never isolated.

2.3.2 Spectrophotometry

The IR spectrum of each compound showed two medium to strong intensity peaks in the range of 883 to 939 cm^{-1}, which are assigned to antisymmetric and symmetric O=Mo=O stretching frequencies. These values fall within the range reported by our group for compound **2a**[68] and also by other researchers working on MoO_2^{2+} complexes.[64, 125] The Mo=O frequencies do not show any trend that can be related to the electronic nature of the R groups. The oxo

bond strength/order also appeared similar for **2.2a**, **2.2c** and **2.2e** (based on Mo-O bond lengths), and only small differences in oxygen transfer capabilities were observed.

The ^{1}H and ^{13}C NMR data are consistent with the structures. Due to the presence of a C_2 axis in **2.2a-f**, the two aryloxy ligands are magnetically equivalent and display a single set of signals. All the peak values and assignments are reported in the experimental section.

Electronic spectra of the complexes in benzene display two intense bands, one of them in the 277-280 nm region and the other in the 346-383 nm region. The first band (B band for aromatic systems)[126] corresponds to a $\pi \rightarrow \pi^*$ transition of the benzene chromophore influenced by the unshared electron pair of the auxochromic oxygen (this band is present in the lithium phenoxides as well as in the plain phenols in about the same region), an auxochrome is a saturated group which, when attached to a chromophore, alters both the wavelength and the intensity of the absorption maxima.[126] These complexes are bright yellow-green when dissolved in benzene (they absorb in the high energy purple region and transmit yellow). Their intense color can be attributed to charge transfer transitions where an electron is transferred from orbitals having mostly ligand character to orbitals having mostly metal character. These LMCT bands probably occur because the ligands have lone pairs of relatively high energy and the metal has low-lying empty orbitals.[127] A nonbonding oxygen-localized 2p electron either in the terminal oxo or in the aryloxide is expected to be transferred to the low lying empty d orbital on molybdenum.

2.3.3 Side-reactions and paramagnetism

The overall reaction for product formation is a simple one; substitution of the aryloxide anion for the chloride anion on the molybdenum. This could be viewed as a transmetallation. However, the ubiquitous phenol, the trend favoring better yields when electron donating groups are present on the aryl ligand, and the presence in some cases of diphenoquinone **3a** or quinones **3b-d** were puzzling aspects.

We initially ascribed phenol side-product formation to adventitious water (moisture present in the solvent hydrolyzing the $MoO_2(OAr)_2$ product or the LiOAr). To investigate this possibility, the following experiments were undertaken.

1) Solutions of LiO-2,6-^{t}Bu$_2$-4-RC$_6$H$_2$ (**2.1a**, R = H; **2.1e**, R = OMe; **2.1h**, R = NO_2) were prepared in THF (hydrophilic hydrocarbon), benzene (hydrophobic hydrocarbon) and CS_2 (hydrophobic non-hydrocarbon). The different solutions were stirred for 12 h (standard reaction time and concentration for the procedures described here). The solvent was removed under vacuum and the samples inspected by ^{1}H NMR; no presence of phenol was detected in any case. For comparison, LiO-2,6-^{t}Bu$_2$-4-RC$_6$H$_2$ (**2.1a**, R = H; **2.1e**, R = OMe; **2.1h**, R = NO_2) dissolved in C_6D_6 reacted immediately to form the respective phenol when water was added.
2) MoO_2Cl_2 + 2 LiO-2,4,6-^{t}Bu$_3$C$_6$H$_2$ in the same molar amounts, were reacted in different volumes of DME (10 and 20 mL). The HOAr:$MoO_2(OAr)_2$ ratio determined by ^{1}H NMR was constant, regardless of the amount of solvent used, indicating no direct correlation between any moisture present in the solvent (< 0.003% water)[128, 129, 130] and the amount of phenol observed.
3) Trace water does not explain the presence of the oxidation products **2.3a**-**d**.

Hydrogen abstraction from molecules of solvent by the reactive LiOAr, to produce HOAr, was also considered, but the pK_a values of the hydrocarbon solvents[131, 132] and the aryl alcohols[133] suggest that the equilibrium ArO$^\ominus$ + solvent-H ⇆ solvent$^\ominus$ + ArOH lies to the left.

The experimental evidence rules out hydrolysis by water or hydrogen abstraction from solvent molecules as the main mechanisms for phenol formation.

We then considered the intervention of a radical species. Molybdenum(VI) can readily undergo reduction to Mo(V),[134] and the diphenoquinone observed in several reactions is well known to emerge via a radical pathway.[120] EPR spectroscopy was used to track the formation of radical species.

Three different LiO-2,6-^{t}Bu$_2$-4-RC$_6$H$_2$ (**2.1e**, R = OMe; **2.1j**, R = ^{t}Bu; and **2.1h**, R = NO$_2$) were analyzed by EPR in solid state, showing almost null activity. R = OMe and NO$_2$ were selected for their strong electron donating and electron withdrawing character. R = ^{t}Bu falls in the middle of this electronic scale; in addition, the phenoxy radical ·O-2,4,6-^{t}Bu$_3$C$_6$H$_2$ (a possible side-product) is stable, known, and easy to synthesize,[107] allowing us the possibility to confirm both paramagnetic and diamagnetic species by running different control experiments.

The reaction of MoO$_2$Cl$_2$ + 2 equiv of LiO-2,6-^{t}Bu$_2$-4-RC$_6$H$_2$ (**2.1e**, R = OMe; **2.1j**, R = ^{t}Bu; and **2.1h**, R = NO$_2$) in benzene was monitored by EPR at room temperature. In contrast with the starting materials alone, strong signals were observed in all of the reaction mixtures (with an intensity comparable to pure ·O-2,4,6-^{t}Bu$_3$C$_6$H$_2$). These signals are attributed to phenoxy radicals. EPR spectra showed that the radicals persisted even after a week of storage in the glove box.

The possible presence of paramagnetic impurities in our purified molybdenum complexes could be the origin of the observed EPR activity. An NMR experiment was performed to investigate the extent of these possible impurities. A ^{1}H NMR spectrum of weighed amounts of **2.2j** and 1,3,5-trimethylbenzene internal standard showed that, within the experimental error, the observed amount of **2.2j** is close to a 100% diamagnetic sample (refer to appendix).

One possible radical initiator would be Li^0 impurity present in the ^{n}BuLi used to synthesize the different lithium aryloxides. Alkali metals are prone to electron transfer; in our system the Mo=O group could be the target. Reactivity of the metal oxo moiety has been compared to that of the carbonyl group in organic chemistry[135] and the radical anion formed by addition of an electron to the low lying π^* orbital of Mo=O might thus be generated by O=Mo^{VI}(O)(OAr)$_2$ + 1e$^-$ → $^{\ominus}$·O-Mo^{V}O(OAr)$_2$. We demonstrated that Li^0 was not the radical source, by using the alkali metal free (Bu$_4$N)OAr as starting material (refer to experimental section for details) and reacting it with MoO$_2$Cl$_2$. Both **2.3a** and phenol were still formed.

Homolysis of $MoO_2(OAr)_2$ into paramagnetic $\cdot Mo^{V}O_2OAr$ and $\cdot OAr$ was considered as a possible explanation for the pronounced EPR activity. Mild EPR activity (see appendix) in solid state was recorded for $MoO_2(2,4,6\text{-}^{t}Bu_3C_6H_2)_2$ (**2.2j**) whereas $\cdot O\text{-}2,4,6\text{-}^{t}Bu_3C_6H_2$ showed stronger activity by one order of magnitude (similar in shape but with slightly different g = 2.0043 and 2.0050, respectively). When benzene is added to the tubes containing these solid samples, the signal strength is of the same order of magnitude (with different shape but similar inflexion points g = 2.0054 and 2.0050[120]). These results imply that the phenoxy radical is indeed formed from the metal complex **2.2j**. It is possible that a fast equilibrium $MoO_2(OAr)_2 \leftrightarrows (\cdot Mo^{V}O_2OAr) + (\cdot OAr)$ occurs in solution. The NMR evidence, though, (see above) indicates that the equilibrium must lie to the left.

Is the radical $\cdot OAr$ from the equilibrium reaction $MoO_2(OAr)_2 \leftrightarrows (\cdot Mo^{V}O_2OAr) + (\cdot OAr)$ the source of the HOAr that we observe? $MoO_2(2,4,6\text{-}^{t}Bu_3C_6H_2)_2$ (**2.2j**) was sealed under vacuum in an NMR tube and allowed to stand for 1 week. There was no significant change in peak intensity (compared against an internal standard). Heating up to 175 °C also did not produce any appreciable variation. If $MoO_2(2,4,6\text{-}^{t}Bu_3C_6H_2)_2$ (**2.2j**) undergoes significant decomposition into phenoxy radical and the respective Mo(V) complex, it would produce a paramagnetic species and therefore a decrease in the intensity of the ^1H NMR signals ($\cdot O\text{-}2,4,6\text{-}^{t}Bu_3C_6H_2$ does not show strong peaks by ^1H NMR).[136] Moreover $HO\text{-}2,4,6\text{-}^{t}Bu_3C_6H_2$, which is the direct product of hydrogen abstraction by $\cdot O\text{-}2,4,6\text{-}^{t}Bu_3C_6H_2$, is not observed.

From these results we concluded that:

1) Phenoxy radical is present in reaction mixtures.
2) Some radical could be formed as part of a fast equilibrium $MoO_2(OAr)_2 \leftrightarrows (\cdot Mo^{V}O_2OAr) + (\cdot OAr)$. If this equilibrium occurs, the NMR evidence shows that the left side is strongly favored.
3) The $\cdot O\text{-}2,6\text{-}^{t}Bu_2\text{-}4\text{-}RC_6H_2$ radicals that produce $HO\text{-}2,6\text{-}^{t}Bu_2\text{-}4\text{-}RC_6H_2$ and **3a**-**d** are generated by a pathway different than the simple homolysis of $MoO_2(OAr)_2$.

Significant aryloxy radical formation is indicated, but not directly from **2.2a**-**h**; it must therefore be formed either by outer-sphere electron transfer or by an inner-sphere process via a competing reaction pathway.

We propose the pathway shown in Scheme 2.2, to account for the formation of phenol and diphenoquinone, benzoquinone or quinone alkylidene sideproducts (**2.3a**-**d**). In this pathway $MoO_2(OAr)_2$ reacts with 1 equiv of LiOAr and forms a 5-coordinate unstable intermediate. This intermediate has two options to relieve the crowding: reverse of **a** or the irreversible homolytic rupture of the Mo-OAr bond forming **B** and the aryl radical species. Complexes analogous to **A** such as $LiMoO_2(OR)_3$,[137] polymeric $NaMoO_2(OR)_3$[122] (R = C_2H_4OMe) and $[Li(12\text{-crown-}4)_2][MoO_2\{O\text{-}2\text{-}(allyl)C_6H_4\}_3]$[89] have been reported and characterized as stable complexes. These alkoxides are sterically less crowded and electronically different from aryloxides. The allyl phenoxide, in spite of similarity importantly to **A**, is less bulky than our 2,6-*tert*-butyl phenoxides. We suggest that **A** is less stable, and we have not yet isolated it.

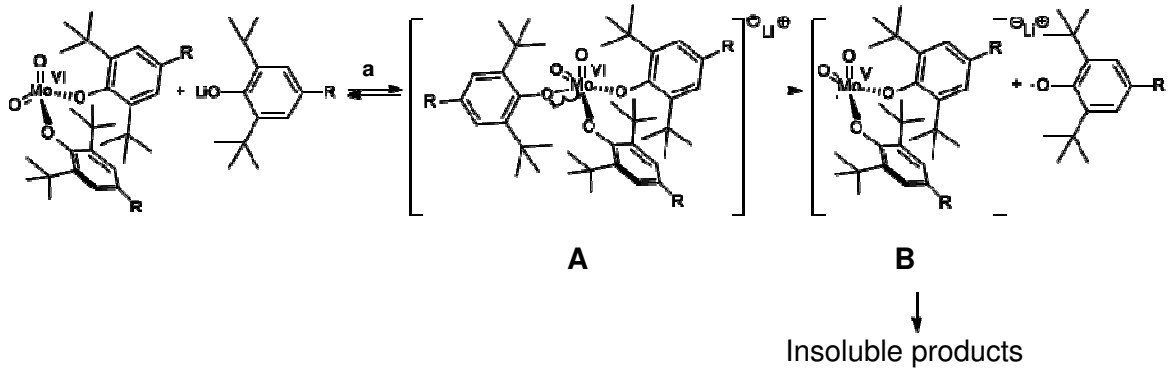

Scheme 2.2 Proposed reaction pathway for formation of the observed phenoxy radicals.

Certain Mo(VI) alkoxides are reported to dissolve better in the presence of LiOR or LiCl.[138] Similar conditions may allow LiOAr and $MoO_2(OAr)_2$ to interact and yield complexes analogous to **A**. This was investigated by ^1H NMR experiments.

Two NMR tubes containing $MoO_2(2,4,6\text{-}^tBu_3C_6H_2)_2$ (**2.2j**) (0.02 M in benzene-d_6, 0.70 mL each) were prepared. One equiv of LiO-2,4,6-$^tBu_3C_6H_2$ (**2.1j**) was added to one while the other

remained as standard. The ^{1}H NMR spectrum of the tube with $MoO_2(OAr)_2$ + LiOAr showed a dramatic decrease in the $MoO_2(OAr)_2$ **2.2j** signals in contrast to the standard. No new peaks were observed. This observation is consistent with the transient formation of **A** and its fast homolysis into the paramagnetic **B**.

Although the proposed intermediate **A** was not isolated, we were able to synthesize an analogue. Complex {MoO_2Cl[2,2'-CH_2(O-6-^{t}Bu-4-$MeC_6H_2)_2$]}Li·3DME (**4**) (Equation 2.1) is analogous to **A**, but stabilized by the chelate effect, and the less sterically crowded environment. Molecule **4** shows that the MoO_2^{2+} coordination sphere can accommodate two $^{\ominus}$O-2,6-^{t}Bu$_2$-4-RC_6H_2 units, and still it is able to accommodate a fifth less sterically bulky group. In contrast, sterics force **A** to reach stability by losing one of the aryloxy ligands.

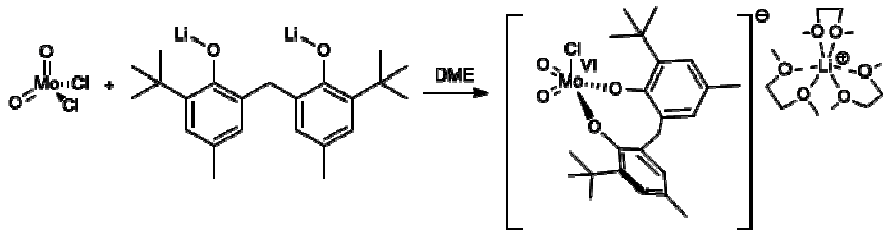

(2.1)

2.4

We propose that two pathways are available to relieve the crowding; 1) reverse of step **a** (Scheme 2), and 2) Mo-O homolysis to form an unstable Mo(V) species **B** and the phenoxy radical. Formation of **A** might be favored by electron-withdrawing groups as they can delocalize the overall negative charge. The consequent formation of free phenoxy radical would be an irreversible process (contrasting with the presumably fast phenoxy radical equilibrium hypothesized for $MoO_2(OAr)_2 \leftrightarrows \cdot Mo^{V}O_2OAr + \cdot OAr$). The phenoxy radical will scavenge for hydrogen from trace moisture, solvent, **B** and/or its decomposition products,[139] to form the observed phenol. The unstable Mo(V) radical is expected to undergo irreversible decomposition to form unsoluble products.

This side-reaction mechanism addresses the electronic effects we have observed. For the case of R = OMe, the electron-donating substituent disfavors the formation of **A**, and we obtain relatively high yield of product **2.2e**. In contrast low yield (R = Br) or no product (R = NO_2)

are observed when R is electron-withdrawing. In this case **A** is favored due to delocalization of electron density, and more side product is formed.

Special attention should be given to compound **2.4**. Analogous alkoxide complexes of this type have been synthesized by more complicated means.[137] Compound **2.4** is formed and crystallized in DME. Its ^{1}H and ^{13}C NMR spectra show nonequivalence between the two phenyl rings that constitute the bisphenoxide; this is due to the lack of symmetry imposed by the ligand distribution around the metallic center (see the crystal structure and three-dimensional geometry section). Three molecules of DME coordinate to the cationic Li. Complex **2.4** is slightly soluble in hydrocarbons (benzene, pentane, hexane). Removal of the supernatant followed by vacuum drying removes the coordinating DME.

The electronic spectrum of **2.4** shows three absorption bands; the B band at 278 nm and two bands at 522 nm and 627 nm. These two bands have ε ($dm^3mol^{-1}cm^{-1}$) > 10^4, and are probably LMCT from the terminal oxo groups or the aryloxide oxygens, and LMCT from the Cl lone pairs to the empty Mo d orbitals. Trigonal bipyramidal complexes are expected to have a smaller d-splitting energy than tetrahedral ones,[140, 141] and therefore absorption is shifted to lower frequencies (green and red) imparting the dark bluish-purple color that is observed in benzene solution. The Mo=O stretching bands fall within the expected range for MoO_2^{2+} complexes.

2.3.4 Catalytic activity

Complexes **2.2c**, **2.2e** and **2.4** were tested as catalysts for oxygen transfer from DMSO to PPh_3. These complexes (4 mol %) display catalytic activity at 120 ^{o}C transforming PPh_3 into $O{=}PPh_3$ within 2 h. A blank study was performed (no catalyst added), and formation of the phosphine oxide was not observed.

2.4 5- and 6-coordinate Mo(VI) dioxo diaryloxides

2.4.1 $MoO_2Cl_2(DMF)_2$ as precursor for molybdenum dioxo aryloxides

A good deal of our research is focused on the synthesis of prospective building blocks for homo- and heterometallic catalyst models. We commonly start from MoO_2Cl_2, which is air and moisture sensitive, but $MoO_2X_2L_2$ adducts attracted our attention. They are air-stable, relatively cheap, and easy to handle; plus could possibly serve as source for new complexes with different degrees of substitution.

Two groups of octahedral adducts $MoO_2X_2L_2$ were investigated (X = halogen, L = neutral ligand): the commonly encountered "*cis*, *trans*, *cis"* arrangement of O, X, L around the Mo atom; and the less common "all *cis*" arrangement of O, X, L. $MoO_2Cl_2(DMF)_2$, $MoO_2Cl_2(CH_3CN)_2$, $MoO_2Cl_2(THF)_2$, $MoO_2Cl_2(DMF)_2$, $MoO_2Cl_2(DMSO)_2$, $MoO_2Br_2(DMF)_2$, $MoO_2Cl_2(OPPh_3)_2$, and MoO_2Cl_2(bipy) belong to the first group, and MoO_2Cl_2(tmen) belongs to the second. Reactions were carried out in Et_2O, and stirred for 12 h at room temperature with a 1:1 ratio of LiO-2,6-^{t}Bu$_2$-4-RC_6H_2:$MoO_2X_2L_2$ (R = H, Et, OMe, NO_2). The products of the reactions were HO-2,6-^{t}Bu$_2$-4-RC_6H_2, free L and $MoO_2(OAr)_2$ **2.2a**, **2.2c** and **2.2e**. In general the neutral ligand L is apparently displaced over the course of the reaction.

$MoO_2Cl_2(DMF)_2$ dissolves in DME and reacts with 2 equiv of LiOAr (**2.1a**, **2.1c**, **2.1e**, and **2.1f**) over 12 h to produce $MoO_2(OAr)_2$ **2.2a**, **2.2c**, **2.2e** and **2.2f**. Molecule **2.2f** was not isolated and **2.1h** just produced phenol. Reactions using $MoO_2Cl_2(DMF)_2$ and different equiv of LiO-2,6-^{t}Bu$_2$-4-RC_6H_2 in DME and Et_2O are summarized in Table 2.2. Two new complexes, **5a** and **5c,** were isolated (entries 16 and 17); refer to the experimental section for synthetic and spectrophotometric details.

Table 2.2 Reactions Between $MoO_2Cl_2(DMF)_2$ and Various LiO-2,6-^{t}Bu$_2$-4-RC_6H_2 (**2.1a**, R = H; **2.1c**, R = OMe; **2.1e**, R = OMe; **2.1f**, R = Br; **2.1h**, R = NO_2) in 1:2 and 1:1 Ratios Using DME and Et_2O as Reaction Solvents.

	R	Eq	Solv.	Product ratios		R	Eq	Solv.	Product ratios
1	H	2	DME	**2.2a**, ArOH, **2.3a** (3:1:1)	11[a]	H	2	Et_2O	**2.5a**, ArOH, **2.3a** (2:1:1)
2	Et	2	DME	**2.2c**, ArOH, **2.3c** (5:1:0.2)	12	Et	2	Et_2O	**2.2c**, ArOH, **2.3c** (3:1:0.1)
3	OMe	2	DME	**2.2e**, ArOH, **2.3b** (3:2:1)	13	OMe	2	Et_2O	**2.2e**, ArOH, **2.3b** (6:1:0.1)
4	Br	2	DME	**2.2h**, ArOH, **2.3a** (2:1:4)	14	Br	2	Et_2O	**2.2h**, ArOH, **2.3a** 1:1.5:1
5	NO_2	2	DME	ArOH	15	NO_2	2	Et_2O	ArOH, **2.3a**, **2.3d** (7:1:0.5)
6[a]	H	1	DME	**2.2a**, ArOH, **2.3a**, **2.5a** (1:3:2:3)	16	H	1	Et_2O	**2.5a**, ArOH, **2.3a** (8:2:1)
7[a]	Et	1	DME	ArOH, **2.5c**, **2.3b** (2:1:2)	17	Et	1	Et_2O	ArOH, **2.5c, 2.3c** (1:3:0.2)
8	OMe	1	DME	ArOH, **2.3b** (2:1)	18	OMe	1	Et_2O	**2.2e**, ArOH, **2.3b** (3:2:2)
9	Br	1	DME	**2.2h**, ArOH, **2.3a** (3:2:1)	19	Br	1	Et_2O	**2.2h**, ArOH, **2.3a** (1:2:1)
10	NO_2	1	DME	ArOH	20	NO_2	1	Et_2O	ArOH, **2.3a** (8:1)

Reaction time = 12 h; room temperature. Approximate ratios are given based on integration of ^{1}H NMR peaks. ([a]) new products detected in small amounts. ArOH = HO-2,6-^{t}Bu$_2$-4-RC_6H_2

In most cases DMF is lost and $MoO_2(OAr)_2$ **2** is formed. We only observed retention of DMF for R = H and Et, and even then, the $MoO_2(OAr)_2(DMF)$ products **2.5a** and **2.5c** were formed in small amounts. It seems that a low concentration of LiOAr (either by using a solvent where LiOAr is not completely soluble, such as Et_2O, or by adding 1 equiv of LiOAr instead of 2), promotes a better product:sideproducts ratio. In our proposed reaction mechanism, unreacted and readily available LiOAr launches the side-reaction described in Scheme 2.2.

2.4.2 Steric substituent effects in reactions with $MoO_2Cl_2(DMF)_2$

Steric factors were studied by using different bulky aryloxide ligands (Scheme 3). We have previously shown that sterics can affect the structure of $MoO_2(OAr)_2(py)_{0-2}$ complexes.[69] Here, $MoO_2Cl_2(DMF)_2$ reactions were performed in Et_2O at room temperature, using LiO-2,6-$Me_2C_6H_3$ (**2.1l**) or LiO-2,6-$^{i}Pr_2C_6H_3$ (**2.1k**) in a 1:1 ratio. **2.1l** yielded product **2.5l** whereas **2.1k** produced as main product **2.5k** and as by-product, a Mo(VI) complex of the form $MoOCl(OAr)_3(DMF)$ that will be presented in Chapter 3. Complexes **2.5a**-**l** demonstrate that as we decrease the steric bulk of the aryloxy coligand, it allows a second molecule of DMF to fit into the coordination sphere.

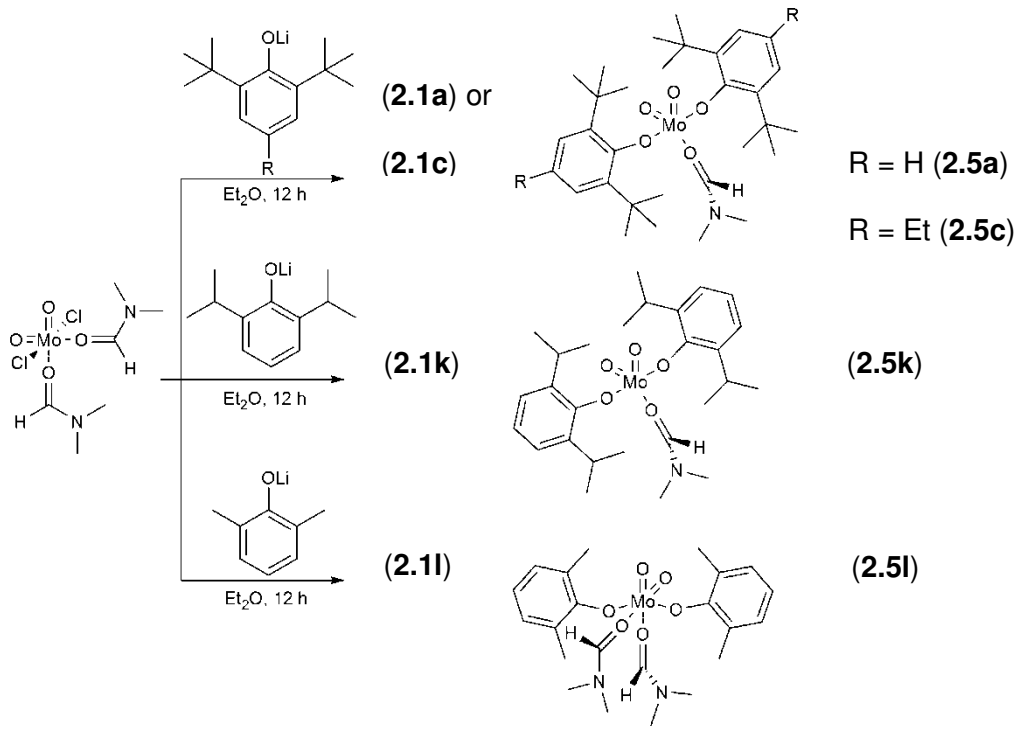

Scheme 2.3 Steric control of coordination number by variation of the steric bulk of the aryloxy ligand in reactions with $MoO_2Cl_2(DMF)_2$.

The ^{1}H NMR spectra of molecules **2.5a** , **2.5c, 2.5k** and **2.5l** are consistent with their C_{2v} molecular symmetry. The phenoxide rings are magnetically equivalent and display only one set of signals. For **2.5l** the DMF molecules are equivalent as well, and only two singlets account for the two amide methyls. The IR spectra show the expected stretching bands for C*H*O (2868-70

cm^{-1}), C=O (1645-49 cm^{-1}) and C-N (1401-13 cm^{-1}). Mo=O stretches fall within the reported values for MoO_2^{2+} species, not revealing any tendency in bond strength. The electronic spectra show three bands: at 278 nm (B band modified by the putative oxygen auxochromic effect), 300 nm (DMF related band), and 619 – 623 nm (low energy absorption, LMCT from terminal oxo or phenoxide to a low energy metal-character orbital: e.g. $t_{2u} \rightarrow t_{2g}$).

2.5 Crystal structure and three-dimensional geometry

Table 2.3 Crystallographic Data and Summary of Data Collection and Structure Refinement

	2.2c	**2.2e**	**2.4**
Formula	$C_{32}H_{50}MoO_4$	$C_{30}H_{46}MoO_6$	$C_{35}H_{60}ClLiMoO_{10}$
fw	594.66	598.61	779.16
crystal system	Monoclinic	Monoclinic	Orthorhombic
space group	C2/c	$P2_1/c$	Fdd2
T, K	213(2) K	223(2) K	213(2) K
a, Å	9.8823(16)	12.537(3)	62.839(15)
b, Å	17.911(3)	18.426(5)	21.386(5)
c, Å	36.339(6)	14.298(4)	12.948(3)
α, deg	90	90	90
β, deg	91.129(3)	112.157(4)	90
γ, deg	90	90	90
V, $Å^3$	6430.8(18)	3058.9(14)	17400(7)
Z	8	4	16
D_{calc}, mg/m^3	1.228	1.300	1.190
θ range (deg) for data collection	2.24 - 23.27	1.89 - 23.26	1.87 - 23.28
$N_{measured}$	18064	18684	23344
$N_{independent}$	4614	4391	5864
R	0.0920	0.0222	0.0479
ωR_2	0.2511	0.0634	0.1265
GOF	1.051	1.023	1.053
largest diff peak and hole ($e \cdot Å^3$)	2.322 and -0.763	0.230 and -0.416	0.715 and -0.325

2.5.1 Coordination number and structural features

The series of molecules **2.2**, **2.4** and **2.5** demonstrates the design of MoO_2^{2+} compounds with 4-, 5- and 6-coordinate environments by using steric hindrance and chelate effect as the controlling factors.

Complexes **2.2c**, **2.2e** (Figures 2.1 and 2.2), **2.4**, and **2.5a**-**l** display the expected geometries (tetrahedral, trigonal bipyramidal and octahedral), though steric effects cause distortion from ideal geometries.

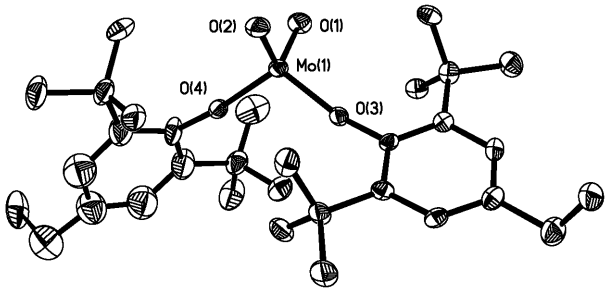

Figure 2.1 ORTEP view of MoO_2(O-2,6-^{t}Bu$_2$-4-EtC_6H_2)$_2$ (**2.2c**) (30% probability). Hydrogen atoms have been omitted for clarity.

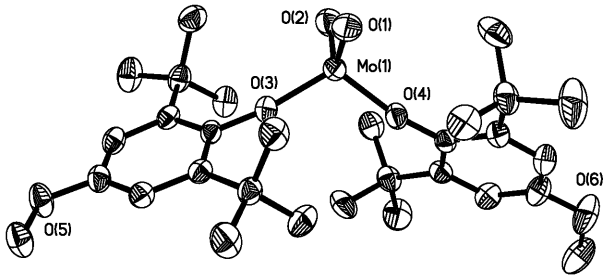

Figure 2.2 ORTEP view of compound MoO_2(O-2,6-^{t}Bu$_2$-4-(OMe)C_6H_2)$_2$ (**2.2e**) (50% probability). Hydrogen atoms have been omitted for clarity.

In the case of complexes **2.2a**,[68] **2.2c** and **2.2e**, the maximum angular deviation is approximately -3.64° from the ideal tetrahedral value, for the narrow ∠O=Mo=O in **2.2e** (Figure 2.2). The mutual steric repulsion exerted by the bulky phenolate ligands widens their angle from 109.5° to a maximum of 112.91(6)° in **2.2e** (there is a small but steady increase of this angle from 111.26(10)° to 112.91(6)° as we shift from R = H to R = OMe). The widening of the ArO-Mo-OAr angle parallels the narrowing of the O=Mo=O angle.

Li{MoO_2Cl[2,2'-CH_2(O-6-^{t}Bu-4-MeC_6H_2)$_2$]}·3DME (**2.4**) is a fine example of the delicate balance between the trigonal (TBP) bipyramidal and square pyramidal (SP) geometries: the

distorted TBP geometry exhibited by **2.4** can be observed as an approach to a SP geometry. In an ideal TBP conformation the equatorial ligands are 120.0° apart, and the apical ligands are 180.0° from each other. The observed angles are 134.8(2)°, 114.4(2)°, 110.7(3)° (equatorial) and 164.83(12)° (apical). The incipient SP character of **2.4** may be driven by the chelating bisphenoxide that would find a less strained bite angle in a SP conformation (≈ 90°) compared to the one imposed by the actual molecular conformation (84.14(16)°). The TBP arrangement is greatly favored by repulsions from bonding pairs: in this conformation the O=Mo=O angle is 110.7(3)° versus the 90° expected if the SP arrangement prevailed. In this TBP conformation the doubly bonded oxygen atoms seek the more spacious equatorial positions and the apical chlorine is bent away from the two equatorial oxo groups. Both oxo moieties require more room than a single bonding pair, and both repel adjacent bonds, thereby distorting the structure so that the ideal 90° O=Mo-Cl angles are not observed; instead the angles 95.62(17)° and 90.34(18)°.

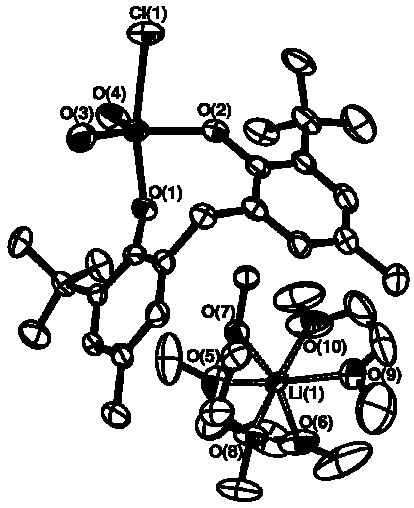

Figure 2.3 ORTEP view of Li{MoO_2Cl[2,2'-CH_2(O-6-^{t}Bu-4-MeC_6H_2)$_2$]}·3DME (**2.4**) (40% probability). Hydrogen atoms have been omitted for clarity.

Tables 2.4 and 2.5 collect important structural information of selected molecules. Bond lengths and bond angles of the complexes $MoO_2(OAr)_2$ **2.2c**, $MoO_2(OAr)_2$(DMF) **2.5c**,

$MoO_2(OAr)_2(DMF)_2$ **5l** are listed and compared with the previously reported $MoO_2(OAr)_2(py)$ and $MoO_2(OAr)_2(py)_2$.[69]

Table 2.4 Selected Bond Lengths (Å)

		Mo=O	Mo-O(aryloxy)	Mo-O(DMF) or Mo-N(py)
4-coordinate				
$MoO_2(OAr)_2$[68]	(**2.2a**)	1.703(2) 1.706(2)	1.857(2) 1.861(2)	
$MoO_2(OAr)_2$	(**2.2c**)	1.679(7) 1.688(6)	1.849(6) 1.860(6)	
5-coordinate				
$MoO_2(OAr)_2(DMF)$	(**2.5c**)	1.689(12) 1.689(12)	1.923(12) 1.939(12)	2.124(12)
$MoO_2(OAr)_2py$[69]		1.701(4) 1.705(4)	1.912(4) 1.909(4)	2.292(5)
6-coordinate				
$MoO_2(OAr)_2(DMF)_2$	(**2.5l**)	1.692(15) 1.700(15)	1.956(2) 1.986(3)	2.238(12) 2.296(14)
$MoO_2(OAr)_2(py)_2$[69]		1.697(5)	1.964(4)	2.421(5)

Table 2.5 Selected Bond Angles (deg)

		O=Mo=O	Mo-O-C(aryloxy)	ArO-Mo-OAr
4-coordinate				
$MoO_2(OAr)_2$[68]	(**2.2a**)	106.5(1)	170.3(2) 174.2(2)	111.26(10)
$MoO_2(OAr)_2$	(**2.2c**)	106.3(3)	164.3(5) 172.3(7)	111.4(2)
5-coordinate				
$MoO_2(OAr)_2(DMF)$	(**2.5c**)	105.6(7)	151.7(12) 147.3(12)	160.4(5)
$MoO_2(OAr)_2py$[69]		110.3(2)[a]	141.6(4) 134.4(4)	92.6(8)[a]
6-coordinate				
$MoO_2(OAr)_2(DMF)_2$	(**2.5l**)	104.06(9)	123.46(11) 135.60(12)	150.3(5)
$MoO_2(OAr)_2(py)_2$[69]		103.9(3)	124.5(4)	154.2(2)

[a] Listed to offer a complete set of parameters; but it cannot be included in any trend because py coordinates in an unusual way to the MoO_2^{2+} unit.

The group of molecules **2.2a**, **2.2c**, **2.2e**, **2.5c**, and **2.5l** demonstrates the design of MoO_2^{2+} compounds with 4-, 5-, and 6-coordinate environments by using steric hindrance as the controlling factor. A similar observation was previously reported by our research group where decreasing the steric bulk of the aryloxy ligand resulted in the coordination of one or two molecules of pyridine.[69]

$MoO_2(OAr)_2(DMF)$ **2.5c** (figure 2.4) displays a slightly distorted TBP geometry. It can be seen as a modified version of **2.2c,** since the only difference is the presence of DMF. The equatorial plane is formed by two oxo ligands and one DMF. DMF is found in between the two aryloxo ligands, widening their angle from 111.4(2)^o (in **2.2c**) to 160.4(5)^o (in **2.5c**). No appreciable difference is noted in the O=Mo=O angle, which goes from 106.3(3)^o (in **2.2c**) to 105.6(7)^o (in **5c**). The Mo-OAr bond lengths in **2.5c** (1.923(12) Å, 1.939(12) Å) are longer than those in **2.2c** (1.849(6) Å, 1.860(6) Å), but shorter than those in $MoO_2(OAr)_2(DMF)_2$ **2.5l**

(1.955(2) Å, 1.980(3) Å). The explanation may be that only one DMF molecule is contributing to the σ* orbital of Mo-OAr instead of none in $MoO_2(OAr)_2$ **2.2c** or two in $MoO_2(OAr)_2(DMF)_2$ **2.5l**.

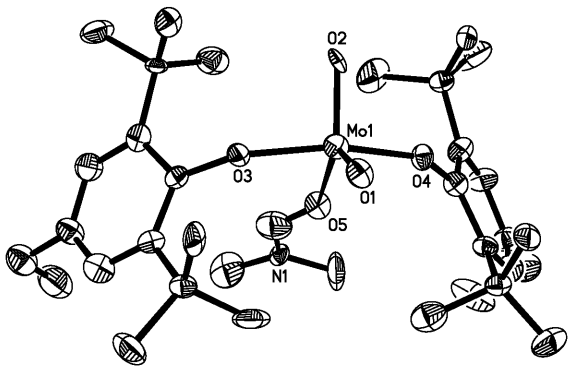

Figure 2.4 ORTEP view of MoO_2(O-2,6-^{t}Bu$_2$-4-Et$C_6H_2)_2$(DMF) (**2.5c**) (50% probability). Hydrogen atoms have been omitted for clarity.

Table 2.6 Crystallographic Data and Summary of Data Collection and Structure Refinement

	2.5c	**2.5l**
Formula	$C_{35}H_{57}MoNO_5$	$C_{22}H_{32}MoN_2O_6$
fw	667.76	516.44
crystal system	Monoclinic	Orthorhombic
space group	$P2_1/n$	$P2_12_12_1$
T, K	223(2)	223(2)
a, Å	9.201(5)	9.3431(8)
b, Å	16.163(9)	14.4151(12)
c, Å	23.891(13)	18.4505(15)
α, deg	90	90
β, deg	92.275(10)	90
γ, deg	90.	90
V, Å^3	3550(3)	2484.9(4)
Z	4	4
D_{calc}, mg/m^3	1.249	1.380
θ range (deg) for data collection	1.52 - 23.28	2.21 - 23.26
$N_{measured}$	21360	12464
$N_{independent}$	5105	3567
R	0.1635	0.0157
ωR_2	0.4062	0.0450
GOF	1.278	0.863
largest diff peak and hole (e·Å^3)	4.008 and -1.370	0.141 and -0.289

$MoO_2(OAr)_2(DMF)_2$ **2.5l** has abnormally long Mo-OAr bonds. The Mo-OAr bond lengths in compounds **2.2a** and **2.2c** range from 1.849(6) Å (**2.2c**) to 1.861(2) Å (**2.2a**), while in **2.5l** the Mo-OAr bond lengths are 1.956(1) and 1.981(1) Å. This lengthening observed in the Mo-OAr bond on going from $MoO_2(OAr)_2$ to $MoO_2(OAr)_2L$, then to $MoO_2(OAr)_2L_2$, is also observed for the analogous $MoO_2(OAr)_2(py)_{0\text{-}2}$ complexes. This phenomenon may be due to the electron donation from the ligand to the metal σ* LUMO (e_g symmetry if viewed as an O_h complex), weakening the Mo-OAr bonds.

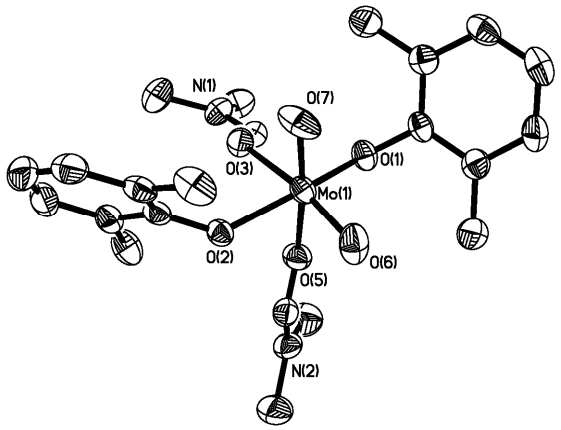

Figure 2.5 ORTEP view of $MoO_2(O\text{-}2,6\text{-}Me_2C_6H_3)_2(DMF)_2$ (**2.5l**) (50% probability). Hydrogen atoms have been omitted for clarity.

Tables 2.4 and 2.5 show that there is a marked decrease in Mo-O-C(aryl) bond angles, increase in Mo-O(aryloxy) bond distances, and increase in Mo-O(DMF) or Mo-N(Py) bond distances, as the coordination number increases. The increase in Mo-ligand distances can be explained in terms of simple steric congestion as we move from coordination numbers 4 to 5. Also, all three trends are consistent with a decrease of electron donation from aryloxy and the DMF or Py ligands to the Mo(VI) center as the coordination number increases.

2.5.2 Electronic unsaturation and structural consequences

Complexes of the series **2.2** and **2.5** are considered to be electronically unsaturated as they have less than 18 electrons in their valence shell. These complexes can relieve the electronic unsaturation by making use of two sources: variable electronic contribution of ligands and contribution of σ-donors.

Oxo, alkoxo and aryloxo ligands can be considered as electron wells, in which electron density can be taken or given as required either for stability of the complex or for chemical transformation in the coordination sphere.

The role of the oxo group as electronic reservoir has been discussed and recognized.[103, 135, 142] A larger degree of electronic contribution by the oxo group to the metal center might be accompanied by a considerable shortening of the Mo=O bond and vice versa. Inspection of Table 2.4 shows that no significant change in any of the listed Mo=O bond lengths is observed for the different coordination numbers. The listed Mo=O bond lengths fall in the range of the observed Mo=O bond distances for various MoO_2^{2+} complexes, which is between 1.667(11) and 1.83(4) Å.[25]

Unlike the Mo=O bond, the Mo-OAr bond differs considerably from one coordination number to another. The observed Mo-OAr bond lengthening parallels the shrinking of the Mo-O-C(aryl) angle. The change of this angle can be seen as a change in the hybridization of the aryloxy oxygen. The electronic contribution of the aryloxy ligands depends on the hybridization of oxygen. Linear oxygen (sp) might contribute up to $6e^-$ to the total electron count, whereas trigonal (sp^2) and tetrahedral oxygens (sp^3) might supply 4 and $2e^-$ respectively, depending on the electronic needs of the complex. In this sense, oxygen in $MoO_2(OAr)_2$ **2c** can be thought to be sp hybridized since the angles are 164.3(5)° and 172.3(7)° (close to 180°). A sp hybridized oxygen implies significant backbonding; this might be the reason for the observed short Mo-OAr bond. In the case of $MoO_2(OAr)_2L$ (L = DMF or Py), the aryloxy oxygen exhibits angles between 134.4(4)° - 151.7(12)°, a little over that expected for a sp^2 hybridization (120°). In this case the

$2e^-$ σ donor DMF or py supplies electronic density to the complex and the metal center demands less contribution from the aryloxy ligand (a longer Mo-OAr bond). For $MoO_2(OAr)_2L_2$ (L = DMF or py), we suggest the same explanation. The aryloxy oxygen displays angles between 103.9(3)° and 104.06(9)°; close to 109.5° for a sp^3 hybridized atom. The Mo-OAr bond lengthens as the need of electronic density is satisfied by the two σ ligands.

This interpretation of how the Mo-O-Ar angles and bond lengths correlate with electron contribution should not be taken as absolute. An study involving Nb(V) and Ta(V) aryloxides found these three parameters to be "flexible" and not correlated, in contrast to our proposed explanation.[143] In any case, the steric and electronic arguments are not opposite but complementary.

2.6 Conclusions

We have presented a series of Mo(VI) dioxo diaryloxide complexes with 4-, 5- and 6-coordinate environments. The electronic nature of the substituents in the aryl ring strongly affects the observed yields of the final molybdenum(VI) dioxo diaryloxides. Electron withdrawing groups produce poor or null yields, whereas electron donating groups favor product formation in relatively good yields. Radical species were observed during the reaction, and their nature and mechanism of formation were proposed. $MoO_2(OAr)_2$ complexes showed catalytic oxygen transfer from DMSO to PPh_3. Inexpensive and stable $MoO_2Cl_2(DMF)_2$ was also a good starting material for some of the complexes presented here. Structural studies indicate that, with increasing coordination, Mo-O(aryloxy) bond lengths increase and Mo-O-C(aryl) bond angle decreases. This behavior can be explained in terms of the steric congestion imposed by the increased coordination number, and/or by the electronic unsaturation of $MoO_2(OAr)_2L_{0-2}$ complexes.

CHAPTER 3

MOLYBDENUM(VI) MONOXO ARYLOXIDES

3.1 Introduction

In the last chapter we discussed the importance of the MoO_2^{2+} unit for the chemistry of molybdenum in high oxidation states. Because of their many applications, MoO_2^{2+} containing complexes are by far the most common in Mo(VI) structural chemistry.[144]

In contrast, the MoO^{4+} core is found in a relatively small number of authenticated structures.[145] This scarcity might be a result of the low stability that some of these products display.[146] Molybdenum(VI) oxo alkoxides, $MoO(OR)_4$, for instance, have a tendency to disproportionate into $MoO_2(OR)_2$ via ether elimination.[147-149] MoO^{4+} species are also highly sensitive to moisture; they hydrolyze upon exposure, a process that is accompanied by the formation of "molybdenum blues".[150]

Molybdenum(VI) complexes that contain a single oxo ligand, or have no oxo moieties, are said to be oxo deficient.[151] It has been observed that strong σ and π donor ligands (e.g. the sulfur containing enedithiolate[145, 152] or the alkoxo[5]/aryloxo ligands[153, 154]) stabilize these oxo-deficient complexes.

MoO^{4+} chemistry has gained special interest in recent years, especially after the discovery of a monooxo Mo(VI) center in the oxidized active site of the dimethylsulfoxide (DMSO) reductase (Chapter 1).[155, 156] Group VI metal aryloxides and oxo aryloxides have become prominent as well, because of their utility as catalyst precursors for the metathesis and metathesis polymerization of functionalized olefins.[157] Compounds of the formula $W(OAr)_{6-n}Cl_n$[158] and the monooxo compounds $MO(OAr)_{4-n}Cl_n$[77, 79, 81, 159, 160] (M = W or Mo), have been shown to act as catalyst precursors in either the presence or absence of cocatalysts.[157, 161] Cocatalysts normally consist of an organometallic compound of a main group metal of groups I-IV. The most commonly used are BuLi, $EtAlCl_2$, R_3Al, and R_4Sn (R = Me, Bu, Ph, etc.).[157] Interestingly, molybdenum-based catalysts are known to be more effective than the

corresponding tungsten-based catalyst in metathesis of olefins (especially for those olefins of molecular weight higher than propene).[157]

It is surprising that very little attention has been given to complexes of the type $MoO(OAr)_{4-n}Cl_n$, considering all of their potential applications. Other than our report on the unexpectedly easy route for the synthesis of $MoO(OAr)_{4-n}Cl_n$ compounds,[81] only one other research group reported its findings on complexes of the type $MoO(OAr)_4$ for several mono- and bidentate aryloxy ligands.[79] The reported $MoO(OAr)_4$ compounds are prepared by the low-temperature reaction of $MoOCl_4$ with the corresponding aryloxy anions, but the yields are low and the characterization minimal.[79]

$WO(OAr)_{4-n}Cl_n$ complexes are prepared by the reaction of $WOCl_4$ with either aryl alcohol or its anion.[162, 163] The molybdenum monooxo analog, $MoOCl_4$, is notoriously more difficult to handle.[57, 164, 165] It is readily attacked by moisture to yield mixed molybdenum(V) and (VI) oxide hydrates.[166] The molybdenum(VI) oxo halide is photo- and thermolabile and prone to disproportionation to form Cl_2 and $MoOCl_3$ products,[166] and it must be freshly prepared before use.[165] In contrast, our research group has reported the facile synthesis of $MoO(OAr)_{4-n}Cl_n$ complexes starting from the more stable MoO_2Cl_2 and the aryl alcohol or its anions at room temperature. In this chapter we will discuss the fundamentals behind this reaction, the proposed reaction mechanisms and their generality. We will also introduce the use of the air and moisture stable $MoO_2Cl_2(DMF)_2$ adduct as a prospective precursor of Mo(VI) monoxo aryloxide complexes.

Table 3.1 introduces the series of the different lithium aryloxides, and the molybenum monooxo aryloxide complexes that will be discussed in this chapter.

Table 3.1 List of Compounds Presented in this Chapter.

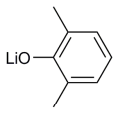

(**3.1a**)

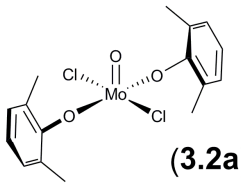

(**3.2a**)

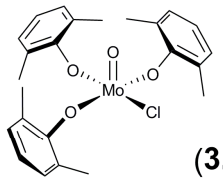

(**3.3a**)

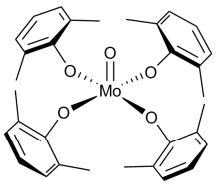

(**3.4a**)

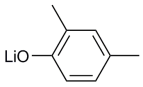

(**3.1b**)

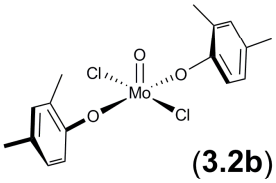

(**3.2b**)

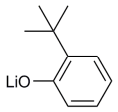

(**3.1c**)

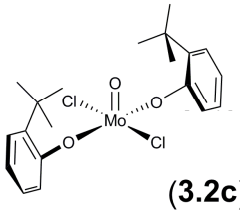

(**3.2c**)

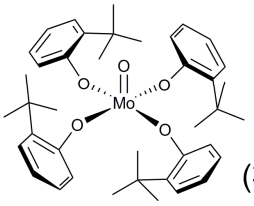

(**3.4c**)

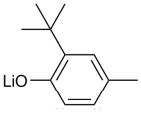

(**3.1d**)

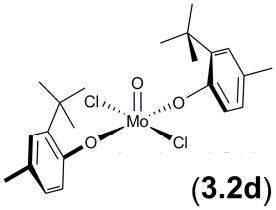

(**3.2d**)

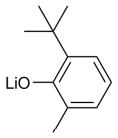

(**3.1e**)

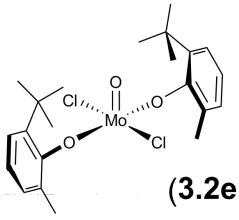

(**3.2e**)

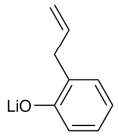

(**3.1f**)

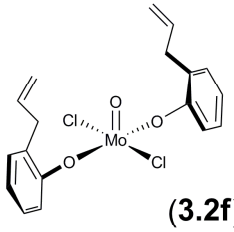

(**3.2f**)

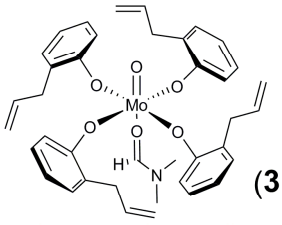

(**3.5f**)

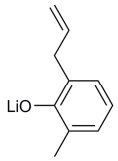

(**3.1g**)

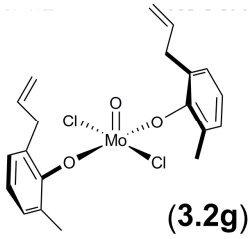

(**3.2g**)

Table 3.1 (Continuation)

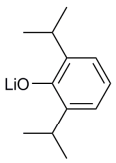

(**3.1h**)

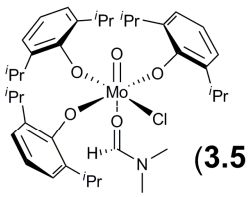

(**3.5h**)

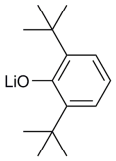

(**3.1i**)

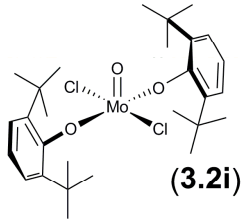

(**3.2i**)

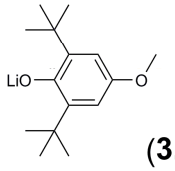

(**3.1j**)

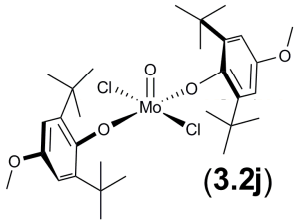

(**3.2j**)

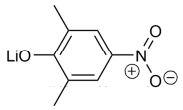

(**3.1k**)

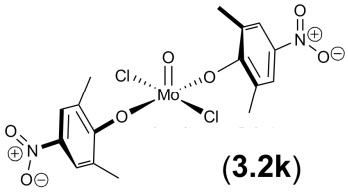

(**3.2k**)

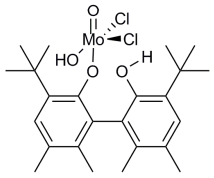

(**3.6**)

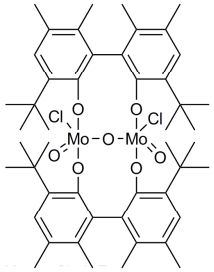

(**3.7**)

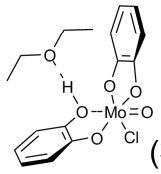

(**3.8**)

3.2 Experimental section

3.2.1 General

All manipulations were performed under dry argon using standard Schlenk techniques or under nitrogen in a NEXUS 1 VAC Atmospheres glovebox. Molybdenum(VI) dichloride dioxide, *n*-butyllithium (2.0 M solution in *n*-pentane), 2,6-dimethylphenol, 2,4-dimethylphenol, 2-*tert*-butyl-6-methylphenol, 2-*tert*-butyl-4-methylphenol, 2-allylphenol, 2-allyl-6-methylphenol, 2,6-diisopropylphenol, 2,6-di-tert-butylphenol, 2,6-di-tert-butyl-4-methoxyphenol, and pyrocatechol were purchased from Aldrich. Racemic-5,5',6,6'-tetramethyl-3,3'-di-*tert*-butyl-1,1'-biphenyl-2,2'-diol, rac-BIPHEN(OH)$_2$, was purchased from Strem Chemicals Company. Aryl alcohols were used as received for the preparation of the lithium aryloxides. For reaction with MoO_2Cl_2, 2,4-dimethylphenol, 2-*tert*-butyl-6-methylphenol, 2-allylphenol, 2-allyl-6-methylphenol and 2,6-diisopropylphenol were stirred for 2 days over CaH_2 under N_2 atmosphere, filtered through a medium pore sintered-glass filter, and stored over molecular sieves for 2 days prior to use. The solid aryl alcohols were recrystallized from Et_2O at -35 ^oC under N_2 atmosphere. 2,6-Dimethyl-4-nitrophenol was prepared from 2,6-dimethylphenol and acetic anhydride (Aldrich) as described elsewhere.[167] MoO_2Cl_2 was obtained from Aldrich and used as received. $MoOCl_4$ was freshly prepared from MoO_3 (J. T. Baker Chemical Company) and newly purchased thionyl chloride (Aldrich) as described previously.[165] The thus synthesized $MoOCl_4$, although reported to be pure for most uses,[165] was further sublimed,[165, 168] and stored in an amber bottle inside the glovebox freezer at -35 ^oC. $MoO(OEt)_4$ was prepared from sodium (Aldrich), ethanol and $MoOCl_4$ as described in the literature.[169] $MoO_2Cl_2(DMF)_2$, LiO-2,6-^{i}Pr$_2$C$_6$H$_3$ (**3.1h**), LiO-2,6-^{t}Bu$_2$C$_6$H$_3$ (**6i**), and LiO-2,6-^{t}Bu$_2$-4-(OMe)C$_6$H$_2$ (**3.1j**) were prepared as described in Chapter 2. “Wet hexane” was prepared freshly each time by sonication of a mixture of 5 mL of water and 40 mL of anhydrous hexanes. The sonicated mixture was saturated with dry argon using a glass sintered bubbler. From this mixture, only 20 mL of hexane, coming from the bottom of the flask, were used to run reactions. Hexanes, 1,2-dimethoxyethane (DME), diethyl ether (Et_2O) and

tetrahydrofuran (THF) were freshly distilled under argon from Na/benzophenone. *n*-Pentane, ethanol and acetonitrile (anhydrous grade) were purchased from Aldrich and stored over molecular sieves. Methanol (HPLC grade, Aldrich) was pre-dried over molecular sieves for 48 h and further refluxed and distilled from CaO under nitrogen. NMR solvents (benzene-d_6, acetonitrile-d_3 and chloroform-d) were degassed and vacuum distilled from CaH_2. Benzene-d_6 was additionally vacuum transferred from Na/benzophenone. All solvents (including NMR solvents) were stored inside the glovebox over 4 Å molecular sieves (previously activated) for 48 h before use.

^1H and ^{13}C NMR spectra were recorded on a Mercury Varian Plus 300 MHz spectrometer. ^1H NMR data are expressed as parts per million (ppm) downfield shift from tetramethylsilane ($\delta_{TMS} = 0$) using either tetramethylsilane or residual solvent as internal reference. Relative integral multiplicity is denoted by s = singlet, d = doublet, t = triplet, m = multiplet, dd = doublet of doublets, td = triplet of doublets. Coupling constants (J) are reported in Hz. ^{13}C NMR spectra were recorded with complete proton decoupling at 300 K. Data are expressed as parts per million (ppm) downfield shift from tetramethylsilane ($\delta_{TMS} = 0$) using either tetramethylsilane or residual solvent as internal reference.

The melting points of the products were observed in sealed capillary tubes on a Mel-temp apparatus (Laboratory Devices, Cambridge, MA). IR spectra were obtained with a MIDAC Corporation M-Series FTIR spectrometer. UV/vis spectra were recorded on an Agilent 8543 UV-visible spectrophotometer.

The complexes described here showed high sensitivity and decomposed upon air exposure. It was decided to submit only 1 sample for microanalysis and 3 for mass spectrometry, since the more stable and structurally related $MoOCl_2$(bisphenoxide) complexes (Chapter 4) performed inadequately under the shipping and analytical conditions of the different facilities. As expected the analysis results were not satisfactory. Elemental analyses were performed at Atlantic Microlab Inc. (Norcross, Georgia). Mass spectrometric analyses were

conducted at the University of California (Berkeley, CA) and at the National Center for Research Resources (St. Louis, MO).

All single crystals were coated with paratone-N oil (Hampton Research), and mounted onto thin glass fibres. Diffraction data were collected using graphite monochromated MoK_α radiation (λ = 0.71073 Å) on a Bruker SMART 1000 CCD area detector diffractometer via ϕ and ω scans. All data were collected at 223 K. The structures were solved using SHELXL-97[117] by direct methods. All structures were refined by least-squares full matrix refinement against F^2 using SHELXL-97 and all fully-occupied non-hydrogen atoms were refined with anisotropic atomic displacement parameters (adps). Hydrogen atoms were geometrically placed and refined as part of a rigid model. Geometric restraints were applied, and partially occupied atom sites were refined with isotropic adps.

Additional details, including solution NMR (^1H and ^{13}C) spectra, can be found in the appendix of this chapter.

3.2.2 Preparation of compounds

3.2.2.1 Synthesis of lithium aryloxides

LiO-2,6-$Me_2C_6H_3$ (3.1a): A 20 mL solution of 2,6-$Me_2C_6H_3OH$ (2.0000 g, 16.372 mmol) in THF was prepared and cooled in an ice bath. ^{n}BuLi (8.19 mL of 2.0 M in pentane, 16 mmol) was mixed with THF (7 mL); the resulting mixture was added dropwise (via addition funnel) to the phenol solution with strong stirring over a period of 30 min at 0 ^oC (the reaction is highly exothermic). The reaction mixture was allowed to reach room temperature over 2 h, stirring constantly. The solvent was evaporated under vacuum and approximately 7 mL of Et_2O were added to the dried yellowish mass. The mixture was stored at -35 ˚C. After 1 day a white crystalline precipitate was observed. The yellowish supernatant was removed with a pipette, and the precipitate was recrystallized from Et_2O (7 mL) two times more. The supernatant was pipetted out and the white powder was dried under vacuum. Yield 1.7122 g (85%). ^1H NMR

(C_6D_6): δ (ppm) 7.07 (d, 2H, *J* = 7.2 Hz, aromatic *H*), 6.71 (t, 1H, *J* = 7.2 Hz, aromatic *H*), 2.22 (s, 6H, C*H*$_3$).

LiO-2,4-Me$_2$C$_6$H$_3$ (3.1b): was prepared in Et_2O following the same procedure as for **1a** but using a dry ice/acetone bath, HO-2,4-$Me_2C_6H_3$ (1.00 mL, *ρ* = 1.011 g/mL at 25 °C, 8.28 mmol) and *n*-BuLi solution (4.14 mL of 2.0 M in pentane, 8.9 mmol). Yield 0.9011 g (82%). ^{1}H NMR (CD_3CN): δ (ppm) 6.73 (d, 1H, *J* = 2.4 Hz, aromatic *H*), 6.65 (dd, 1H, *J* = 2.4 Hz and 7.8 Hz, aromatic *H*), 6.50 (d, 1H, *J* = 8.1 Hz, aromatic *H*), 2.12 (s, 3H,C*H*$_3$), 2.06 (s, 3H,C*H*$_3$).

LiO-2-^{t}BuC$_6$H$_4$ (3.1c): was prepared in Et_2O following the same procedure as for **1a** but using HO-2-^{t}BuC$_6$H$_4$ (1.00 mL, *ρ* = 0.978 g/mL at 25 °C, 6.51 mmol) and ^{n}BuLi solution (3.25 mL of 2.0 M in pentane, 6.5 mmol). The product precipitated as a grey powder. Yield 0.9701 g (95%). ^{1}H NMR (DMSO-d_6): δ (ppm) 6.74 (dd, H, *J* = 1.8 and 7.5 Hz, aromatic *H*), 6.58 (td, 1H, *J* = 1.8 and 7.5 Hz, aromatic *H*), 6.18 (d, 1H, *J* = 7.5 Hz, aromatic *H*), 5.86 (t, 1H, *J* = 6.9 Hz, aromatic *H*), 1.33 (s, 9H,C(C*H*$_3$)). Note: higher resolution would be expected to show a dd at 6.18 ppm and a td at 5.86 ppm.

LiO-2-^{t}Bu-4-MeC$_6$H$_3$ (3.1d): was prepared in Et_2O following the same procedure as for **1a** but using HO-2-^{t}Bu-4-MeC_6H_3 (1.0000 g, 6.0886 mmol) and ^{n}BuLi solution (3.04 mL of 2.0 M in pentane, 6.1 mmol). LiO-2-^{t}Bu-4-MeC_6H_3 was twice recrystallized from pentane. Yield 0.8901 g (86%). ^{1}H NMR (DMSO-d_6): δ (ppm) 6.56 (s, 1H, aromatic *H*), 6.40 (d, 1H, *J* = 8.1 Hz, aromatic *H*), 8.1 Hz (d, 1H, *J* = 6.9 Hz, aromatic *H*), 2.34 (s, 3H,C*H*$_3$), 1.35 (s, 9H,C*H*$_3$).

LiO-2-^{t}Bu-6-MeC$_6$H$_3$ (3.1e): was prepared in Et_2O following the same procedure as for **1a** but using HO-2-^{t}Bu-6-MeC_6H_3 (1.00 mL, *ρ* = 0.967 g/mL at 25 °C, 5.89 mmol) and ^{n}BuLi solution (2.94 mL of 2.0 M in pentane, 5.9 mmol). Yield 0.8918 g (89%). ^{1}H NMR (CD_3Cl): δ (ppm) 7.03 (dd, 1H, *J* = 1.5 and 7.9 Hz, aromatic *H*), 6.91 (dd, 1H, *J* = 1.5 and 7.9 Hz, aromatic *H*), 6.39 (t, 1H, *J* = 7.5 Hz, aromatic *H*), 2.16 (s, 3H, C*H*$_3$), 1.40 (s, 9H,C(C*H*$_3$)$_3$).

LiO-2-(allyl)C$_6$H$_4$ (3.1f): was prepared in Et_2O following the same procedure as for **1a** but using HO-2-(allyl)C_6H_4 (1.00 mL, *ρ* = 1.028 g/mL at 25 °C, 7.66 mmol) and ^{n}BuLi solution

(3.83 mL of 2.0 M in pentane, 7.7 mmol). Yield 0.8821 g (82%). ^{1}H NMR (CD_3CN): δ (ppm) 6.90 (m, 2H, aromatic *H*), 6.64 (d, 1H, *J* = 7.8, aromatic *H*), 6.42 (t, 1H, *J* = 7.8 Hz, aromatic *H*), 5.99 (m, 1H, H_2C=C*H*CH_2-), 5.00 (m, 2H, *H*$_2$C=CHCH_2-), 3.34 (d, 2H, *J* = 7.2 Hz, H_2C=CHC*H*$_2$-).

LiO-2-(allyl)-6-MeC_6H_3 (3.1g): was prepared in Et_2O following the same procedure as for **1a** but using HO-2-(allyl)-6-MeC_6H_3 (2.00 mL, *ρ* = 0.992 g/mL at 25 °C, 13.4 mmol) and ^{n}BuLi solution (6.69 mL of 2.0 M in pentane, 13 mmol). Yield 1.7010 g (83%). The product was poorly soluble in most deuterated solvents and meaningful integrations were not obtained. ^{1}H NMR (C_6D_6): δ (ppm) 7.09-6.70 (m, aromatic *H*), 4.80 (m, H_2C=C*H*CH_2-), 4.76 (m, *H*$_2$C=CHCH_2-), 3.16 (d, *J* = 5.6 Hz, H_2C=CHC*H*$_2$-), 2.00 (s, C*H*$_3$).

LiO-2,6-Me$_2$-4-(NO$_2$)C_6H_2 (3.1k): was prepared in Et_2O following the same procedure as for **1a** but using HO-2,6-Me$_2$-4-(NO$_2$)C_6H_2 (0.500 g, 2.99 mmol) and ^{n}BuLi solution (1.50 mL of 2.0 M in pentane, 3.0 mmol). Yield 0.5039 g (97%). No recrystallization was done. ^{1}H NMR (DMSO-d_6): δ (ppm) 7.63 (s, 2H, aromatic *H*), 1.87 (s, 6H, C*H*$_3$).

3.2.2.2 Reactions between MoO_2Cl_2 and aryl alcohols

MoO(O-2,6-Me$_2$$C_6H_3$)$_2$$Cl_2$ (3.2a): HO-2,4-Me$_2$$C_6H_3$ (0.1256 g, 1.028 mmol) and MoO_2Cl_2 (0.1011 g, 0.5084 mmol) were dissolved, each in 10 mL of Et_2O. The aryl alcohol solution was added dropwise to the light blue MoO_2Cl_2 suspension with rapid stirring at room temperature, forming a dark blue solution. After 12 h, the reaction mixture was filtered through a medium pore sintered glass frit, the filtrate was concentrated under vacuum to 5 mL, and kept at -35 °C. Dark solid precipitated after 4 days; the supernatant was withdrawn and the solid recrystallized once more from pentane. The ^{1}H NMR data matched those reported in the literature.[81] The proposed structure was corroborated by low resolution mass spectrometry.

MoO(O-2,4-Me$_2$$C_6H_3$)$_2$$Cl_2$ (3.2b): HO-2,4-Me$_2$$C_6H_3$ (0.12 mL, 0.99 mmol) and MoO_2Cl_2 (0.1000 g, 0.5029 mmol) were dissolved, each in 10 mL of hexanes. The aryl alcohol solution was added dropwise to the light blue MoO_2Cl_2 suspension with rapid stirring at room

temperature, forming a deep blue solution. After 12 h, the reaction mixture was filtered through a medium pore sintered glass frit and the filtrate was dried under vacuum. A ^{1}H NMR spectrum of the crude reaction mixture (after filtration) revealed two major components; MoO(O-2,4-$Me_2C_6H_3)_2Cl_2$ (**3.2b**) and HO-2,4-$Me_2C_6H_3$. Et_2O (5 mL) was added to the dry dark blue mass and the mixture was stored at -35 ^{o}C for 5 days affording crystalline dark blue solid. The supernatant was withdrawn and recrystallization in Et_2O was performed twice more. The crystals were dried under vacuum. Yield 0.0840 g (39%), m.p. 138-140 ^{o}C. ^{1}H NMR ($CDCl_3$): δ 6.92 (d, 2H, *J* = 7.8 Hz, aromatic *H*), 6.81 (d, 2H, *J* = 8.4 Hz, aromatic *H*), 6.75 (s, 2H, aromatic *H*), 2.22 (s, 6H, C*H*$_3$), 2.02 (s, 6H, C*H*$_3$). ^{13}C{^{1}H} NMR ($CDCl_3$): δ 161.9 (*ipso C*), 133.6 (*meta C*), 130.6 (*para* C), 127.2 (*meta C*), 127.0 (*ortho C,* next to Me), 119.9 (*ortho C*), 20.8 (*C*H$_3$), 16.4 (*C*H$_3$). IR (cm^{-1}, KBr): 3398br, 1593w, 1514w, 1263w, 1219m, 1149w, 1120m, 972m (Mo=O), 926w, 918w, 839w, 808s, 553m. UV-vis (C_6H_6) λ_{max}/nm (ε/dm^{3}mol^{-1}cm^{-1}): 286 (5996), 621 (2781).

MoO(O-2-^{t}BuC$_6$H$_4$)$_2$Cl$_2$ (3.2c): HO-2-^{t}BuC$_6$H$_4$ (0.15 mL, 1.0 mmol) and MoO_2Cl_2 (0.1000 g, 0.5029 mmol) were dissolved, each in 10 mL of Et_2O or hexanes. The aryl alcohol solution was added dropwise to the light blue MoO_2Cl_2 solution with rapid stirring at room temperature, forming a dark blue solution. After 12 h, the reaction mixture was filtered through a medium pore sintered glass frit and the the filtrate was dried under vacuum. A ^{1}H NMR spectrum of the crude reaction mixture (after filtration) revealed two major components; presumably MoO(O-2-^{t}BuC$_6$H$_4$)$_2$Cl$_2$ (**3.2c**) and HO-2-^{t}BuC$_6$H$_4$. Either Et_2O or hexanes (5 mL) was added to the dry dark blue mass and the mixture was stored at -35 ^{o}C for several days. Isolation of the product was unsuccessful and the amount of aryl alcohol increased as repeated recrystallizations were performed. ^{1}H NMR ($CDCl_3$): δ 7.21 (dd, 2H, *J* = 1.2 and 9 Hz, aromatic *H*), 7.14 (td, 2H, *J* = 1.5 and 7.8 Hz, aromatic *H*), 6.01 (d, 2H, aromatic *H* overlapping with aryl alcohol signal), 6.77 (td, 2H, *J* = 1.2 and 7.6 Hz, aromatic *H*), 1.33 (s, 18H,C(C*H*$_3$)$_3$).

$MoO(O\text{-}2\text{-}^{t}Bu\text{-}4\text{-}MeC_6H_3)_2Cl_2$ (3.2d): HO-2-^{t}Bu-4-MeC_6H_3 (0.1652 g, 1.006 mmol) and MoO_2Cl_2 (0.1000 g, 0.5029 mmol) were dissolved, each in 10 mL of hexane. The aryl alcohol solution was added dropwise to the light blue MoO_2Cl_2 solution with rapid stirring at room temperature. A ^{1}H NMR spectrum of the crude reaction mixture revealed two major components; $MoO(O\text{-}2\text{-}^{t}Bu\text{-}4\text{-}MeC_6H_3)_2Cl_2$ (**3.2d**) and HO-2-^{t}Bu-4-MeC_6H_3. The solution was concentrated to 10 mL and the mixture was filtered through a medium pore sintered glass frit. The solid in the frit was rinsed once more with hexane and dried under vacuum. Yield 0.1010 g (39%), m.p. 141.5-142 ^{o}C. ^{1}H NMR ($CDCl_3$): δ 7.20 (d, 2H, *J* = 2.1 Hz, aromatic *H*), 7.10 (dd, 2H, *J* = 1.8 and 8.2 Hz, aromatic *H*), 6.88 (d, *J* = 8.1 Hz, 2H, aromatic *H*), 2.50 (s, 6H, C*H*$_3$), 1.48 (s, 18H, C(C*H*$_3$)$_3$). ^{13}C{^{1}H} NMR ($CDCl_3$): δ 163.8 (*ipso C*), 140.9 (*ortho C,* next to C(CH_3)$_3$), 140.5 (*para* C), 128.6 (*meta C*), 128.3 (*meta C*), 127.1 (*ortho C*), 35.1 (*C*(CH_3)$_3$), 30.3 (C(*C*H$_3$)$_3$), 21.9 (*C*H$_3$). IR (cm^{-1}, KBr): 3385br, 2964m, 2916m, 2868w, 1592s, 1471m, 1392w, 1363w, 1286w, 1257w, 1208s, 1136m, 1086m, 1024w, 985s (Mo=O), 926s, 804s. UV-vis (C_6H_6) λ_{max}/nm (ε/dm^{3}mol^{-1}cm^{-1}, C_6H_6): 286 (5118), 732 (3015).

$MoO(O\text{-}2\text{-}^{t}Bu\text{-}6\text{-}MeC_6H_3)_2Cl_2$ (3.2e): HO-2-^{t}Bu-6-MeC_6H_3 (0.17 mL, 1.0 mmol) and MoO_2Cl_2 (0.1000 g, 0.5029 mmol) were dissolved, each in 10 mL of Et_2O. The aryl alcohol solution was added dropwise to the light blue MoO_2Cl_2 solution with rapid stirring at room temperature. After 12 h, the reaction mixture was filtered through a medium pore sintered glass frit and the filtrate was dried under vacuum. A ^{1}H NMR spectrum of the crude reaction mixture (after filtration) revealed two major components; $MoO(O\text{-}2\text{-}^{t}Bu\text{-}6\text{-}MeC_6H_3)_2Cl_2$ (**3.2e**) and HO-2-^{t}Bu-6-MeC_6H_3. The dry dark blue mass was very soluble in most organic solvents. Partial purification by reprecipitation was accomplished in hexane (10 mL) and the mixture was stored at -35 ^{o}C for 2 days affording a dark blue solid precipitate. The dark solid was dried under vacuum and used for NMR analysis. ^{1}H NMR ($CDCl_3$): δ 7.28 (d, 2H, *J* = 8.1 Hz, aromatic *H*), 7.10 (d, 2H, *J* = 8.1, aromatic *H*), 7.03 (t, 2H, *J* = 7.5 Hz, aromatic *H*), 2.50 (s, 6H, C*H*$_3$), 1.56 (s, 18H, C(C*H*$_3$)$_3$). ^{13}C{^{1}H} NMR ($CDCl_3$): δ 143.6 (*ortho C,* next to C(CH_3)$_3$), 135.6 (*meta* C), 129.5

(*ortho C*, next to CH_3), 129.3 (*meta C*), 124.6 (*para C*), 35.4 ($C(CH_3)_3$), 30.0 ($C(CH_3)_3$), 19.4 (CH_3). The *ipso* carbon was not observed due to the low concentration of the sample.

$MoO(O\text{-}2\text{-}(allyl)C_6H_4)_2Cl_2$ (3.2f): HO-2-(allyl)C_6H_4 (0.13 mL, 1.0 mmol) and MoO_2Cl_2 (0.1000 g, 0.5029 mmol) were dissolved, each in 10 mL of pentane. The aryl alcohol solution was added dropwise to the light blue MoO_2Cl_2 solution with rapid stirring at room temperature, forming a deep blue solution. After 12 h, the reaction mixture was filtered through a fine pore sintered glass frit and the volatiles were removed under vacuum. A ^1H NMR spectrum of the crude reaction mixture (after filtration) revealed as major component $MoO(O\text{-}2\text{-}(allyl)C_6H_4)_2Cl_2$ (**3.2f**), and a little HO-2-(allyl)C_6H_4. Attempts to recrystallize **7f** at -35 °C from Et_2O, pentane, hexane, or mixtures of solvents, were unsuccessful. Formation of $MoO(O\text{-}2\text{-}(allyl)C_6H_4)_2Cl_2$ (**3.2f**) is not observed if Et_2O is used as reaction solvent. $MoO(O\text{-}2\text{-}(allyl)C_6H_4)_2Cl_2$ was isolated from a different reaction (refer to section 3.2.2.4).

$MoO(O\text{-}2\text{-}(allyl)\text{-}6\text{-}MeC_6H_3)_2Cl_2$ (3.2g): HO-2-(allyl)-6-MeC_6H_3 (0.15 mL, 1.0 mmol) and MoO_2Cl_2 (0.1000 g, 0.5029 mmol) were dissolved, each in 10 mL of pentane. The aryl alcohol solution was added dropwise to the light blue MoO_2Cl_2 solution with rapid stirring at room temperature, forming a dark blue solution. After 12 h, the reaction mixture was filtered through a medium pore sintered glass frit and the volatiles were removed under vacuum. A ^1H NMR spectrum of the crude reaction mixture (after filtration) revealed three major components; $MoO(O\text{-}2\text{-}(allyl)\text{-}6\text{-}MeC_6H_3)_2Cl_2$ (**3.2g**), HO-2-(allyl)-4-MeC_6H_3 and possibly $MoO(O\text{-}2\text{-}(allyl)\text{-}6\text{-}MeC_6H_3)_3Cl$. The solid was dried under vacuum. Pentane (10 mL) and 5 drops of THF were added to the dark blue solid. After 2 weeks of storage at -35 °C a crystalline precipitate was observed. The supernatant was withdrawn and the solid dried under vacuum. Yield 0.0719 g (30%). The resulting product was sticky and hard to fit into a capillary tube for melting point measurement. ^1H NMR ($CDCl_3$): δ 7.12 (two overlapping doublets: 4H, aromatic *H*), 7.01 (m, 2H, *J* = 7.5 Hz), 5.99 (m, 2H, $H_2C{=}CHCH_2$-), 5.15 (m, 4H, $H_2C{=}CHCH_2$-), 3.60 (d, 4H, *J* = 6.3, $H_2C{=}CHCH_2$-), 2.50 (s, 6H, CH_3). $^{13}C\{^1H\}$ NMR ($CDCl_3$): δ 168.0 (*ipso C*), 135.2 ($H_2C{=}CHCH_2$-),

134.1 (*meta* C), 132.8 (*ortho C,* next to allyl), 129.2 (*meta C*), 128.7 (*ortho*, next to Me), 127.1 (*para C*), 116.9 (H_2C=CHCH$_2$-), 34.8 (H_2C=CHCH$_2$-), 17.4 (CH$_3$). UV-vis (C_6H_6) λ_{max}/nm (ε/dm^{3}mol^{-1}cm^{-1}): 280 (5120), 742 (3030). Mass spectrometric analysis was performed with unsatisfactory results.

MoO(O-2,6-^{t}Bu$_2$C$_6$H$_3$)$_2$Cl$_2$ (3.2i): HO-2,6-^{t}Bu$_2$C$_6$H$_3$ (0.2075 g, 1.006 mmol) and MoO_2Cl_2 (0.1000 g, 0.5029 mmol) were dissolved, each in 10 mL of Et_2O. The aryl alcohol solution was added dropwise to the light blue MoO_2Cl_2 solution with rapid stirring at room temperature, immediately affording a green solution. After 12 h, a sample was taken and dried under vacuum for NMR analysis. The ^{1}H NMR spectrum revealed just starting material. Product **3.2i** was not observed. Heating in pentane at 40 ^{o}C for 12 h was performed with no success.

MoO(O-2,6-^{t}Bu$_2$-4-(OMe)C$_6$H$_2$)$_2$Cl$_2$ (3.2j): HO-2,6-^{t}Bu$_2$-4-(OMe)C$_6$H$_2$ (0.2377 g, 1.006 mmol) and MoO_2Cl_2 (0.1000 g, 0.5029 mmol) were dissolved, each in 10 mL of Et_2O. The aryl alcohol solution was added dropwise to the light blue MoO_2Cl_2 solution with rapid stirring at room temperature, immediately affording a dark blue solution. After 12 h, a sample was taken and dried under vacuum for NMR analysis. The ^{1}H NMR spectrum revealed just starting material. Product **3.2j** was not observed. Heating in pentane at 40 ^{o}C for 12 h was performed with no success. MoO(O-2,6-^{t}Bu$_2$-4-(OMe)C$_6$H$_2$)$_2$Cl$_2$ (**3.2j**) was isolated from a different reaction (refer to section 3.2.2.4).

MoO(O-2,6-Me$_2$-4-(NO$_2$)C$_6$H$_2$)$_2$Cl$_2$ (3.2k): HO-2,6-Me$_2$-4-(NO$_2$)C$_6$H$_2$ (0.1681 g, 1.006 mmol) and MoO_2Cl_2 (0.1000 g, 0.5029 mmol) were dissolved, each in 10 mL of pentane. The aryl alcohol solution was added dropwise to the light blue MoO_2Cl_2 suspension with rapid stirring at room temperature. After 24 h, a sample was taken and dried under vacuum for NMR analysis. The ^{1}H NMR spectrum revealed just starting material. Et_2O and benzene with heating to 75 ^{o}C were tried without success. Product **3.2k** was not observed.

3.2.2.3 Reactions between MoO_2Cl_2 and bidentate phenols (biphenol and catechol)

[Mo(O)Cl]$_2${[μ-rac-BIPHEN(O)$_2$-κ^2*O:O'*]$_2$-(μ-O)} (3.7): Method A. rac-BIPHEN(OH)$_2$ (0.1782 g, 0.5026 mmol) and MoO_2Cl_2 (0.1000 g, 0.5029 mmol) were dissolved, each in 10 mL of pentane. The aryl alcohol solution was added dropwise to the light blue MoO_2Cl_2 suspension with rapid stirring at room temperature to form a dark blue solution, then heated at 40 ^oC for 12 h. After 12 h, an aliquot was taken from the dark blue reaction mixture for NMR analysis. The ^1H NMR spectrum of the crude reaction mixture revealed two major components; rac-BIPHEN(OH)$_2$ and possibly Mo(O)(OH)[rac-BIPHEN(O)(OH)]Cl$_2$ (**3.6**). Attempts to purify **3.6** by recrystallization or reprecipitation from concentrated or dilute solutions in Et_2O, pentane, hexane or any other solvent mixtures at -35 ^oC were unsuccessful. The reaction mixture containing **3.6** was stored in pentane (15 mL) at -35 ^oC. After 2 months, vapor deposited dark blue solid was observed in the walls of the container. The supernatant was withdrawn with a pipette and the solid dried under vacuum. The ^1H NMR spectrum of the solid revealed formation of [Mo(O)Cl]$_2${[μ-rac-BIPHEN(O)$_2$-κ^2*O:O'*]$_2$-(μ-O)} (**3.7**). A ^1H NMR spectrum of the supernatant revealed two major components; [rac-BIPHEN(OH)$_2$] and [Mo(O)Cl]$_2${[μ-rac-BIPHEN(O)$_2$-κ^2*O:O'*]$_2$(μ-O)} (**3.7**). Method A yielded 0.0245 g (10%) of [Mo(O)Cl]$_2${[μ-rac-BIPHEN(O)$_2$-κ^2*O:O'*]$_2$(μ-O)} (**3.7**).

Method B. rac-BIPHEN(OH)$_2$ (0.1782 g, 0.5026 mmol) and MoO_2Cl_2 (0.1000 g, 0.503 mmol) were dissolved, each in 10 mL of pentane. The aryl alcohol solution was added dropwise to the light blue MoO_2Cl_2 suspension with rapid stirring at room temperature to form a dark blue solution, then heated at 40 ^oC. After 12 h, stirring was stopped and the volatiles were removed under vacuum. The dry dark blue mass was transferred to a sublimator apparatus. Sublimation was accomplished by heating at 100 ^oC using a dynamic vacuum of 0.1 mm Hg. Liquid nitrogen was used as cooling agent. After 30 minutes heating and vacuum were stopped and the little dark blue crystals deposited in the cold finger were rinsed out with pentane. Pentane was evaporated under vacuum and a ^1H NMR spectrum identified this solid to be [Mo(O)Cl]$_2${[μ-rac-

BIPHEN(O)$_2$-κ^2*O:O'*]$_2$(μ-O)} (**3.7**). Method B yielded 0.0142 g (6%) of [Mo(O)Cl]$_2${[μ-rac-BIPHEN(O)$_2$-κ^2*O:O'*]$_2$-(μ-O)} (**3.7**). Mo(O)(OH)[rac-BIPHEN(O)(OH)]Cl$_2$ (**3.6**); ^{1}H NMR ($CDCl_3$): δ 7.33 (s, 1H, aromatic *H*), 7.21 (s, 1H, aromatic *H*), 4.60 (s, 1H, Mo(O)(O*H*)), 3.06 (s, 3H, CH_3), 2.77 (s, 1H, rac-BIPHEN(O*H*)), 1.89 (s, 3H, CH_3), 1.63 (s, 3H, CH_3), 1.51 (s, 9H, C(CH_3)$_3$), 1.50 (s, 3H, CH_3), 1.38 (s, 9H, C(CH_3)$_3$). [Mo(O)Cl]$_2${[μ-rac-BIPHEN(O)$_2$-κ^2*O:O'*]$_2$(μ-O)} (**3.7**); ^{1}H NMR ($CDCl_3$): δ 7.01 (s, 2H, aromatic *H*), 6.98 (s, 2H, aromatic *H*), 2.45 (s, 6H, CH_3), 2.21 (s, 6H, CH_3), 1.61 (s, 6H, CH_3), 1.56 (s, 6H, CH_3), 1.29 (s, 18H, C(CH_3)$_3$), 1.06 (s, 9H, C(CH_3)$_3$). ^{13}C{^{1}H} NMR ($CDCl_3$): δ 170.0 (*ipso C*), 164.6 (*ipso C*), 140.5 (*ortho C,* next to C(CH_3)$_3$), 139.0 (*ortho C,* next to C(CH_3)$_3$), 137.3 (*para* C), 137.2 (*para* C), 135.8 (*meta* C), 134.6 (*meta* C), 133.1 (*ortho C,* next to C-C bridge), 129.3 (*ortho C,* next to C-C bridge), 128.7 (*meta* C, next to CH_3), 126.1 (*meta* C, next to CH_3), 34.5 (*C*(CH_3)$_3$), 34.4 (*C*(CH_3)$_3$), 30.9 (C(*C*H$_3$)$_3$), 30.4 (*C*(*C*H$_3$)$_3$), 21.4 (*C*H$_3$), 20.4 (*C*H$_3$), 17.8 (*C*H$_3$), 16.4 (*C*H$_3$). IR (cm^{-1}, KBr): 2958s, 2915sh, 2869sh, 1576s, 1539w, 1456s, 1362s, 1251w, 1220vs, 1165m, 1047vs, 970vs (Mo=O), 924w, 877m, 802m, 737vs (Mo-O-Mo). UV-vis (C_6H_6) λ_{max}/nm (ε/dm^{3}mol^{-1}cm^{-1}): 278 (14112), 349 (8629), 672 (11343). X-ray quality crystals of [Mo(O)Cl]$_2${[μ-rac-BIPHEN(O)$_2$-κ^2*O:O'*]$_2$(μ-O)} (**3.7**) were obtained from a concentrated solution in Et_2O at -35 ^{o}C after 2 weeks. The crystals were formed by vapor deposition of solid in the walls of the container.

Mo(O)Cl($C_6H_4O_2$-κ^2*O,O'*)(C_6H_4O(OH)-κ^2*O,O'*)·Et_2O (3.8): Catechol (0.0553 g, 0.5029 mmol) and MoO_2Cl_2 (0.1000 g, 0.5029 mmol) were dissolved, each in 10 mL of pentane. The catechol solution was added dropwise to the light blue MoO_2Cl_2 solution with rapid stirring at room temperature, forming a dark red solution. After 12 h, the reaction mixture was concentrated to approximately 5 mL and stored at -35 ^{o}C. After 2 days, crystalline dark red precipitate was observed. The supernatant was withdrawn and the solid dried under vacuum. Yield 0.0578 g (53%). ^{1}H NMR ($CDCl_3$): δ 7.34-7.12 (m, 4H, aromatic *H*), 6.88 (dd, 2H, *J* = 3.6 and 6.3 Hz, aromatic *H*), 6.55 (dd, 2H, *J* = 3.6 and 6.3 Hz, aromatic *H*), 2.34 (s, 1H, O*H*). ^{13}C{^{1}H} NMR ($CDCl_3$): δ 158.5 (aromatic *C*, next to O), 156.6 (aromatic *C*, next to O), 153.3

(aromatic *C*, next to O), 149.7 (aromatic *C*, next to O), 130.0 (aromatic *C*), 123.6 (aromatic *C*), 123.1 (aromatic *C*), 122.4 (aromatic *C*), 118.6 (aromatic *C*), 114.4 (aromatic *C*), 114.0 (aromatic *C*), 113.8 (aromatic *C*). IR (cm^{-1}, KBr): 1580s, 1455s, 1247s, 1147m, 1100m, 965s (Mo=O), 802m, 760sh, 747s, 659m. UV-vis (C_6H_6) λ_{max}/nm ($\varepsilon/dm^3mol^{-1}cm^{-1}$): 319 (48388), 485 (84304), 804 (28220). X-ray quality crystals were obtained from a concentrated solution in Et_2O of **3.8** at -35 ^oC after 1 week. The crystals were formed by vapor deposition of solid in the walls of the container.

3.2.2.4 Reactions between MoO_2Cl_2 and lithium aryloxides

3.2.2.4.1 Reactions in a 1:2 MoO_2Cl_2:LiOAr ratio

$MoO(O\text{-}2,4\text{-}Me_2C_6H_3)_3Cl$ (3.3a): LiO-2,6-$Me_2C_6H_3$ (**3.1a**) (0.1288 g, 1.006 mmol) and MoO_2Cl_2 (0.1000 g, 0.5029 mmol) were dissolved, each in 10 mL of Et_2O. The lithium aryloxide solution was added dropwise to the light blue MoO_2Cl_2 solution with rapid stirring at room temperature. After 12 h, a sample was taken for ^1H NMR analysis. The ^1H NMR spectrum of the dark blue crude reaction mixture revealed the quantitative formation of $MoO(O\text{-}2,4\text{-}Me_2C_6H_3)_3Cl$ (**3.3a**). The reaction mixture was filtered through a medium pore glass sintered filter and concentrated under vacuum to approximately 5 mL. The concentrated dark blue solution was kept at -35 ^oC. After 5 days dark blue crystalline solid was formed. The supernatant was withdrawn and the solid dried under vacuum. The ^1H NMR spectrum of the solid confirmed it to be $MoO(O\text{-}2,4\text{-}Me_2C_6H_3)_3Cl$ (**3.3a**). The ^1H NMR data matched those reported in the literature.[81]

Other lithium aryloxides were explored using these reaction conditions: LiO-2,4-$Me_2C_6H_3$ (**3.1b**), LiO-2-^{t}Bu-4-MeC_6H_3 (**3.1d**), LiO-2-^{t}Bu-4-MeC_6H_3 (**3.1d**), and LiO-2-^{t}Bu-6-MeC_6H_3 (**3.1e**); yielding the $MoO(OAr)_2Cl_2$ products described in section 3.2.2.2. LiO-2-(allyl)-6-MeC_6H_3 (**3.1g**) forms a mixture of $MoO(O\text{-}2\text{-}(allyl)\text{-}6\text{-}MeC_6H_3)_2Cl_2$ (**3.2g**) and possibly $MoO(O\text{-}2\text{-}(allyl)\text{-}6\text{-}MeC_6H_3)_3Cl$.

$MoO(O\text{-}2\text{-}(allyl)C_6H_4)_2Cl_2$ (3.2f): LiO-2-(allyl)C_6H_4 (**3.1f**) (0.1409 g, 1.006 mmol) and MoO_2Cl_2 (0.1000 g, 0.5029 mmol) were dissolved, each in 10 mL of DME. The aryl alcohol solution was added dropwise to the light blue MoO_2Cl_2 solution with rapid stirring at room temperature affording a bright orange solution. After 12 h, the stirring was stopped and the volatiles were removed under vacuum leaving behind a dark mass. A ^{1}H NMR spectrum of the crude reaction mixture revealed two major components; $MoO(O\text{-}2\text{-}(allyl)C_6H_4)_2Cl_2$ (**3.2f**) and HO-2-(allyl)C_6H_4. Pentane (20 mL) was added to the dark mass and the mixture was stirred for 6 hours. The dark suspension was filtered through a medium pore sintered glass filter. The filtrate was dried under vacuum and Et_2O (15 mL) was added. The resulting dark blue solution was stored at -35 ^{o}C. After 1 week crystalline solid was observed, the supernatant was withdrawn with a pipette and the solid dried under reduced pressure (when Et_2O, hexane and pentane were used as reaction solvents, product **3.2f** and aryl alcohol were observed, but isolation only could be accomplished in DME). Yield 0.0789 g (35%), m.p. = 138-141 ^{o}C ^{1}H NMR ($CDCl_3$): δ 7.30 (dd, 2H, *J* = 1.2 and 7.5 Hz, aromatic *H*), 6.89 (m, 4H, aromatic *H*), 6.65 (td, *J* = 1.2 and 7.5 Hz, 2H, aromatic *H*), 5.78 (m, 2H, CH_2=C*H*-CH_2-), 4.99 (m, 4H, C*H*$_2$=CH-CH_2-), 2.79 (d, 4H, *J* = 6.3 Hz, CH_2=CH-C*H*$_2$-). ^{13}C{^{1}H} NMR ($CDCl_3$): δ 162.5 (*ipso C*), 136.4 (CH_2=*C*H-CH_2-), 129.5 (*meta* C), 129.2 (*ortho C*, next to allyl), 127.2 (*meta C*), 124.5 (*para C*), 120.7 (*C*H_2=CH-CH_2-), 116.0 (*ortho C*), 34.3 (CH_2=CH-*C*H_2-). IR (cm^{-1}, KBr): 3485br, 2960m, 2920m, 1630m, 1583w, 1471s, 1260s, 1194s, 1093m, 1024w, 982s (Mo=O), 915s, 773sh, 748sh, 563m. UV-vis (C_6H_6) λ_{max}/nm (ε/dm^{3}mol^{-1}cm^{-1}): 295 (2677), 326 (2866), 336 (2904), 697 (11202).

3.2.2.4.2 Reactions in a 1:4 MoO_2Cl_2:LiOAr ratio in “wet hexane”

$MoO(O\text{-}2,4\text{-}Me_2C_6H_3)_4$ (3.4a): LiO-2,6-$Me_2C_6H_3$ (**3.1a**) (0.2577 g, 2.012 mmol) and MoO_2Cl_2 (0.1000 g, 0.5029 mmol) were suspended, each in 10 mL of wet hexane. The lithium aryloxide suspension was added dropwise to the light blue MoO_2Cl_2 suspension with rapid

stirring at room temperature. The reaction mixture turned dark blue slowly as the reaction progressed. After 12 h, a sample was taken for ^{1}H NMR analysis. The ^{1}H NMR spectrum of the dark blue crude reaction mixture revealed the formation of MoO(O-2,4-$Me_2C_6H_3)_4$ (**9a**). The reaction mixture was filtered through a medium pore glass sintered filter and concentrated under vacuum to approximately 5 mL. The concentrated dark blue solution was kept at -35 °C. After 5 days dark blue crystalline solid was formed. The supernatant was withdrawn and the solid dried under vacuum. The ^{1}H NMR spectrum of the solid confirmed this solid to be MoO(O-2,4-$Me_2C_6H_3)_4$ (**9a**). m.p. 170-172 °C. ^{1}H NMR (C_6D_6): δ 6.99 (d, 8H, *J* = 7.5 Hz, aromatic *H*), 6.70 (t, 4H, *J* = 7.5 Hz, aromatic *H*), 2.16 (s, 24H, C*H*$_3$). ^{13}C{^{1}H} NMR ($CDCl_3$): δ 128.9 (*meta C*), 124.5 (*para C*), 117.2 (*ortho C*). *Ipso C* was not observed probably due to dilute sample. IR (cm^{-1}, C_6H_6): 3229m, 3085m, 2974w, 2382w, 2275vs, 1973w, 1612m, 1447m, 1325s, 1030m (Mo=O), 810vs, 662m, 484m. UV-vis (C_6H_6) λ_{max}/nm (ε/dm^{3}mol^{-1}cm^{-1}): 276 (3894), 325 (4922), 618 (7552). Anal. Calcd. for $C_{32}H_{36}O_5Mo$: C, 64.03; H, 6.08. Found: C, 61.41; H, 5.47. If 1 equiv of Li_2O is added: Anal. Calcd. for $C_{32}H_{36}Li_2O_6Mo$: C, 61.35; H, 5.79. Found: C, 61.41; H, 5.47.

Other synthetic alternatives for this compound were explored: reactions of MoO(O-2,4-$Me_2C_6H_3)_2Cl_2$ (**3.2a**) + 2 quiv of LiO-2,4-$Me_2C_6H_3$ (**3.1a**); MoO(O-2,4-$Me_2C_6H_3)_3Cl$ (**3.2a**) + 1 equiv of LiO-2,4-$Me_2C_6H_3$ (**3.1a**); $MoO(OEt)_4$ + 4/5/6 HO-2,4-$Me_2C_6H_3$; and $MoOCl_4$ + 4 equiv of LiO-2,4-$Me_2C_6H_3$ (**3.1a**) in different solvents and reaction conditions. These alternatives yielded mixtures of the aryl alcohol, di- (**3.2a**), and tri-aryloxy (**3.3a**) monooxo complexes.

MoO(O-2-^{t}BuC$_6$H$_4$)$_4$ (3.4c): LiO-2-^{t}BuC_6H_4 (**6a**) (0.3141 g, 2.012 mmol) and MoO_2Cl_2 (0.1000 g, 0.5029 mmol) were suspended, each in 10 mL of wet hexane. The lithium aryloxide solution was added dropwise to the light blue MoO_2Cl_2 suspension with rapid stirring at room temperature. The reaction mixture turned dark blue slowly as the reaction progressed. After 12 h, a sample was taken for ^{1}H NMR analysis. The ^{1}H NMR spectrum of the dark blue crude reaction mixture revealed the possible formation of MoO(O-2-^{t}Bu$C_6H_4)_4$ (**3.4c**). The reaction mixture was filtered through a medium pore glass sintered filter and concentrated under vacuum

to approximately 3 mL. The concentrated dark blue solution was kept at -35 °C. After 5 days dark solid was formed. The supernatant was withdrawn and the solid dried under vacuum. The yield was poor after the first recrystallization; only NMR analyses were obtained. ^{1}H NMR ($CDCl_3$): δ 7.17 (d, 4H, *J* = 7.8 Hz, aromatic *H*), 7.09 (d, 4H, *J* = 7.8 Hz, aromatic *H*), 7.00 (t, 4H, *J* = 6.9 Hz, aromatic *H*), 6.82 (t, 4H, *J* = 7.2 Hz, aromatic *H*), 1.23 (s, 36H, C(C*H*$_3$)$_3$). ^{13}C{^{1}H} NMR ($CDCl_3$): δ 163.35 (*ipso C*), 138.45 (*ortho C*, next to ^{t}Bu), 127.05 (*meta C*), 126.23 (*meta C*), 124.06 (*para C*), 123.70 (*ortho C*), 34.90 (*C*(CH$_3$)$_3$), 30.06 (C(*C*H$_3$)$_3$).

3.2.2.4.3 Reactions between LiOAr and $MoOCl_4$

$MoO(O\text{-}2,6\text{-}^{t}Bu_2\text{-}4\text{-}(OMe)C_6H_2)_2Cl_2$ (3.2j): LiO-2,6-^{t}Bu$_2$-4-(OMe)C$_6$H$_2$ (**3.1j**) (0.0955 g, 0.394 mmol) and $MoOCl_4$ (0.0500 g, 0.197 mmol) were dissolved, each in 10 mL of Et_2O. The lithium aryloxide solution was added dropwise to the dark red $MoOCl_4$ solution with rapid stirring at room temperature. The reaction mixture turned dark red. After 12 h, stirring was stopped and an aliquot was taken for NMR analysis. The ^{1}H NMR spectrum of the crude reaction mixture revealed two major components; MoO(O-2,6-^{t}Bu$_2$-4-(OMe)C$_6$H$_2$)$_2$Cl$_2$ (**3.1j**) and HO-2,6-^{t}Bu$_2$-4-(OMe)C$_6$H$_2$. The reaction mixture was concentrated under vacuum to approximately 5 mL and stored at -35 °C. After 1 day, dark purple precipitate was observed, then separated from the supernatant by centrifugation. Yield: 0.0651 g, (51%), m. p. 189-192 °C. ^{1}H NMR ($CDCl_3$): δ 6.87 (d, 2H, *J* = 2.7 Hz, aromatic *H*), 6.82 (d, 2H, *J* = 2.7 Hz, aromatic *H*), 3.90 (s, 6H, OC*H*$_3$,), 1.64 (s, 18H, C(C*H*$_3$)$_3$), 1.46 (s, 18H, C(C*H*$_3$)$_3$). ^{13}C{^{1}H} NMR ($CDCl_3$): δ 169.9 (*para C*), 158.7 (*ipso C*), 149.2 (*ortho C*), 148.5 (*ortho C*), 111.2 (*meta C*), 111.0 (*meta C*), 55.4 (O*C*H$_3$), 37.0 (*C*(CH$_3$)$_3$), 36.3 (*C*(CH$_3$)$_3$), 34.0 (C(*C*H$_3$)$_3$), 30.7 (C(*C*H$_3$)$_3$). IR (cm^{-1}, KBr): 3455br, 2966w, 2929w, 1584vs, 1286s, 1221s, 1142s, 1103w, 1059w, 1014w, 999w, 939m (possibly Mo=O), 887m, 873w, 850m, 758m, 653m, 575m. UV-vis (C_6H_6) λ_{max}/nm (ε/dm^{3}mol^{-1}cm^{-1}): 289 (8061), 543 (3170), 621(2427), 923 (27860). The proposed structure was confirmed by low resolution mass spectrometry (FAB), refer to the appendix of this chapter.

Use of LiO-2,6-$^{t}Bu_2C_6H_3$ and LiO-2,6-Me_2-4-$(NO_2)C_6H_2$ was explored under these reaction conditions; but only formation of phenol was observed by ^{1}H NMR.

3.2.2.5 Reactions between LiOAr and $MoO_2Cl_2(DMF)_2$

$MoO(O\text{-}2\text{-}(allyl)C_6H_4)_4(DMF)$ (3.5f): A solution of LiO-2-(allyl)C_6H_4 (0.1218 g, 0.8695 mmol) in 10 mL of Et_2O was added dropwise to a stirring suspension of $MoO_2Cl_2(DMF)_2$ (0.3000 g, 0.8695 mmol) in 10 mL of Et_2O at room temperature. After 12 h stirring was stopped and the volatiles were removed under vacuum. Hexane (15 mL) was added to the dry dark mass and the mixture was stirred for 5 hours at room temperature. The resulting suspension was filtered through a medium pore frit to separate the insoluble and unreacted $MoO_2Cl_2(DMF)_2$ from the reaction products. The filtrate was concentrated under vacuum to ca. 5 mL and stored at -35 ^{o}C. After 5 days dark crystals were observed in the bottom and walls of the vial. The supernatant was withdrawn with a pipette, and some crystals were separated for X-ray diffraction; the rest were dried under reduced pressure. The dried solid was identified as MoO(O-2-(allyl)$C_6H_4)_4$(DMF) (**2.5f**). Yield 0.0099 g (7%). ^{1}H NMR ($CDCl_3$): δ 7.95 (s, 1H, H of DMF), 7.15 (d, 4H, *J* = 7.8 Hz, aromatic *H*), 7.04 (m, 8H, aromatic *H*), 6.82 (t, 4H, *J* = 0.9 and 6.7 Hz, aromatic *H*), 5.78 (m, 4H, CH_2=C*H*CH_2-), 4.92 (m, 8H, C*H*$_2$=CHCH_2-), 3.18 (d, 8H, J = 6 Hz, CH_2=CHC*H*$_2$-), 2.87 (s, 3H, C*H*$_3$ of DMF), 2.82 (s, 3H, C*H*$_3$ of DMF). ^{13}C{^{1}H} NMR ($CDCl_3$): δ 165.1 (*C*=O of DMF), 163.3 (*ipso C*), 137.2 (CH_2=*C*HCH_2-), 129.3 (*ortho C*, next to allyl), 129.0 (meta C), 127.2 (para C), 123.0 (meta C), 120.2 (ortho C), 115.3 (*C*H_2=CHCH_2-), 37.6 (*C*H_3 of DMF), 34.4 (CH_2=CH*C*H_2-), 32.5 (CH_3 of DMF). IR (cm^{-1}, KBr): 3435br, 3064w, 2967w, 2912w, 1657sh, 1647vs, 1519sh, 1477w, 1456m, 1448m, 1368m, 1226vs, 1108w, 1103w, 1034w, 999w (possibly Mo=O) 935w, 912w, 875w, 798w, 756s, 683w, 657m, 632w. UV-vis (C_6H_6) λ_{max}/nm (ε/dm^{3}mol^{-1}cm^{-1}): 281 (5507), 346 (7433), 570 (2589).

$MoO(O\text{-}2,6\text{-}^{i}Pr_2C_6H_3)_3(DMF)Cl$ (3.5h): A solution of LiO-2,6-$^{i}Pr_2C_6H_3$ (0.1602 g, 0.8697 mmol) in 10 mL of Et_2O was added dropwise to a stirring suspension of $MoO_2Cl_2(DMF)_2$ (0.3000

g, 0.8695 mmol) in 10 mL of Et_2O at room temperature. After 12 h stirring was stopped and the reaction was filtered through a medium pore frit to separate the insoluble and unreacted $MoO_2Cl_2(DMF)_2$ from the reaction products. The resulting ethereal reaction mixture was concentrated under vacuum to ca. 15 mL and stored at -35 °C. After 3 days a small amount of dark blue crystals was observed. The supernatant was withdrawn, and the crystals inspected by X-ray diffraction. The crystals were identified as $MoO(O\text{-}2,6\text{-}^{i}Pr_2C_6H_3)_3(DMF)Cl$ (**3.5h**). The supernatant was deposited in a separate vial and stored at -35 °C. After 2 weeks a greenish precipitate was observed. The supernatant was removed and the solid dried under vacuum. The solid was identified as $MoO_2(O\text{-}2,6\text{-}^{i}Pr_2C_6H_3)_2(DMF)$ (**2.5k**) by ^1H NMR spectroscopy (refer to chapter 2). Purification of $MoO(O\text{-}2,6\text{-}^{i}Pr_2C_6H_3)_3Cl$ via recrystallization from Et_2O, hexanes or pentane was unsuccessful; it appears as a mixture of $MoO(O\text{-}2,6\text{-}^{i}Pr_2C_6H_3)_3Cl$ and $MoO_2(O\text{-}2,6\text{-}^{i}Pr_2C_6H_3)_2(DMF)$ (**2.5k**). ^1H NMR ($CDCl_3$): δ 7.97 (s, 1H, H of DMF), 7.11-6.92 (m, 9H, aromatic *H*), 3.69 (m, *J* = 6.9 Hz , 2H, C*H*$(CH_3)_2$), 3.38 (m, *J* = 6.9 Hz , 4H, C*H*$(CH_3)_2$), 2.93 (s, 3H, CH_3 of DMF), 2.75 (s, 3H, CH_3 of DMF), 1.28 (d, 24H, *J* = 6.6 Hz, CH(C$H_3)_2$), 1.13 (d, 12H, *J* = 6.6, CH(C$H_3)_2$).

3.3 Results and discussion

Although MoO^{4+} complexes are known, they are less numerous than those that feature the MoO_2^{2+} unit. The simplest set of complexes that contain the MoO^{4+} core is the $MoOX_4$ group (X = F, Cl, Br).[145]

MoO^{4+} complexes are stabilized by ligands that are good σ and π donors, enabling the transfer of sufficient charge density to the electronically deficient Mo^{VI} center. Ligands with nonbonding filled p orbitals are preferred, predominantly oxygen-,[138, 146, 148, 170, 171] nitrogen-,[80, 172, 173] and sulfur-based ligands.[80, 174] MoO^{4+} complexes almost always exhibit coordination numbers seven and five in a pentagonal bipyramidal or square pyramidal geometry, respectively.[80, 170]

Molybdenum(VI) monooxo alkoxides are of interest because of their potential use as molecular precursors for high purity metal oxides using sol–gel, metal-organic chemical vapor deposition (MOCVD) or metalorganic decomposition (MOD) technologies.[146, 175] Molybdenum alkoxides and oxo alkoxides have been proposed to serve as models for metal oxides,[176, 177] making these molecules suitable targets of study.

Despite their versatility, Mo(VI) oxo alkoxides are unstable. They have a significant tendency to disproportionate via ether elimination, they are highly sensitive to hydrolysis,[146] and they are prone to dimerization and/or polymerization.[153, 169] The isolation and characterization of mononuclear oxo alkoxide complexes is a difficult task.[146] The use of aryloxide groups might circumvent these difficulties without sacrificing the stability that the oxygen π-donor ligand conveys to the Mo(VI) center.

In the field of group (VI) oxo aryloxides, monooxo complexes $WO(OAr)_{4-n}Cl_n$ have been demonstrated to be suitable procatalysts for ROMP metathesis.[77, 159, 178] They are prepared by reacting the commercially available $WOCl_4$ with either aryl alcohol or its anion.[77, 162, 163] For the molybdenum analogues, there is only one entry in the literature, other than our report.[81] Hayano et al. reported the synthesis of $MoO(OAr)_4$ for several mono- and multidentate aryloxy ligands by the low-temperature reaction of $MoOCl_4$ with the corresponding aryloxy anions. They demonstrated that their $MoO(OAr)_4$ complexes could serve as procatalysts for metathesis polymerization.[79]

Our interest in Mo(VI) monooxo aryloxides is in the production of molecules that can be used as:

1) molecular precursors to produce high purity inorganic materials. Mo(VI) oxo aryloxides might permit a better and more versatile control over the composition, structure and morphology of the inorganic materials produced,
2) models that can lead to a better mechanistic understanding of chemical transformations, e.g. the SOHIO process[21, 38]or olefin metathesis reaction,[157] and

3) cost effective complexes for use in catalytic processes such as C-H activation, oxygen transfer, epoxidation, etc.

Molybdenum(VI) and tungsten(VI) monooxo complexes have been demonstrated to be suitable compounds for catalysis.[157] Following this trend, we intend to produce prospective catalyst precursors with tunable attributes of stability, reactivity, and good selectivity. In this sense, the use of bulky aryloxide ligands has certain advantages over the alkoxides:[77]

1) the solubility of the complex can be controlled by the aryloxide ligand and its substituents,
2) bulky aryloxide ligands avoid catalyst decomposition pathways that involve the dimerization of the metal centers.
3) the ligands sculpt the shape of the reaction site by means of their steric bulk, and
4) the electronic character of the reaction site can be tuned by variation of the electronic nature of the substituents in the the aryloxide ligand.

As noted above, synthesis of some $MoO(OAr)_4$ complexes has already been accomplished;[79] but the proposed methodology is inconvenient and it was observed by us that in one case the identity of the final product was mistaken. In contrast, we propose the facile synthesis of different $MoO(OAr)_{4-n}Cl_n$ with n = 2, 1 and 0, starting from the more stable MoO_2Cl_2 and $MoO_2Cl_2(DMF)_2$ precursors. The extent of aryloxide substitution in the final product might impact its final reactivity and selectivity towards the substrate. Our methodology led to products with different degrees of aryloxide substitution at the MoO^{4+} center in a relatively general process.

3.3.1 Synthesis of products and reaction mechanisms

3.3.1.1 Products from addition of mono and bidentate aryl alcohols to MoO_2Cl_2

The $MoO(OAr)_{4-n}Cl_n$ complexes described in this chapter were prepared by the reaction of MoO_2Cl_2 with various aryl alcohols or their lithium aryloxides in nonpolar solvents (preferably Et_2O or pentane). Different degrees of aryloxide substitution in the MoO^{4+} core were reached by changing the nature of the ligand starting material and its stoichiometry.

Previously our research group reported that the reaction of a suspension of MoO_2Cl_2 with 1 equiv of LiO-2,6-$Me_2C_6H_3$ in ether at room temperature immediately formed a dark blue solution characteristic of d^0 group VI monooxo aryloxides. The resulting product was identified as $MoOCl_2$(O-2,6-$Me_2C_6H_3)_2$ (**3.2a**) (Equation 3.1).[81] It was also noted that there was a cleaner and easier alternative for the preparation of this compound that is the addition of 2 equiv of HO-2,6-$Me_2C_6H_3$ to MoO_2Cl_2 in Et_2O (Equation 3.2).[81]

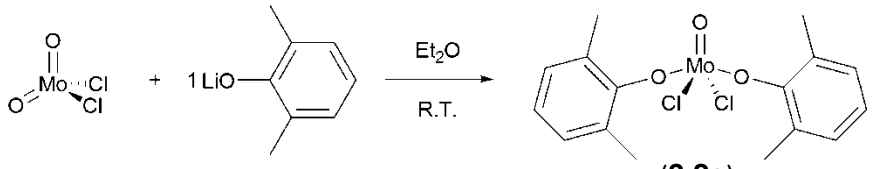

(**3.2a**) (3.1)

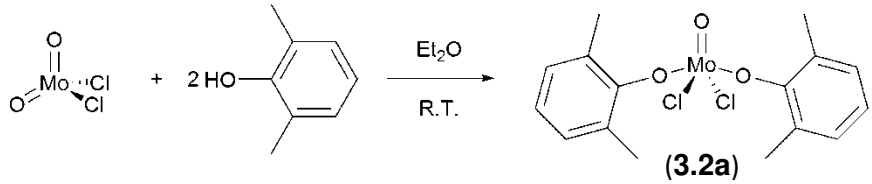

(**3.2a**) (3.2)

The reaction shown in Equation 3.2 appeared to be a convenient way to prepare $MoOCl_2(OAr)_2$ complexes starting from the commercially available MoO_2Cl_2 precursor and different aryl alcohols without the need of preparing the respective lithium aryloxides. The generality of Equation 3.2 was explored using aryl alcohols with different alkyl substituents in different positions of the aromatic ring. In this way compounds **3.2b**-**3.2g** were prepared by addition of the parent aryl alcohol to MoO_2Cl_2 in non-polar solvents such as Et_2O, pentane or hexane, immediately forming dark blue solutions at room temperature. Use of polar solvents

such as CH_3CN or THF prevents the reaction, yielding only aryl alcohol starting material. A summary of the results obtained for this reaction with different aryl alcohol substrates is shown in Scheme 3.1.

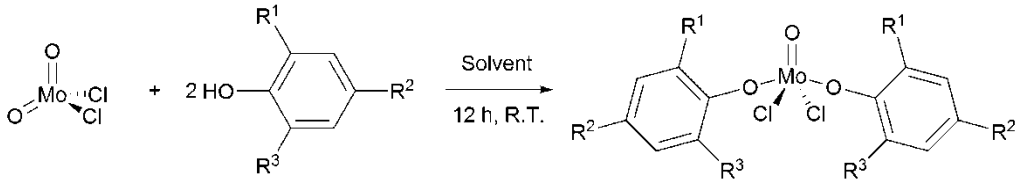

3.2a-g

Label	R^1	R^2	R^3	Solvent	Yield (%)
a	Me	H	Me	Et_2O	49
b	Me	Me	H	Hexane	39
c	^{t}Bu	H	H	Et_2O	NMR only
d	^{t}Bu	Me	H	Hexane	39
e	^{t}Bu	H	Me	Et_2O	NMR only
f	allyl	H	H	Pentane	NMR only*
g	allyl	H	Me	Pentane	30
i	^{t}Bu	H	^{t}Bu	Et_2O	Not observed
j	^{t}Bu	OMe	^{t}Bu	Et_2O	Not observed
k	Me	NO_2	Me	Et_2O	Not observed

* Isolated from a different reaction.

Scheme 3.1 Reaction of MoO_2Cl_2 with various aryl alcohols.

The synthesis of complexes **3.2a**-**g** is believed to happen via the reaction mechanism shown in Scheme 3.2.

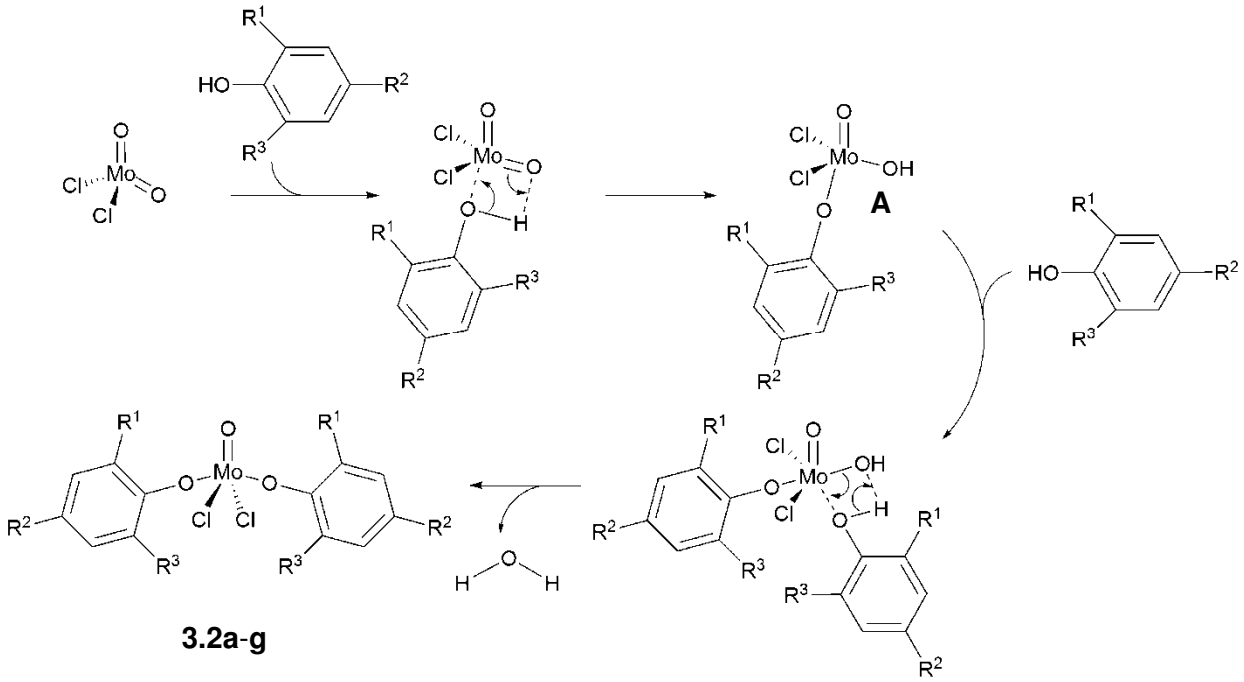

Scheme 3.2 Concerted aryl alcohol addition across the Mo=O bond.

We propose that the formation of $MoOCl_2(OAr)_2$ complexes follows these steps:

1) pre-coordination of the aryl alcohol to the molybdenum center.

   The Mo=O···H-OAr coordination has previously been reported by our research group for the molybdenum dioxo diaryloxide MoO_2(O-2,6-^{t}Bu$_2$C$_6$H$_3$)$_2$ (**2.2a**) (X-ray structure is shown in Chapter 1), which cocrystallizes with 1 equiv of phenol. No evidence of proton transfer was found in that system,[68] probably because the phenol is not acidic enough to protonate the Mo=O unit, and the *tert*-butyl groups are too sterically demanding to allow OH coordination to the molybdenum core.[68] This observation is supported by a similar study by Kühn et al.[179] and by the non-productive attempts to produce molecules **3.2i**-**j** by adding HO-2,6-^{t}Bu$_2$-4-RC$_6$H$_2$ (R = H, OMe) to MoO_2Cl_2 (refer to experimental section and Scheme 3.1).

2) bond metathesis between the coordinated OH group and the Mo=O bond

   A similar associative mechanism has been proposed for the alcoholysis of tungsten(VI) amides,[180] and for the reaction of $MoO_2Cl_2L_2$ with HOO^{t}Bu.[179] The formation of the four-membered metallacycle might additionally be favored by the "spectator oxo group stabilization" (the Mo=O group not involved in the reaction changes from a double to a "virtual" triple bond Mo$\equiv$O. The dotted line represents an acceptor-donor σ bond)[103]

3) formation of the $Mo(O)(OH)Cl_2(OAr)$ intermediate **A** (not isolated).

   Formation of a similar intermediate has been previously proposed by Kühn et al.,[179] and although its identity has just been supported by IR spectroscopy, its feasibility has been supported by DFT calculations.[181] Since protonation of the Mo=O unit is not observed by pure interaction with HO-2,6-^{t}Bu$_2$-4-RC_6H_2 (R = H, OMe), formation of $Mo(O)(OH)Cl_2(OAr)$ necessarily requires the coordination of the aryl alcohol before the Mo=O bond protonates. We proposed that the steric hindrance imposed by the *tert*-butyl groups prevents the correct alignment of the aryl alcohol with respect to the molybdenum center and the reaction does not take place. In the case of HO-2,6-Me_2-4-$(NO_2)C_6H_2$, the steric factor is no longer an issue, but the strong electron withdrawing nature of the *para*-nitro lowers the basicity of the oxygen and makes it unlikely to react.

4) addition of a second molecule of aryl alcohol to the $Mo(O)(OH)Cl_2(OAr)$ intermediate and H_2O side product formation.

   This step has two possible driving forces: a) DFT calculations on the reaction of $MoO_2X_2L_2$ and HOO^{t}Bu have found that the protonation of the Mo=O bond leads to a pronounced increase in the Lewis acidity of the molybdenum center,[181] favoring the Lewis acid-base interaction between $Mo(O)(OH)Cl_2(OAr)$ and HOAr, and b) the formation of the two stable molecules H_2O and $MoOCl_2(OAr)_2$ as reaction products.

Although unusual, the proposed [2+2] addition of the OH group to the Mo=O bond is well-precedented for several metal oxo complexes[182] as well as for other molybdenum-

containing compounds.[151, 183-186] Theoretical studies on the O-H and C-H bond activations by different d^0 transition metal oxo complexes found the [2+2] addition across the oxo bond to be a favorable process.[187, 188]

This theoretical argument is further supported by experimental observations found in the synthesis of complexes **3.6**-**3.8** (Schemes 3.3 and 3.4).

The proposed structure of intermediate **3.6** is analogous to the $Mo(O)(OH)Cl_2(OAr)$ intermediate **A** described in Scheme 3.2. Complex **3.6** is formed by addition of rac-$BIPHEN(OH)_2$ to MoO_2Cl_2 in pentane. This complex was stable enough to attempt its isolation by repeated reprecipitation, and to be detected by ^1H NMR spectrometry (refer to the experimental section). When two units of the intermediate complex **3.6** condense (condensation can be induced by heating or just by allowing them to interact for long enough; refer to the experimental section), formation of the stable and characterized complex **3.7** takes place. The proposed reaction mechanism for the formation of **3.6** and **3.7** is shown in Scheme 3.3.

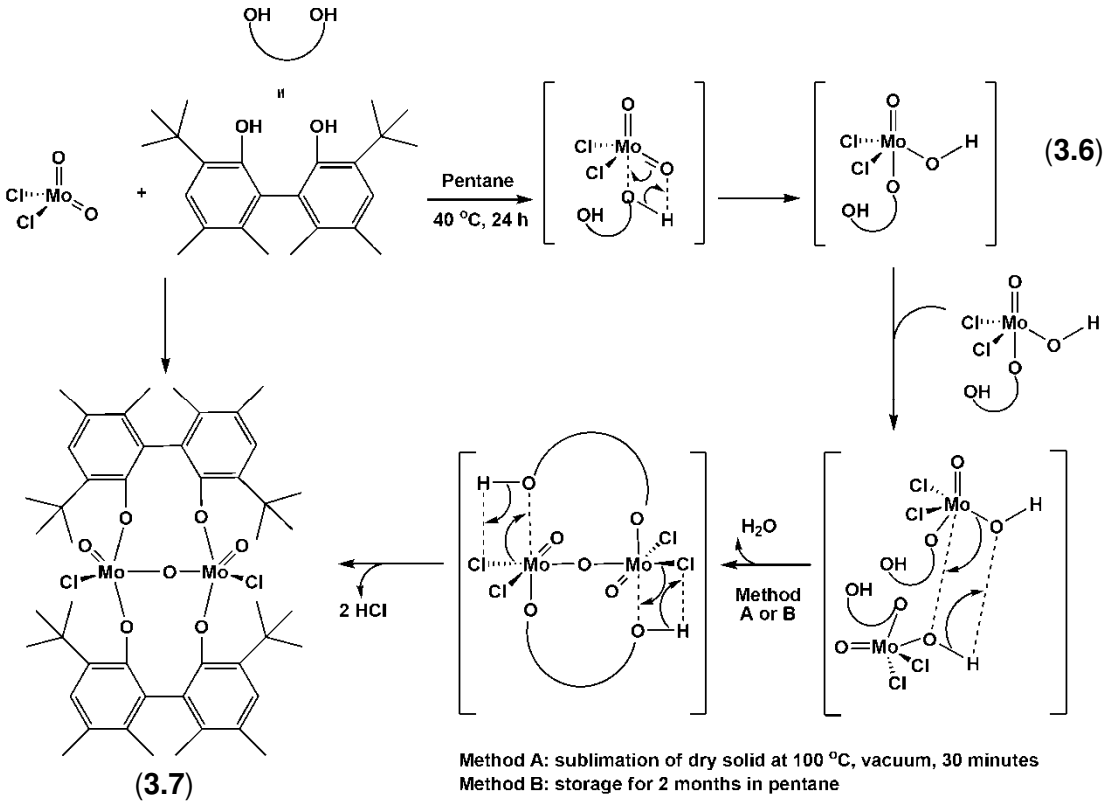

Scheme 3.3 Proposed reaction pathway for the formation of Mo(O)(OH)[rac-BIPHEN(O)(OH)]Cl_2 (**3.6**) and [Mo(O)Cl]$_2${[μ-rac-BIPHEN(O)$_2$-κ^2*O:O*']$_2$(μ-O)} (**3.7**).

Although **3.6** has not been completely characterized, isolation of **3.7** provides support for the formation of a molybdenum oxo hydroxide species, since conceptually it may be viewed as arising from condensation of two Mo(O)(OH)[rac-BIPHEN(O)(OH)]Cl_2 (**3.6**) fragments. A similar assumption was made by others to rationalize the formation of the tetranuclear molybdenum complex [Mo_4(N-2,6-^{i}Pr$_2$C$_6$H$_3$)$_6$(O-^{t}Bu)$_2$(μ-O)$_4$(μ_3-OH)$_2$] from the [Mo(O)(OH)(NAr)(O-^{t}Bu)] and [$Mo(NAr)_2$(O)] fragments.[189]

Mo(O)Cl($C_6H_4O_2$-κ^2*O,O'*)(C_6H_4O(OH)-κ^2*O,O'*)·Et_2O (**3.8**) is synthesized from MoO_2Cl_2 and catechol (1:1) in Et_2O at room temperature. The proposed reaction mechanism is shown in Scheme 3.4.

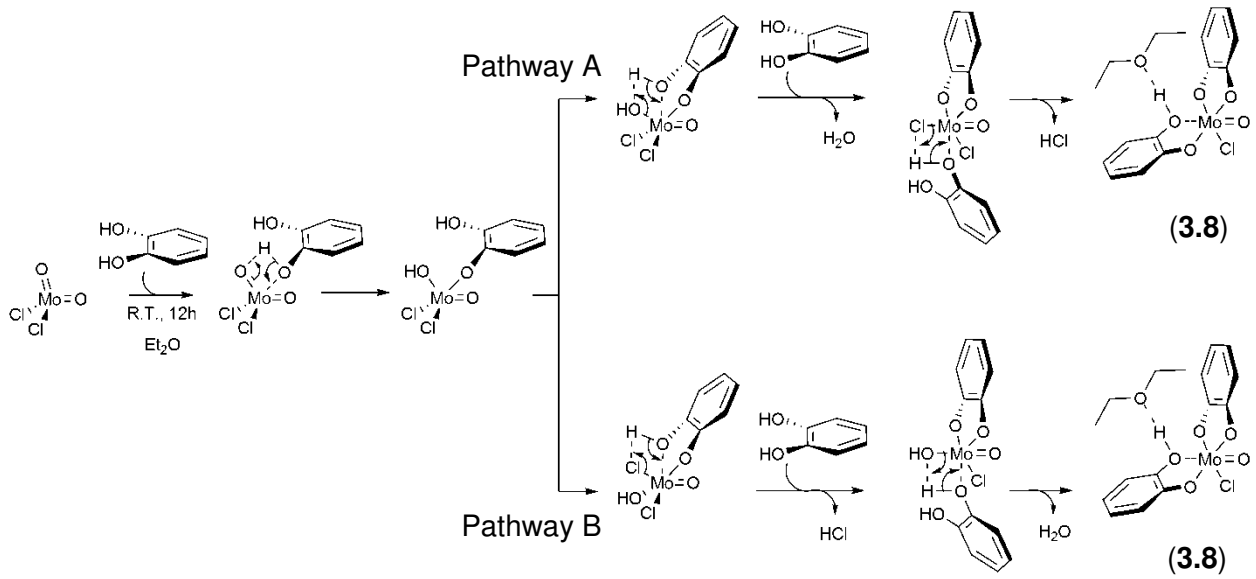

Scheme 3.4 Proposed reaction mechanisms for the formation of Mo(O)Cl($C_6H_4O_2$-κ^2*O,O'*)(C_6H_4O(OH)-κ^2*O,O'*)·Et_2O (**3.8**).

The proposed mechanism involves the coordination of the aryl alcohol to the MoO_2^{2+} core, followed by the addition of the first catechol (OH) across the Mo=O bond, forming the Mo(VI) oxo hydroxide intermediate. This intermediate will further react with the second OH from the same catechol in either of two ways (Pathway A or B). Pathway A involves bond metathesis with a Mo-OH bond and production of 1 equiv of H_2O. The Mo(O)Cl_2(catecholate) then reacts with 1 equiv of catechol to form HCl via σ-bond metathesis, yielding the observed product.

Pathway B: Involves bond metathesis with the Mo-Cl bond and release of one molecule of HCl. The Mo(O)(OH)Cl(catecholate) then reacts with 1 equiv of catechol to form H_2O via σ-bond metathesis, yielding the observed product.

Based on our experimental evidence we believe that pathway B is the operating mechanism. It has been demonstrated that $MoOCl_2(OAr)_2$ complexes do not react with further HOAr,[81] making reaction pathway A unlikely. On the other hand, reaction pathway B includes the formation of HCl via bond metathesis with the Mo-Cl bond. The chelating catechol has a small bite angle, that might prevent it from reacting with the Mo-OH bond, and so it reacts instead with the closest Mo-Cl substituent. This mechanism suggests that the *cis*- and *trans*-orientations of the substituents in the final product (*trans*-aryloxy, *trans*-chloro MoO^{4+} complexes) are defined early in the reaction pathway. The second catechol molecule will react with the Mo(O)(OH)Cl(catecholate) via *σ*-bond metathesis with the Mo-OH group yielding 1 equiv of H_2O. The driving force for the addition of the second molecule of catechol to Mo(O)(OH)Cl(catecholate) is the formation of the stable Mo(O)Cl($C_6H_4O_2$-κ^2*O,O'*)(C_6H_4O(OH)-κ^2*O,O'*)·Et_2O (**3.8**) and water.

Independently of the reaction pathway, it is important to notice that only one hydroxyl group of the second catechol molecule reacts with the Mo center, while the second –OH group coordinates to the Mo(VI) center (similar to the pre-coordination of ArOH to MoO_2Cl_2), and hydrogen bonds to a molecule of Et_2O. This lack of reactivity might be understood in terms of the "spectator oxo effect".[103] The remaining molybdenum oxo bond in **3.8** after addition of the first molecule of catechol (Scheme 3.4), has a virtual triple bond character Mo≡≡O.[103] The energetic consequence of this effect is that the molybdenum monooxo bond is stronger than the Mo=O bonds in dioxo species, making it unlikely to react under these conditions.

3.3.1.2 Products from addition of LiOAr to MoO_2Cl_2 (2:1)

Our research group previously reported the synthesis of $MoOCl(O\text{-}2,6\text{-}Me_2C_6H_3)_3$ (**3.3a**) by addition of 2 equiv of $LiO\text{-}2,6\text{-}Me_2C_6H_3$ to MoO_2Cl_2 in Et_2O (Equation 3.3).[81]

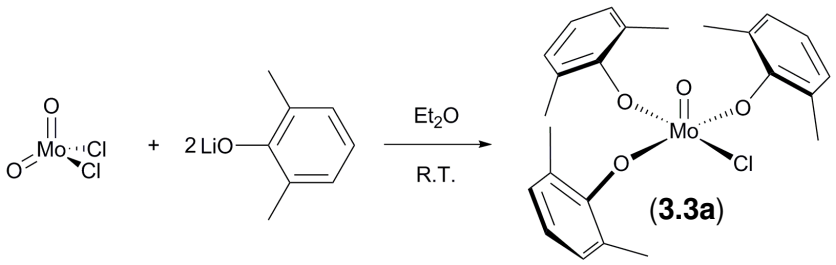

(**3.3a**) (3.3)

Synthesis of $MoOCl(OAr)_3$ complexes was explored using different lithium aryloxides, having as precedent the reaction shown in Equation 3.3.

Addition of different LiOAr (**3.2b**-**g**) to MoO_2Cl_2 in Et_2O led to the formation of $MoOCl_2(OAr)_2$ complexes (Equation 3.4) instead.

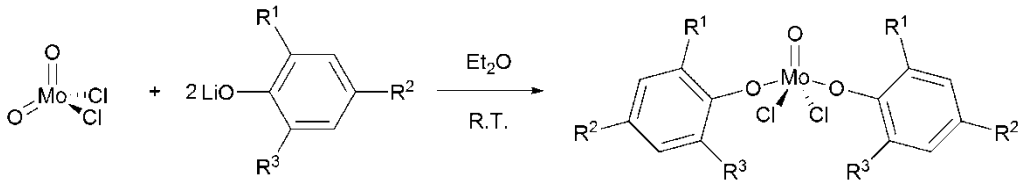

(**3.1b-g**) (**3.2b-g**) (3.4)

Complex **3.2f** was isolated using this procedure. When the LiOAr **3.1g** was used, formation of $MoOCl_2(OAr)_2$ **3.2g** and possibly $MoOCl(OAr)_3$ **3.3g** were observed by ^1H NMR spectroscopy.

We can conclude that the extent of product substitution is highly sensitive to the nature of the ligand. Formation of the tris-aryloxide ligand should be possible using different stoichiometries for each lithium aryloxide.

3.3.1.3 Products from addition of LiOAr to MoO_2Cl_2 (4:1) in “wet hexane”

The synthesis of $MoO(OAr)_4$ complexes represented a real challenge. Our chemistry is usually conducted under rigorous moisture and oxygen free conditions. Attempts to synthesize $MoO(OAr)_4$ complexes in these conditions were unsuccessful. Synthesis of MoO(O-2,6-

$Me_2C_6H_3)_4$ was accomplished by reacting MoO_2Cl_2 and 4 equiv of LiO-2,6-$Me_2C_6H_3$ in "wet hexane" at room temperature (refer to the experimental section) (Equation 3.5).

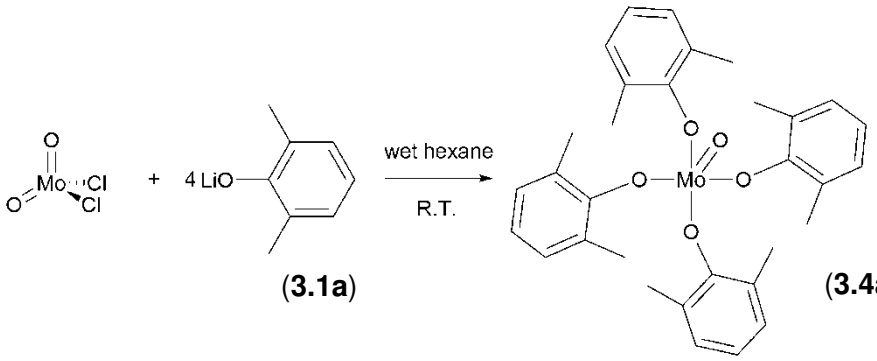

(3.5)

Based on our previous observations of ArOH addition to MoO_2Cl_2, we proposed the reaction mechanism described in Scheme 3.5.[81]

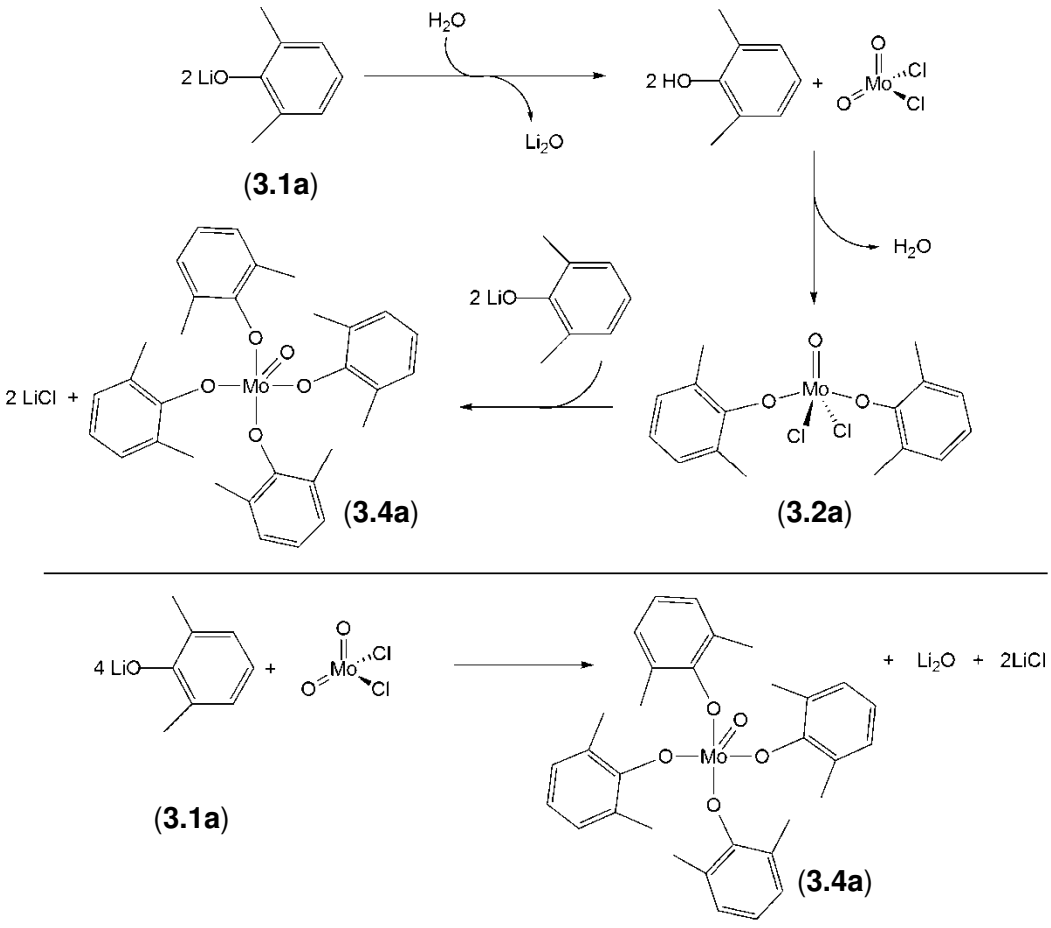

Scheme 3.5 Proposed reaction mechanism for the formation of $MoO(OAr)_4$ complexes.[81]

The reaction pathway described in Scheme 3.5 is thought to be water catalyzed. Lack of water indeed prevents the formation of $MoO(OAr)_4$ and instead, mixtures of $MoOCl(OAr)_3$ and $MoOCl_2(OAr)_2$ are observed when 4 equiv of LiOAr are added to MoO_2Cl_2 under anhydrous conditions. If "wet hexane" is used, successful formation of **3.4a** and **3.4c** is observed. Elemental analysis for **3.4a** gave satisfactory agreement with the theoretical values if one equiv of the proposed Li_2O side product is added to the calculation.

A drawback in the mechanism proposed in Scheme 3.5 is that mixtures of complexes **3.2a** and **3.3a** are formed when LiOAr **3.1a** is added to $MoOCl(OAr)_3$ or to $MoOCl_2(OAr)_2$ in different ratios.

Attempts to synthesize $MoO(O\text{-}2,6\text{-}Me_2C_6H_3)_4$ from the reaction between 4 equiv LiO-2,6-$Me_2C_6H_3$ (**3.1a**) and $MoOCl_4$ in Et_2O at -78 ^oC[79] produced $MoOCl_2(O\text{-}2,6\text{-}Me_2C_6H_3)_2$ (**3.2a**). Alternative reactions with different precursors and ligands were attempted (refer to experimental section) with no success.

Successful synthesis of $MoO(O\text{-}2\text{-}^tBuC_6H_4)_4$ (**3.4c**) was accomplished using the reaction conditions shown in Equation 3.5. Unfortunately complete isolation of **3.4c** was not accomplished and its identity was established by ^1H and ^{13}C NMR spectroscopy alone.

$MoOCl(O\text{-}2,6\text{-}Me_2C_6H_3)_3$ (**3.3a**) is expected to be formed throughout the mechanism shown in Scheme 3.5. Use of 3 equiv of LiOAr yielded $MoOCl_2(O\text{-}2,6\text{-}Me_2C_6H_3)_2$ (**3.2a**) instead of the trisubstituted monooxo complex.

3.3.1.4 Products from addition of LiOAr to $MoO_2Cl_2(DMF)_2$ (1:1)

When 1 equiv of the respective LiOAr **3.1f** and **3.1h** was reacted with $MoO_2Cl_2(DMF)_2$ in Et_2O, 6-coordinate $MoO(OAr)_4(DMF)$ **3.5f** and $MoOCl(OAr)_3(DMF)$ **3.5h** complexes were produced. The extent of the aryloxide substitution in the MoO^{4+} core seems to be highly sensitive to the structure of the ligand. The unpredictability of the final product substitution

makes it difficult to establish a protocol with the $MoO_2Cl_2(DMF)_2$ precursor, unlike the reliable reaction of MoO_2Cl_2 + 2 HOAr.

One of the main motivations for synthesizing molybdenum(VI) oxo complexes with allyl substituents is that possible Mo···CH_2=CH-CH_2- (allyl) interactions could be studied, and the knowledge used to understand activation of unsaturated substrates as CH_2=CH-CH_3 (propylene) on the surface of the SOHIO catalyst.[89] MoO(O-2-(allyl)$C_6H_4)_4$(DMF) (**3.5f**) was produced and characterized by different spectroscopic methods and X-ray diffraction. Unfortunately the allyl moiety in the aromatic ring was too far from the Mo(VI) center to yield any kind of meaningful interaction. Model complex [MoO_2(O-2-(allyl)$C_6H_4)_3$]Li·2(12-crown-4) was synthesized by Limberg et al.[89] in a similar attempt to produce a tether interaction between the high valent molybdenum core and the aryloxo/olefin ligand; but in their case, the olefin functions also remained dangling.

3.3.2 Spectroscopic characterization

3.3.2.1 Products from addition of monodentate aryl alcohols to MoO_2Cl_2

The ^{1}H and ^{13}C NMR spectra of the molybdenum(VI) monooxo diaryloxides **3.2a**-**g** are consistent with their structures. Due to the presence of a C_2 axis in **3.2a**-**g**, the two aryloxy ligands are magnetically equivalet and display a single set of signals. The observed magnetic equivalence is in agreement with the X-ray structures obtained for **3.2a**[81] and **3.2b** (section 3.3.3). The structural arrangement for these two complexes can be extended by analogy to the complexes **3.2c**-**3.2g**, on the basis of the spectroscopic evidence. All the peak values and assignments are reported in the experimental section.

The IR spectrum of each compound showed one medium to strong intensity peak in the range of 939-982 cm^{-1}, which is assigned to the Mo=O stretching frequency. These values fall within the range reported by our group for compound **3.2a**[81] and also by other researchers working on MoO^{4+} complexes.[74, 80, 173, 190] The Mo=O frequencies do not show any trend that can

be related to the alkyl substitution patterns. The oxo bond lengths also appeared similar for **3.2a** and **3.2b**.

Electronic spectra of the complexes in benzene display two intense bands, one of them in the 278-295 nm region and the other in the 620-730 nm region. The first band (B band for aromatic systems)[126] corresponds to a $\pi \rightarrow \pi^*$ transition of the benzene chromophore influenced by the unshared electron pair of the auxochromic oxygen (this band is present in the lithium phenoxides as well as in the plain phenols in about the same region). For the specific case of compound **3.2g** the appearance of absorption bands at 326 and 336 might correspond to the auxochromic effects resulting from the π-π conjugated aryl-allyl system. These complexes are dark blue when dissolved in benzene (they absorb in the low energy yellow-orange region and transmit the blue-purple). Their deep blue color can be attributed to charge transfer transitions where an electron is transferred from orbitals having mostly ligand character to orbitals having mostly metal character.

These complexes possess a square pyramidal geometry (C_{2V}); unlike the bright and colorful complexes of Chapter 2, their LMCT bands occur in a low energy region, due to a smaller band gap between the A_1 and the A_2 levels in a SP arrangement. The ligands have lone pairs of relatively high energy and the metal has low-lying A_1 empty orbitals. A nonbonding oxygen-localized 2p electron either in the terminal oxo or in the aryloxide is expected to be transferred to the low lying empty d orbital on molybdenum.

Low resolution mass spectrometry was attempted for complexes **3.2a** and **3.2g**. Only **3.2a** passed satisfactorily. The high sensitivity of these complexes to moisture and oxygen may cause degradation under analytical conditions. Molybdenum monooxo complexes are oxophilic[151] and their electronic unsaturation ($12e^-$) forces them to accept electron density from a lone pair of any available heteroatom (e.g. from O_2 or H_2O).

3.3.2.2 Products from addition of bidentate aryl alcohols to MoO_2Cl_2

Complexes **3.6**-**3.7** display very distinctive structural features that arise from the bidentate nature of their ligands (Schemes 3.3 and 3.4).

Mo(O)(OH)[rac-BIPHEN(O)(OH)]Cl_2 (**3.6**) was not isolated. Its separation from the parent biphenol was attempted via consecutive reprecipitations. Pentane or hexanes worked, although 7 reprecipitations were required to obtain a significant amount of **3.6**, but it was still contaminated with starting biphenol. Ether was not appropriate for purification of **3.6** because it induced decomposition of **3.6** into biphenol starting material. Mo(O)(OH)[rac-BIPHEN(O)(OH)]Cl_2 (**3.6**) was characterized by ^{1}H NMR spectroscopy as a mixture of **3.6** and the biphenol. Mo(O)(OH)[rac-BIPHEN(O)(OH)]Cl_2 (**3.6**) is asymmetric and shows different signals for each alkyl group and aryl proton of its structure. The OH peak at rac-BIPHEN(O*H*) was assigned by analogy with compound **3.8** (vide infra); and the Mo(OH) was assigned by process of elimination.

Mo(O)(OH)[rac-BIPHEN(O)(OH)]Cl_2 (**3.6**) is a d^0 five coordinate species, therefore a SP geometry is expected around the Mo(VI) center. As in the case of complexes **3.2a**-**g**, **3.6** is dark blue in solid and solution states.

[Mo(O)Cl]$_2${[μ-rac-BIPHEN(O)$_2$-κ^2*O:O*']$_2$(μ-O)} (**3.7**) is a binuclear complex of Mo(VI) that shows a much simpler ^{1}H NMR spectrum than that of compound **3.6**. The crystal structure (section 3.3.3) shows that the bridging oxygen lies at a crystallographic center of symmetry. The number of ^{1}H NMR peaks is therefore halved due to the magnetic equivalence of the protons in opposite sides of the mirror plane (refer to appendix for a graphical ^{1}H and ^{13}C peak assignment based on this center of symmetry observed by X-ray diffraction).

The IR spectrum of **3.7** identifies two peaks of very strong intensity. One peak is at 970 cm^{-1}, which is in the range assigned to the Mo=O vibrations for mononuclear complexes, and the Mo-O-Mo stretch is at 737 cm^{-1}. The assignment of these IR signals agrees with those reported by other research groups working with dinuclear oxo-bridged Mo^{VI} complexes.[145]

Electronic spectra of complex **3.7** in benzene display three bands at 278, 349 and 672 nm. The first band (B band for aromatic systems)[126] corresponds to a $\pi \rightarrow \pi^*$ transition of the benzene chromophore influenced by the unshared electron pair of the auxochromic oxygen of the bisphenoxide. The second band (R band)[126] might correspond to a $n \rightarrow \pi^*$ transition of the nonbonding free electrons from the bridging oxo group to the antibonding orbitals of the aromatic ring. The band at 672 nm can be catalogued as a LMCT band. This LMCT band occurs in a low energy region, due probably to small band gap of the trigonal bipyramidal arrangement of each of the Mo units.[220]

Mo(O)Cl($C_6H_4O_2$-κ^2O,O')(C_6H_4O(OH)-κ^2O,O')·Et_2O (**3.8**) exhibits the strong characteristic peak for a Mo=O vibration at 965 cm^{-1}.The electronic spectrum of **3.8** features three bands at 319, 485, and 804 nm. In the literature, these three bands are assigned to charge-transfer transitions produced by catechol coordination.[190] The ^1H and ^{13}C NMR spectra of molecule **3.8** are complex and reveal the magnetic nonequivalency of the two catecholate rings.

3.3.2.3 Products from addition of LiOAr and MoO_2Cl_2 (4:1) in "wet hexane"

Production of $MoO(OAr)_4$ complexes has been reported previously by Hayano et. al.[79] and by our research group.[81] Hayano's procedure requires the use of $MoOCl_4$ as precursor; in our case MoO_2Cl_2 is used as starting material. Hayano et al. reported the synthesis of MoO(O-2,6-$Me_2C_6H_3)_4$ (**3.4a**).[79] In our hands his methodology yielded $MoOCl_2$(O-2,6-$Me_2C_6H_3)_2$ (**3.2a**) instead. Hayano et al. reported ^1H NMR and X-ray characterization, but their reported ^1H NMR spectrum corresponds to our $MoOCl_2$(O-2,6-$Me_2C_6H_3)_2$ (**3.2a**). Although the X-ray structure corresponds to that of MoO(O-2,6-$Me_2C_6H_3)_4$ (**3.4a**), is likely that the tetraaryloxide complex was formed as the minor product. In our case, elemental analysis[81] and low resolution mass spectrometry confirm the identity of $MoOCl_2$(O-2,6-$Me_2C_6H_3)_2$ (**3.2a**). Elemental analysis of MoO(O-2,6-$Me_2C_6H_3)_4$ (**3.4a**) is satisfactory if 1 molecule of Li_2O is included in the calculation (Li_2O is a side product according to our proposed reaction mechanism, Scheme 3.5).

The use of “wet hexane” as reaction solvent for the production of complexes with the generic structure $MoO(OAr)_4$ was tested with the lithium aryloxide **3.1c**, yielding the product $MoO(O\text{-}2\text{-}^tBuC_6H_4)_4$ (**3.4c**).

The ^1H and ^{13}C NMR data are consistent with a SP structure. Due to the presence of a C_4 axis in **3.4a** and **3.4c**, the four aryloxy ligands are magnetically equivalent and display a single set of signals. The observed magnetic equivalence is in agreement with the X-ray structures obtained for **3.4a** (section 3.3.3). All the peak values and assignments are reported in the experimental section.

The IR spectrum of **3.4a** showed one intense peak in 1030 cm^{-1}, which we believe might correspond to the Mo=O stretching frequency. This value is a little off from the range expected (890-998 cm^{-1}) for Mo=O bond frequencies in MoO^{4+} complexes reported previously,[74, 80, 81, 145, 173, 190] but comparable with that of $MoOF_4$ (1030 cm^{-1}).[145] Despite this value, the Mo=O bond length in $MoO(O\text{-}2,6\text{-}Me_2C_6H_3)_4$ (**3.4a**) is similar to that observed for the Mo=O bonds in $MoOCl_2(O\text{-}2,6\text{-}Me_2C_6H_3)_2$ (**3.2a**) and $MoOCl_2(O\text{-}2,4\text{-}Me_2C_6H_3)_2$ (**3.2b**), based on their X-ray structures.

The electronic spectrum of complex **3.4a** in benzene displays three intense bands at 276, 325 and 618 nm. The first band is again identified as the B band for aromatic systems, and the second and the third band might correspond to LMCT transitions that occur in the low energy region of the visible spectra (orange-yellow). This compound is dark blue.

3.3.2.4 Products from addition of LiOAr to $MoOCl_4$

Synthesis of $MoOCl_2(O\text{-}2,6\text{-}^tBu_2\text{-}4\text{-}RC_6H_2)_2$ (R = H, OMe) and $MoOCl_2(O\text{-}2,6\text{-}Me_2\text{-}4\text{-}(NO_2)C_6H_2)_2$ was attempted by addition of 2 equiv of $HO\text{-}2,6\text{-}^tBu_2\text{-}4\text{-}RC_6H_2$ (R = H, OMe) or $HO\text{-}2,6\text{-}Me_2\text{-}4\text{-}(NO_2)C_6H_2$ to MoO_2Cl_2 (refer to the experimental section, 3.2.2.3.1) but the desired product was not observed. An alternative synthesis was the reaction between $MoOCl_4$ + 2 equiv of $LiO\text{-}2,6\text{-}^tBu_2\text{-}4\text{-}RC_6H_2$ (R = H, OMe) or $LiO\text{-}2,6\text{-}Me_2\text{-}4\text{-}(NO_2)C_6H_2$ in Et_2O (Scheme 3.6).

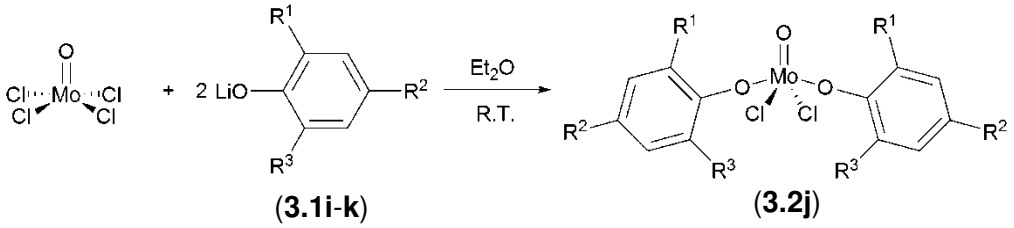

(**3.1i-k**) (**3.2j**)

Label	R^1	R^2	R^3	Yield (%)
i	^{t}Bu	H	^{t}Bu	not observed
j	^{t}Bu	OMe	^{t}Bu	51
k	Me	NO_2	Me	not observed

Scheme 3.6 Alternative synthesis of $MoOCl_2(OAr)_2$ complexes for ligands with sterically congested or highly electron-withdrawing substituents.

LiO-2,6-^{t}Bu$_2$C$_6$H$_3$ and LiO-2,6-Me$_2$-4-(NO$_2$)C$_6$H$_2$ afforded only parent aryl alcohol, whereas LiO-2,6-^{t}Bu$_2$-4-(OMe)C$_6$H$_2$ produced the dark red complex $MoOCl_2$(O-2,6-^{t}Bu$_2$-4-(OMe)C$_6$H$_2$)$_2$. Unfortunately suitable crystals for X-ray diffraction were not obtained, and the structure assignment has been made on the basis of the ^{1}H NMR, ^{13}C NMR, and low resolution mass spectrometry data.

The ^{1}H and ^{13}C NMR data are consistent with a structure containing a C_2 axis (as for molecules **3.2a**-**g**). The two aryloxy ligands are magnetically equivalent and display a single set of signals. Unlike in the complexes $MoOCl_2(OAr)_2$ **3.2a**-**g**, in the case of $MoOCl_2$(O-2,6-^{t}Bu$_2$-4-(OMe)C$_6$H$_2$)$_2$ (**3.2j**) each of the *tert*-butyl groups and aryl protons for the same aryl ring are nonequivalent to each other. This asymmetry may be caused by the lack of free rotation around the Mo-O-Ar axis due to the bulkiness imposed by the *tert*-butyl groups. All the peak values and assignments are reported in the experimental section. Low resolution mass spectrometry is in agreement with the proposed structure for $MoOCl_2$(O-2,6-^{t}Bu$_2$-4-(OMe)C$_6$H$_2$)$_2$ (**3.2j**).

The IR spectrum of **3.2j** showed a weak peak at 939 cm^{-1}, which is assigned to the Mo=O stretching frequency. These values fall within the range reported for MoO^{4+} complexes [74, 80, 81, 173, 190].

The electronic spectra of complex **3.2j** in benzene displays four bands at 289, 543, 621, and 923 nm. The band at 289 nm (B band for aromatic systems)[126] corresponds to a $\pi \rightarrow \pi^*$ transition of the benzene chromophore, while the other 3 bands should correspond to LMCT transitions. The strong electron donation of the *para*-OMe substituent causes more than one transition across the small band gap of the proposed SP geometry for this molecule. The absorption bands at 543, 621 and 923 nm are green, yellow and orange (transmits red and blue); this complex has a dark red coloration in solution and solid state.

3.3.2.5 Products from addition of LiOAr and $MoO_2Cl_2(DMF)_2$

We investigated the synthesis of Mo(VI) monooxo aryloxides starting from $MoO_2Cl_2(DMF)_2$. Addition of 1 equiv of LiO-2,6-^{i}Pr$_2$C$_6$H$_3$ to $MoO_2Cl_2(DMF)_2$ in Et_2O and stirred overnight produced a mixture of complexes $MoOCl(O\text{-}2,6\text{-}^i Pr_2C_6H_3)_3(DMF)$ (**3.5h**) and $MoO_2(O\text{-}2,6\text{-}^i Pr_2C_6H_3)_2(DMF)$ (**2.5k**). The monooxo complex **3.5h** was only present in small amounts. The complex **3.5h** yielded one crystal that was inspected by X-ray diffraction. The ^{1}H and ^{13}C NMR data are in agreement with the structure obtained by X-ray diffraction (refer to the appendix of this this chapter for the symmetry and peak assignments). The ^{1}H NMR showed two aryl groups in a 1:2 ratio, as expected due to its C_s symmetry.

Addition of 1 equiv of LiO-2-(allyl)C_6H_4 to $MoO_2Cl_2(DMF)_2$ in Et_2O and stirred overninght overnight yielded $MoO(O\text{-}2\text{-}(allyl)C_6H_4)_4$ (**3.5f**). The ^{1}H and ^{13}C NMR data agree with the X-ray structure: the four aryl rings and the allyl moieties are equivalent to each other as consequence of its C_{4v} symmetry. The Mo=O stretching frequency in the IR spectrum is at 999 cm^{-1}. The electronic spectrum shows three absorption bands at 281, 346, and 570 nm. The absorption band at 346 nm might result from the auxochromic effects of the π-π conjugated aryl-allyl system. The band at 281 nm (B band) is again from the benzene chromophore. It is important to mention that the LMCT occurs at a higher energy (frequency) than in the other cases. This complex has a pseudooctahedral geometry, so it is expected that the energy required to excite

an electron from the t_{2g} level to the e_g level will be larger than for a SP or TBP arrangement. Complex **3.5f** absorbs in the medium frequency region of green and transmits purple and red; this accounts for the dark purple coloration observed for this complex in solution.

3.3.3 Crystal structure and three-dimensional geometry.

Table 3.2 Crystallographic Data and Summary of Data Collection and Structure Refinement.

	3.2b	**3.4a**	**3.5f**	**3.5h**
Formula	$C_{20}H_{26}Cl_2MoO_4$	$C_{32}H_{36}MoO_5$	$C_{39}H_{43}MoNO_6$	$C_{39}H_{58}ClMoNO_5$
fw	497.25	596.55	717.68	752.25
crystal system	Monoclinic	Tetragonal	Monoclinic	Orthorhombic
space group	$P2_1/c$	P4/n	$P2_1/c$	$P2_12_12_1$
T, K	223(2) K	213(2) K	218(2) K	218(2) K
a, Å	7.902(3)	14.0914(10)	23.008(4)	13.6523(9)
b, Å	32.721(10)	14.0914(10)	8.3675(14)	15.9547(11)
c, Å	8.817(3)	7.4079(10)	18.483(3)	18.7218(12)
α, deg	90	90	90	90
β, deg	103.001(6)	90	93.798(3)	90
γ, deg	90	90	90	90
V, Å^3	2221.4(12)	1471.0(2)	3550.6(10)	4078.0(5)
Z	4	2	4	4
D_{calc}, mg/m^3	1.487	1.347	1.343	1.225
θ range (deg) for data collection	2.45 – 23.28	2.04 – 28.19	2.21 – 25.00	1.68 – 25.00
$N_{measured}$	13618	11668	9522	11324
$N_{independent}$	3195	1729	5639	6794
R	0.0398	0.0234	0.0421	0.0248
ωR_2	0.0901	0.0639	0.1026	0.0660
GOF	1.101	1.152	0.993	1.018
largest diff peak and hole (e·Å^3)	0.540 and -0.364	0.543 and -0.189	0.756 and -0.734	0.426 and -0.209

MoO^{4+} complexes are found in coordination numbers of 5-[170], 6-[190] and 7,[145, 191] exhibiting square pyramidal,[164, 192] trigonal bipyramidal,[57] octahedral[24, 74, 75] and pentagonal bipyramidal geometries.[57, 145]

The different $MoO(OAr)_{4-n}Cl_nL_{0-1}$ (L = THF, DMF) complexes described in this chapter are either 5-coordinate with a distorted square pyramidal geometry (**3.2a**,[81] **3.3a**[81] and **3.4a**) or 6-coordinate with a distorted octahedral arrangement (**3.2b**, **3.5f** and **3.5h**).

Tables 3.2 and 3.3 collect important structural information of selected molecules. Bond lengths and bond angles of the complexes $MoO(OAr)_2Cl_2$ **3.2b**, $MoO(OAr)_4$ **3.4a**, $MoO(OAr)_4(DMF)$ **3.5f**, and $MoO(OAr)_3Cl(DMF)$ **3.5h** are listed and compared with the previously reported $MoO(OAr)_2Cl_2$ and $MoO(OAr)_3Cl$.[81]

Table 3.3 Selected Bond Lengths (Å)

		Mo=O	Mo-O(aryloxy)	Mo···O(DMF) or (THF)
5-coordinate				
$MoOCl_2(OAr)_2$[81]	(**3.2a**)	1.628(13)	1.838(10) 1.856(11)	
$MoOCl(OAr)_3$[81]	(**3.3a**)	1.667(3)	1.862(3) 1.891(4) 1.893(3)	
$MoO(OAr)_4$	(**3.4a**)	1.685(2)	1.8825(11)	
6-coordinate				
$MoOCl_2(OAr)_2(THF)$	(**3.2b**)	1.670(3)	1.870(3) 1.883(3)	2.315(3)
$MoOCl(OAr)_3(DMF)$	(**3.5h**)	1.6676(16)	1.8688(15) 1.8765(16) 1.9267(15)	2.2750(17)
$MoOCl(OAr)_4(DMF)$	(**3.5f**)	1.682(3)	1.904(3) 1.915(2) 1.923(3) 1.947(2)	2.257(2)

Table 3.4 Selected Bond Angles (deg)

		O=Mo-OAr	Mo-O-C(aryloxy)	ArO-Mo-OAr
5-coordinate				
$MoOCl_2(OAr)_2$[81]	(**3.2a**)	101.0(5)	156.5(10)	
		101.3(6)	167.2(12)	
$MoOCl(OAr)_3$[81]	(**3.3a**)	101.22(15)	148.1(3)	91.84(14)
		101.57(15)	134.2(3)	87.14(14)
		110.20(15)	147.5(3)	
$MoO(OAr)_4$	(**3.4a**)	104.71(4)	147.45(10)	86.30(2)
6-coordinate				
$MoOCl_2(OAr)_2(THF)$	(**3.2b**)	99.65(13)	136.9(3)	
		96.86(13)	157.9(3)	
$MoOCl(OAr)_3(DMF)$	(**3.5h**)	97.63(8)	163.79(15)	90.64(7)
		102.23(8)	128.79(14)	89.01(7)
		96.58(8)	163.40(18)	
$MoOCl(OAr)_4(DMF)$	(**3.5f**)	99.94(12)	137.4(2)	94.10(11)
		96.11(12)	135.2(2)	98.85(13)
		98.85(13)	135.4(2)	89.54(11)
		96.72(11)	138.1(3)	85.42(11)

In complexes **3.2a**, **3.3a**, and **3.4a** (Figure 3.1) the central atom is above the basal square plane by an average of 10° (the O=Mo-OAr angles are larger than the ideal 90° for a SP geometry). The apical bond is the shortest (higher bond order) among all the ligands, as expected for a d^0 species.[193]

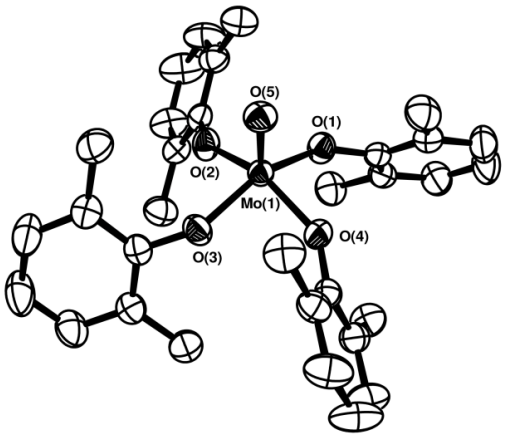

Figure 3.1 ORTEP view of $MoO(O\text{-}2,4\text{-}Me_2C_6H_3)_4$ (**3.4a**) (50% probability). Hydrogen atoms have been omitted for clarity.

The formation of the distorted octahedral complexes **3.2b** (Figure 3.2), **3.5f** (Figure 3.3), and **3.5h** (Figure 3.4), is the result of the addition of a sixth weakly bonded ligand (THF or DMF) *trans* to the Mo=O bond. The *trans* ligand for a d^0 species such as Mo(VI) is usually either a N- or O-donor (although exceptions have been observed[69]).[194]

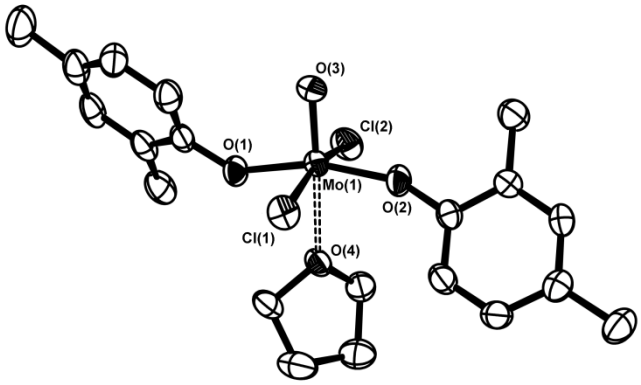

Figure 3.2 ORTEP view of MoO(O-2,4-$Me_2C_6H_3)_2Cl_2$·(THF) (**3.2b**) (50% probability). Hydrogen atoms have been omitted for clarity.

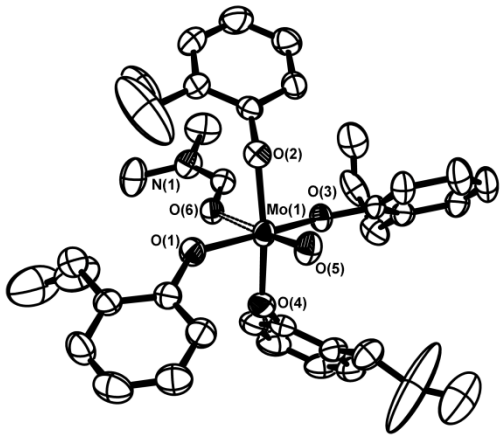

Figure 3.3 ORTEP view of MoO(O-2-(allyl)$C_6H_4)_4$(DMF) (**3.5f**) (50% probability). Hydrogen atoms have been omitted for clarity.

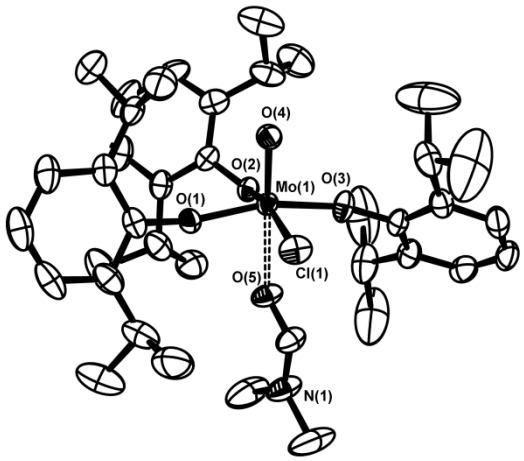

Figure 3.4 ORTEP view of MoO(O-2,6-$^{i}Pr_2C_6H_3)_3Cl(DMF)$ (**3.5h**) (50% probability). Hydrogen atoms have been omitted for clarity.

In complexes of d^0 metals, the length of the metal-oxo bond is fairly stable and depends on the number of oxo groups in the complex. In the case of Mo(VI), the length of the Mo=O bond in MoO^{4+} complexes is 1.61-1.68 Å, while the length of the average Mo=O bond in MoO_2^{2+} complexes is 1.67-1.72 Å. In some trioxo complexes the Mo=O lengths are approximately 1.74 Å.[194] The Mo=O bond in MoO^{4+} complexes approaches a bond order of 3 (and in dioxo complexes a bond order of 2.5). Rather than rationalizing the Mo=O short bond in MoO^{4+} complexes as $^{\ominus}Mo{\equiv}O^{\oplus}$ (ab initio calculations have shown no net charge transfer for the analogous Cr=O),[142] Rappé and Goddard favor the partial triple bond representation Mo$\equiv\!\!-$O from results of ab initio calculations (a large amount of electron density back donated to the d^0 center).[70, 142] The complexes listed in Table 3.2 show Mo=O bond lengths that are in agreement with the trends discussed above.

Three interesting trends are present in Tables 3.2 and 3.3:

1. lengthening of the Mo=O bond lengths with the presence of a *trans*-ligand,
2. lengthening of the Mo=O bond as the number of OAr substituents increases, and
3. shrinking of the Mo-O-C(aryloxy) angle as the number of OAr substituents increases.

Weakening (lengthening) of the Mo=O bond due to the presence of a *trans*-partner is expected. If we compare molecules **3.2a** and **3.2b** (almost identical aryloxide groups) this lengthening is obvious (1.628(13) and 1.670(3) Å respectively). The absence of a ligand in the *trans* position to the Mo=O bond in **3.2a** produces electron deficiency at the molybdenum center and enables donation of more electron density from the oxygen (Mo≡O). A longer Mo=O bond distance is therefore observed when THF (**3.2b**, 1.670(3) Å) or DMF (**3.5h**, 1.6676(16) Å and **3.5f,** 1.682(3) Å) are coordinated.

Lengthening of the Mo=O bond is observed in going from $MoOCl_2(OAr)_2$ **3.2a** (1.628(13) Å) to $MoOCl(OAr)_3$ **3.2a** (1.667(3) Å) to $MoO(OAr)_4$ **3.3a** (1.685(2) Å), and in general when we increase the number of aryloxide substituents in the molybdenum center. The lengthening of the Mo=O bond parallels the shrinking of the Mo-O-C(aryl) angle. The latter trend was observed in Chapter 2, but in that case no change was observed for the Mo=O bond lengths. The Mo=O bond variation observed for the monooxo complexes may be due to the availability of only one oxo group to compensate for the electronic demands of the Mo(VI) center, whereas in the MoO_2^{2+} unit the two oxo groups distribute the electronic demands, lessening any change in their bond order.

The complexes listed in Tables 3.2 and 3.3 are considered to be electronically unsaturated as they have less than 18 electrons in their valence shell. These complexes can relieve the electronic unsaturation by making use of two sources: variable electronic contribution of ligands and contribution of σ-donors.

It was noted in Chapter 2 that oxo, alkoxo, and aryloxo ligands can be considered as electronic reservoirs, in which electron density can be taken or given as required either for stability of the complex or for chemical transformation in the coordination sphere.

Both the Mo=O bond (1.628(13)–1.685(2) Å), and the Mo-OAr bond (1.838(10)-1.8825(11) Å) lengthen as we progress from from di- (**3.2a**) to tri- (**3.3a**) to tetra-aryloxide (**3.4a**) complexes. The observed Mo-OAr bond lengthening parallels the shrinking of the Mo-O-C(aryl)

angle (167.2(12)°-147.45(10)°). The change of this angle can be seen as a change in the hybridization of the aryloxy oxygen, and the electronic contribution of the aryloxy ligands. Linear oxygen (sp) might contribute up to $6e^-$ to the total electron count, whereas trigonal (sp^2) and tetrahedral oxygens (sp^3) might supply 4 and $2e^-$ respectively, depending on the electronic needs of the complex.

If we change from one coordination number to another, this trend is no longer evident. The steric effects imposed by the ligand environment are apparently stronger than the electronic demands of the metallic center.

As pointed out in chapter 2, the steric and electronic arguments are not opposite but complementary.

Table 3.5 Crystallographic Data and Summary of Data Collection and Structure Refinement.

	3.7	**3.8**
Formula	$C_{48}H_{64}Cl_2Mo_2O_7$	$C_{16}H_{19}ClMoO_6$
fw	1015.77	438.70
crystal system	Monoclinic	Monoclinic
space group	C2/c	$P2_1/c$
T, K	213(2) K	223(2) K
a, Å	24.975(9)	9.5612(8)
b, Å	12.491(4)	19.4516(15)
c, Å	17.398(6)	12.2800(7)
α, deg	90	90
β, deg	118.733(4)	128.399(4)
γ, deg	90	90
V, $Å^3$	4759(3)	1789.9
Z	4	4
D_{calc}, mg/m^3	1.418	1.628
θ range (deg) for data collection	1.86 – 25.00	2.36 – 24.99
$N_{measured}$	14229	4792
$N_{independent}$	4181	2612
R	0.0512	0.0284
ωR_2	0.1398	0.0787
GOF	1.123	1.018
largest diff peak and hole ($e \cdot Å^3$)	2.178 and -0.365	0.342 and -0.304

Complexes **3.7** (Figure 3.5) and **3.8** (Figure 3.6) were synthesized by similar procedures as compounds **3.2a**-**g** (Scheme 3.1). Complexes **3.7** and **3.8**, however, have very different

structural attributes. Their importance lies primarily in the information that these molecules provide to support the aryl alcohol addition across the Mo=O bond.

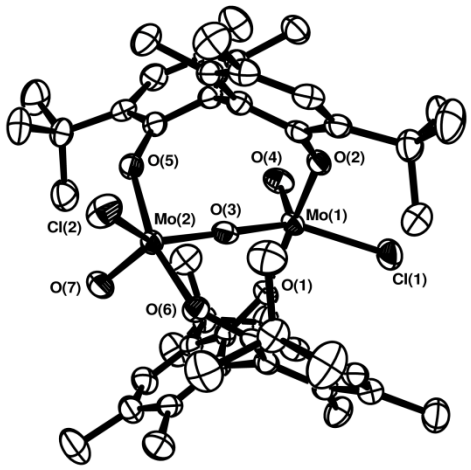

Figure 3.5 ORTEP view of [Mo(O)Cl]$_2${[μ-rac-BIPHEN(O)$_2$-κ^2*O:O'*]$_2$(μ-O)} (**3.7**) (50% probability). Hydrogen atoms have been omitted for clarity. Selected bond distances (Å) and bond angles (deg): Mo(1)-O(1) 1.874(3), Mo(1)-O(2) 1.901(3), Mo(1)-O(3) 1.8982(7), Mo(1)-O(4) 1.665(3), O(1)-Mo(1)-O(3) 83.83(12), O(2)-Mo(1)-O(3) 85.13(13), O(3)-Mo(1)-Cl(1) 140.70(12), O(4)-Mo(1)-Cl(1) 106.74(14), O(4)-Mo(1)-O(3) 112.56(17).

In addition to the multitude of mononuclear and heteropolynuclear complexes that contain Mo(VI), there are a significant number of dinuclear complexes.[145]

In molecule **3.7** the bridging oxygen atom O(1) lies at a crystallographic center of symmetry, and the Mo(1)-O(1)-Mo(2) bridge is linear (178.0(3)^o) and symmetrical. The array of one chlorine and four oxygen atoms about each molybdenum atom forms a distorted TPB geometry. The Mo(1)-O(3) length of 1.8982(7) Å lies in the normal range for oxo bridged complexes[145] with a bond order of one.[195, 196]

The Mo=O bond length 1.665(3) Å and Mo-OAr distances (1.874(3)-1.901(3) Å) fall within the values observed for molecules listed in Table 3.2.

Although the MoO^{4+} core of this complex is 5-coordinate, it does not display the square pyramidal geometry observed in complexes **3.2a**, **3.3a** and **3.4a**; instead it is trigonal bipyramidal. This geometrical arrangement is probably due to steric requirements of the

bidentate ligand rac-BIPHEN$(OH)_2$. Contrary to expectation for d^0 species (electronegative elements prefer axial positions),[193] the electronegative chlorine, the oxo, and *μ*-O ligands occupy the equatorial plane, again probably due to the steric limitations of the chelating ligand.

Molecules whose helical sense is maintained through hindered rotation (due to steric congestion) about a single bond are said to have a chiral axis in the bond.[197] This is the case of rac-BIPHEN$(OH)_2$, which can exist as the R or S isomer or "atropisomer" (from Greek *a* meaning not, and *tropos* meaning turn).[197] Notice the twisted conformation of the biphenolate in Figure 3.5. The synthesis of molecules Mo(O)(OH)[rac-BIPHEN(O)(OH)]Cl_2 **3.6** and $[Mo(O)Cl]_2\{[\mu\text{-rac-BIPHEN}(O)_2\text{-}\kappa^2O{:}O']_2(\mu\text{-O})\}$ (**3.7**) was accomplished starting from the achiral MoO_2Cl_2 and the racemic mixture of BIPHEN$(OH)_2$ (Scheme 3.3). In the case of molecule **3.6**, enantiomers Mo(O)(OH)[(a*S*)-BIPHEN(O)(OH)]Cl_2 and Mo(O)(OH)[(a*R*)-BIPHEN(O)(OH)]Cl_2 (the descriptors a*R* and a*S* are used to distinguish axial chirality from other types)[197]should be formed in equal proportions since there is no optically pure substrate that favors one or the other enantiomer. The condensation of two Mo(O)(OH)[rac-BIPHEN(O)(OH)]Cl_2 units yields product **3.7**. Inspection of the configuration and the ring pattern substitution in the biphenolate rings of **3.7** (Figure 3.5) permits the identification of the $[Mo(O)Cl]_2\{[\mu\text{-(a}S\text{,a}S\text{)-BIPHEN}(O)_2\text{-}\kappa^2O{:}O']_2(\mu\text{-O})\}$ isomer. Although the X-ray structure just shows one of the two enantiomers, the formation of $[Mo(O)Cl]_2\{[\mu\text{-(a}R\text{,a}R\text{)-BIPHEN}(O)_2\text{-}\kappa^2O{:}O']_2(\mu\text{-O})\}$ is expected since we started with a racemic mixture of **3.6**. No evidence of the formation of the diastereoisomers (a*R*,a*S*) or (a*S*,a*R*) was found in the ^1H and ^{13}C NMR spectra of the crude reaction mixtures or in the supernatant from which **3.7** was separated (refer to the experimental section and to the appendix of this chapter). It is interesting to observe that the condensation step (**3.6** + **3.6** → **3.7**) occurs with selectivity, probably due to the steric requirements of each enantiomer.

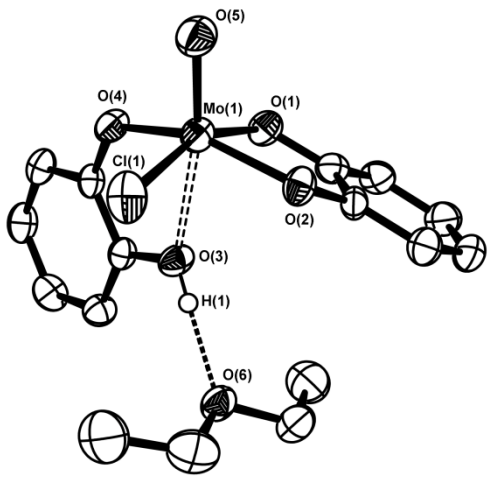

Figure 3.6 ORTEP view of Mo(O)Cl($C_6H_4O_2$-κ^2O,O')(C_6H_4O(OH)-κ^2O,O')·Et_2O (**3.8**) (50% probability). Hydrogen atoms have been omitted for clarity. Selected bond distances (Å) and bond angles (deg): Mo(1)-O(1) 1.966(2), Mo(1)-O(2) 1.947(2), Mo(1)-O(3) 2.349(2), Mo(1)-O(4) 1.899(2), Mo(1)-O(5) 1.675(2) Mo(1)-O(6) 1.6675(2), H(1)···O(6) 1.772, O(1)-Mo(1)-O(2) 78.22(10), O(1)-Mo(1)-O(4) 89.91(10), O(4)-Mo(1)-Cl(1) 99.75(8), Cl(1)-Mo(1)-O(2) 87.34(7), O(1)-Mo(1)-O(5) 103.13(12), O(1)-Mo(1)-O(3) 80.11(9).

The Mo-OAr bond lengths in molecule **3.6** (1.966(2), 1.947(2), and 1.899(2) Å) are similar to those reported for complex **3.5h** (1.904(3)-1.947(2) Å), with long Mo-OAr bonds. The Mo=O bond length (1.675(2) Å) falls within the normal values (Table 3.2). In comparison with molecule **3.6**, other MoO^{4+} catecholates display similar Mo=O bond lengths (1.690(5) Å) and Mo-OAr lengths (1.929(3)-1.993(3) Å).[151] This complex displays a distorted octahedral arrangement imposed by the small bite angle of the catecholate rings. A similar pseudo octahedral arrangement has been observed for MoO^{4+} catecholates with mixed sulfur and nitrogen ligands.[74, 190]

The interesting feature of this molecule is the Mo(1)···O(3) interaction with a length of 2.349(2) Å. This interaction may be compared to the Lewis acid-base interaction between Mo(VI) and the hydroxyl groups of the aryl alcohols described in section (3.3.1.1). Although the hydrogen was not located, O(3) was modeled as a hydroxyl moiety. A Mo(1)-O(3) covalent bond (2.349(2) Å) would have been extremely long (normal range 1.929(3)-1.993(3) Å)[151] and the final oxidation state of Mo(VI) would require the presence of a counter ion that was not

observed. The Mo(1)···O(3) bond length is comparable to those for weakly coordinated solvents in Table 3.2 (2.257(2)-2.315(3) Å). HO/water ligands in Mo(VI) centers have been assigned lengths of 2.3 Å.[198]

3.4 Conclusions

The synthesis of different $MoO(OAr)_{4-n}Cl_nL_{0-1}$ (L = THF, DMF) complexes was accomplished by reacting MoO_2Cl_2 and $MoO_2Cl_2(DMF)_2$ precursors with aryl alcohols or their lithium aryloxides.

We have demonstrated the facile and general synthesis of $MoOCl_2(OAr)_2$ complexes starting from the commercially available and easy to handle MoO_2Cl_2, and the parent aryl alcohol. Our research group is the only one to report the synthesis of MoO^{4+} complexes starting from a dioxo precursor.

The extent of product substitution is highly sensitive to the structure of the ligand and to stoichiometry.

The formation of $MoOCl_2(OAr)_2$ is likely to proceed via an associative mechanism where pre-coordination of the parent aryl alcohol to the Mo(VI) is followed by a [2+2] addition to the M=O bond. We have proposed a reaction mechanism and supporting evidence for this new reaction.

CHAPTER 4

MOLYBDENUM(VI) MONOOXO BISPHENOXIDES

4.1 Introduction

The stability, reactivity and selectivity of organometallic complexes, especially those designed for catalytic applications, are parameters that result from the combination of the metal center and its ligands.

Ligands containing elements such as O, S, and N are of interest because they can donate p electron density to high valent metal centers, stabilizing the catalysts and often improving their reactivity.[199, 200] For this reason, alkoxo and aryloxo ligands play an important and almost ubiquitous role in the design of high oxidation state molybdenum (and in general group VI metal) complexes. Alkoxo and aryloxo complexes are used for classic catalysis (e.g. olefin metathesis polymerization[79, 157, 201, 202] and oxygen transfer reactions[23]), and modeling of catalytic processes[176, 177] such as the SOHIO process[91] or isomerization of allyl alcohols,[203] among others.[57]

Alkoxo and aryloxo ligands are considered good candidates for ancillary ligands in organometallic chemistry and catalysis with early transition metal complexes for several reasons:[201]

1) Early transition metal alkoxides are relatively stable (e.g. they do not readily undergo *β*-hydride elimination)[201] often yielding characterizable complexes;[175, 177] in this respect, aryloxide ligands have been shown to perform better than their alkoxide counterparts.[204, 205]
2) In solution, the relatively high electrophilicity of early transition metals disfavors the dissociation of the alkoxo or aryloxo ions from the metallic center.[201]
3) Polymerization or oligomerization of the metal complexes can be prevented by increasing the steric hindrance of the alkoxo or aryloxo ligands; again aryloxo ligands

are thought to perform better as their structures possess inherent bulkiness and structural rigidity.

4) Alkoxo and aryloxo ligands can be considered as electronic reservoirs, from where electron density can be taken or given as required either for stability of the complex or for chemical transformation in the coordination sphere.
5) The reactivity of organometallic complexes is often strongly dependent on the electron density at the metal center, and this can be tuned by changing the substituents on the alkoxo or aryloxo ligand.
6) Alkoxo and aryloxo ligands impart solubility to the complexes, enhancing their use as homogeneous models for catalytic processes.

In conclusion, alkoxo and aryloxo ligands display steric flexibility and electronic adaptability to the changing requirements of the metal atom, including during the course of reaction.

In the past chapters we have described the chemistry and structural features of molybdenum(VI) dioxo- and monooxo complexes with monodentate aryloxide ligands. In addition, our group has explored the use of calixarenes as ligands to produce Mo(VI) complexes as catalyst models.[183] An obvious next step is to combine the characteristics of the acyclic and calixarene ligands by using bidentate aryloxides (bisphenoxides) that can be viewed as “half calixarenes”.[206] This new set of ligands led us to the preparation of the molybdenum(VI) monoxo bisphenoxide complexes that are described in this chapter. The use of chelating bisphenoxide ligands can provide structurally well defined molybdenum(VI) monoxo complexes that can be further used for catalytic purposes.[67, 207, 208]

Table 4.1 introduces the series of the different bisphenols, lithium bisphenoxides, and the molybenum monooxo aryloxide complexes that will be discussed in this chapter.

Table 4.1 List of Compounds Presented in this Chapter

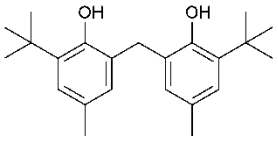

(**4.1a**)

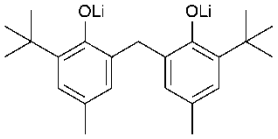

(**4.2a**)

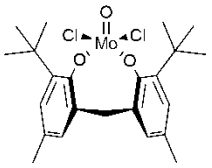

(**4.3a**)

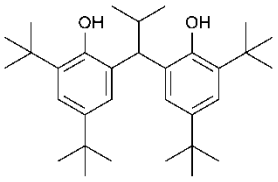

(**4.1b**)

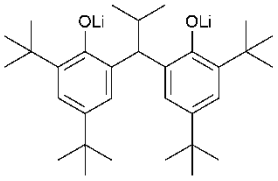

(**4.2b**)

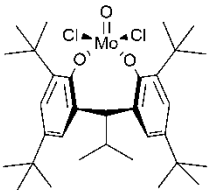

(**4.3b**)

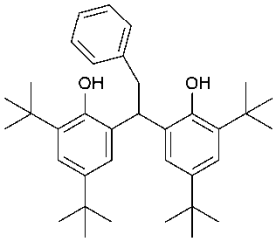

(**4.1c**)

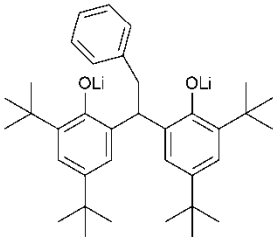

(**4.2c**)

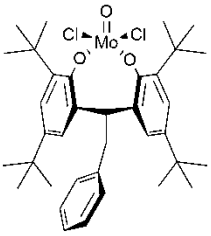

(**4.3c**)

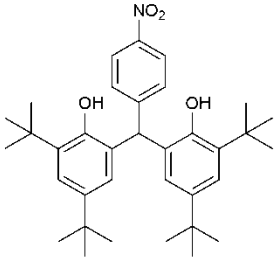

(**4.1d**)

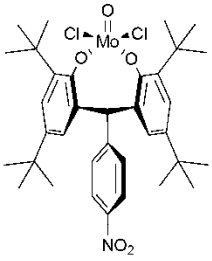

(**4.3d**)

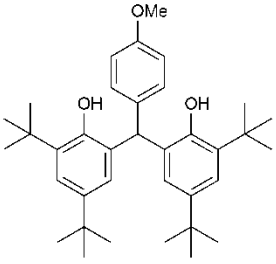

(**4.1e**)

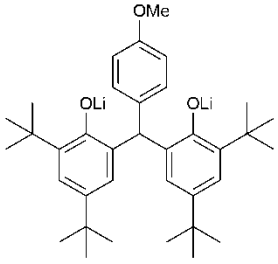

(**4.2e**)

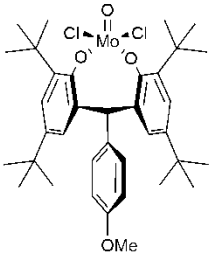

(**4.3e**)

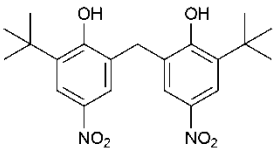

(**4.1f**)

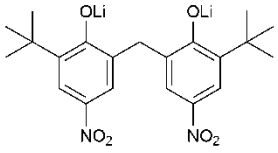

(**4.2f**)

4.2 Experimental section

4.2.1 General

All manipulations were performed under dry argon using standard Schlenk techniques or under nitrogen in a NEXUS 1 Vac Atmospheres glovebox. Molybdenum(VI) dichloride dioxide, *n*-butyllithium (2.0 M solution in *n*-pentane), 2,2'-methylenebis(6-*tert*-butyl-4-methylphenol) (**4.1a**), 2,4-di-*tert*-butylphenol, 2-*tert*-butylphenol, *p*-formaldehyde, isobutyraldehyde, phenylacetaldehyde, 4-nitrobenzaldehyde, 4-methoxybenzaldehyde, boron trifluoride diethyl etherate, xylenes, heptane, sodium bicarbonate and magnesium sulfate were purchased from Aldrich. Hydrochloric acid and methanol were purchased from AAPER, glacial acetic acid and nitric acid were obtained from EMScience, and sulfuric acid was purchased from VWR.

2,2'-methylenebis(6-*tert*-butylphenol) was synthesized from 2-*tert*-butylphenol and *p*-formaldehyde in anhydrous xylenes following a literature procedure.[209] The reaction was performed in a glass pressure tube with Teflon® screw cap. 2,2'-isobutylidenebis(4,6-di-*tert*-butylphenol), (2,2'-CH(^{i}Pr)(4,6-^{t}Bu$_2$C$_6$H$_2$OH)$_2$, **4.1b**) was prepared from 2,4-di-*tert*-butylphenol, isobutyraldehyde, boron trifluoride diethyl etherate and acetic acid as described elsewhere.[210] The synthesized phenols were dried for two days in a drying pistol at 78.4 ^{o}C under vacuum. Anhydrous hydrogen chloride gas was produced from hydrochloric acid and concentrated sulfuric acid.[211] The evolved gas was passed through a drying tube packed with drierite™ as desiccant. $MoOCl_4$ was freshly prepared from MoO_3 (J. T. Baker Chemical Company) and newly purchased thionyl chloride (Aldrich) as described previously.[165] The thus synthesized $MoOCl_4$, although reported to be pure for most uses,[165] was further sublimed,[165, 168] and stored in an amber bottle inside the glovebox freezer at -35 ^{o}C.

Hexanes, diethyl ether (Et_2O) and tetrahydrofuran (THF) were freshly distilled under argon from Na/benzophenone. *n*-Pentane (anhydrous grade) was purchased from Aldrich and stored over molecular sieves. Methanol, heptanes and xylenes were pre-dried over 4 Å molecular sieves (previously activated) for 48 h and further refluxed and distilled from CaO

(methanol) or CaH_2 (heptanes and xylenes) under argon. Acetone (HPLC grade, Aldrich) was dried over activated 4 Å molecular sieves for 48 h. NMR solvents (DMSO-d_6, benzene-d_6, THF-d_8 and chloroform-d) were degassed and vacuum distilled from CaH_2. All solvents (including NMR solvents) were stored inside the glovebox over 4 Å molecular sieves (previously activated) for 48 h before use.

^1H and ^{13}C NMR spectra were recorded on a Mercury Varian Plus 300 MHz spectrometer. ^1H NMR data are expressed as parts per million (ppm) downfield shift from tetramethylsilane ($\delta_{TMS} = 0$) using either tetramethylsilane or residual solvent as internal reference. Relative integral multiplicity is denoted by s = singlet, d = doublet, t = triplet, m = multiplet. Coupling constants (J) are reported in Hz. ^{13}C NMR spectra were recorded with proton decoupling at 300 K. The melting points of the products were observed in sealed capillary tubes on a Mel-temp apparatus (Laboratory Devices, Cambridge, MA). IR spectra were obtained with a MIDAC Corporation M-Series FTIR spectrometer. UV/vis spectra were recorded on an Agilent 8543 UV-visible spectrophotometer.

The complexes described in this chapter showed high sensitivity and decomposed upon air exposure. It was decided to submit only 2 samples for mass spectrometry. Since the analysis results were not satisfactory, the others were not submitted. Mass spectrometric analyses were conducted at the National Center for Research Resources (St. Louis, MO). Samples were not submitted for elemental analysis due to the poor performance of this compound type under analytical protocols.

All single crystals were coated with paratone-N oil (Hampton Research), and mounted onto thin glass fibres. Diffraction data were collected using graphite monochromated MoK_α radiation ($\lambda = 0.71073$ Å) on a Bruker SMART 1000 CCD area detector diffractometer via ϕ and ω scans. All data were collected at 223 K. The structures were solved using SHELXL-97[117] by direct methods. All structures were refined by least-squares full matrix refinement against F^2 using SHELXL-97 and all fully-occupied non-hydrogen atoms were refined with anisotropic

atomic displacement parameters (adps). Hydrogen atoms were geometrically placed and refined as part of a rigid model. Geometric restraints were applied, and partially occupied atom sites were refined with isotropic adps.

Solution NMR (^{1}H and ^{13}C) spectra can be found in the appendix of this chapter.

4.2.2 Preparation of compounds

4.2.2.1 Synthesis of bisphenols

Bisphenols **4.1c**-**e** were prepared according to a literature procedure.[212] For the synthesis of bisphenols **4.1d**-**e**, instead of using a stock solution of $HCl_{(g)}$ in methanol, anhydrous $HCl_{(g)}$ was continuously flowed into the reaction mixture to ensure completion of reaction.

2,2'-CH(Bn)(4,6-^{t}Bu$_2$C$_6$H$_2$OH)$_2$, 2,2'-phenylethylenebis(4,6-di-*tert*-butylphenol) (4.1c): 2,6-di-*tert*-butylphenol (2.063 g, 10.00 mmol), phenylacetaldehyde (0.661 g, 5.50 mmol), heptane (30 mL) and conc. H_2SO_4 (1 mL) were added together with strong stirring into a 100 mL round bottom flask equipped with condenser. The reaction mixture was refluxed for 8 h and then allowed to cool down to room temperature. The reaction mixture was washed twice with a saturated solution of $NaHCO_3$ and the organic phase separated and dried with $MgSO_4$. The solvents were evaporated from the organic phase, leaving behind an orange residue. A mixture of water:methanol (1:6, 50 mL) was added to the residue, boiled for 25 minutes, and then allowed to reach room temperature, affording a yellow precipitate. The yellow solid was recrystallized from a 20 mL mixture of chloroform and hexanes (1:10). Yield 2.020 g (78%). ^{1}H NMR (C_6D_6): δ (ppm) 7.38 (d, 2H, *J* = 2.4 Hz, aromatic *H*), 7.36 (d, 2H, *J* = 2.4 Hz, aromatic *H*), 6.97 (m, 3H, aromatic *H*), 6.86 (m, 2H, aromatic *H*), 5.35 (s, 2H, O*H*), 4.64 (t, 1H, *J* = 7.8 Hz, C*H*(CH_2Ph)), 3.40 (d, 2H, 7.8 Hz, CH(C*H*$_2$Ph)), 1.39 (s, 18H, C(C*H*$_3$)$_3$), 1.27 (s, 18H, C(C*H*$_3$)$_3$).

2,2'-CH[4-(NO$_2$)C$_6$H$_4$](4,6-^{t}Bu$_2$C$_6$H$_2$OH)$_2$, 2,2'-(4-nitrobenzylene)bis(4,6-di-*tert*-butylphenol) (4.1d): 2,6-di-*tert*-butylphenol (2.063 g, 10.00 mmol) and 4-nitrobenzaldehyde

(0.831 g, 5.50 mmol) were dissolved in anhydrous methanol (40 mL) in a 100 mL three neck flask. The first neck was attached to a mild argon flow, the second neck was equipped with a glass sintered bubbler that provided a mild anhydrous hydrogen chloride gas flow during the course of the reaction, and the third neck was connected to a trap used to quench the excess of HCl gas with a saturated solution of K_2CO_3. The reaction mixture was stirred at room temperature. After 2 days, stirring was stopped, the precipitate was collected by filtration, and it was recrystallized from hexanes at -15 °C yielding a yellowish crystalline solid. Yield 1.971 g (72%). ^{1}H NMR ($CDCl_3$): δ (ppm) 8.19 (d, 2H, *J* = 8.7 Hz, aromatic *H*), 7.33 (d, 2H, *J* = 8.7 Hz, aromatic *H*), 7.27 (d, 2H, *J* = 2.4 Hz, aromatic *H*), 6.65 (d, 2H, *J* = 2.4 Hz, aromatic *H*), 5.85 (s, 1H, C*H*(4-(NO_2)C_6H_4)), 4.89 (s, 2H, O*H*), 1.39 (s, 18H, C(C*H*$_3$)$_3$), 1.16 (s, 18H, C(C*H*$_3$)$_3$).

2,2'-CH[4-(OMe)C_6H_4](4,6-^{t}Bu$_2$$C_6H_2$OH)$_2$, 2,2'-(4-methoxybenzylene)bis(4,6-di-*tert*-butylphenol) (4.1e): 2,6-di-*tert*-butylphenol (2.063 g, 10.00 mmol) and 3-methoxybenzaldehyde (0.749 g, 5.50 mmol) were dissolved in anhydrous methanol (40 mL) in a 100 mL three neck flask. The first neck was attached to a mild argon flow, the second neck was equipped with a glass sintered bubbler that provided a mild anhydrous hydrogen chloride gas flow during the course of the reaction, and the third neck was connected to a trap used to release the excess HCl gas with a saturated solution of K_2CO_3. The reaction mixture was stirred at room temperature. After 2 days, stirring was stopped, the precipitate was collected by filtration, and it was recrystallized from hexanes at -15 °C yielding a white powder. Yield 2.008 g (76%). ^{1}H NMR (C_6D_6): δ (ppm) 7.52 (d, 2H, *J* = 2.4 Hz, aromatic *H*), 7.03 (two overlapping d, 4H, aromatic *H*), 6.65 (d, 2H, *J* = 8.7 Hz, aromatic *H*), 5.60 (s, 1H, C*H*(4-(OMe)C_6H_4)), 4.95 (s, 2H, O*H*), 3.17 (s, 3H, OC*H*$_3$), 1.55 (s, 18H, C(C*H*$_3$)$_3$), 1.21 (s, 18H, C(C*H*$_3$)$_3$).

2,2'-CH_2[4-(NO_2)-6-^{t}Bu$_2$$C_6H_2$OH]$_2$, 2,2'-methylenebis(4-nitro-6-*tert*-butylphenol) (4.1f): 2,2'-methylenebis(6-*tert*-butylphenol) (4.300 g, 13.76 mmol) was dissolved in cyclohexane (50 ml) in a 250 mL round bottom flask. The flask was equipped with an addition funnel. The system was placed in an ice bath at 0 °C. A HNO_3/AcOH mixture (1:1) (3.3 mL) was

prepared and suspended in cyclohexane (20 mL). The suspension was transferred to the addition funnel and added dropwise to the bisphenol solution with strong stirring at 0 °C over a period of 10 min, forming a dark brown-orange mixture (direct addition of the HNO_3/AcOH mixture to the bisphenol solution without cooling or dissolving will cause nitration in more than one position). Then, 50 mL of cool water were added, and stirring was continued for 10 min more. The resulting mixture was vacuum filtered through a fine pore filter paper, washed thoroughly with hexane and allowed to dry affording a yellowish powder. Yield 2.030 g, (37%). ^{1}H NMR (C_6D_6): δ (ppm) 8.07 (d, 2H, *J* = 2.4 Hz, aromatic *H*), 7.84 (d, 2H, *J* = 2.4 Hz, aromatic *H*), 6.00 (s, 2H, O*H*), 3.22 (s, 2H, CH_2), 1.11 (s, 18H, C(CH_3)$_3$).

4.2.2.2 Synthesis of lithium bisphenoxides.

The detailed preparation for compound **4.2a** is described below. The rest of the lithium bisphenoxides were synthesized following similar procedures.

2,2'-CH_2(LiO-6-^{t}Bu-4-MeC_6H_2)$_2$ (4.2a): A 15 mL solution of 2,2'-CH_2(6-^{t}Bu-4-MeC_6H_2OH)$_2$ (1.0000 g, 2.9368 mmol, **4.1a**) in Et_2O was prepared and cooled in an ice bath. ^{n}BuLi (2.93 mL of 2.0 M in pentane, 5.8 mmol) was mixed with Et_2O (7 mL); the resulting mixture was added dropwise (via addition funnel) to the phenol solution with strong stirring over a period of 30 min at 0 °C (the reaction is highly exothermic). The reaction mixture was allowed to reach room temperature over 2 h, stirring constantly. The solvent was concentrated in vacuo to *ca.* 5 mL and the mixture stored at -35 ˚C. After 1 day a white crystalline precipitate formed. The yellowish supernatant was removed with a pipette, and the precipitate was crystallized from Et_2O (7 mL) a second time. The supernatant was pipetted out and the white powder was dried under vacuum. Yield 0.7884 g (75%). ^{1}H NMR (CD_3CN): δ (ppm) 6.79 (s, 2H, aromatic *H*), 6.64 (s, 2H, aromatic *H*), 3.71 (s, 2H, methylene CH_2), 2.10 (s, 6H, CH_3), 1.31 (s, 18H, C(CH_3)$_3$).The ^{1}H NMR spectrum for this compound was reported before in Chapter 2, labeled as (**2.1i**).

2,2'-CH(^{i}Pr)(LiO-4,6-^{t}Bu$_2$C$_6$H$_2$)$_2$ (4.2b): was prepared following the same procedure as for **4.1a** but using 2,2'-CH(^{i}Pr)(4,6-^{t}Bu$_2$C$_6$H$_2$OH)$_2$ (1.0000 g, 2.1421 mmol, **4.1b**) and ^{n}BuLi solution (2.14 mL of 2.0 M in pentane, 4.3 mmol). White crystalline solid was obtained after recrystallization from Et_2O. Yield 0.7583 g (74%). 2,2'-CH(^{i}Pr)(LiO-4,6-^{t}Bu$_2$C$_6$H$_2$)$_2$ (**4.2b**) was poorly soluble in the available deuterated solvents and meaningful NMR data could not be obtained.

2,2'-CH(Bn)(LiO-4,6-^{t}Bu$_2$C$_6$H$_2$)$_2$ (4.2c): was prepared following the same procedure as for **4.1a** but using 2,2'-CH(Bn)(4,6-^{t}Bu$_2$C$_6$H$_2$OH)$_2$ (1.000 g, 1.9425 mmol, **4.1c**) and ^{n}BuLi solution (1.94 mL of 2.0 M in pentane, 3.9 mmol). White crystalline solid was obtained after recrystallization from Et_2O. Yield 0.7912 g (77%). 2,2'-CH(Bn)(LiO-4,6-^{t}Bu$_2$C$_6$H$_2$)$_2$ (**4.2c**) was poorly soluble in the available deuterated solvents and meaningful NMR data could not be obtained.

2,2'-CH[4-(OMe)C$_6$H$_4$](LiO-4,6-^{t}Bu$_2$C$_6$H$_2$)$_2$ (4.2e): was prepared following the same procedure as for **4.1a** but using 2,2'-CH[4-(OMe)C$_6$H$_4$](4,6-^{t}Bu$_2$C$_6$H$_2$OH)$_2$ (1.0000 g, 1.8840 mmol, **4.1e**) and ^{n}BuLi solution (1.88 mL of 2.0 M in pentane, 3.8 mmol). White powder was obtained after solvent evaporation and reprecipitation from pentane. Yield 0.8021 g (78%). 2,2'-CH[4-(OMe)C$_6$H$_4$](LiO-4,6-^{t}Bu$_2$C$_6$H$_2$)$_2$ (**4.2e**) was poorly soluble in the available deuterated solvents and meaningful NMR data could not be obtained.

2,2'-CH$_2$[LiO-4-(NO$_2$)-6-^{t}BuC$_6$H$_2$]$_2$ (4.2f): was prepared following the same procedure as for **4.1a** but using 2,2'-CH$_2$[4-(NO$_2$)-6-^{t}BuC$_6$H$_2$OH]$_2$ (1.0000 g, 2.4848 mmol, **4.1f**) and ^{n}BuLi solution (2.48 mL of 2.0 M in pentane, 4.97 mmol). An orange powder was obtained after solvent evaporation and reprecipitation from pentane. Yield 0.8901 g (86%). ^{1}H NMR (DMSO-d_6): δ (ppm) 7.69 (d, 2H, J = 2.7 Hz, aromatic *H*), 7.60 (d, 2H, J = 2.7 Hz, aromatic *H*), 3.40 (s, 2H, methylene C*H*$_2$), 1.28 (s, 18H, C(C*H*$_3$)$_3$).

4.2.2.3 Synthesis of Mo(VI) monooxo *cis* chloro *cis* bisphenoxides

$Mo(O)Cl_2${2,2'-CH_2(O-6-^{t}Bu-4-MeC_6H_2)$_2$-κ^2*O,O'*} (4.3a): was prepared by two methods. Method A: 2,2'-CH_2(6-^{t}Bu-4-$MeC_6H_2OH)_2$ (0.1712 g, 0.5029 mmol, **4.1a**) and MoO_2Cl_2 (0.1000 g, 0.5029 mmol) were dissolved, each in 10 mL of pentane. The bisphenol solution was added dropwise to the MoO_2Cl_2 suspension with rapid stirring at room temperature affording a dark purple-blue solution. After 12 h, the reaction mixture was filtered through a medium pore sintered glass frit and the solid remaining in the frit was reprecipitated from pentane (10 mL) two times more at -35 ^{o}C. The final precipitate was dried under vacuum. Note: Et_2O can be used instead as reaction solvent, but the product is mildly soluble in this solvent and the easy separation by filtration cannot be achieved without affecting the final yield. Yield 0.1701 g (65%). Method B: 2,2'-CH_2(LiO-6-^{t}Bu-4-$MeC_6H_2)_2$ (0.1389 g, 0.3941 mmol, **4.2a**) and $MoOCl_4$ (0.1000 g, 0.3941 mmol) were dissolved, each in 10 mL of Et_2O. The lithium bisphenoxide solution was added dropwise to the $MoOCl_4$ solution with rapid stirring at room temperature affording a dark purple-blue solution. After 12 h, the reaction mixture was concentrated under vacuum to ca. 5 mL and stored at -35 ^{o}C in the glovebox freezer. After one week dark purple needles were observed. X-ray quality crystals were selected and the remaining crystals were dried under vacuum. Yield 0.1201 g (58%). ^{1}H NMR ($CDCl_3$): δ 6.95 (s, 2H, aromatic *H*), 6.92 (s, 2H, aromatic *H*), 4.12 (d, 1H, J = 15.9 Hz, C*H*$_2$), 3.96 (d, 1H, J = 15.9 Hz, C*H*$_2$), 2.41 (s, 6H, C*H*$_3$) 1.35 (s, 18H,C(C*H*$_3$)$_3$). ^{13}C{^{1}H} NMR ($CDCl_3$): δ 161.5 (*ipso C*), 141.4 (*ortho* C), 140.7 (*para C*), 136.0 (*ortho C*), 129.0 (*meta C*), 126.5 (*meta C*), 40.1 (*C*H$_2$), 35.7 (*C*(CH$_3$)$_3$), 30.5 (C(*C*H$_3$)$_3$), 21.9 (*C*H$_3$). IR (cm^{-1}, KBr): 3415br, 2960s, 2914sh, 2873sh, 1591s, 1464w, 1292w, 1246w, 1209s, 1093w, 991vs (Mo=O), 910m, 866m, 796w, 621w, 578w. UV-vis (C_6H_6) λ_{max}/nm (ε/dm^{3}mol^{-1}cm^{-1}) : 289 (4949), 380 (2559), 540 (7468). Low resolution mass spectrometry results were unsatisfactory.

$Mo(O)Cl_2${2,2'-CH(^{i}Pr)(O-4,6-^{t}Bu$_2C_6H_2$)$_2$-κ^2*O,O'*} (4.3b): was prepared by two methods. Method A: 2,2'-CH(^{i}Pr)(4,6-^{t}Bu$_2C_6H_2OH)_2$ (0.2347 g, 0.5029 mmol, **4.1b**) and MoO_2Cl_2 (0.1000

g, 0.5029 mmol) were dissolved, each in 10 mL of pentane or Et_2O. The bisphenol solution was added dropwise to the MoO_2Cl_2 suspension with rapid stirring at room temperature affording a dark purple-blue solution. After 12 h, the reaction was concentrated under vacuum to ca. 5 mL and stored at -35 °C in the glovebox freezer. After 1 week crystalline solid in the walls of the vial was observed. The supernatant was withdrawn and recrystallization in pentane (5 mL) and 2 drops of benzene was performed once more. X-ray quality crystals were selected from the last recrystallization and the remaining crystals were dried under vacuum. Yield 0.1981 g (57%). Method B: 2,2'-CH(^{i}Pr)(LiO-4,6-^{t}Bu$_2$C$_6$H$_2$)$_2$ (0.1886 g, 0.3941 mmol, **4.2b**) and $MoOCl_4$ (0.1000 g, 0.3941 mmol) were dissolved, each in 10 mL of Et_2O. The lithium bisphenoxide solution was added dropwise to the $MoOCl_4$ solution with rapid stirring at room temperature affording a dark purple-blue solution. After 12 h, the reaction mixture was concentrated to ca. 7 mL and stored at -35 °C. After one week dark purple needles were observed. The supernatant was withdrawn and a second recrystallization from pentane was performed. The resulting needles were dried under vacuum. Yield 0.1701 g (67%). ^{1}H NMR (C_6D_6): δ 7.13 (d, 2H, *J* = 2.4 Hz, aromatic *H*), 7.10 (d, 2H, *J* = 2.4 Hz, aromatic *H*), 4.23 (d, 1H, *J* = 9.6 Hz, C*H*-^{i}Pr), 2.55 (m, 1H, C*H*(CH$_3$)$_2$), 1.34 (s, 18H, C(C*H*$_3$)$_3$), 1.27 (d, 6H, *J* = 6.6 Hz, CH(C*H*$_3$)$_2$), 1.11 (s, 18H,C(C*H*$_3$)$_3$). ^{13}C{^{1}H} NMR (C_6D_6): δ 161.6 (*ipso C*), 153.0 (*para* C), 141.6 (*ortho C*), 141.5 (*ortho C*), 122.3 (*meta C*), 122.0 (*meta C*), 57.0 (*C*H-^{i}Pr), 36.1 (*C*H(CH$_3$)$_2$), 35.3 (*C*(CH$_3$)$_3$), 32.4 (*C*(CH$_3$)$_3$), 31.1 (C(*C*H$_3$)$_3$), 30.6 (C(*C*H$_3$)$_3$), 21.3 (CH(*C*H$_3$)$_2$). IR (cm^{-1}, KBr): 3055br, 2991s, 1973s, 1845s, 1835s, 1590m, 1484m, 1438s, 1397sh, 1312m, 1271s, 1191m, 1120m, 1071m, 995s (Mo=O), 971s, 939m, 924w. UV-vis (C_6H_6) λ_{max}/nm (ε/dm^{3}mol^{-1}cm^{-1}): 290 (1180), 388 (1369), 540 (4789). Low resolution mass spectrometry results were unsatisfactory.

Mo(O)Cl$_2$\{2,2'-CH(Bn)(O-4,6-^{t}Bu$_2$C$_6$H$_2$)$_2$-*κ*^{2}*O,O'*\} (4.3c): was prepared by two methods. Method A: 2,2'-CH(Bn)(4,6-^{t}Bu$_2$C$_6$H$_2$OH)$_2$ (0.2589 g, 0.5029 mmol, **4.1c**) and MoO_2Cl_2 (0.1000 g, 0.5029 mmol) were dissolved, each in 10 mL of pentane or Et_2O. The bisphenol solution was added dropwise to the MoO_2Cl_2 suspension with rapid stirring at room temperature affording a

dark purple-blue solution. After 12 h, the reaction was concentrated under vacuum to ca. 5 mL and stored at -35 °C in the glovebox freezer. After 1 week solid was observed on the walls of the vial. The supernatant was withdrawn and recrystallization in pentane (5 mL) was performed once more. The crystals were dried under vacuum. Yield 0.1981 g (57%). Method B: 2,2'-CH(Bn)(LiO-4,6-^{t}Bu$_2$C$_6$H$_2$)$_2$ (0.2075 g, 0.3941 mmol, **4.2c**) and $MoOCl_4$ (0.1000 g, 0.3941 mmol) were dissolved, each in 10 mL of Et_2O. The lithium bisphenoxide solution was added dropwise to the $MoOCl_4$ solution with rapid stirring at room temperature affording a dark purple-blue solution. After 12 h, the reaction mixture was concentrated to ca. 7 mL and stored at -35 °C. After one week dark purple needles were observed. The supernatant was withdrawn and a second recrystallization from Et_2O was performed. The resulting needles were dried under vacuum. Yield 0.1567 g (57%). ^{1}H NMR ($CDCl_3$): δ 7.31 (d, 2H, *J* = 7.2 Hz, aromatic *H*), 7.21-7.08 (m, 7H, aromatic *H*), 4.57 (t, 1H, *J* = 6.9 Hz, C*H*-Bn), 3.53 (d, 2H, *J* = 6.9 Hz, CH-C*H*$_2$Ph), 1.31 (s, 18H, C(C*H*$_3$)$_3$) 1.28 (s, 18H, C(C*H*$_3$)$_3$). ^{13}C{^{1}H} NMR ($CDCl_3$): δ 161.4 (*ipso C*), 152.8 (*para* C), 141.2 (*ortho C*), 141.1 (*ortho C*), 137.2 (*ipso C* of Bn), 129.8 (*meta C* of Bn), 128.3 (*ortho C* of Bn), 126.8 (*para C* of Bn), 122.1 (*meta C*), 122.0 (*meta C*), 48.8 (*C*H$_2$ of Bn), 39.5 (*C*H-Bn), 35.9 (*C*(CH$_3$)$_3$), 35.5 (*C*(CH$_3$)$_3$), 31.2 (C(*C*H$_3$)$_3$), 30.6 (C(*C*H$_3$)$_3$). IR (cm^{-1}, KBr): 3436br, 2963vs, 2906sh, 2870sh, 1586s, 1458w, 1423w, 1392w, 1363m, 1240w, 1194m, 1137m, 991vs (Mo=O), 909w, 745m, 701m, 567m, 477m. UV-vis (C_6H_6) λ_{max}/nm (ε/dm^{3}mol^{-1}cm^{-1}): 287 (4653), 390 (2212), 554 (7414). Low resolution mass spectrometry results were unsatisfactory.

$MoOCl_2${2,2'-CH[4-(NO_2)C_6H_4](O-4,6-^{t}Bu$_2$C$_6$H$_2$)$_2$-κ^2*O,O'*} (4.3d): 2,2'-CH[4-(NO_2)C_6H_4](4,6-^{t}Bu$_2$C$_6$H$_2$OH)$_2$ (0.2745 g, 0.5029 mmol, **4.1d**) and MoO_2Cl_2 (0.1000 g, 0.5029 mmol) were dissolved, each in 10 mL of pentane. The bisphenol solution was added dropwise to the MoO_2Cl_2 suspension with rapid stirring at room temperature affording a dark blue solution. After 12 h, the reaction was concentrated under vacuum to ca. 5 mL and stored at -35 °C in the glovebox freezer. After 1 week a small amount of dark blue solid precipitate was observed. The supernatant was withdrawn and reprecipitation in pentane (5 mL) was performed twice more.

The solid was dried under vacuum. Yield 0.0429 g (12%). Complete purification was not accomplished. This product seems to gradually decompose into something different from the starting bisphenol, during the recrystallization period. Attempts to purify **4.3d** from Et_2O, hexanes, toluene, THF and their mixtures were unsuccessful. ^{1}H NMR ($CDCl_3$): δ 8.25 (d, 2H, *J* = 9.3 Hz, aromatic *H*), 7.64 (d, 2H, *J* = 9.3 Hz, aromatic *H*), 7.16 (d, 2H, *J* = 2.4 Hz, aromatic *H*), 6.90 (d, 2H, *J* = 2.4 Hz, aromatic *H*), 6.06 (s, 1H, C*H*[4-$(NO_2)C_6H_4$]), 1.41 (s, 18H, C(CH_3)$_3$), 1.21 (s, 18H, C(CH_3)$_3$). ^{13}C{^{1}H} NMR ($CDCl_3$): δ 161.3 (*ipso C*), 153.3 (*para C*), 147.2 (*ipso C* of [4-$(NO_2)C_6H_4$]), 146.4 (*para C* of [4-$(NO_2)C_6H_4$]), 141.8 (*ortho C*), 139.7 (*ortho C* of [4-$(NO_2)C_6H_4$]), 130.6 (*meta C* of [4-$(NO_2)C_6H_4$]), 124.5 (*ortho C*), 123.6 (*meta C*), 122.9 (*meta C*), 51.7 (*C*H[4-$(NO_2)C_6H_4$]), 36.1 (*C*(CH_3)$_3$), 35.5 (*C*(CH_3)$_3$), 31.0 (C(*C*H_3)$_3$), 30.6 (C(*C*H_3)$_3$). UV-vis (C_6H_6) λ_{max}/nm (ε/dm^{3}mol^{-1}cm^{-1}): 281 (11786), 582 (4952).

Mo(O)Cl$_2${2,2'-CH[4-(OMe)C$_6$H$_4$](O-4,6-^{t}Bu$_2$C$_6$H$_2$)$_2$-*κ*^{2}*O,O'*} (4.3e): was prepared by two methods. Method A: 2,2'-CH[4-(OMe)C_6H_4](4,6-^{t}Bu$_2$$C_6H_2$OH)$_2$ (0.2669 g, 0.5029 mmol, **4.1e**) and MoO_2Cl_2 (0.1000 g, 0.5029 mmol) were dissolved, each in 10 mL of pentane or Et_2O. The bisphenol solution was added dropwise to the MoO_2Cl_2 suspension with rapid stirring at room temperature affording a dark purple-blue solution. After 12 h, the reaction was concentrated under vacuum to ca. 5 mL and stored at -35 °C in the glovebox freezer. After 1 week solid precipitate was observed. The supernatant was withdrawn and reprecipitation from pentane (5 mL) was performed twice more, but **4.3e** could not be separated from the starting bisphenol. Et_2O and hexanes were used as recrystallization solvents with no success. Method B: 2,2'-CH[4-(OMe)C_6H_4](LiO-4,6-^{t}Bu$_2$$C_6H_2$)$_2$ (0.2138 g, 0.3941 mmol, **4.2e**) and $MoOCl_4$ (0.1000 g, 0.3941 mmol) were dissolved, each in 10 mL of Et_2O. The lithium bisphenoxide solution was added dropwise to the $MoOCl_4$ solution with rapid stirring at room temperature affording a dark purple-blue solution. After 12 h, the reaction mixture was concentrated to ca. 7 mL and stored at -35 °C. After one week dark blue precipitate was observed. The supernatant was withdrawn and recrystallization from Et_2O was performed twice more. Complete purification was not

accomplished and **4.3a** could not be separated from the starting bisphenol. Recrystallization attempts included pentane, hexanes, toluene and their mixtures with no success. ^{1}H NMR ($CDCl_3$): δ 7.31 (d, 2H, *J* = 8.4 Hz, aromatic *H*), 7.14 (d, 2H, *J* = 2.4 Hz, aromatic *H*), 7.02 (d, 2H, *J* = 2.4 Hz, aromatic *H*), 6.89 (d, 2H, *J* = 9.0 Hz, aromatic *H*), 5.97 (s, 1H, C*H*[4-(OMe)C_6H_4]), 3.84 (s, 3H, OCH_3), 1.40 (s, 18H, C(CH_3)$_3$), 1.16 (s, 18H, C(CH_3)$_3$).

$Mo(O)Cl_2${2,2'-CH_2[O-4-(NO_2)-6-^{t}Bu$_2$$C_6H_2$]$_2$-$\kappa^2$*O,O'*} (4.3f): was attempted by two methods. Method A: 2,2'-CH_2[4-(NO_2)-6-^{t}Bu$_2$$C_6H_2$OH]$_2$ (0.2024 g, 0.5029 mmol, **4.1f**) and MoO_2Cl_2 (0.1000 g, 0.5029 mmol) were dissolved, each in 10 mL of pentane. The bisphenol solution was added dropwise to the MoO_2Cl_2 suspension with rapid stirring at room temperature affording a purple solution. After 12 h, the reaction mixture was dried under vacuum. A ^{1}H NMR spectrum of the crude reaction mixture revealed just the presence of bisphenol **4.1f**. Pentane, hexanes and heating at 45, 75 and 110 °C for 12 h were tried with no success. Product **4.3f** was not observed and bisphenol **4.1f** was formed at all times. Method B: 2,2'-CH_2[LiO-4-(NO_2)-6-^{t}Bu$_2$$C_6H_2$]$_2$ (0.1633 g, 0.3941 mmol, **4.2f**) and $MoOCl_4$ (0.1000 g, 0.3941 mmol) were dissolved, each in 10 mL of Et_2O. The lithium bisphenoxide solution was added dropwise to the $MoOCl_4$ solution with rapid stirring at room temperature affording a dark purple-blue solution. After 12 h, the reaction mixture was dried under vacuum. A ^{1}H NMR spectrum of the crude reaction mixture revealed the presence of bisphenol **4.1f** as the only product. Pentane, hexanes and heating at 45, 75 and 110 °C for 12 h were tried with no success. Product **4.3f** was not observed and bisphenol **4.1f** was formed at all times.

4.3 Results and discussion.

The chemistry of chelating aryloxide ligands has attracted increased interest within the last few years.[208, 213] Their rich coordination chemistry and capability to undergo backbone modifications to modify steric and electronic attributes, makes them suitable candidates as chelating ligands for early transition elements.[214, 215] For instance, it has been demonstrated that

the addition of bulky aryl substituents can influence the structures and reactivities of metal complexes by sterically crowding the metal coordination environment.[216-218] The possible effects of these chelating ligands on the chemistry of molybdenum(VI) oxo complexes inspired the synthesis of different bisphenols, for use as bidentate ligands.

Bisphenols **4.1b**-**e** were synthesized from 2,4-di-*tert*-butylphenol and the respective aldehyde (Scheme 4.1). Bisphenol **4.1f** was prepared by nitration of 2,2'-methylenebis(6-*tert*-butylphenol). Attempts to synthesize **4.1f** starting from 2-tert-butyl-4-nitrophenol and formaldehyde were unsuccessful. The summary of the reaction conditions for the synthesis of bisphenols **4.1a**-**f** is found in Scheme 4.1.

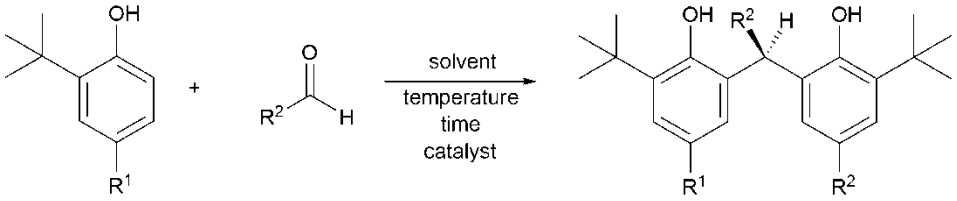

4.1b-**f**

Label	Substituents		Reaction conditions				Yield (%)
	R^1	R^2	solvent	Temp	time	catalyst	
4.1b	^{t}Bu	^{i}Pr	AcOH	0 °C to R.T.	23 h	$BF_3{\cdot}Et_2O$	74
4.1c	^{t}Bu	Bn	heptane	Reflux	8 h	H_2SO_4	78
4.1d	^{t}Bu	4-$(NO_2)C_6H_4$	MeOH	R.T.	48 h	$HCl_{(g)}$	76
4.1e	^{t}Bu	4-$(OMe)C_6H_4$	MeOH	R.T.	48 h	$HCl_{(g)}$	72
4.1f[a]	H	H	xylenes	175 °C	10 h	-	90

[a] The nitrated bisphenol was synthesized starting from this bisphenol and HNO_3/AcOH.

Scheme 4.1 Reaction conditions for the synthesis of different disphenols.

Since our intention in the synthesis of these organic molecules is their application and use as prospective ligands, the preparation of their lithium salts was accomplished. Synthesis of lithium aryloxides has been a common practice throughout this dissertation, as they offer a reliable way to access to different molybdenum(VI) oxo aryloxides by their reaction with a molybdenum(VI) oxo halide via simple substitution.

The synthesis of lithium bisphenoxides was performed by hydrogen abstraction from the OH function using ^{n}BuLi. The resulting lithium bisphenoxides **4.2a**-**f**, with the exception of **4.2a** and **4.2f**, were poorly soluble in deuterated solvents, preventing them from being characterized by ^{1}H NMR.

The bisphenols **4.1a**-**f** and their lithium bisphenoxides **4.2a**-**f** were reacted as shown in Scheme 4.2. These reactions led to the different molybdenum(VI) monooxo bisphenoxides that will be discussed in this chapter.

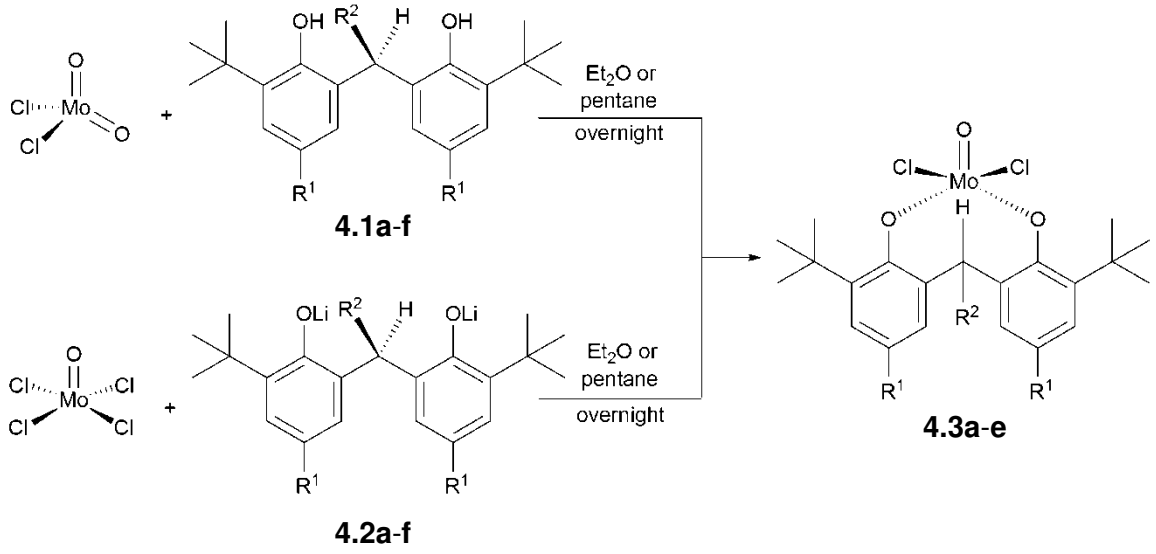

4.1a-f

4.2a-f

4.3a-e

Label	Substituents			Yield (%)
	Precursor	R^1	R^2	
a	bisphenol	Me	H	65
	lithium bisphenoxide			58
b	bisphenol	^{t}Bu	^{i}Pr	57
	lithium bisphenoxide			67
c	bisphenol	^{t}Bu	Bn	57
	lithium bisphenoxide			57
d	bisphenol	^{t}Bu	4-(NO_2)C_6H_4	12
	lithium bisphenoxide			-
e	bisphenol	^{t}Bu	4-(OMe)C_6H_4	not isolated
	lithium bisphenoxide			not isolated
f	bisphenol	NO_2	H	not observed
	lithium bisphenoxide			not observed

Scheme 4.2 Synthetic routes for the syntheses of Mo(VI) monooxo bisphenoxides.

The synthesis of the different chelated molybdenum(VI) monooxo bisphenoxides was accomplished in nonpolar solvents such as pentane and Et_2O, according to the reaction described in Scheme 4.2.

MoO_2Cl_2 reacts with 1 equiv of bisphenol to instantaneously form dark purple-blue solutions from which $MoOCl_2$(bisphenoxides) **4.3a**-**e** are isolated. In the same way $MoOCl_4$ reacts with 1 equiv of the lithium bisphenoxides to yield dark purple blue solutions that contain the $MoOCl_2$(bisphenoxide) product. Direct addition of bisphenol to the molybdenum(VI) dioxo precursor is a very convenient and easy 1-step synthesis to produce molybdenum(VI) monoxo bisphenoxide complexes (although it does not always offer the best yields).

The series of bisphenols shown in Scheme 4.1 were produced in order to explore the steric and electronic effects that the ligand might exert in the shape and reactivity of the final complexes. Tuning of the steric factor was accomplished first, by addition of substituents with different steric demands on the methylene bridge. The *tert*-butyl groups were kept constant along the series. Adjustment of the electronic properties of the ligand came next. We added electron withdrawing (NO_2) and electron donating (OMe) groups to different parts of the bisphenol backbone. By combining steric and electronic effects we produced a set of ligands that will allow us to study and understand the chemistry of Mo(VI) monooxo bisphenoxides.

4.3.1 Spectroscopy

The IR spectrum of each compound showed one medium to strong intensity peak in the range of 991 to 995 cm^{-1}, which is assigned to the Mo=O stretching frequency. These values fall within the normal range for MoO^{4+} complexes.[25, 57, 81] The similar Mo=O bond stretching frequencies are consistent with the oxo bond strength/order obtained from the X-ray structures of molecules **4.3a** and **4.3b** (based on Mo=O bond lengths) and with other MoO^{4+} cored molecules previously reported.[25, 57]

The ^{1}H NMR spectra of the synthesized bisphenols **2.1a-f** as well as the ^{1}H and ^{13}C NMR spectra of the $MoOCl_2$(bisphenoxide) complexes **2.3a**-**e** prepared with them, reveal the existence of a mirror plane that crosses each molecule through the methylene bridge. The number of ^{1}H and ^{13}C NMR peaks observed for molecules **2.1a-f** and **2.3a**-**e** is therefore halved due to the magnetic equivalence of the nuclei (Hs and Cs) in opposite sides of the mirror plane with a bridging methylene (or substituted methylene) as center of symmetry. All the peak values and assignments are reported in the experimental section (refer to appendix for a graphical ^{1}H and ^{13}C peak assignment). In the case of complex **4.3a**, the methylene protons in the chelate backbone are diastereotopic. They are exposed to different magnetic environments: one pointing to the metal center (*endo*[219]) and the other pointing down from the coordination sphere (*exo*[219]), therefore the ^{1}H NMR spectrum shows two doublets (in the parent phenol the methylene protons are a singlet).

Electronic spectra of the complexes in benzene display three intense bands, one of them in the 287-290 nm region, the second in the 380-390 nm region, and a third one in the 540-582 nm region. The first band (B band for aromatic systems)[126] corresponds to a $\pi \rightarrow \pi^*$ transition of the benzene chromophore influenced by the unshared electron pair of the auxochromic oxygen (this band is present in the lithium phenoxides as well as in the plain phenols in about the same region). The remaining two bands at 380-390 nm and 540-582 nm can be identified as LMCT bands. These complexes possess a square pyramidal geometry and, unlike the bright complexes of Chapter 2, they are dark blue (absorb purple and green and transmit blue and red = dark blue). These LMCT bands might account for low energy transitions (weak band at 388 nm and intense absorption at 540-554 nm) due to a small band gap between the a_1 and the b_2 levels in a SP arrangement.[220] The ligands have lone pairs of relatively high energy and the metal has low-lying a_1 empty orbitals.[220] It is likely that a nonbonding oxygen-localized 2p electron in the oxo (Figure 4.1a) or aryloxide ligand (Figure 4.1b) might be transferred to the low lying empty d orbital on molybdenum. The strong LMCT band at 540-554 nm may involve a

contribution from the in-plane mixing of oxygen and molybdenum orbitals shown in Figure 4.1.[192] Complexes **4.3a** and **4.3b** exhibit a "folded" SP arrangement where the central atom lies above the basal plane (based on their X-ray structure, which will be discussed in section 4.3.2). The interaction between non-bonding oxygen orbitals and empty Mo d orbitals (Figure 4.1b) should facilitate the electron transfer. Similar behavior has been investigated in molybdenum oxo enzymes where dithiolate ligands contribute to the electronic structure of a molybdenum oxo center.[192]

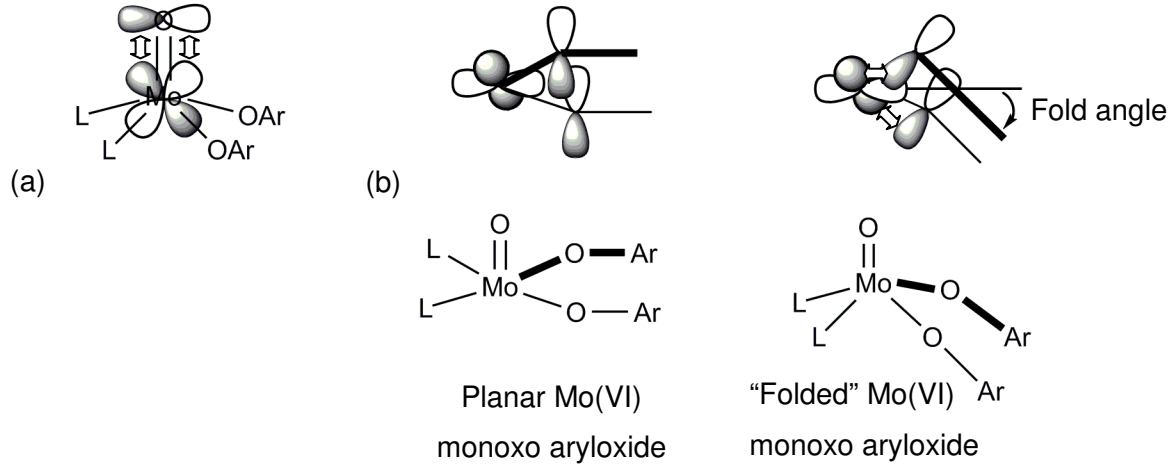

Figure 4.1 Possible interactions between ligand and metal orbitals that might account for the observed LMCT bands. (a) Electronic contribution from a non bonding p orbital located in the oxo ligand (adapted from ref.[201]). (b) Electronic contribution from the oxo bisphenoxide p orbitals to the molybdenum center. Complexes **4.3a**-**b** exhibit an SP arrangement where the central atom lies above the basal plane, facilitating the interaction between the p and d orbitals. In a regular SP geometry this interaction would not be possible. (adapted from ref.[192])

4.3.2 Electronic and Structural Effects

Products **4.3a**-**f** were synthesized from the reaction of bisphenol and MoO_2Cl_2 or by the reaction between the lithium bisphenoxide and $MoOCl_4$ (Scheme 4.2).

It is interesting to observe that what we learned from the synthesis of $MoOCl_2(OAr)_2$ complexes (Chapter 3) has direct application to the synthesis of these chelated complexes. The proposed addition of the O-H function across the Mo=O bond is a process that can be extended from monodentate aryl alcohols to bidentate aryl alcohols. Differences and similarities can be found between mono and bidentate ligands.

The mechanism of O-H addition across the Mo=O in monodentate aryl alcohols yields a *trans*-aryloxide, *trans*-chloride Mo(VI) monooxo complex. When using bidentate aryl alcohols, a *cis*-bisphenoxo, *cis*-chloride arrangement is observed around the MoO^{4+} center. This is not surprising, as chelates are likely to occupy *cis*-positions when the coordinate to the same metal center.

Electronic effects again play an important role in the outcome of the reaction. In chapters 2 and 3 we learned that aryl alcohols or aryloxides bearing a strong electron withdrawing group (e. g. NO_2) led to no product (usually just the starting phenol is observed). In the same manner, bisphenol 2,2'-CH_2[4-(NO_2)-6-^{t}$Bu_2C_6H_2OH]_2$ (**4.1h**) and MoO_2Cl_2 were reacted but the desired product was not observed (even if the lithium bisphenoxide **4.2h** is reacted with the $MoOCl_4$ precursor).

The position of the electron-withdrawing/donating group is also of crucial importance. Bisphenols 2,2'-CH[4-(NO_2)C_6H_4](4,6-^{t}$Bu_2C_6H_2OH)_2$ (**4.1d)** and 2,2'-CH_2[4-(NO_2)-6-^{t}$Bu_2C_6H_2OH]_2$ (**4.1h**) bear nitro substituents in different positions. **4.1d** has a *para*-nitro group in the aryl ring attached to the methylene bridge, whereas **4.1h** has the nitro substituents *para* to the binding phenoxy oxygens. Product **4.3d** was synthesized and characterized, but product **4.3h** was not observed. Electronic effects are apparently more important for the binding of the bisphenoxide ligand when the electron withdrawing/donating substituents are present in the phenoxy rings. Synthesis of a bisphenoxide bearing electron donating groups in the *para* position was attempted in order to compare its electronic effects with the bisphenol **4.1h** and its lithium salt **4.2h**, but we did not succeed in its preparation.

Electron withdrawing/donating substituents that are not directly attached to the phenoxy rings, do not play a major role in the binding process of the chelating bisphenols/bisphenoxides to the molybdenum center, but they might affect the reactivity of the C-H bond of the methylene bridge.[206]

4.3.3. Crystal structure and three-dimensional geometry

Table 4.2 Crystallographic Data and Summary of Data Collection and Structure Refinement

	4.3a	**4.3b**
Formula	$C_{23}H_{30}Cl_2MoO_3$	$C_{32}H_{48}Cl_2MoO_3 \cdot C_6H_6$
fw	521.31	726.25
crystal system	Monoclinic	Monoclinic
space group	C2/c	$P2_1/c$
T, K	213(2) K	213(2) K
a, Å	29.919(8)	9.6850(10)
b, Å	10.905(3)	21.184(2)
c, Å	19.220(5)	18.1866(19)
α, deg	90	90
β, deg	129.05(3)	93.945(2)
γ, deg	90	90
V, Å^3	4870(2)	3058.9(14)
Z	8	4
D_{calc}, mg/m^3	1.422	1.252
θ range (deg) for data collection	2.26-25.00	1.45-28.39
$N_{measured}$	14933	29152
$N_{independent}$	4280	9071
R	0.0454	0.0427
ωR_2	0.1078	0.1176
GOF	1.107	1.027
largest diff peak and hole (e·Å^3)	0.576 and -0.548	0.685 and -0.409

Tables 4.2 and 4.3 collect important structural information of selected molecules. The 5-coordinate SP $MoOCl_2(OAr)_2$ **3.2a**,[81] $MoOCl(OAr)_3$ **3.3a**,[81] and $MoO(OAr)_4$ complexes are listed for comparison (Chapter 3).

Table 4.3 Selected Bond Lengths (Å)

		Mo=O	Mo-O(aryloxy)
5-coordinate			
$MoOCl_2(OAr)_2$[81]	(**3.2a**)	1.628(13)	1.838(10) 1.856(11)
$MoOCl(OAr)_3$[81]	(**3.3a**)	1.667(3)	1.862(3) 1.891(4) 1.893(3)
$MoO(OAr)_4$	(**3.4a**)	1.685(2)	1.882(1)
$MoOCl_2[CH_2(OAr)_2]$	(**4.3a**)	1.659(3)	1.870(3) 1.874(3)
$MoOCl_2[CH(^iPr)(OAr)_2]$	(**4.3b**)	1.656(1)	1.869(1) 1.875(1)

Table 4.4 Selected Bond Angles (deg)

		O=Mo-OAr	Mo-O-C(aryloxy)	ArO-Mo-OAr
5-coordinate				
$MoOCl_2(OAr)_2$[81]	(**3.2a**)	101.0(5) 101.3(6)	156.5(10) 167.2(12)	
$MoOCl(OAr)_3$[81]	(**3.3a**)	101.22(15) 101.57(15) 110.20(15)	148.1(3) 134.2(3) 147.5(3)	91.84(14) 87.14(14)
$MoO(OAr)_4$	(**3.4a**)	104.71(4)	147.45(10)	86.30(2)
$MoOCl_2[CH_2(OAr)_2]$	(**4.3a**)	104.66(14) 103.24(13)	141.9(2) 142.3(3)	89.66(12)
$MoOCl_2[CH(^iPr)(OAr)_2]$	(**4.3b**)	103.61(9) 103.83(9)	143.75(16) 142.55(16)	91.29(7)

In complexes **4.3a** and **4.3b** (Figures 4.2 and 4.3) the central atom is above the basal square plane by an average of 13° (the O=Mo-OAr angles are bigger than the ideal 90° for a SP geometry), 3° more than that observed for $MoOCl_n(OAr)_{n-1}$ complexes. The apical bond is the shortest (higher bond order) among all the ligands as expected for a d^0 species.[193]

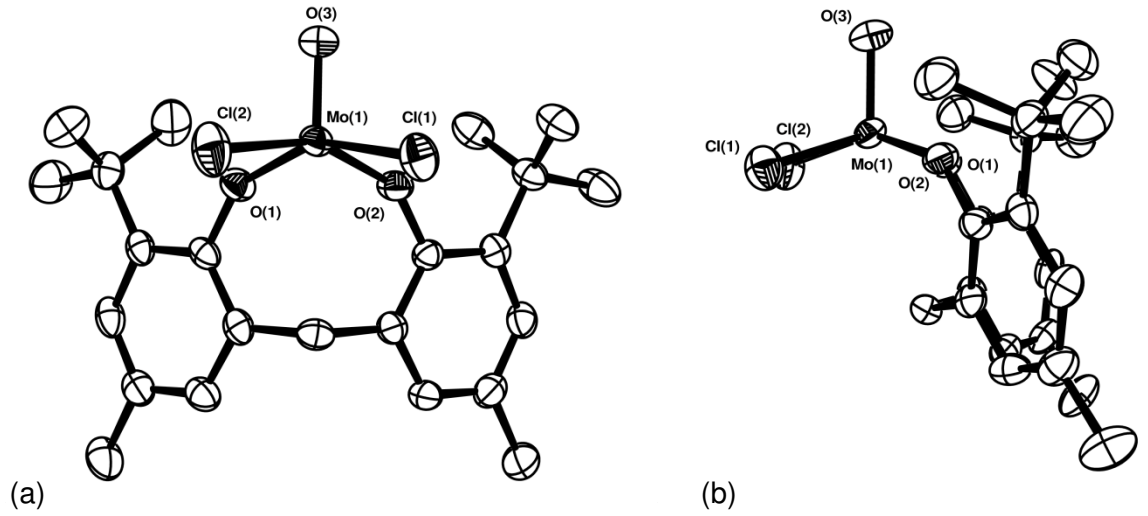

Figure 4.2 ORTEP view of Mo(O)Cl_2{2,2'-CH_2(O-6-^{t}Bu-4-Me$C_6H_2)_2$-κ^2*O,O'*} (**4.3a**) (50% probability). Hydrogen atoms have been omitted for clarity. (a) front view (b) side view.

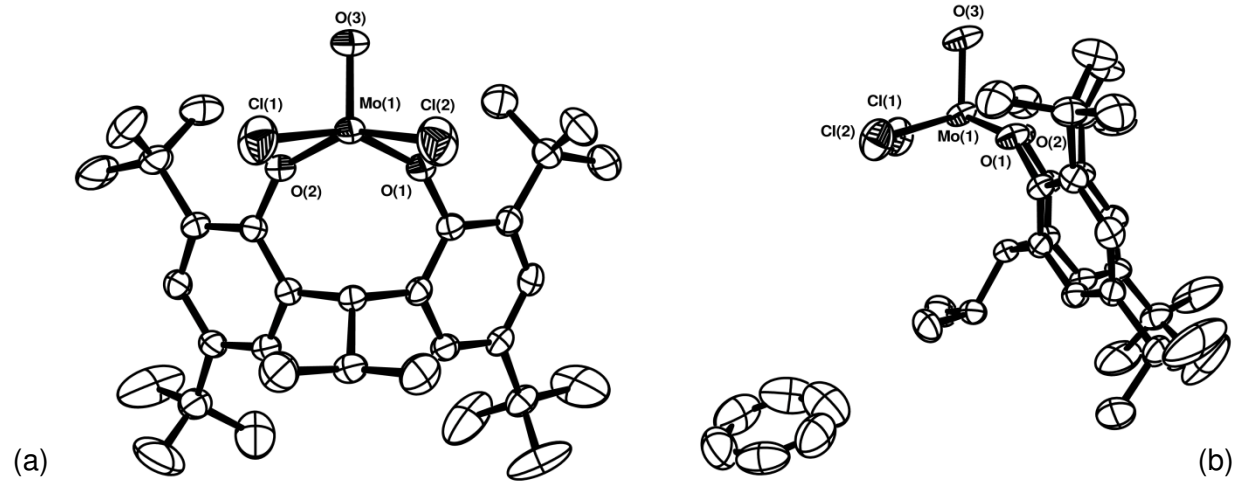

Figure 4.3 ORTEP view of Mo(O)Cl_2{2,2'-CH(^{i}Pr)(O-4,6-^{t}Bu$_2C_6H_2)_2$-κ^2*O,O'*} (**4.3b**) (50% probability). Hydrogen atoms have been omitted for clarity. (a) front view, omitting benzene molecule of co-crystallization (b) side view, including benzene molecule.

From tables 4.3 and 4.4 we can extract important information regarding similarities between $MoOCl_n(OAr)_{n-1}$ complexes and $MoOCl_2[CHR(OAr)_2]$ (R = H, **4.3a** and R= ^{i}Pr, **4.3b**). For example, the Mo=O bond length for complexes **4.3a** (1.659(3) Å) and **4.3b** (1.656(1) Å) falls in the range of the observed lengths for the $MoOCl_n(OAr)_{n-1}$ compounds of 1.628(13) to 1.685(2) Å. The Mo-O-Ar average bond length of 1.870(3) for **4.3a** and 1.875(1) Å for **4.3b** are similar to

the observed range of bond lengths in their $MoOCl_n(OAr)_{n-1}$ counterparts of 1.838(10) to 1.893(3) Å.

As noted above, the MoO^{4+} moiety in complexes **4.3a** and **4.3b** is farther above their square basal plane than the MoO^{4+} moiety in the $MoOCl_n(OAr)_{n-1}$ complexes (**3.2a**-**3.4a**). This might be a product of the *cis*-oriented ligand structural and sterical requirements that force the MoO^{4+} to rise above its basal plane (as when the two ends of a plastic bar are pushed at the same time and the center rises above the plane to relieve the pressure).

The addition of alkyl or aryl groups to the methylene bridge of the different bisphenols had little effect on the MoO^{4+} center. As can be seen from Figures 4.2 and 4.3 the methylene carbon points away from the MoO^{4+} center (it folds “inside-out” and this folding induces the methylene to point down). A dialkyl bridge will presumably have a larger effect on the MoO^{4+} group.

Although certain Mo(IV) complexes bearing the bisphenol 2,2’-CH_2(-6-^{t}Bu-4-MeC_6H_2-OH)$_2$ (**4.1a**) have shown agostic C-H···MoO^{4+} interactions,[206] we observed no such interaction in our case.

In general bond angles and lengths are consistent between the complexes presented here and those presented in Chapter 3.

4.4 Conclusion

The facile synthesis of different bisphenols was accomplished in order to use them as chelating ligands to synthesize Mo(VI) complexes. Tuning of steric properties was achieved by addition of different alkyl and aryl moieties. Adjustment of the electronic effect was achieved by using electron donating or electron withdrawing groups on the aryl rings.

Mo(VI) monooxo bisphenoxide complexes were synthesized by two routes: aryl alcohol addition across the Mo=O bond and by the reaction of lithium bisphenoxides with the $MoOCl_4$ precursor (simple substitution).

The MoO^{4+} complexes synthesized using bisphenol/bisphenolate ligands, displayed a *cis*-, *cis*- arrangement between the two chlorine atoms and the aryl units that form the bisphenol, with the strong Mo=O group in the apical position as expected for complexes displaying a square pyramidal geometry.

CHAPTER 5

RING-OPENING METATHESIS POLYMERIZATION OF NORBORNENE USING MOLYBDENUM(VI) MONOOXO ARYLOXO- AND BISPHENOXO COMPLEXES.

5.1 Introduction

The word metathesis is derived from the Greek *meta* (change) and *tithemi* (place), meaning transposition of two sounds or letters in a word. In chemistry it refers to the interchange of atoms between two molecules.[157] Olefin metathesis is the (apparent) interchange of carbon atoms between a pair of double bonds.[157] More precisely olefin metathesis is a catalytic reaction in which alkenes are converted into new products via the rupture and reformation of carbon-carbon double bonds.[221]

Olefin metathesis is a useful reaction where olefins exchange the groups connected by a double bond resulting in a variety of different new products that would be otherwise inaccessible or difficult to produce.[222-224] Since the first reports of olefin metathesis in the early 1960s,[225-227] tremendous progress has been made in the field of this novel reaction. Today olefin metathesis is a popular reaction with many applications,[228] from drug development to industrial elastomer production.[229] Indeed in 2005 the Nobel Prize in Chemistry was awarded to Chauvin, Grubbs, and Schrock for the development of this useful catalytic reaction.[230]

Among the members of the olefin metathesis family of reactions, the most studied are: cross-metathesis (CM), the interchange of groups between two acyclic olefins; ring-closing metathesis (RCM), closure of large rings; ring opening metathesis (ROM), the formation of dienes from cyclic and acyclic olefins; and ring opening metathesis polymerization (ROMP), the polymerization of cyclic olefins.[231] The overall chemistry (but not the mechanism) is shown in Scheme 5.1. The reactions are generally reversible and, with the right catalyst system, equilibrium can be attained in a matter of seconds.[157]

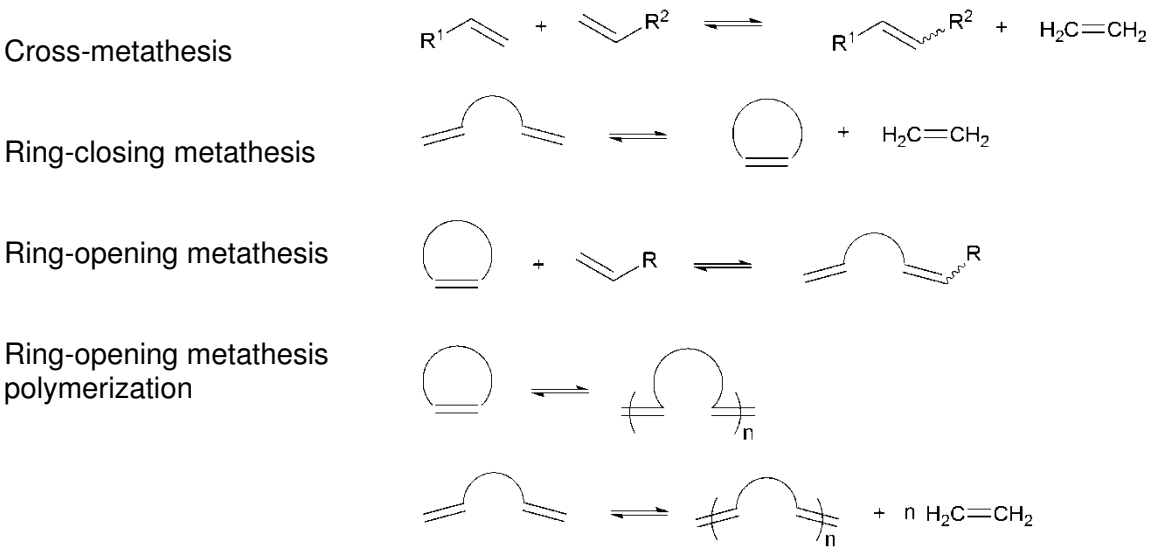

Scheme 5.1 Most studied olefin metathesis reactions.

Catalyst systems for olefin metathesis almost invariably contain a transition metal compound. These are sometimes effective by themselves but often require the presence of a second compound (co-catalyst), and sometimes a third (promoter). The systems most commonly used are based on the chlorides, oxides, or other easily accessible compounds of Mo, Ru, W, or Re.[157, 232] Os, Ir, Ti, V, Cr and Ta are sometimes used.[157] Typical co-catalysts are $EtAlCl_2$, R_3Al and R_4Sn (R = Ph, Me, Et, Bu), while promoters often contain oxygen, e.g. O_2, EtOH, PhOH.[157] Representative examples of extremely active systems at room temperature are WCl_6/EtOH/$EtAlCl_2$, $MoCl_2(NO)_2L_2$/Me_3Al and $WOCl_4$/Me_4Sn.[232]

The mechanism of reaction by which the transition metal “exchanges” the alkylidene moieties was a puzzling question. The first mechanism proposed by Bradshaw (1976) involved a “quasi-cyclobutane” complex.[232] In this model two double bonds come together in the vicinity of the transition metal site and the orbitals of the transition metal overlap with those of the double bonds in a way that would allow the exchange to occur via a cyclobutane-type complex (Scheme 5.2).[157]

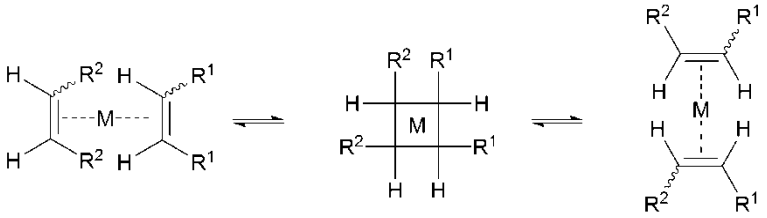

Scheme 5.2 The “pairwise” exchange of alkylidene fragments between two olefins (adapted from ref.[232]).

After collection of theoretical and experimental evidence, the “pairwise” mechanism was eventually discarded in favor of the “metal carbene chain mechanism” or “carbene mechanism”, proposed by Hérrison and Chauvin.[232] In this mechanism the active species is a metal carbene complex formed from the catalyst/substrate system. The reaction is assumed to proceed via a metallacyclobutane intermediate (not normally detected) and a metal carbene complex is regenerated at every stage (Scheme 5.3).[157]

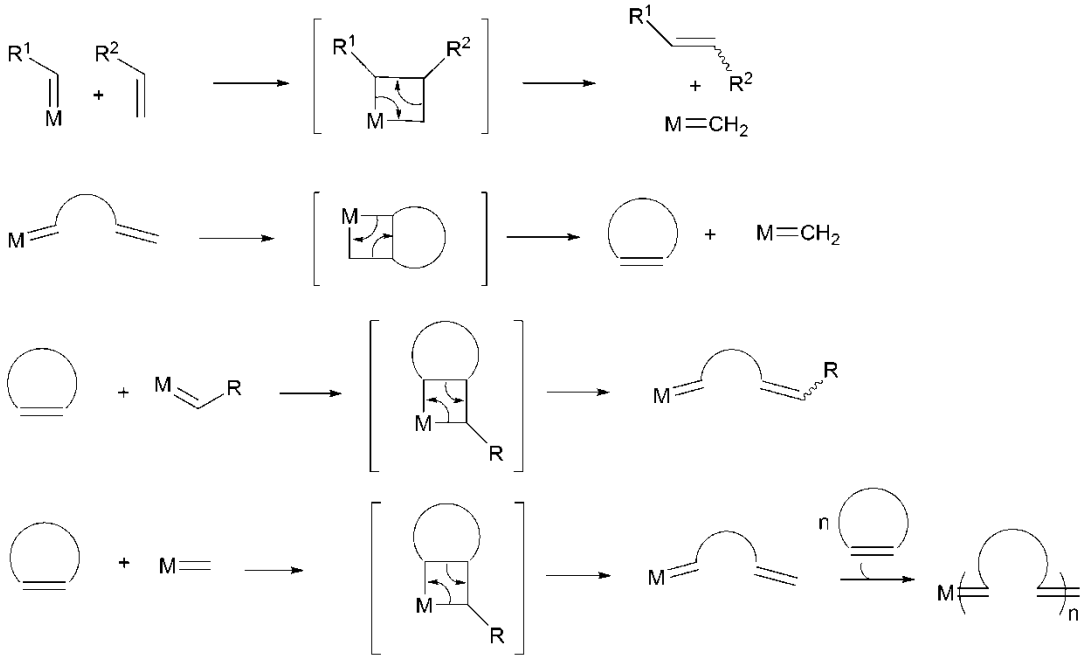

Scheme 5.3 Olefin metathesis reaction mechanism. The metallacyclobutane intermediate is in brackets. M represents the transition metal (other ligands have been omitted for clarity).

The advent of the “carbene mechanism” gave rise to intense research that has yielded the synthesis of more specific and well-defined catalysts such as those developed by Grubbs

and Schrock, containing metal carbene (metal-alkylidene) moieties.[233, 234] The so-called Grubbs and Schrock catalysts were developed through focused research programs going back to the 1970s.[231] In the mid-1980s, Schrock developed highly reactive systems based on tungsten and then on molybdenum (W=CRR' or Mo=CRR').[235] In 1992 Grubbs developed his first ruthenium catalysts (Ru=CRR').[231, 236] Both catalysts have been refined over the years to improve selectivities and reactivities.[231]

The power of olefin metathesis is that it transforms the carbon-carbon double bond, a functional group that is generally unreactive. With certain catalysts, new carbon-carbon double bonds are formed at or near room temperature even in aqueous media from starting materials that bear a variety of functional groups.[237] The catalysts are commercially available, making the reaction accessible to everyone. In this way olefin metathesis has become a very versatile tool with academic and industrial applications.[228]

The research in the past two decades has yielded structurally well-defined catalysts for olefin metathesis that are used to synthesize an array of molecules with unprecedented efficiency.[237] Nonetheless, the field of olefin metathesis is full of challenges that require the synthesis of new catalytic systems capable of higher reactivities and selectivities.

Our motivation in doing the studies presented in this chapter was to add to ongoing research in the field of the metathesis polymerization reaction, which is catalogued as one of the most important types of olefin metathesis in polymer chemistry.[228] In this chapter we will introduce the use of different molybdenum(VI) monooxo aryloxo- and bisphenoxo complexes as initiators for this fundamental reaction, and we will illustrate how the structure of these complexes affects their reactivity. The composition of a catalyst (or pro-catalyst) is certainly important but deeply dependent of the structure of the catalyst (or pro-catalyst) complex.

5.2 Experimental section

5.2.1 General

All manipulations were performed under dry argon using standard Schlenk techniques or under nitrogen in a NEXUS 1 Vac Atmospheres glovebox. Molybdenum(VI) dichloride dioxide, *n*-butyllithium (2.0 M solution in *n*-pentane), phenyllithium (1.9 M solution in cyclohexane/ether), triethylaluminum (1.0 M solution in hexane), phenylmagnesium bromide (1.0 M solution in Et_2O), *sec*-butyllithium (1.4 M solution in cyclohexane), benzylmagnesium chloride solution (2.0 M in THF), neopentyl chloride, norbornene (NBE), 2,2'-methylenebis(6-tert-butyl-4-methylphenol), lithium wire, and cyclohexene were purchased from Aldrich and used as received. Diphenylmercury and racemic-5,5',6,6'-tetramethyl-3,3'-di-*tert*-butyl-1,1'-biphenyl-2,2'-diol, rac-BIPHEN$(OH)_2$ were purchased from Strem Chemicals Company and used without further purification. MeOH and 2-propyl alcohol were obtained from AAPER.

$MoOCl_4$ was freshly prepared from MoO_3 (J. T. Baker Chemical Company) and newly purchased thionyl chloride (Aldrich) as described previously.[165] The thus synthesized $MoOCl_4$, although reported to be pure for most uses,[165] was further sublimed,[165, 168] and stored in an amber bottle inside the glovebox freezer at -35 °C.

MoO(O-2,6-$Me_2C_6H_3)_2Cl_2$ (**3.2a**), MoO(O-2,6-$Me_2C_6H_3)_3Cl$ (**3.2b**), Mo(O)Cl_2{2,2'-CH_2(O-6-^{t}Bu-4-$MeC_6H_2)_2$-κ^2*O,O'*} (**4.3a**), Mo(O)Cl_2{2,2'-CH(^{i}Pr)(O-4,6-$^t Bu_2C_6H_2)_2$-κ^2*O,O'*} (**4.3b**) were synthesized according to the procedures and starting materials described in Chapters 3 and 4 of this dissertation. MoO(rac-biphenolate)$_2$ and MoO[2,2'-methylenebis(6-tert-butyl-4-methylphenolate)]$_2$ were prepared from $MoOCl_4$, *n*-BuLi, rac-BIPHEN$(OH)_2$ or 2,2'-methylenebis(6-tert-butyl-4-methylphenol) in Et_2O as described in the literature.[79]

Benzyllithium was prepared from toluene, THF and sec-butyllithium as described elsewhere.[238] Neopentyllithium was prepared from a solution of neopentyl chloride and lithium wire in pentane as reported previously.[239]

Toluene and diethyl ether (Et_2O) were freshly distilled under argon from Na/benzophenone. *n*-Pentane and cyclohexane (anhydrous grade) was purchased from Aldrich and stored over molecular sieves. Cyclohexene (Aldrich) was pre-dried over 4 Å molecular sieves (previously activated) for 48 h and further refluxed and distilled from CaH_2 under argon. NMR solvents (benzene-d_6 and chloroform-d) were degassed and vacuum distilled from CaH_2. All solvents (including NMR solvents) were stored inside the glovebox over 4 Å molecular sieves (previously activated) for 48 h before use.

^1H spectra were recorded on a Mercury Varian Plus 300 MHz spectrometer. ^1H NMR data are expressed as parts per million (ppm) downfield shift from tetramethylsilane ($\delta_{TMS} = 0$) using either tetramethylsilane or residual solvent as internal reference. The melting points of the products were observed in sealed capillary tubes on a Mel-temp apparatus (Laboratory Devices, Cambridge, MA). IR spectra were obtained with a MIDAC Corporation M-Series FTIR spectrometer. UV/vis spectra were recorded on an Agilent 8543 UV-visible spectrophotometer.

5.2.2 Polymerization reactions

5.2.2.1 Polymerization trials using $MoO(OAr)_{4-n}Cl_{n = 0-2}$ complexes

The detailed procedure for polymerization of norbornene (NBE) with compound **3.1a**, is described below. The rest of polymerizations of this section were accomplished with similar procedures. The polymerization procedure used here is an adaptation of that used by Hayano et al. to produce polyNBE starting from different Mo(VI) monooxo aryloxides.[79]

Polymerization of NBE was accomplished in a two necked Schlenk flasks. One neck was attached to an addition funnel and the other neck was equipped with a condenser attached to a Teflon valve connected to an oil trap to allow release of pressure. Yields were determined by the equation % yield = (wt. of polyNBE)/(wt. of monomer)*100. *Cis* (c) to *trans* (t) ratios (c:t) were determined by integration of the two distinctive ^1H NMR signals of polyNBE at 5.50 (m, 1H,

trans-polyNBE, =C-*H*) and 5.35 (m, 1H, *cis*-polyNBE, =C-*H*) ppm in C_6D_6 as described in the literature.[229] The pro-catalyst:NBE ratio was 1:100 at all times.

ROMP of NBE by **3.2a** and 2 equiv of ^{n}BuLi: a solution of MoO(O-2,6-$Me_2C_6H_3)_2Cl_2$ (0.0043 g, 0.010 mmol, **3.2a**) in toluene (5 mL) was mixed with ^{n}BuLi (0.01 mL of 2.0 M in pentane, 0.02 mmol) at -78 °C with strong stirring. The resulting dark blue mixture was allowed to warm to room temperature. After 15 min, the solution turned a reddish orange color. A solution of NBE (0.0942 g, 1.00 mmol) in cyclohexane (15 mL) was added to the mixture via addition funnel at 80 °C. After stirring for 2 h, heating was stopped and the reaction was quenched with 2-propanol or MeOH (5 mL). The quenched mixture was stirred for 30 minutes (allowing it to reach room temperature). Formation of a white elastic solid was observed. The supernatant was withdrawn with a pipette. The solid was dried under vacuum overnight. A sample of this white gummy solid was dissolved in C_6D_6 with heating (30 °C) due to its poor solubility. The ^{1}H NMR spectrum revealed the formation of polyNBE. (c:t) = 0.58:1.00. Yield 0.0088 (9%).

A solution of NBE (0.0942 g, 1.00 mmol) in cyclohexane (15 mL) was added to a solution of MoO(O-2,6-$Me_2C_6H_3)_2Cl_2$ (0.0043 g, 0.010 mmol, **3.2a**) in toluene (5 mL) with no co-catalyst at 80 °C with stirring. After 2 h the reaction was quenched with 2-propyl alcohol (5 mL) and stirring was continued for 30 minutes more. A sample from the quenched reaction was dried under vacuum for NMR spectroscopy. The ^{1}H NMR spectrum of the reaction mixture revealed only unreacted complex **3.2a** and NBE.

ROMP of NBE by **3.3a** and 2 equiv of ^{n}BuLi: was prepared following the same procedure as **3.2a**, but using MoO(O-2,6-$Me_2C_6H_3)_3Cl$ (0.0051 g, 0.010 mmol, **3.3a**) and ^{n}BuLi co-catalyst (0.01 mL of 2.0 M in pentane, 0.02 mmol). (c:t) = 0.51:1.00. Yield 0.0037 g (4%).

ROMP of NBE by MoO(rac-biphenolate)$_2$[79] and 2 equiv of ^{n}BuLi: was prepared following the same procedure as **3.2a**, but using MoO[2,2'-methylenebis(6-*tert*-butyl-4-methylphenolate)]$_2$

(0.0082 g, 0.010 mmol) and ^{n}BuLi (0.01 mL of 2.0 M in pentane, 0.02 mmol). (c:t) = 1.00:0.72. Yield 0.0039 g (4%).

5.2.2.2 Polymerization trials using MoO(O-2,6-$Me_2C_6H_3)_2Cl_2$ (**3.2a**) as pro-catalyst and ^{n}BuLi co-catalyst in different ratios

MoO(O-2,6-$Me_2C_6H_3)_2Cl_2$ (**3.2a**) and 0.5, 1.0, 1.5, 2.0, 2.5 and 3.0 equiv of ^{n}BuLi: MoO(O-2,6-$Me_2C_6H_3)_2Cl_2$ (0.0043 g, 0.010 mmol, **3.2a**) were dissolved in toluene (5 mL) to make six solutions. ^{n}BuLi (0.10 mL, 2.0 mmol) was dissolved in pentane to prepare a 10.00 mL, 0.02 M stock solution (in a 10.00 mL Pyrex® Class A volumetric flask, tolerance ± 0.02). The six solutions containing **3.2a** were cooled at -35 °C for 30 minutes in the glove box freezer. Addition of ^{n}BuLi (0.02 M in pentane, 0.25 mL, 0.0050 mmol; 0.50 mL, 0.010 mmol; 0.75 mL, 0.015 mmol; 1.00 mL, 0.020 mmol; 1.25 mL, 0.025 mmol; 1.50 mL, 0.030 mmol) to each of to the cooled solutions was done at room temperature with stirring forming dark blue solutions. After 15 minutes the solutions became red-orange. Solutions of NBE (0.0942 g, 1.00 mmol) in cyclohexane (13 mL) were added to each of the six mixtures of complex **3.2a** with x equiv of ^{n}BuLi. Stirring was continued outside the glovebox at room temperature. After 2 h, the vials containing the reaction mixtures were opened and the reactions quenched with 5 mL of MeOH. Stirring was continued for 30 minutes more. Formation of a tacky solid was observed. The supernatants were withdrawn with a pipette and the solids were dried under vacuum overnight.

Complex **3.2a** with 0.5 equiv of ^{n}BuLi: (c:t) = 0.56:1.00. Yield 0.0940 g (100%).

Complex **3.2a** with 1.0 equiv of ^{n}BuLi: (c:t) = 0.81:1.00. Yield 0.0758 g (80%).

Complex **3.2a** with 1.5 equiv of ^{n}BuLi: (c:t) = 1.00:0.58. Yield 0.0286 g (30%).

Complex **3.2a** with 2.0 equiv of ^{n}BuLi: (c:t) = 1.00:0.72. Yield 0.0192 g (20%).

Complex **3.2a** with 2.5 equiv of ^{n}BuLi: (c:t) = 1.00:0.87. Yield 0.0097 g (10%).

Complex **3.2a** with 3.0 equiv of ^{n}BuLi: (c:t) = 0.85:1.00. Yield 0.0099 g (11%).

Polymerization reactions with 0.5 and 1.0 equiv of ^{n}BuLi were repeated on three different days to ensure reproducibility using the described procedure. The results are listed below. No (c:t) ratio was measured.

(Day 1): complex **3.2a** with 0.5 equiv of ^{n}BuLi: (c:t) = 0.56:1.00. Yield 0.0833 g (88%).

(Day 1): complex **3.2a** with 1.0 equiv of ^{n}BuLi: (c:t) = 0.81:1.00. Yield 0.0940 g (100%).

(Day 2): complex **3.2a** with 0.5 equiv of ^{n}BuLi: (c:t) = 1.00:0.58. Yield 0.0484 g (51%).

(Day 2): complex **3.2a** with 1.0 equiv of ^{n}BuLi: (c:t) = 1.00:0.72. Yield 0.0129 g (14%).

Other co-catalysts such as Et_3Al, $PhCH_2MgCl$, $PhCH_2Li$ and PhLi were attempted in a 2:1 co-catalyst:**3.2a** ratio, but no polymerization activity was observed.

5.2.2.3 Persistence of the molybdenum active intermediate.

The experiments of this section were done in two different weeks to study their reproducibility. The pro-catalyst:NBE ratio was 1:100 at all times.

ROMP of NBE by **3.2a** and 0.5 equiv of ^{n}BuLi: $MoO(O\text{-}2,6\text{-}Me_2C_6H_3)_2Cl_2$ (0.0511 g, 0.120 mmol, **3.2a**) was dissolved in toluene (60.0 mL) and cooled at -35 ^{o}C in the glovebox freezer for 1 h. ^{n}BuLi (0.03 mL of 2.0 M in pentane, 0.06 mmol) was added to the cooled solution of **3.3a** with stirring. The resulting dark blue mixture was allowed to warm to room temperature. After 15 min, the solution became red orange. Four 5 mL aliquots of the red orange solution were taken and deposited in four vials. NBE (0.0942 g, 1.00 mmol) dissolved in cyclohexane (15 mL) was added to each of the three vials containing the active species at room temperature with stirring (the content of the fourth vial was dried under vacuum and used for ^{1}H NMR analysis). Stirring was continued outside the glovebox. After 2 h, stirring was stopped and the reaction was quenched with MeOH (5 mL). The quenched mixture was stirred for 30 minutes. Formation of a tacky white solid was observed. The supernatant was withdrawn with a pipette. The solid was dried under vacuum overnight. Yields were measured. The content of the fourth vial was dried under vacuum for ^{1}H NMR analysis. The rest of the solution containing the

mixture of the complex **3.2a** with 0.5 equiv of ^{n}BuLi was stored at -35 ^{o}C in the glovebox freezer. This procedure (including the NMR analysis) was repeated two times more in consecutive days, (c:t) ratios were not measured.

(Week 1, day 1): yield$_1$ 0.0352 g (37%), yield$_2$ 0.0249 g (26%), yield$_3$ 0.0471 g (50%).

(Week 1, day 2): yield$_1$ 0.0421 g (45%), yield$_2$ 0.0422 g (45%), yield$_3$ 0.0521 g (55%).

(Week 1, day 3): yield$_1$ 0.0762 g (81%), yield$_2$ 0.0776 g (82%), yield$_3$ 0.0749 g (80%).

The dried aliquots of the red orange solution were poorly soluble in C_6D_6. The ^{1}H NMR spectra revealed the presence of HO-2,6-$Me_2C_6H_3$ along with other unidentified products were observed.

The results for the second week were:

(Week 2, day 1): yield$_1$ 0.0073 g (8%), yield$_2$ 0.0047 g (5%), yield$_3$ 0.0021 g (2%).

(Week 2, day 2): yield$_1$ 0.0205 g (22%), yield$_2$ 0.0388 g (41%), yield$_3$ 0.0027 g (3%).

(Week 2, day 3): yield$_1$ 0.0039 g (4%), yield$_2$ (0%), yield$_3$ 0.0197 g (21%).

5.2.2.4 Polymerization trials using $MoOCl_2$(bisphenoxides)

The detailed procedure for polymerization of norbornene (NBE) with compound **4.3a**, is described below. The rest of the polymerizations of this section were accomplished with similar procedures. The pro-catalyst:NBE ratio was 1:100 at all times.

ROMP of NBE by **4.3a** and 0.5 equiv of ^{n}BuLi: Mo(O)Cl_2{2,2'-CH_2(O-6-^{t}Bu-4-$MeC_6H_2)_2$-κ^2*O,O*'} (0.0626 g, 0.120 mmol, **4.3a**) was dissolved in toluene (60.0 mL) and cooled at -35 ^{o}C in the glovebox freezer for 1 h. ^{n}BuLi (0.03 mL of 2.0 M in pentane, 0.06 mmol) was added to the cooled solution of **4.3a** with stirring. The resulting dark purple mixture was allowed to warm to room temperature. After 15 min, the solution became dark orange. Three 5 mL aliquots of the orange solution were taken and deposited in three vials. NBE (0.0942 g, 1.00 mmol) dissolved in cyclohexane (15 mL) was added to each of the three vials containing the active species at room temperature with stirring. Stirring was continued outside the glovebox. After 2 h, stirring

was stopped and the reaction was quenched with MeOH (5 mL). The quenched mixture was stirred for 30 minutes. Formation of a tacky white solid was observed. The supernatant was withdrawn with a pipette. The solid was dried under vacuum overnight. Yields were measured. The content of the fourth vial was dried under vacuum for ^{1}H NMR analysis. The rest of the solution containing the mixture of the complex **4.3a** with 0.5 equiv of ^{n}BuLi was stored at -35 ^{o}C in the glovebox freezer. This procedure was repeated two times more in consecutive days, (c:t) ratios were not measured.

(Week 1, day 1): yield$_1$ 0.0234 g (25%), yield$_2$ 0.0237 g (25%), yield$_3$ 0.0239 g (25%).

(Week 1, day 2): yield$_1$ 0.0554 g (59%), yield$_2$ 0.0557 g (59%), yield$_3$ 0.0938 g (100%).

(Week 1, day 3): yield$_1$ 0.0469 g (50%), yield$_2$ 0.0318 g (34%), yield$_3$ 0.0468 g (50%).

Each day, 0.50 mL aliquots from the mixture **4.3a**/^{n}BuLi were taken and dried under vacuum for ^{1}H NMR analysis in C_6D_6. The ^{1}H NMR spectrum showed the presence of 2,2'-methylenebis(6-tert-butyl-4-methylphenol), MoO[2,2'-methylenebis(6-tert-butyl-4-methylphenolate)]$_2$,[79] unreacted complex **4.3a**, and other unidentifiable products. The amount of bisphenol increased while the presence of the other two complexes decreased towards the third day.

This experiment was performed under the same conditions a week later. The results for the second week were:

(Week 2, day 1): yield$_1$ 0.0233 g (25%), yield$_2$ 0.0239 g (25%), yield$_3$ 0.0236 g (25%).

(Week 2, day 2): yield$_1$ 0.0562 g (60%), yield$_2$ 0.0568 g (60%), yield$_3$ 0.0566 g (60%).

(Week 2, day 3): yield$_1$ 0.0469 g (50%), yield$_2$ 0.0451 g (48%), yield$_3$ 0.0453 g (48%).

ROMP of NBE by **4.3a** and 1.0 equiv of ^{n}BuLi: was prepared following the same procedure as **4.3a** (above), but using Mo(O)Cl$_2${2,2'-CH$_2$(O-6-^{t}Bu-4-MeC$_6$H$_2$)$_2$-κ^2*O,O'*} (0.0626 g, 0.120 mmol, **4.3a**), and ^{n}BuLi (0.06 mL of 2.0 M in pentane, 0.12 mmol). (c:t) Ratios were measured only for the first run of each day of the first week. The yields were:

(Week 1, day 1): $yield_1$ 0.0938 g (100%), (c:t) = 0.64:1.00; $yield_2$ 0.0669 g (71%), $yield_3$ 0.0940 g (100%).

(Week 1, day 2): $yield_1$ 0.0886 g (94%), (c:t) = 0.72:1.00; $yield_2$ 0.0940 g (100%), $yield_3$ 0.0939 (100%).

(Week 1, day 3): $yield_1$ 0.7610 g (76%), (c:t) = 0.50:1.00; $yield_2$ 0.0684 g (73%), $yield_3$ 0.0752 g (80%).

A 0.50 mL aliquot from the mixture **4.3a**/^{n}BuLi was taken at day 1 and dried under vacuum for ^{1}H NMR analysis in C_6D_6. The ^{1}H NMR spectrum revealed the probable presence MoO[2,2'-methylenebis(6-tert-butyl-4-methylphenolate)]$_2$[79] along with other unidentified products.

The results for the second week were:

(Week 2, day 1): $yield_1$ 0.0941 g (100%), $yield_2$ 0.0850 g (90%), $yield_3$ 0.0939 g (100%).

(Week 2, day 2): $yield_1$ 0.0940 g (100%), $yield_2$ 0.0923 g (98%), $yield_3$ 0.0939 g (100%).

(Week 2, day 3): $yield_1$ 0.0750 g (80%), $yield_2$ 0.0752 g (80%), $yield_3$ 0.0736 g (78%).

ROMP of NBE by **4.3a** and 1.5 equiv of ^{n}BuLi: was prepared following the same procedure as **4.3a** (above), but using Mo(O)Cl$_2${2,2'-CH$_2$(O-6-^{t}Bu-4-MeC$_6$H$_2$)$_2$-κ^2*O,O*'} (0.0626 g, 0.120 mmol, **4.3a**), and ^{n}BuLi (0.09 mL of 2.0 M in pentane, 0.18 mmol). (c:t) Ratios were measured only for the first run of each day of the first week. The yields were:

(Week 1, day 1): $yield_1$ 0.0333 g (35%), (c:t) = 1.00:0.88; $yield_2$ 0.0408 g (43%), $yield_3$ 0.0332 g (35%).

(Week 1, day 2): $yield_1$ 0.0263 g (28%), (c:t) = 1.00:0.66; $yield_2$ 0.0262 g (28%), $yield_3$ 0.0762 g (81%).

(Week 1, day 3): $yield_1$ 0.0216 g (23%), (c:t) = 0.59:1.00; $yield_2$ 0.0159 g (17%), $yield_3$ 0.0215 g (23%).

A 0.50 mL aliquot from the mixture **4.3a**/^{n}BuLi was taken at day 1 and dried under vacuum for ^{1}H NMR analysis in C_6D_6. The ^{1}H NMR spectrum was complex and did not reveal the presence of any known species or give enough information to identify a new one.

The results for the second week were:

(Week 2, day 1): $yield_1$ 0.0356 g (38%), $yield_2$ 0.0327 g (35%), $yield_3$ 0.0357 g (38%).

(Week 2, day 2): $yield_1$ 0.0264 g (28%), $yield_2$ 0.0263 g (28%), $yield_3$ 0.0287 g (30%).

(Week 2, day 3): $yield_1$ 0.0205 g (22%), $yield_2$ 0.0191 g (20%), $yield_3$ 0.0198 g (21%).

ROMP of NBE by **4.3a** and 2.0 equiv of ^{n}BuLi: was prepared following the same procedure as **4.3a** (above), but using Mo(O)Cl_2{2,2'-CH_2(O-6-^{t}Bu-4-Me$C_6H_2)_2$-κ^2*O,O*'} (0.0626 g, 0.120 mmol, **4.3a**), and ^{n}BuLi (0.12 mL of 2.0 M in pentane, 0.24 mmol). This experiment was done only for one week. The yields were:

(Week 1, day 1): $yield_1$ 0.0009 g (1%), $yield_2$ 0.0011 g (1%), $yield_3$ 0.0013 g (1%).

(Week 1, day 2): $yield_1$ 0%, $yield_2$ 0%, $yield_3$ 0%.

(Week 1, day 3): $yield_1$ 0.0060 g (6%), $yield_2$ 0.0084 g (9%), $yield_3$ 0.0076 g (8%).

ROMP of NBE by **4.3a** and 2.5 equiv of ^{n}BuLi: was prepared following the same procedure as **4.3a** (above), but using Mo(O)Cl_2{2,2'-CH_2(O-6-^{t}Bu-4-Me$C_6H_2)_2$-κ^2*O,O*'} (0.0626 g, 0.120 mmol, **4.3a**), and ^{n}BuLi (0.15 mL of 2.0 M in pentane, 0.30 mmol). This experiment was done only for one week. The yields were:

(Week 1, day 1): $yield_1$ 0.0008 g (1%), $yield_2$ 0.0009 g (1%), $yield_3$ 0.0012 g (1%).

(Week 1, day 2): $yield_1$ 0%, $yield_2$ 0%, $yield_3$ 0%.

(Week 1, day 3): $yield_1$ 0%, $yield_2$ 0%, $yield_3$ 0%.

ROMP of NBE by **4.3a** and 3.0 equiv of ^{n}BuLi: was prepared following the same procedure as **4.3a** (above), but using Mo(O)Cl_2{2,2'-CH_2(O-6-^{t}Bu-4-Me$C_6H_2)_2$-κ^2*O,O*'} (0.0626 g, 0.120 mmol, **4.3a**), and ^{n}BuLi (0.18 mL of 2.0 M in pentane, 0.30 mmol). This experiment was done only for one week. The yields were:

(Day 1): $yield_1$ 0.0012 g (1%), $yield_2$ 0.0010 g (1%), $yield_3$ 0.0009 g (1%).

(Day 2): yield$_1$ 0%, yield$_2$ 0%, yield$_3$ 0%.

(Day 3): yield$_1$ 0%, yield$_2$ 0%, yield$_3$ 0%.

ROMP of NBE by **4.3a** and 0.5 equiv of Et_3Al: was prepared following the same procedure as **4.3a** (above), but using Mo(O)Cl$_2${2,2'-CH$_2$(O-6-^{t}Bu-4-MeC$_6$H$_2$)$_2$-κ^2*O,O*'} (0.0470 g, 0.0901 mmol, **4.3a**), and Et_3Al (0.04 mL of 1.0 M in hexane, 0.04 mmol). This experiment was done only for one week. (c:t) Ratios were measured only for the first run of each day. The yields were:

(Day 1): yield$_1$ 0.0940 g (100%), (c:t) = 0.47:1.00; yield$_2$ 0.0939 g (100%), yield$_3$ 0.0939 g (100%).

(Day 2): yield$_1$ 0.0940 g (100%), (c:t) = 0.42:1.00; yield$_2$ 0.0941 g (100%), yield$_3$ 0.0939 g (100%).

A 0.50 mL aliquot from the mixture **4.3a**/Et_3Al was taken at day 1 and dried under vacuum for ^{1}H NMR analysis in C_6D_6. The ^{1}H NMR was complex, but it revealed the presence of unreacted Mo(O)Cl$_2${2,2'-CH$_2$(O-6-^{t}Bu-4-MeC$_6$H$_2$)$_2$-κ^2*O,O*'} (**4.3a**) and 2,2'-CH$_2$(6-^{t}Bu-4-MeC$_6$H$_2$OH)$_2$ along with other unidentified products.

ROMP of NBE by **4.3a** and 1.0 equiv of Et_3Al: was prepared following the same procedure as **4.3a** (above), but using Mo(O)Cl$_2${2,2'-CH$_2$(O-6-^{t}Bu-4-MeC$_6$H$_2$)$_2$-κ^2*O,O*'} (0.0470 g, 0.0901 mmol, **4.3a**), and Et_3Al (0.09 mL of 1.0 M in hexane, 0.09 mmol). This experiment was done only for one week. The yields were:

(Day 1): yield$_1$ 0.0877 g (93%), (c:t) = 0.35:1.00; yield$_2$ 0.0790 g (84%), yield$_3$ 0.0794 g (84%).

(Day 2): yield$_1$ 0.0566 g (60%), (c:t) = 0.39:1.00; yield$_2$ 0.0620 g (66%), yield$_3$ 0.0634 g (67%).

A 0.50 mL aliquot was taken from the mixture **4.3a**/Et_3Al at day 1 and dried under vacuum for ^{1}H NMR analysis in C_6D_6. The ^{1}H NMR spectrum was complex, but 2,2'-CH$_2$(6-^{t}Bu-4-MeC$_6$H$_2$OH)$_2$ was observed along with other unidentified products.

ROMP of NBE by **4.3a** and 0.5 equiv of $PhCH_2MgCl$: was prepared following the same procedure as **4.3a** (above), but using Mo(O)Cl$_2${2,2'-CH$_2$(O-6-^{t}Bu-4-MeC$_6$H$_2$)$_2$-κ^2*O,O*'} (0.0470 g,

0.090 mmol, **4.3a**), and $PhCH_2MgCl$ (0.02 mL of 2.0 M in THF, 0.04 mmol). This experiment was done only for one week. The yields were:

(Day 1): $yield_1$ 0.0987 g (70%), $yield_2$ 0.0887 g (94%), $yield_3$ 0.0648 g (69%).

(Day 2): $yield_1$ 0.0839 g (89%), $yield_2$ 0.0569 g (60%), $yield_3$ 0.0922 g (98%).

A 0.50 mL aliquot was taken from the mixture **4.3a**/$PhCH_2MgCl$ at day 1 and dried under vacuum for ^1H NMR analysis in C_6D_6. The sample showed poor solubility in the deuterated solvent. The ^1H NMR spectrum showed mainly 2,2'-CH_2(6-^{t}Bu-4-$MeC_6H_2OH)_2$ and unreacted complex **4.3a**.

ROMP of NBE by **4.3a** and 1.0 equiv of $PhCH_2MgCl$: was prepared following the same procedure as **4.3a** (above), but using Mo(O)Cl_2{2,2'-CH_2(O-6-^{t}Bu-4-$MeC_6H_2)_2$-κ^2*O,O*'} (0.0470 g, 0.0901 mmol, **4.3a**), and $PhCH_2MgCl$ (0.04 mL of 2.0 M in THF, 0.08 mmol). This experiment was done only for one week. (c:t) Ratios were measured only for the first run of each day. The yields were:

(Day 1): $yield_1$ 0.0847 g (90%), (c:t) = 0.72:1.00; $yield_2$ 0.0851 g (90%), $yield_3$ 0.0852 g (90%).

(Day 2): $yield_1$ 0.0745 g (79%), (c:t) = 0.71:1.00; $yield_2$ 0.0743 g (79%), $yield_3$ 0.0729 g (77%).

A 0.50 mL aliquot was taken from the mixture **4.3a**/$PhCH_2MgCl$ at day 1 and dried under vacuum for ^1H NMR analysis in C_6D_6. The sample showed poor solubility in the deuterated solvent. The ^1H NMR spectrum showed the presence of 2,2'-CH_2(6-^{t}Bu-4-$MeC_6H_2OH)_2$ along with other unidentified products.

ROMP of NBE by **4.3a** and 0.5 equiv of Et_3Al: was prepared following the same procedure as **4.3a** (above), but using Mo(O)Cl_2{2,2'-CH_2(O-6-^{t}Bu-4-$MeC_6H_2)_2$-κ^2*O,O*'} (0.0052 g, 0.010 mmol, **4.3a**), and Et_3Al (0.05 mL of 0.10 M in hexane, 0.0050 mmol). The 0.10 M Et_3Al was made by dilution of Et_3Al (1.00 mL of 1.0 M in hexane, 1.0 mmol) in hexane to prepare a 10.00 mL, 0.10 M stock solution (in a 10.00 mL Pyrex® Class A volumetric flask, tolerance ± 0.02). NBE (0.0942 g, 10.0 mmol) was dissolved in THF (15 mL) instead of cyclohexane. (c:t) Ratio = 1.00:0.09. Yield 0.0940 g (100%).

Polymerization with **4.3a** and 0.5 and1.0 equiv of PhLi, PhMgBr, diphenylmercury and neopentyllithium were attempted but no ROMP activity was observed.

ROMP of NBE by **4.3b** and 1.0 equiv of ^{n}BuLi: was prepared following the same procedure as **4.3a** (above), but using Mo(O)Cl$_2${2,2'-C(^{i}Pr)(O-4,6-^{t}Bu$_2$C$_6$H$_2$)$_2$-κ^2*O,O*'} (0.0777 g, 0.120 mmol, **4.3a**), and ^{n}BuLi (0.12 mL of 2.0 M in pentane, 0.24 mmol). (c:t) Ratios were measured only for the first run of each day. The yields were:
(Day 1): yield$_1$ 0.0333 g (35%), (c:t) = 0.52:1.00; yield$_2$ 0.0328 g (35%), yield$_3$ 0.0334 g (35%).
(Day 2): yield$_1$ 0.0265 g (28%), (c:t) = 0.87:1.00; yield$_2$ 0.0267 g (28%), yield$_3$ 0.0219 g (23%).
(Day 3): yield$_1$ 0.0196 g (21%), (c:t) = 0.79:1.00; yield$_2$ 0.0157 g (17%), yield$_3$ 0.0186 g (20%).

5.2.2.5 Reactions with Cyclohexene

Mo(O)Cl$_2${2,2'-CH$_2$(O-6-^{t}Bu-4-MeC$_6$H$_2$)$_2$-κ^2*O,O*'} (0.0470 g, 0.0901 mmol, **4.3a**) was dissolved in toluene (15.0 mL) and cooled to -35 ^{o}C in the glovebox freezer for 1 h. ^{n}BuLi (0.02 mL of 2.0 M in pentane, 0.040 mmol) was added to the cooled solution of **4.3a** with stirring. The resulting dark purple mixture was allowed to warm to room temperature. After 15 min, the solution became dark orange. Cyclohexene (0.0037 g, 0.045 mmol) dissolved in cyclohexane (5 mL) was added to the mixture of **4.3a**/^{n}BuLi. After 2 h, stirring was stopped and the reaction was dried under vacuum overnight. A sample was taken for ^{1}H NMR analysis in C$_6$D$_6$. The ^{1}H NMR spectrum was complex in the alkyl area, but one signal at 11.07 ppm (m, probably M=C*H*R) was observed.

5.3 Results and discussion

Olefin metathesis and specifically ROMP has grown to become one of the most important tools for the formation of C-C bonds.[240] A broad variety of initiators have been used for olefin metathesis polymerization. The first initiators were formed in situ from transition metal halide precursors and main group metal alkyl co-catalysts.[157] These catalytic systems are cheap

and, therefore, are often used in industrial applications with certain restrictions.[228] These restrictions arise from the lack of control in the reaction because the propagating species is, in general, not quantitatively formed and not defined.[228] It is assumed that a metal carbene complex is formed in situ from the transition metal compound and its interaction with the substrate or the respective co-catalyst.[157] The development of well defined initiators mostly based on molybdenum, tungsten,[234, 235] and ruthenium alkylidenes,[233] which are co-catalyst free systems, allowed control of different aspects of the polymerization process: precise adjustment of the molecular weight, low polydispersities and high catalyst recyclability.[228] Although these new homogeneous and well-defined catalysts do not yet play a major role in the industrial scenarios, they are starting to emerge as attractive alternatives in the areas of polymer, oleochemical and fine chemicals industries due to their precision and high reactivity.[231]

The number of catalyst that initiate ring opening metathesis polymerization is large,[157, 240] but there is still need of new catalysts capable of tolerating monomer functionalities and with better selectivities.[237] Knowing that the ROMP scenario is still an open field, we resolved to explore the activity of some of the molybdenum(VI) oxo complexes synthesized in chapters 3 and 4 as C-C bond forming facilitators.

5.3.1 The procatalysts

Molybdenum aryloxides are known to display ROMP activity in the presence of strained olefins.[79,158] Compounds of the formula $M(OAr)_{6-n}Cl_n$ (M = W or Mo) and the monooxo compounds $WO(OAr)_{4-n}Cl_n$ have been shown to act as catalyst precursors in the presence of co-catalysts such as alkylaluminum, alkyltin or alkyllithium.[77, 157-161, 241] Recently, Hayano et al.[79] has reported the successful use of monooxo molybdenum(VI) tetraaryloxides as procatalysts for metathesis polymerization when combined with ^{n}BuLi and Et_3Al in different proportions. Although W and Mo based catalysts are both popular for olefin metathesis, it has been noted

that Mo based catalysts are generally more effective than the corresponding W analogues for olefin metathesis.[157]

Complexes $MoO(OAr)_{4-n}Cl_n$ (chapter 3) and $MoO(bisphenoxide)Cl_2$ (chapter 4) resemble those used by other researchers for ring opening metathesis polymerization of strained olefins. We selected four complexes in order to investigate their activity and the consequences that their structure might have in the reaction course and product characteristics.

The molecules used for olefin metathesis polymerization trials in this chapter are shown in Figure 5.1.

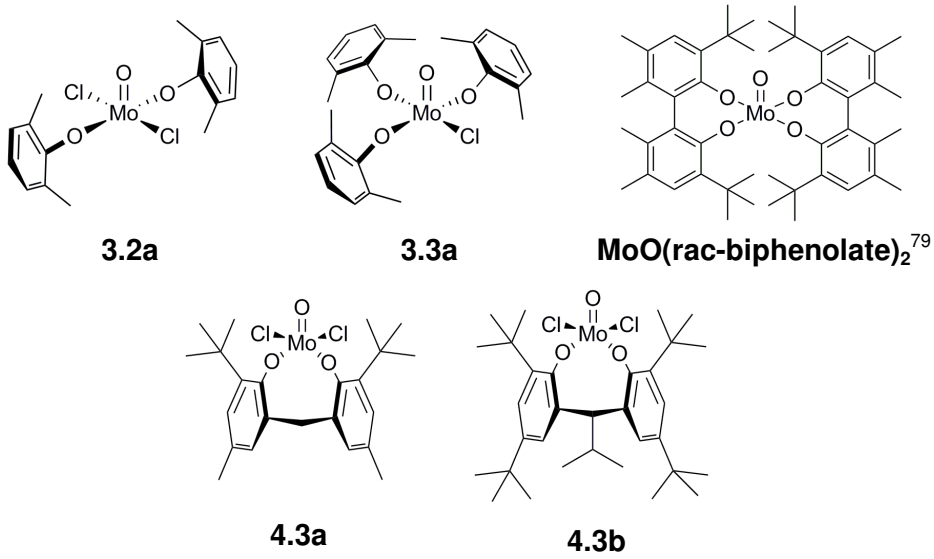

Figure 5.1 Molybdenum(VI) monooxo complexes used as procatalysts for polymerization of NBE.

According to Ivin et al.,[157] catalyst systems may be divided into three types:

1. well defined metal carbenes, such as $W(=CPh_2)(CO)_5$,
2. those containing an alkyl or allyl group in one of the components, e.g. $EtAlCl_2$, from which a metal carbene ligand can readily be generated, and
3. those having neither a preformed carbene nor an alkyl group in any component.

In conformity with this classification, our MoO^{4+} complexes belong to the category number 3. Therefore an alkylating agent such as ^{n}BuLi, Et_3Al or $PhCH_2MgCl$ (co-catalyst) was required to produce an active intermediate.

It is suggested that the precursor undergoes substitution at the halogen ligands to form an alkylated intermediate (the alkylation of transition metals by organometallic compounds is well known).[242] The alkylated intermediate is responsible for the generation of a metal carbene species (M=CRR') via an α-H abstraction step between two alkyl groups.[232, 235, 243] Those derivatives with one or more chlorine substituents are expected to be more active than those with none.[81]

Complexes **3.2a**, **3.3a** and MoO(rac-biphenolate)$_2$[79] display di-, tri- and tetrasubstitution at the Mo^{4+} center. Although the tetrasubstituted complex was not synthesized by us, it has been shown to work successfully as precursor for ROMP catalysis,[79] giving us a "standard" of performance. Complexes **4.3a** and **4.3b** were selected because of their *cis*-bisphenoxo, *cis*-chloro structure around the MoO^{4+} unit. The molybdenum(VI) oxo complexes **3.2a**, **3.3a**, **4.3a** and **4.3b** are believed to undergo alkylation at the chlorine positions, and then produce a molybdenum-alkylidene moiety via α-hydrogen abstraction. This is a well-precedented mechanism for early transition metal complexes in high oxidation states (Scheme 5.4).[232, 242-244]

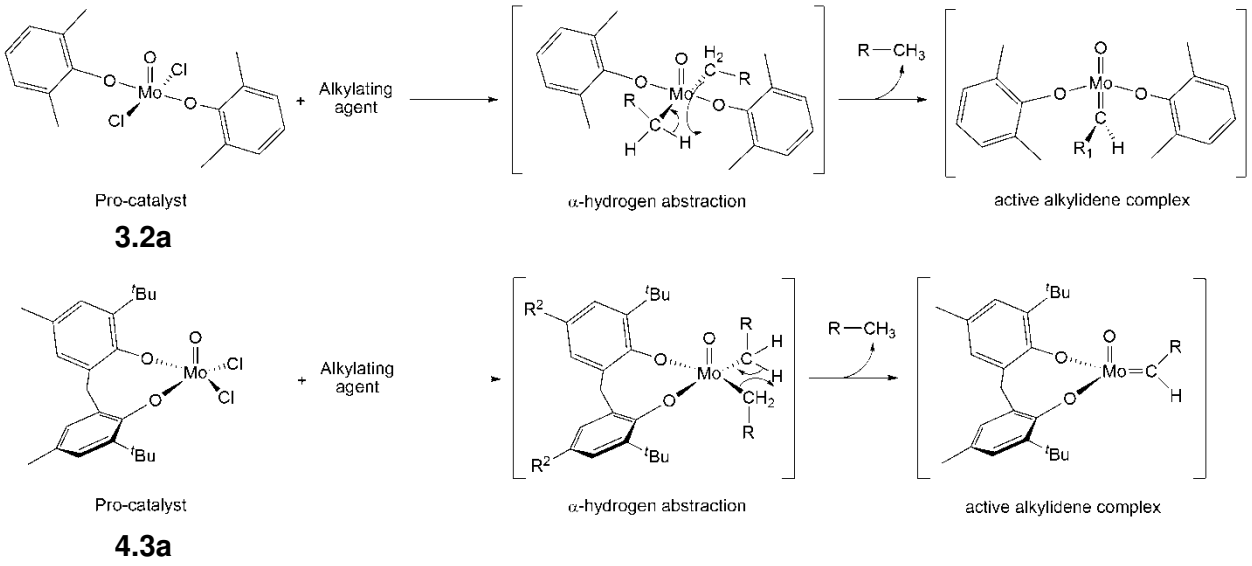

3.2a

4.3a

Scheme 5.4 Generation of the proposed active Mo(VI) monooxo catalysts. Complexes **3.2a** and **4.3a** are used as models. The complexes are expected to undergo alkylation, then α-hydrogen abstraction between the newly generated alkyl ligands, and formation of the active alkylidene complex (Mo=CHR).

5.3.2 The mechanism

The commonly accepted mechanism for the olefin metathesis reaction was proposed by Chauvin[157, 232] and involves:

1) generation of the initial carbene catalyst,
2) a [2+2] cycloaddition reaction between a transition metal alkylidene complex and the olefin to form an intermediate metallacyclobutane.[157]
3) metallacycle cleavage, and formation of the propagating metal carbene olefin complex.[157]

Scheme 5.5 shows the proposed propagation steps after the carbene complex has been generated via alkylation of complex **4.3a**. This mechanism is well-known for different metal alkylidenes,[157, 240] and molecule **4.3a** has been used as model (the proposed Mo=CRR' complexes in this chapter could not be isolated). The propagation should occur in a similar manner for all the tested complexes (double bonds in the aryl rings have been omitted for clarity).

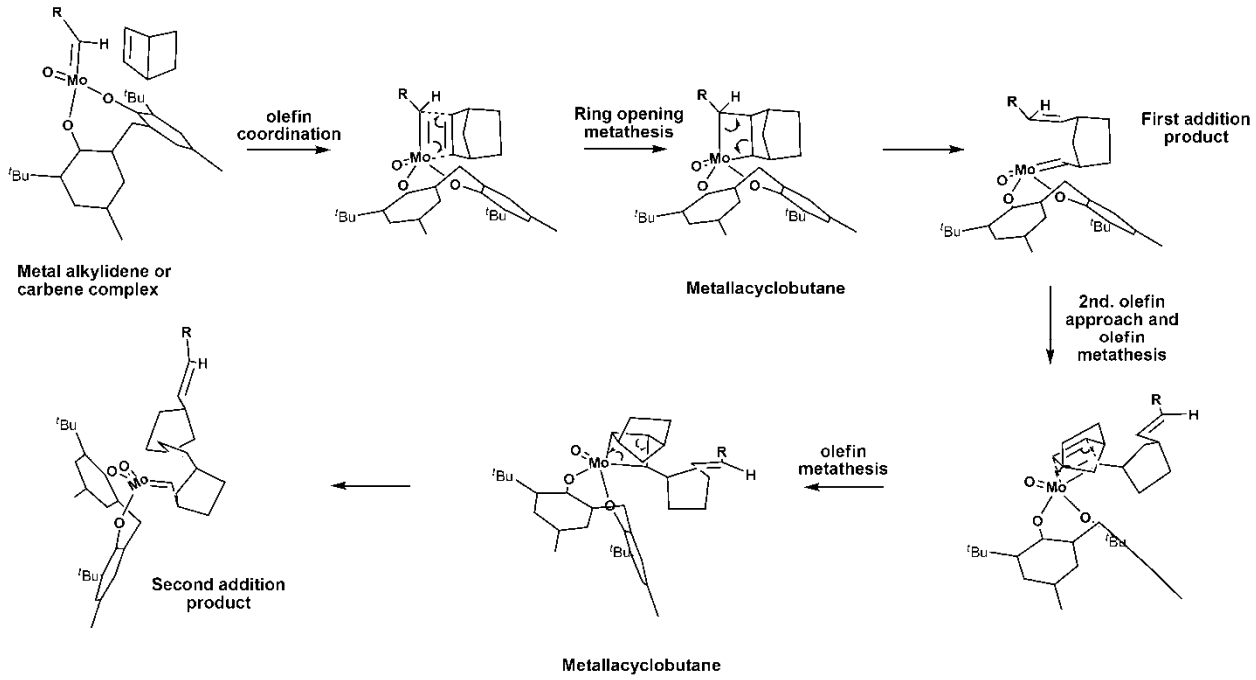

Scheme 5.5 Ring opening metathesis polymerization of NBE. The carbene complex derived from molecule **4.3a** was not isolated. Its proposed structure serves as model for the propagating metal carbene complex that is believed to be form in situ in our polymerization trials. *cis*:*trans* Stereochemistry in the polyNBE chain has been randomly assigned.

5.3.3 The monomer and the stereochemistry of the polymer

Norbornene (NBE) is a commonly used monomer for ROMP reactions. NBE contains strained rings and its ROMP can be readily initiated by a wide range of catalyst systems. Less strained rings such as cyclopentene generally require more active catalyst systems.[157]

Polymers formed by ROMP reactions are characterized by the fact that the double bonds of the monomeric molecules that mediated the polymerization, reappear in the polymeric product. The newly formed double bonds may be *cis* (c) or *trans* (t), and the c:t ratio is often seen as the primary microstructural variant. The four stereochemical variations that are possible for monomer dyad units in the polymer formed from NBE are shown in Scheme 5.6.[245]

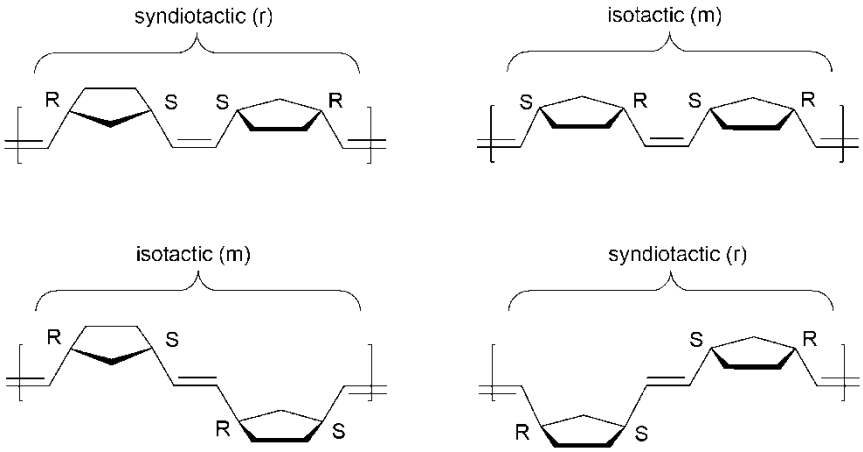

Scheme 5.6 Different possible combinations of dyad tacticity and double bond stereochemistry in polyNBE.[245]

Information on the stereochemical composition of a given polymer is necessary because it leads ultimately to an understanding of the factors that produced such stereochemistry (solvent, temperature, electronic and steric variations in the catalyst, reaction time, etc.).[245] A fair measure of success has been achieved in identifying the c:t ratio using ^{1}H NMR spectroscopy. ^{1}H NMR has the advantage of small sample and short time acquisition requirements. Unfortunately little information is obtained concerning stereochemical sequences along the chain (syndiotactic or isotactic). ^{13}C NMR spectroscopy is a suitable technique to measure c:t ratio and tacticity,[245] but its interpretation is beyond the scope of this study. This chapter is not intended to be a deep discussion of the ROMP reaction. As our first approach to this type of reactivity, our knowledge in this field is limited. Therefore we decided to measure c:t ratios by ^{1}H NMR spectroscopy as shown in Figure 5.2.

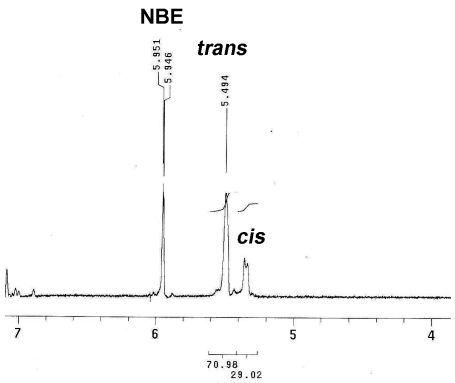

Figure 5.2 ^{1}H NMR spectrum in C_6D_6 (expansion) of a polyNBE. *cis*- and *trans*-PolyNBE are labeled according to the literature.[229] The c:t ratio is 0.41:1.0.

5.3.4 Polymerization trials

Polymerization of NBE was first attempted as described by Hayano et al. for a series of Mo(VI) monooxo tetraaryloxide complexes.[79] The active species (Scheme 5.4) was generated by mixing the Mo(VI) monooxo complex (procatalyst) and the alkylating agent (^{n}BuLi) at -75 °C in toluene. The mixture was allowed to reach the room temperature (15 min) and then mixed with 100 equiv of NBE (see experimental section).

The results from this first trial are summarized in Scheme 5.7.

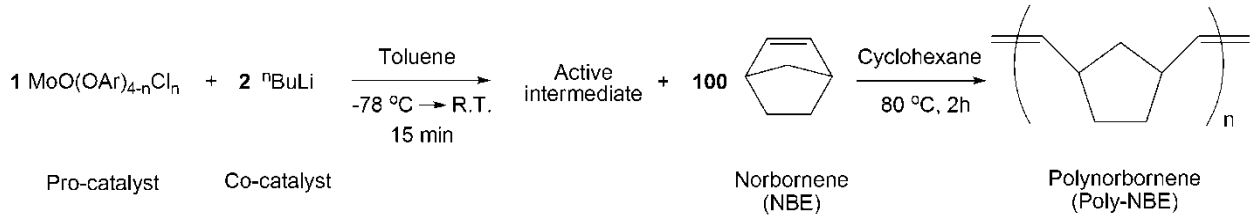

Initiator	label	Yield (%)	*cis*:*trans*
$MoO(O\text{-}2,6\text{-}Me_2C_6H_3)_2Cl_2$	**3.2a**	9	0.58:1.0
$MoO(O\text{-}2,6\text{-}Me_2C_6H_3)_3Cl$	**3.3a**	4	0.51:1.0
$MoO(rac\text{-}biphenolate)_2$	ref[79]	4	1.0:0.72

Scheme 5.7 Polymerization of NBE using Mo(VI) monooxo di-, tri-, and tetraaryloxo complexes.

The yields of polyNBE obtained after this first trial were low, but it was observed that complex **3.2a** (disubstituted) performed better than the tri- **3.3a**, and tetrasubstituted complexes. This difference was expected, as noted in section 5.3.2,because the complexes are believed to undergo alkylation at the chloro sites; a dialkylated complex might undergo an easier α-

hydrogen abstraction and the consequent Mo=CRR' moiety might be generated faster (Scheme 5.4). A singly alkylated complex might need to undergo ligand exchange with another Mo(VI) monooxo molecule before being able to undergo α-hydrogen abstraction. (tungsten alkyl complexes have shown to be active catalysts for metathesis in presence of $WOCl_4$, suggesting a ligand exchange process).[232]

In our hands, the MoO(rac-biphenolate)$_2$ complex performed poorly. In the literature this complex is reported to catalyze 100% conversion of NBE into polyNBE under these reaction conditions when mixed in a 1:2:100 procatalyst:^{n}BuLi:monomer ratio.[79]

MoO(O-2,6-$Me_2C_6H_3)_2Cl_2$ (**3.2a**) not only performed better in the first screening test; but in addition, it has a one-step preparation (chapter 3). These elements made it a suitable candidate for more polymerization trials. The next step was a variation on the amounts of ^{n}BuLi. Two variations were introduced in the initial polymerization procedure:

1) the "activation" temperature was changed from -75 °C (dry ice/acetone bath) to -35 °C (glove box freezer), and
2) the polymerization was run at room temperature and not 80 °C.

In this way polymerization trials would be easier to perform in glovebox conditions (the initial reaction conditions required use of Schlenk techniques which do not allow several reactions at the same time).

The results from addition of different equiv of ^{n}BuLi to MoO(O-2,6-$Me_2C_6H_3)_2Cl_2$ (**3.2a**) at -35 °C for room temperature polymerization of NBE, are shown in Scheme 5.8. Reactions with 0.5 and 1.0 equiv of ^{n}BuLi (best yields of polyNBE) were repeated 2 more times in two different days (for details refer to the experimental section of this chapter).

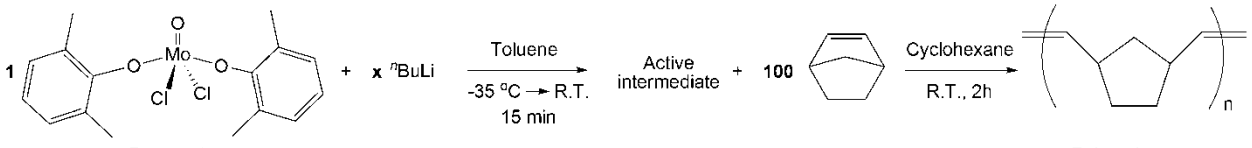

3.2a

Initiator	equiv	Day 1		Day 2		Day 3	
		Yield (%)	*cis*:*trans*	Yield (%)	*cis*:*trans*	Yield (%)	*cis*:*trans*
3.2a	0.5	100	0.56:1.0	88	0.56:1.0	51	1:0:0.58
3.2a	1.0	80	0.81:1.0	100	0.81:1.0	14	1.0:0.72
3.2a	1.5	30	1.0:0.58	-	-	-	-
3.2a	2.0	20	1.0:0.72	-	-	-	-
3.2a	2.5	10	1.0:0.87	-	-	-	-
3.2a	3.0	11	0.85:1.0	-	-	-	-

Scheme 5.8 Polymerization of NBE using $MoO(O\text{-}2,6\text{-}Me_2C_6H_3)_2Cl_2$ (**3.2a**) and ^{n}BuLi in different ratios.

From the table in Scheme 5.8 we can infer the following:

1) the best yields are obtained when ^{n}BuLi is added in 0.5 or 1.0 equiv,
2) the *cis*:*trans* ratio is sometimes erratic and it is difficult to predict in this system, and
3) there is no reproducibility for consecutive runs of the same experiment .

In order to check reproducibility, a stock solution of $MoO(O\text{-}2,6\text{-}Me_2C_6H_3)_2Cl_2$ with 0.5 equiv of ^{n}BuLi was prepared. This same solution was used to run 3 experiments in parallel per day, three different days, ensuring that the same conditions were observed in the preparation of each of the "active intermediates" used for each polymerization trial. Solutions were stored in the glovebox freezer at -35 °C after use. This experiment was performed in two different weeks. (c:t) Ratios were not measured as the primary goal of this experiment was to investigate yield reproducibility. The results are summarized in Table 5.1 (for details refer to the experimental section of this chapter).

Table 5.1 Yields of PolyNBE Using a Stock Solution of Complex **3.2a** as Precursor and 0.5 equiv of ^{n}BuLi (3 runs per day on three different days; repeated in two different weeks).

Initiator	^{n}BuLi equiv	Week 1			Week 2		
		$Yield_{day1}$ (%)	$Yield_{day\ 2}$ (%)	$Yield_{day\ 3}$ (%)	$Yield_{day1}$ (%)	$Yield_{day\ 2}$ (%)	$Yield_{day\ 3}$ (%)
3.2a	0.5	37	45	81	8	25	4
3.2a	0.5	26	45	82	5	41	0
3.2a	0.5	50	55	80	2	3	21

It was surprising that the active intermediate is still active after 3 days of storage at -35 ^{o}C, but the disparity in the yields was a problem. Attempts to characterize the active intermediate by analyzing samples of the active species solution by ^{1}H NMR spectroscopy was unsuccessful and often complex ^{1}H NMR spectra were observed.

Results from week one and week two are very different, and so are the parallel runs in the same day. We believe that this lack of the reproducibility observed with complex **3.2a** is connected to the formation of the initiator. In Scheme 5.4 it is shown how the complex **3.2a** is hypothetically alkylated in the chlorine positions that are *trans* to each other. The α-hydrogen abstraction step might require the proximity of the two alkyl moieties to produce a transition state favorable for a σ-bond metathesis. Complex **3.2a** does not offer this proximity (from its X-ray structure[81]), and as a consequence the active species might not be formed equally at all times. On the other hand *cis*-alkyl moieties should undergo α-hydrogen abstraction more easily. Complexes Mo(O)Cl_2{2,2'-CH_2(O-6-^{t}Bu-4-Me$C_6H_2)_2$-κ^2*O,O*'} (**4.3a**) and Mo(O)Cl_2{2,2'-CH(^{i}Pr)(O-4,6-$^{t}Bu_2C_6H_2)_2$-κ^2*O,O*'} (**4.3b**) have a *cis*-chloro *cis*-bisphenoxo arrangement around the MoO^{4+} center. Their performance was therefore tested with different co-catalysts in different ratios.

Stock solutions of complex **4.3a** and 0.5, 1.0 and 1.5 equiv of ^{n}BuLi were prepared at -35 ^{o}C to run 3 polymerizations at room temperature in parallel per day, for 3 days. These experiments were repeated twice in two different weeks. Experiments using complex **4.3a** and 2.0, 2.5 and 3.0 equiv were done in the same manner as those above, but only for 1 week. Solutions were stored in the glovebox freezer at -35 ^{o}C after use. The results are displayed in Scheme 5.9.

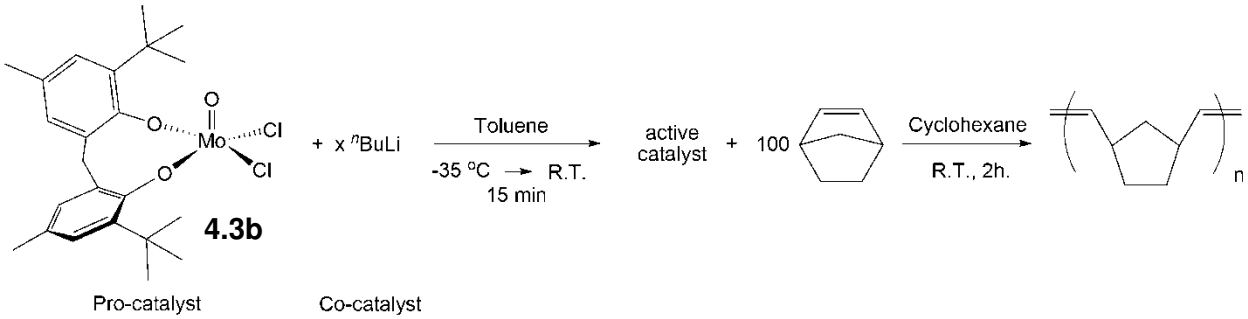

4.3b

Pro-catalyst Co-catalyst

Initiator	^{n}BuLi equiv	Week 1			Week 2		
		$Yield_{day1}$ (%)	$Yield_{day\ 2}$ (%)	$Yield_{day\ 3}$ (%)	$Yield_{day1}$ (%)	$Yield_{day\ 2}$ (%)	$Yield_{day\ 3}$ (%)
4.3a	0.5	25	59	50	25	60	50
4.3a	0.5	25	59	34	25	60	48
4.4a	0.5	25	100	50	25	60	48
4.4a	1.0	100	94	76	100	100	80
4.4a	1.0	71	100	73	90	98	80
4.4a	1.0	100	100	80	100	100	78
4.4a	1.5	35	28	23	38	28	22
4.4a	1.5	43	28	17	35	28	20
4.4a	1.5	35	81	23	38	30	21
4.4a	2.0	1	0	6	-	-	-
4.4a	2.0	1	0	9	-	-	-
4.4a	2.0	1	0	8	-	-	-
4.4a	2.5	1	0	0	-	-	-
4.4a	2.5	1	0	0	-	-	-
4.4a	2.5	1	0	0	-	-	-
4.4a	3.0	1	0	0	-	-	-
4.4a	3.0	1	0	0	-	-	-
4.4a	3.0	1	0	0	-	-	-

Scheme 5.9 Polymerization of NBE using a stock solution of **4.3a** and ^{n}BuLi in different ratios. Reactions were done in triplicate each day for three days. Polymerizations were performed in two different weeks.

From the table in Scheme 5.9 we can observe that high yields of polyNBE are obtained when we use 1.0 equiv of ^{n}BuLi. More interesting, is the fact that reproducibility was reached for parallel experiments when we use the complex $Mo(O)Cl_2\{2,2'\text{-}CH_2(O\text{-}6\text{-}^{t}Bu\text{-}4\text{-}MeC_6H_2)_2\text{-}\kappa^2O,O'\}$ (**4.3a**) as initiator. This supports our hypothesis about the need of a *cis*-alkyl arrangement around the MoO^{4+} moiety for successful α-hydrogen abstraction step. Attempts to identify the active species by ^{1}H NMR spectroscopy were unsuccessful, due to the complexity of the ^{1}H NMR spectra.

Unfortunately *cis*:*trans* ratios were not improved and they were an average of 0.62:1.0 when 1 equiv of ^{n}BuLi was used as co-catalyst.

Other co-catalysts were attempted, with Et_3Al and $PhCh_2MgCl$ yieldeding the best results.

Stock solutions of complex **4.3a** were prepared with 0.5 and 1.0 equiv of Et_3Al and $PhCh_2MgCl$ at -35 °C. These solutions were use to run two polymerizations at room temperature per day during three days. The solutions were kept in the glovebox freezer at -35 °C after use. The results are shown in the Scheme 5.10.

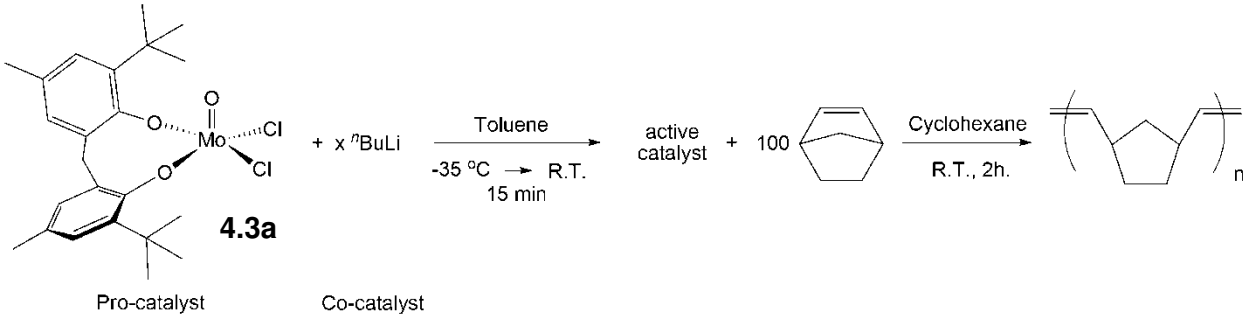

Initiator	cocatalys	equiv	Week 1		
			$Yield_{day1}$ (%)	$Yield_{day\ 2}$ (%)	$Yield_{day\ 3}$ (%)
4.3a	Et_3Al	0.5	100	100	100
4.3a	Et_3Al	0.5	100	100	100
4.4a	Et_3Al	1.0	93	84	84
4.4a	Et_3Al	1.0	60	66	67
4.4a	$PhCH_2MgCl$	0.5	70	94	69
4.4a	$PhCH_2MgCl$	0.5	89	60	98
4.4a	$PhCH_2MgCl$	1.0	90	90	90
4.4a	$PhCH_2MgCl$	1.0	79	79	77

Scheme 5.10 Polymerization trials with **4.3a** using 0.5 and 1.0 equiv of Et_3Al and $PhCH_2MgCl$ as co-catalysts.

Superior conversion was obtained when the precursor **4.3a** was used with 0.5 equiv of Et_3Al, (c:t) ratios were an average of 0.44:1.0. The active intermediate is stable in solution and yields reproducible results. Attempts to characterize the active intermediate by analyzing aliquots of the stock solutions by ^{1}H NMR spectroscopy were not successful. The *cis*:*trans* ratios were still broad (no stereocontrol in the reaction).

Mo(O)Cl_2{2,2'-CH_2(O-6-^{t}Bu-4-Me$C_6H_2)_2$-κ^2*O,O'*} (**4.3a**) was reacted with 0.5 equiv of Et_3Al at -35 °C, and polymerization of NBE at room temperature was attempted using THF as reaction solvent. The yield was 100% and the (c:t) was 1.0:0.89 (Figure 5.2). This result indicates that the cis:trans ratio is strongly dependent on the reaction solvent. This is in agreement with previous reports where has been noted that the stereochemistry of the final product might be determined by a group of factors such as solvent, additives, temperature, reaction time, and the monomer.[228]

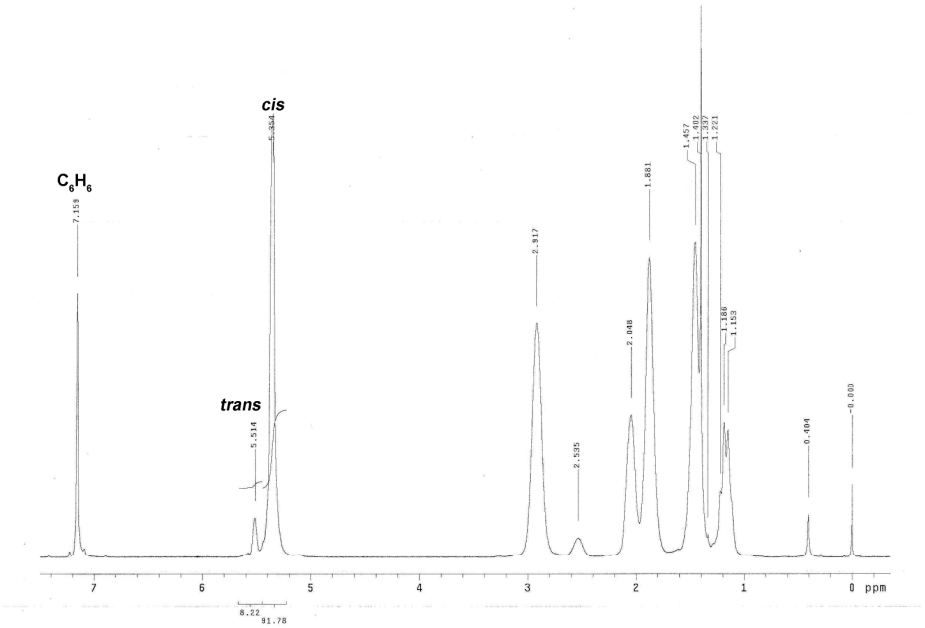

Figure 5.3 ^{1}H NMR spectrum in C_6D_6 of polyNBE generated from the precursor **4.3a** and 0.5 equiv of Et_3Al in THF at room temperature.

The complex Mo(O)Cl_2{2,2'-C(^{i}Pr)(O-4,6-^{t}Bu$_2C_6H_2)_2$-κ^2*O,O'*} (**4.3b**) was explored as catalyst precursor. Complex **4.3b** has an isopropyl group at the methylene bridge and, its X-ray structure (chapter 4) shows that the isopropyl substituent points out and down from the coordination sphere of the MoO^{4+} unit. This might not provide enough steric hindrance to the MoO^{4+} center to direct the approach of the monomer, but the catalytic activity of the complex **4.3b** was investigated. A stock solution of complex **4.3b** was prepared with 1.0 equiv of ^{n}BuLi at -35 °C (1.0 equiv of ^{n}BuLi produced the best yields with complex **4.3a**, Scheme 5.9). The stock solution

was used to run three polymerizations at room temperature per day during three days. The solution was kept in the glovebox freezer at -35 °C after use. The results are shown in the Scheme 5.11.

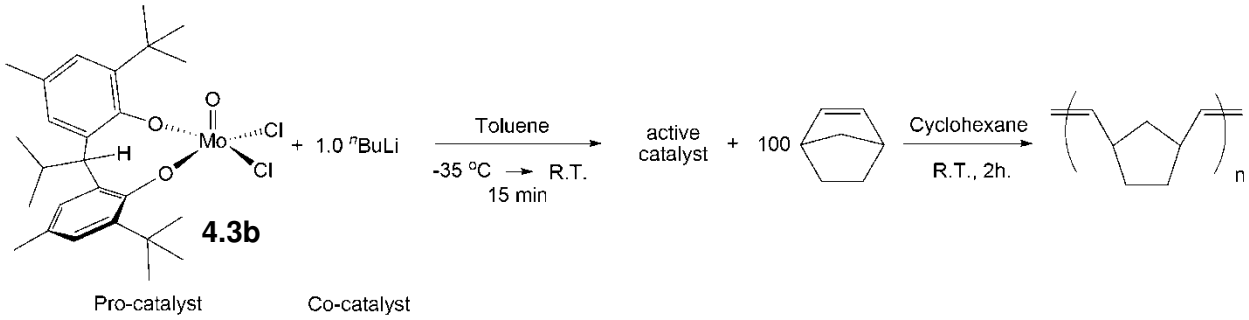

Initiator	$Yield_{day1}$ (%)	$Yield_{day\ 2}$ (%)	$Yield_{day\ 3}$ (%)
4.3b	35	28	21
4.3b	35	28	17
4.4b	35	23	20

Scheme 5.11 Polymerization of NBE with complex **4.3b** as initiator and 1.0 equiv of ^{n}BuLi.

Although the yield reproducibility for parallel runs in the same day was good, the *cis*:*trans* ratios averaged 0.72:1.0. This result implies that the isopropyl substituent in the methylene bridge does not affect the stereochemistry (Scheme 5.5). Addition of a second substituent at the methylene bridge might produce steric hindrance at the MoO^{4+} unit and probably direct the approach of the monomer. Use of different co-catalysts and different solvents (such as THF) might also give a better stereocontrol in the final polymer.

5.4 Conclusions

The complexes $MoO(O\text{-}2,6\text{-}Me_2C_6H_3)_2Cl_2$ (**3.2a**), $MoO(O\text{-}2,6\text{-}Me_2C_6H_3)_3Cl$ (**3.2b**), $Mo(O)Cl_2\{2,2'\text{-}CH_2(O\text{-}6\text{-}^{t}Bu\text{-}4\text{-}MeC_6H_2)_2\text{-}\kappa^2O,O'\}$ (**4.3a**), $Mo(O)Cl_2\{2,2'\text{-}CH(^{i}Pr)(O\text{-}4,6\text{-}^{t}Bu_2C_6H_2)_2\text{-}\kappa^2O,O'\}$ (**4.3b**) were tested as precursors for ring opening metathesis polymerization of norbornene. A metal carbene intermediate is believed to be formed in situ upon addition of

alkylating agents such as ^{n}BuLi, Et_3Al or $PhCH_2MgCl$. In systems like ours an α-hydrogen abstraction between the generated alkyl moieties might produce the metal alkylidene complex responsible for the observed ROMP activity. It was observed that MoO^{4+} complexes with lesser degree of aryloxide substitution performed better than those fully substituted. Among the disubstituted complexes, those that had *cis*-chloro moieties such as Mo(O)Cl_2{2,2'-CH_2(O-6-^{t}Bu-4-$MeC_6H_2)_2$-κ^2*O,O*} (**4.3a**), Mo(O)Cl_2{2,2'-CH(^{i}Pr)(O-4,6-$^{t}Bu_2C_6H_2)_2$-κ^2*O,O*} (**4.3b**) offered more consistent reactivities, translated into reproducible yields.

The research described in this chapter was our first approach to the field of olefin metathesis polymerization. Further adjustments in our polymerization procedures have to be made in order to offer a more complete discussion and understanding of the different factors that might affect the reaction course and the characteristics of the final product. More detailed work involving temperatures, solvents and reaction times is required.

Appendix for Chapter 2

^{1}H and ^{13}C NMR Spectra

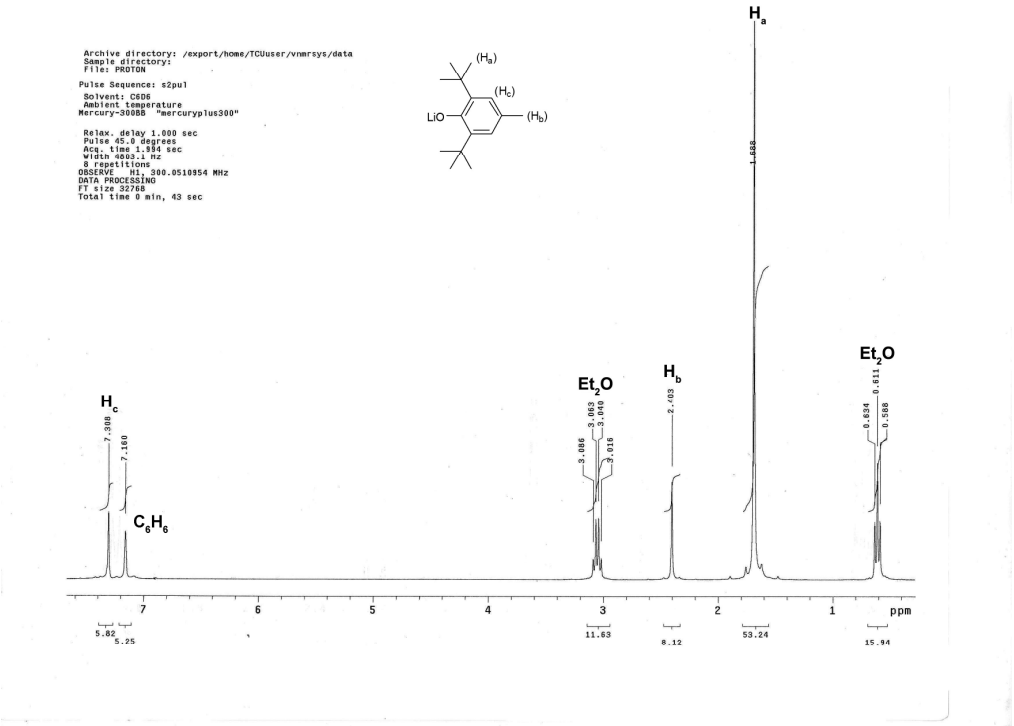

Figure A2.1. ^{1}H NMR of LiO-2,6-$^{t}Bu_2$-4-MeC_6H_2 (**2.1b**) in C_6D_6

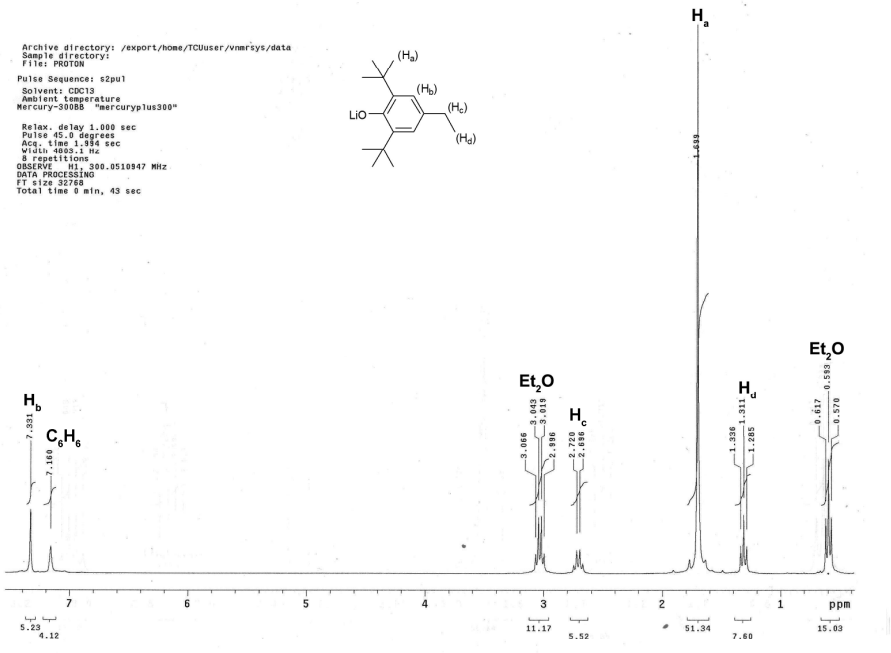

Figure A2.2. ^{1}H NMR of LiO-2,6-$^{t}Bu_2$-4-EtC_6H_2 (**2.1c**) in $CDCl_3$

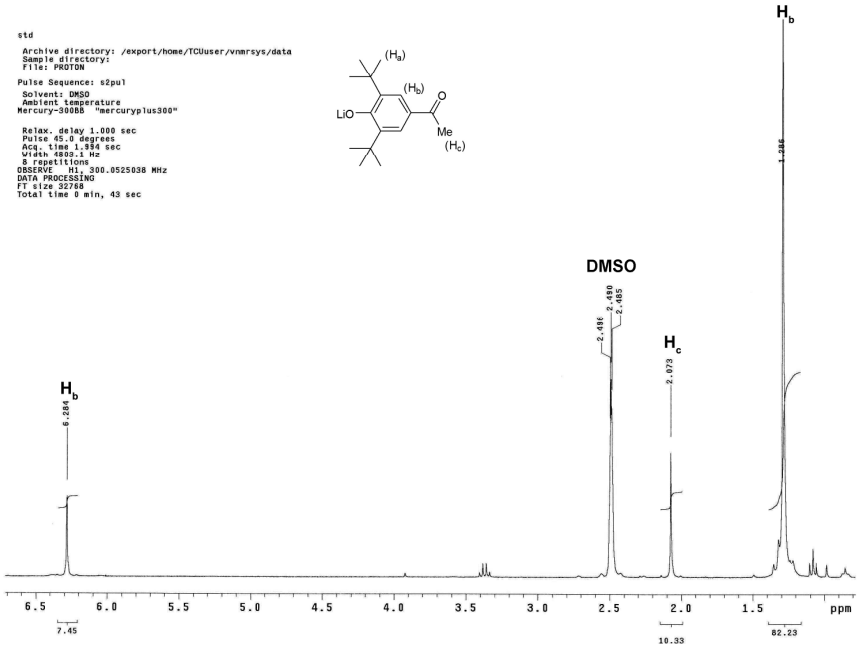

Figure A2.3. ^{1}H NMR of LiO-2,6-^{t}Bu$_2$-4-[OC(O)Me]C$_6$H$_2$ (**2.1d**) in DMSO-d$_6$

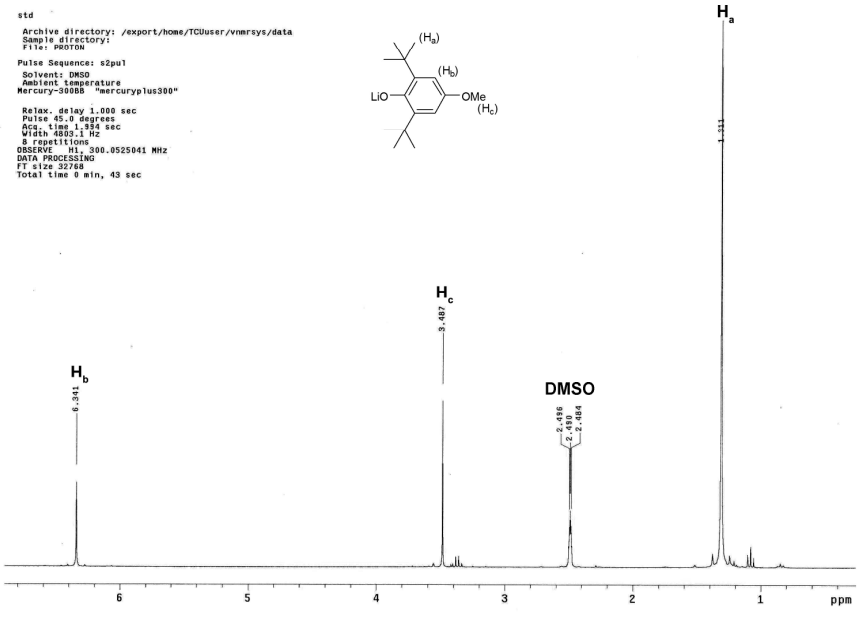

Figure A2.4. ^{1}H NMR of LiO-2,6-^{t}Bu$_2$-4-(OMe)C$_6$H$_2$ (**2.1e**) in DMSO-d$_6$

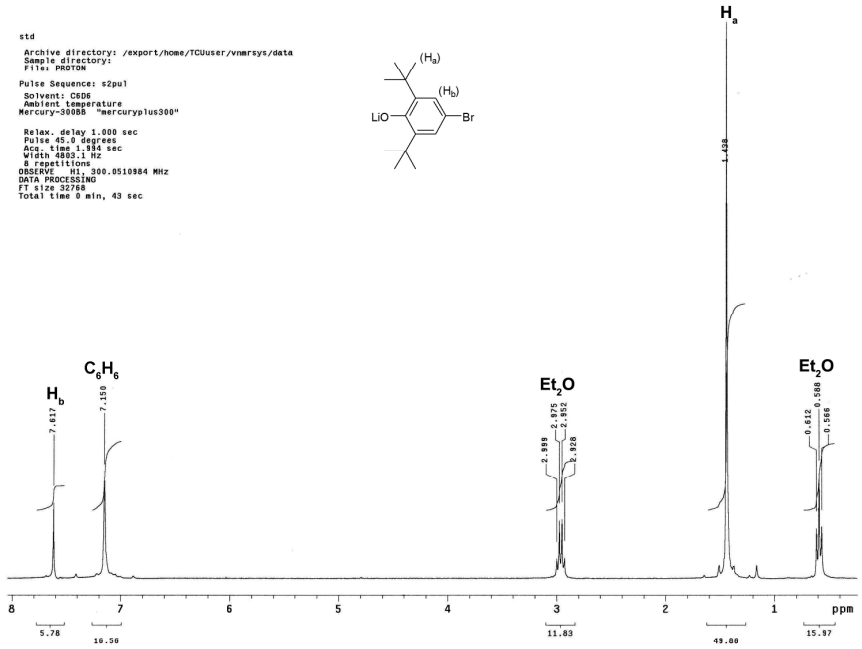

Figure A2.5. ^{1}H NMR of LiO-2,6-^{t}Bu$_2$-4-BrC$_6$H$_2$ (**2.1f**) in C$_6$D$_6$

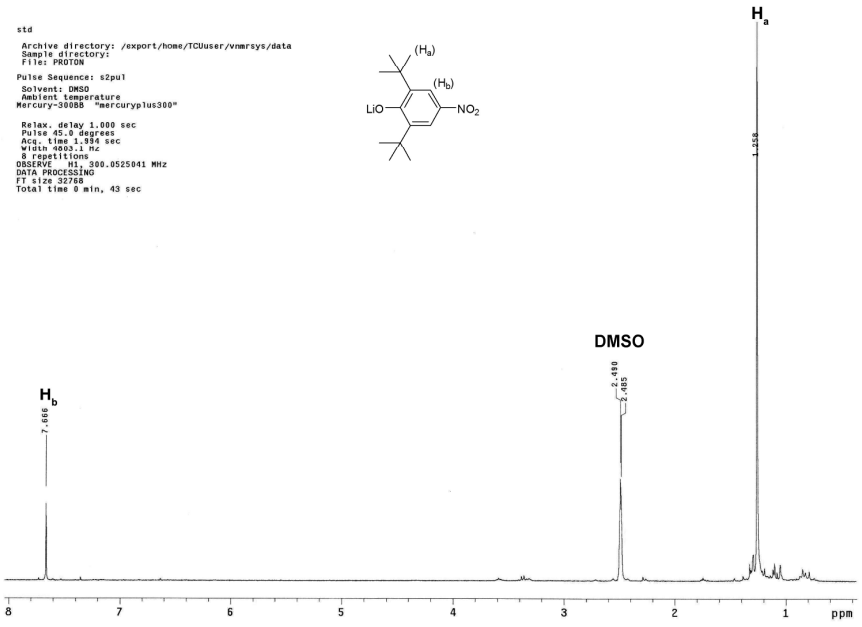

Figure A2.6. ^{1}H NMR of LiO-2,6-^{t}Bu$_2$-4-(NO$_2$)C$_6$H$_2$ (**2.1h**) in DMSO-d$_6$

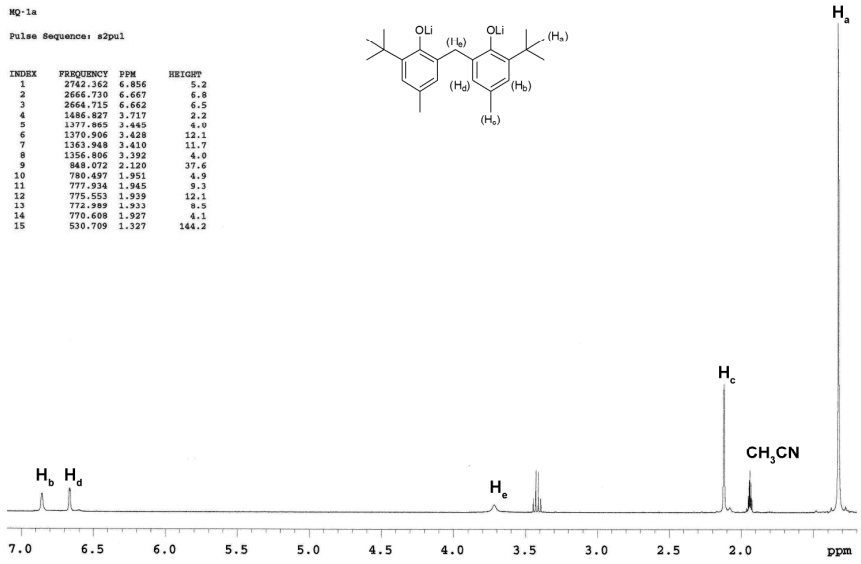

Figure A2.7. ^{1}H NMR of 2,2'-CH_2(LiO-6-^{t}Bu-4-MeC_6H_2)$_2$ (**2.1i**) in CD_3CN

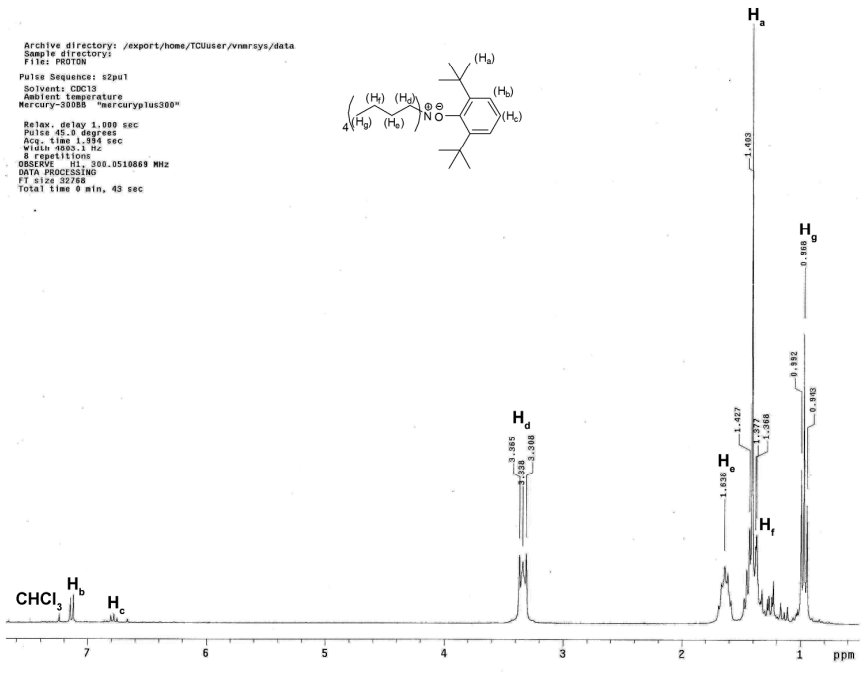

Figure A2.8. ^{1}H NMR of (Bu_4N)(O-2,6-^{t}Bu$_2C_6H_3$) (**2.1m**) in $CDCl_3$

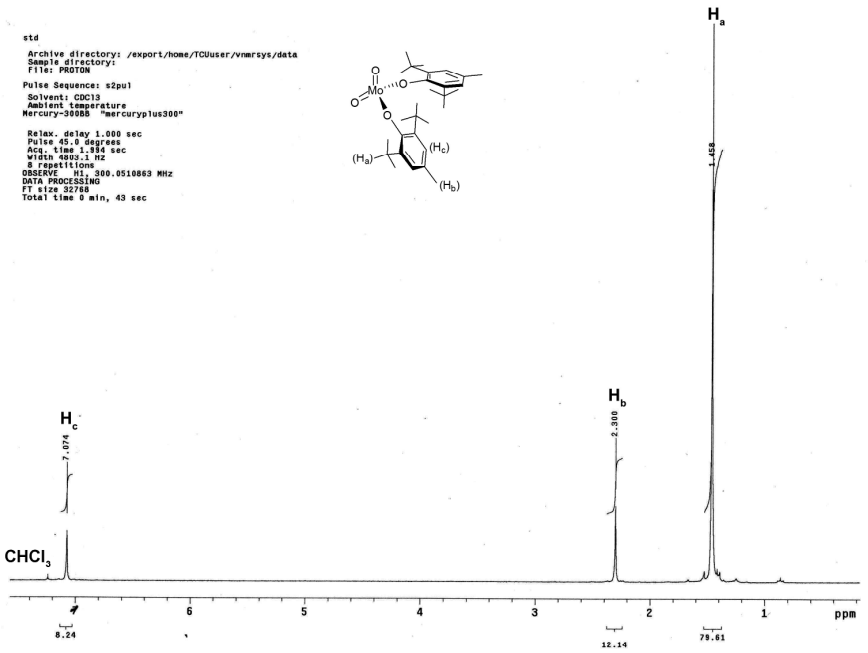

Figure A2.9. ^{1}H NMR of MoO_2(O-2,6-^{t}Bu$_2$-4-MeC_6H_2)$_2$ (**2.2b**) in $CDCl_3$

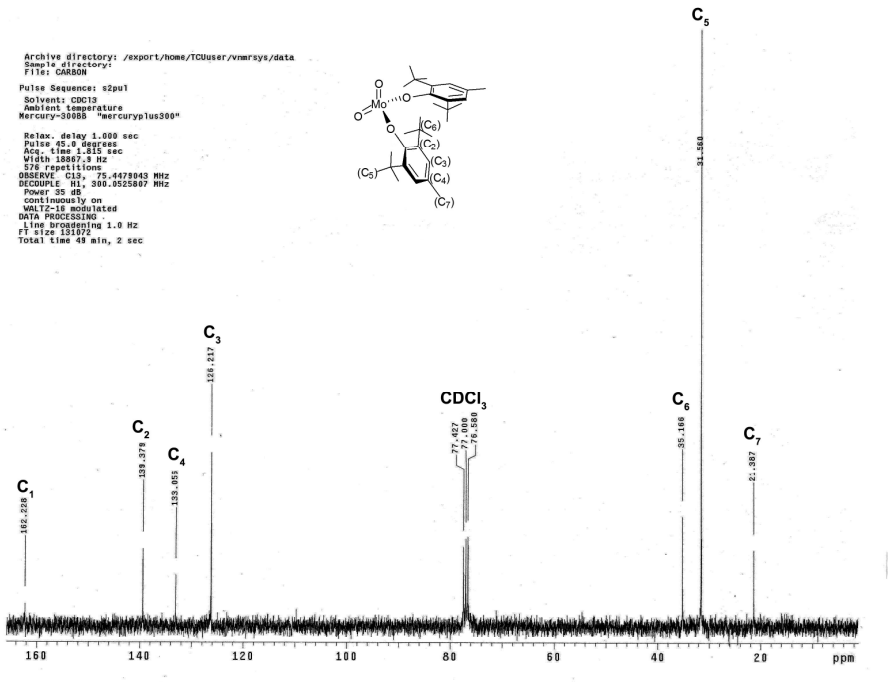

Figure A2.10. ^{13}C NMR of MoO_2(O-2,6-^{t}Bu$_2$-4-MeC_6H_2)$_2$ (**2.2d**) in $CDCl_3$

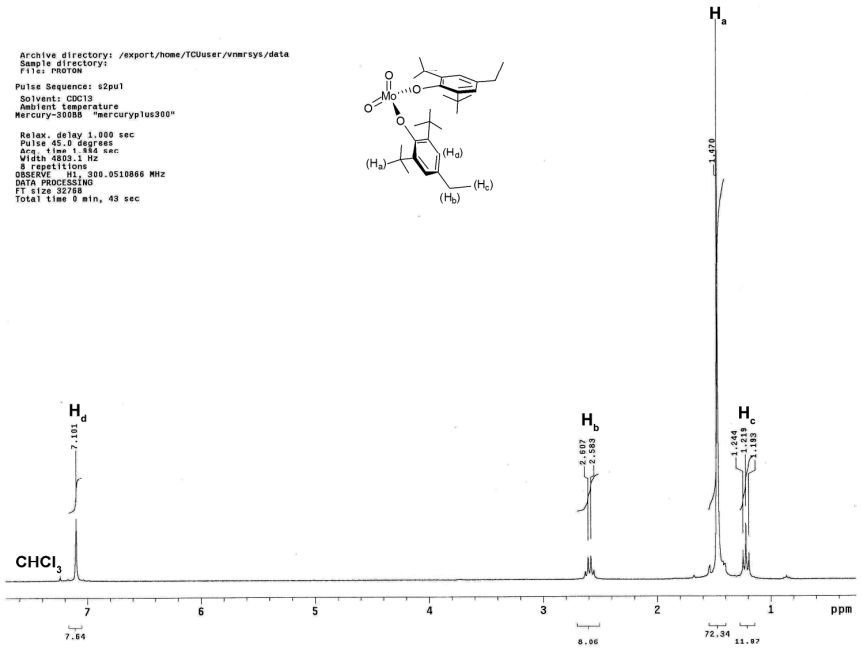

Figure A2.11. ^{1}H NMR of MoO_2(O-2,6-^{t}Bu$_2$-4-EtC_6H_2)$_2$ (**2.2c**) in $CDCl_3$

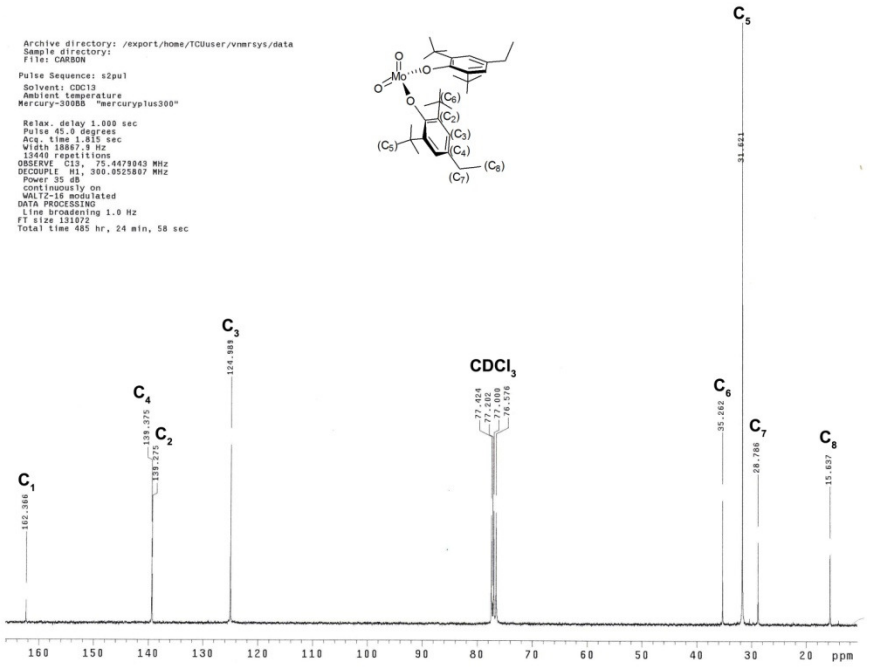

Figure A2.12. ^{13}C NMR of MoO_2(O-2,6-^{t}Bu$_2$-4-EtC_6H_2)$_2$ (**2.2c**) in $CDCl_3$

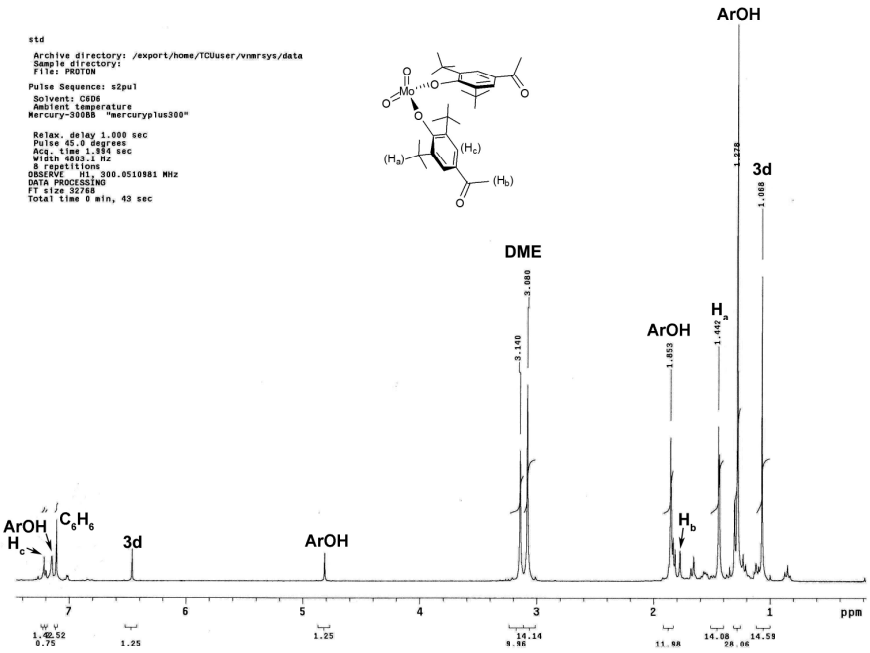

Figure A2.13. ^{1}H NMR of MoO_2(O-2,6-^{t}Bu$_2$-4-[OC(O)Me]C_6H_2)$_2$ (**2.2d**) in C_6D_6

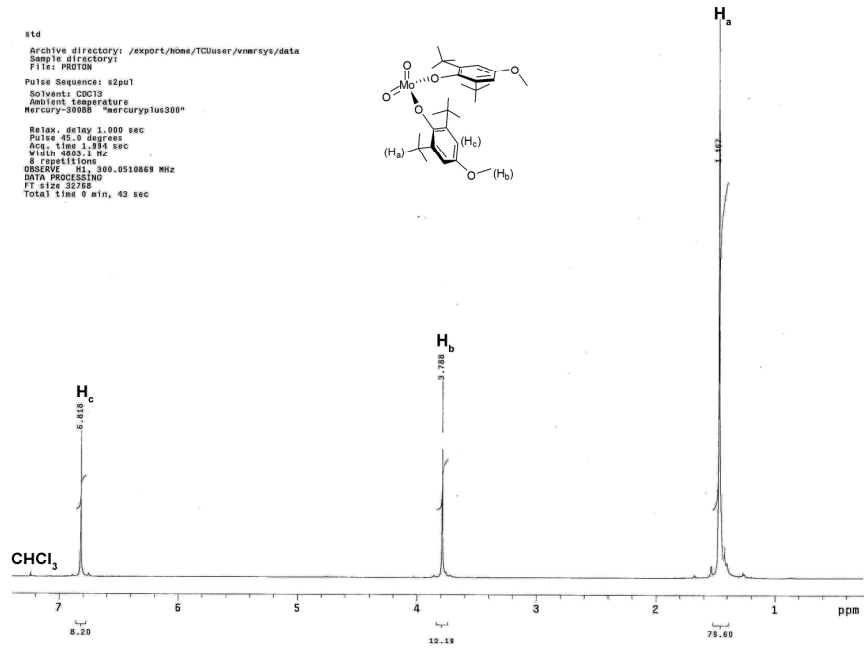

Figure A2.14. ^{1}H NMR of MoO_2(O-2,6-^{t}Bu$_2$-4-(OMe)C_6H_2)$_2$ (**2.2e**) in $CDCl_3$

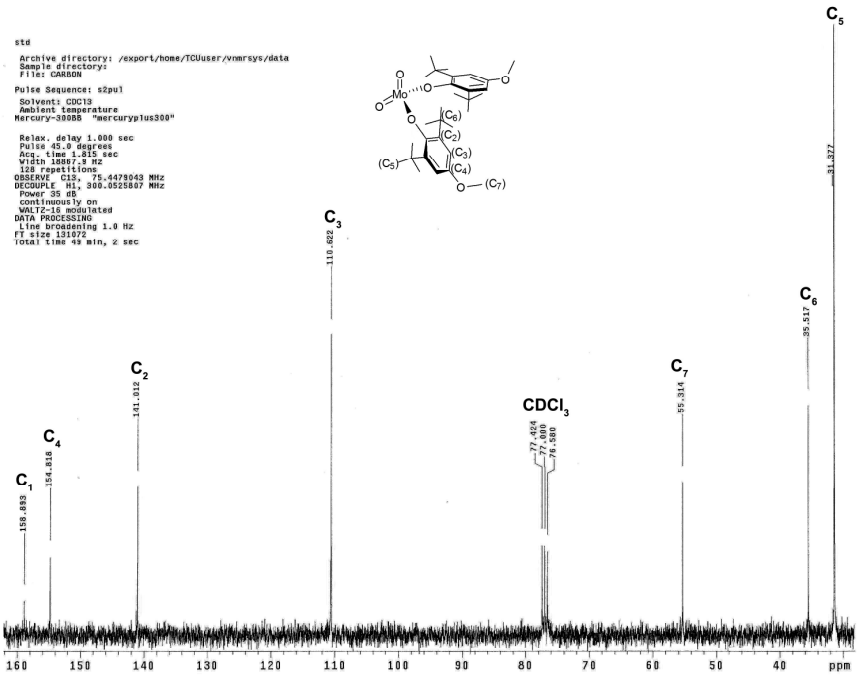

Figure A2.15. ^{13}C NMR of MoO_2(O-2,6-^{t}Bu$_2$-4-[OC(O)Me]C_6H_2)$_2$ (**2.2e**) in $CDCl_3$

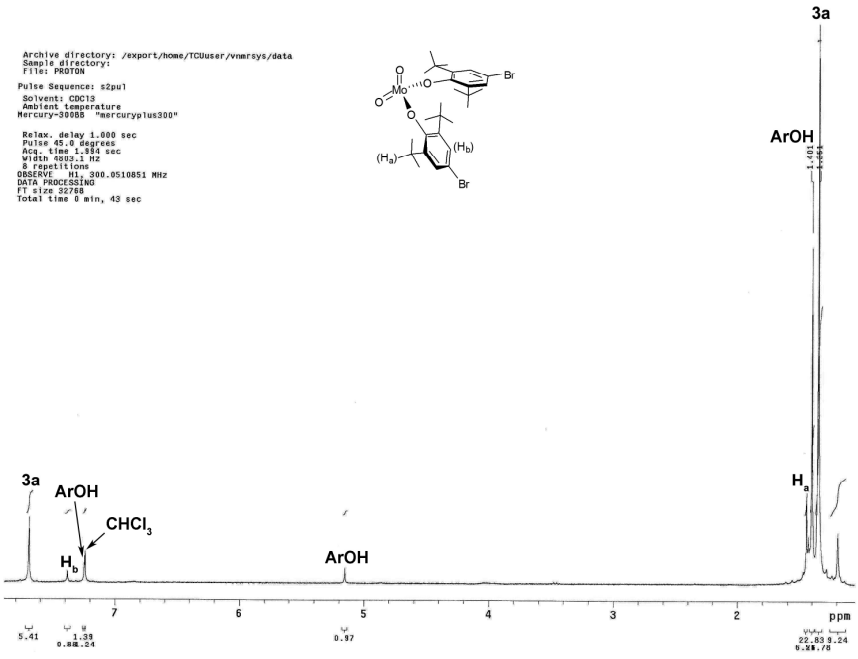

Figure A2.16. ^1H NMR of MoO_2(O-2,6-^{t}Bu$_2$-4-BrC_6H_2)$_2$ (**2.2f**) in $CDCl_3$

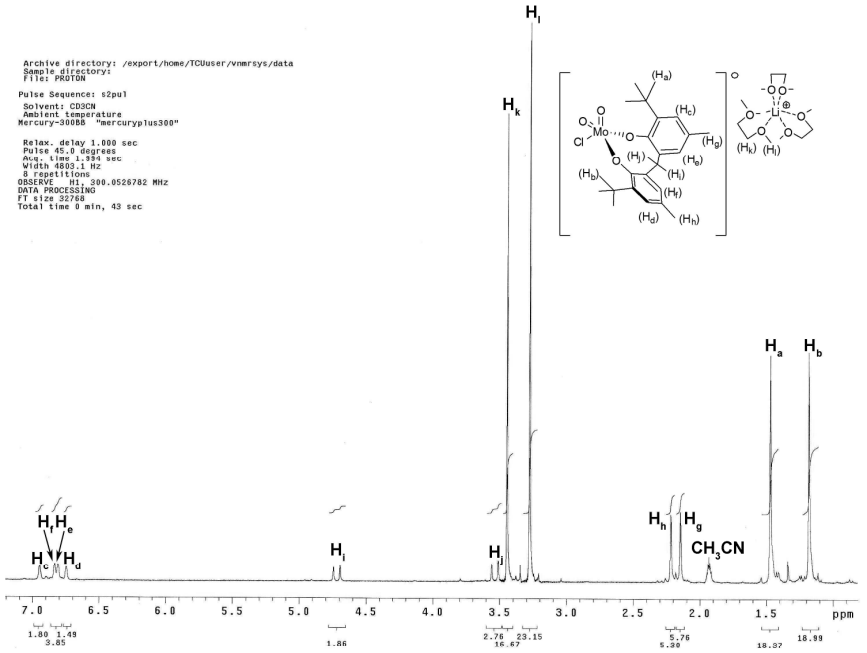

Figure A2.17. ^{1}H NMR of {$MoO_2Cl[2,2'\text{-}CH_2(O\text{-}6\text{-}^{t}Bu\text{-}4\text{-}MeC_6H_2)_2]$}Li·3DME (**2.4**) in CD_3CN

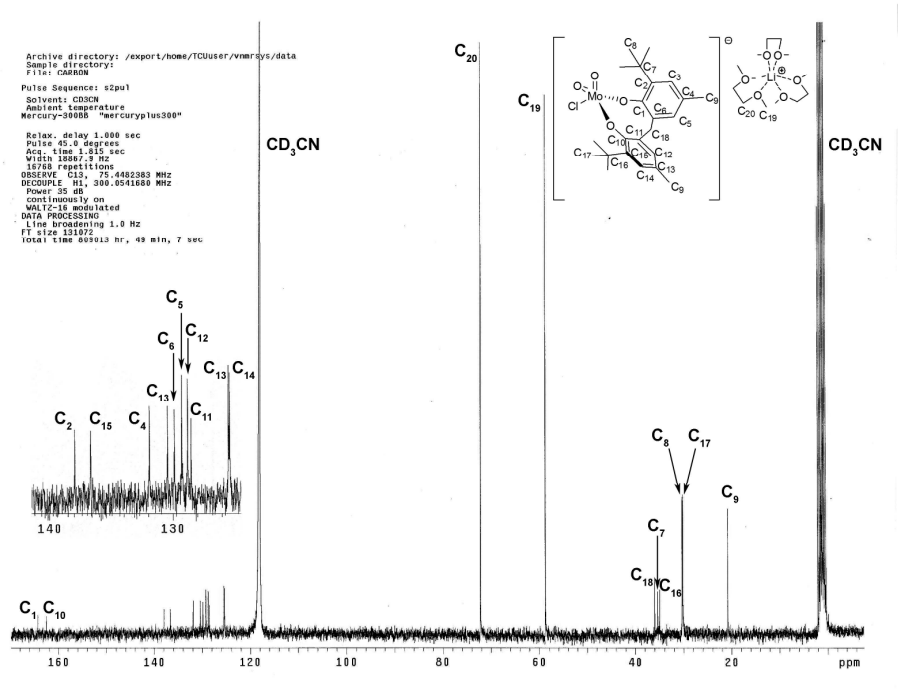

Figure A2.18. ^{13}C NMR of {$MoO_2Cl[2,2'\text{-}CH_2(O\text{-}6\text{-}^{t}Bu\text{-}4\text{-}MeC_6H_2)_2]$}Li·3DME (**2.4**) in CD_3CN

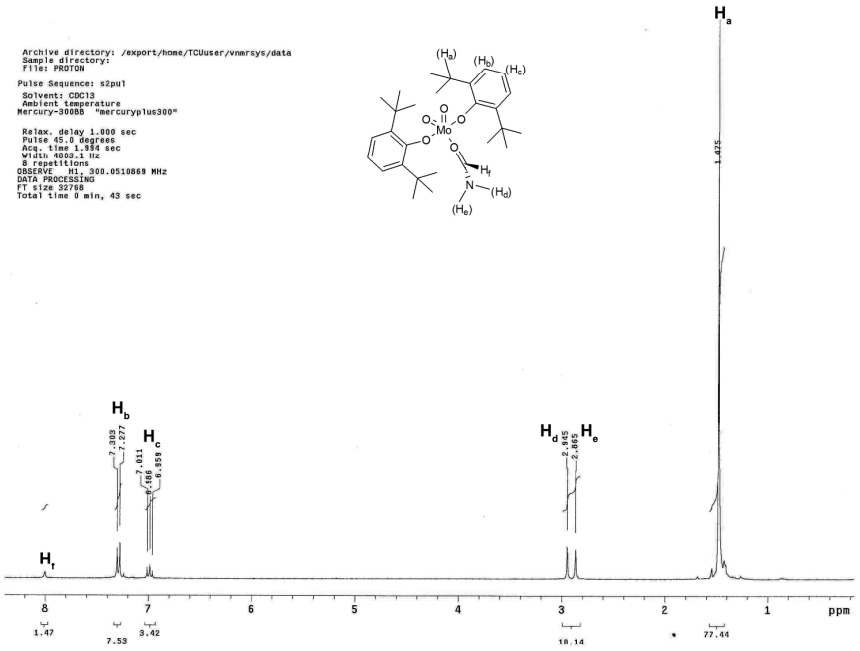

Figure A2.19. ^{1}H NMR of MoO_2(O-2,6-$^{t}Bu_2C_6H_3)_2$(DMF) (**2.5a**) in $CDCl_3$

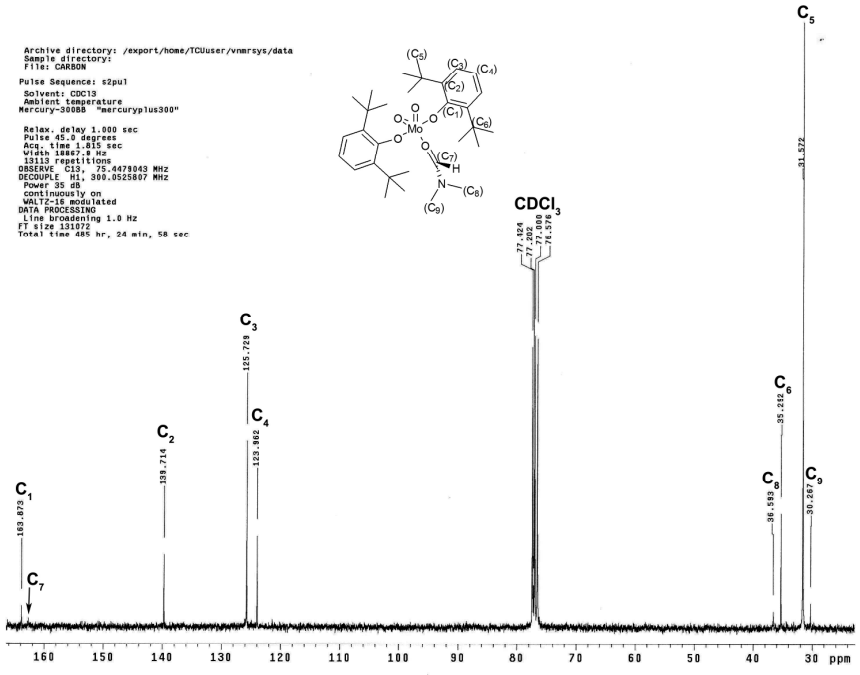

Figure A2.20. ^{13}C NMR of MoO_2(O-2,6-$^{t}Bu_2C_6H_3)_2$(DMF) (**2.5a**) in $CDCl_3$

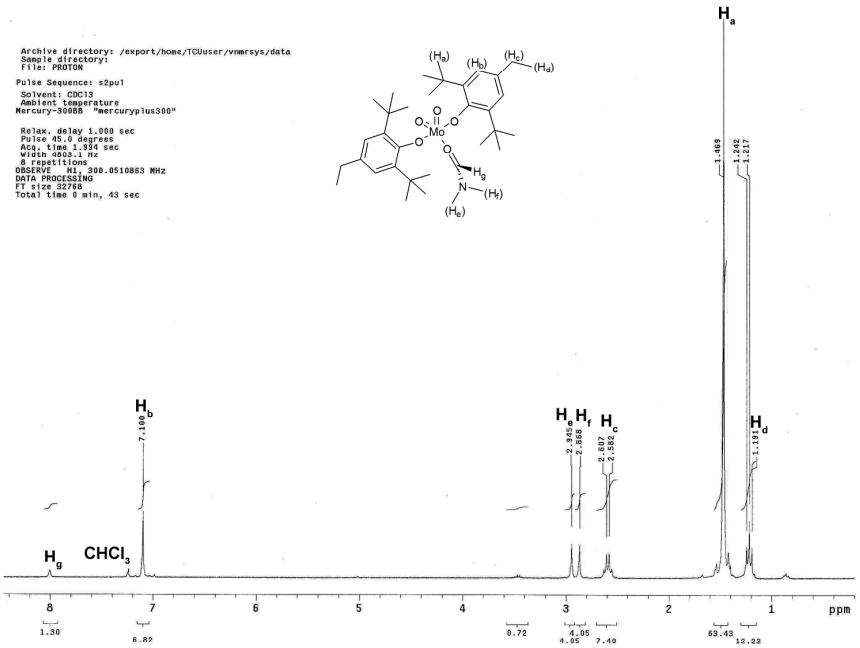

Figure A2.21. ^{1}H NMR of MoO_2(O-2,6-^{t}Bu$_2$-4-EtC_6H_2)$_2$(DMF) (**2.5c**) in $CDCl_3$

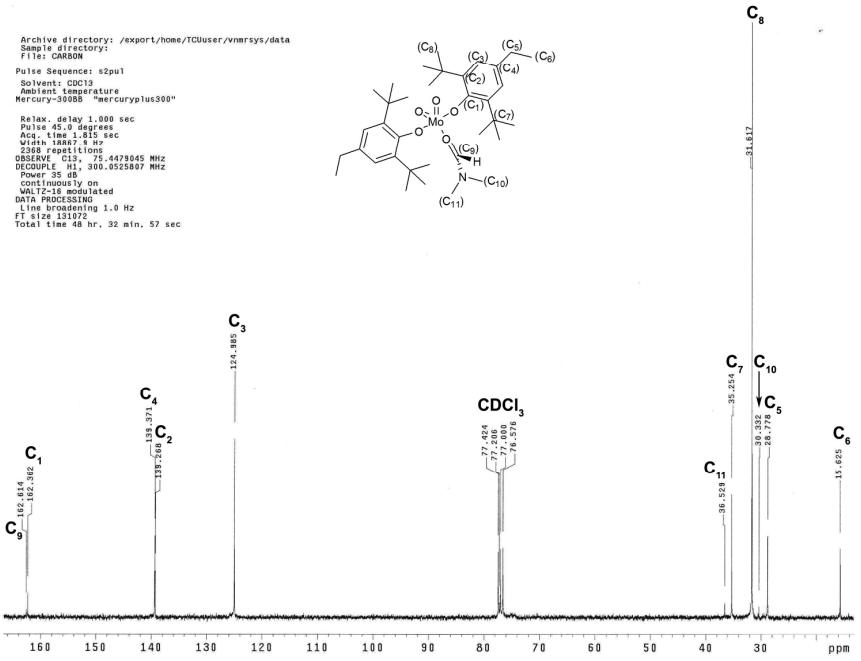

Figure A2.22. ^{13}C NMR of MoO_2(O-2,6-^{t}Bu$_2$-4-EtC_6H_2)$_2$(DMF) (**2.5c**) in $CDCl_3$

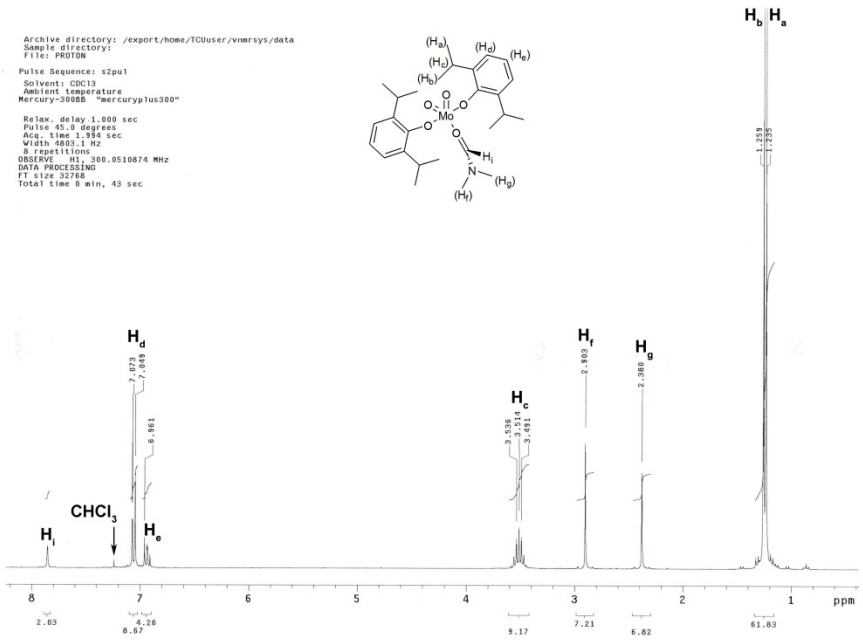

Figure A2.23. ^{1}H NMR of MoO_2(O-2,6-$^{i}Pr_2C_6H_3)_2$(DMF) (**2.5k**) in $CDCl_3$

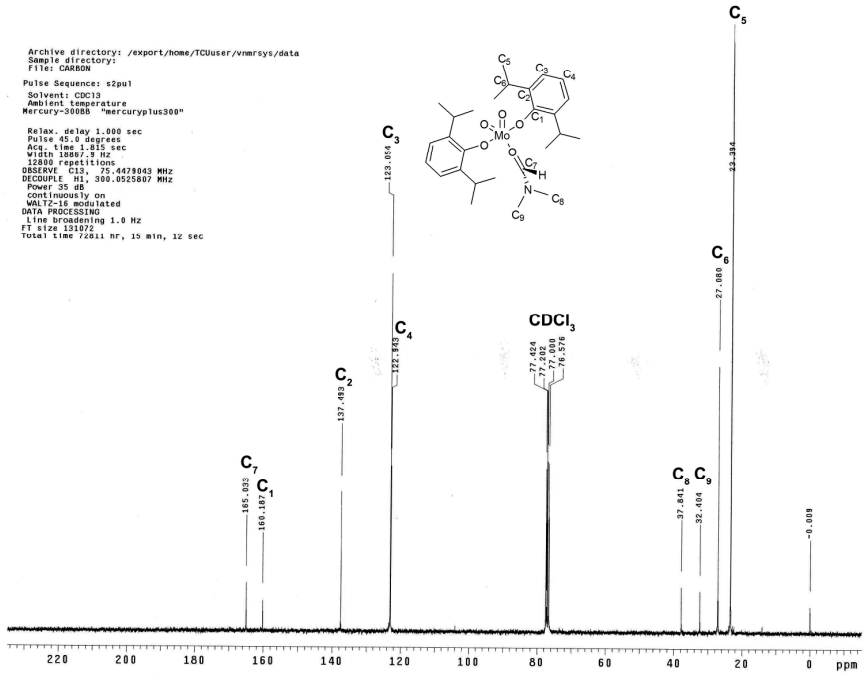

Figure A2.24. ^{13}C of NMR MoO_2(O-2,6-$^{i}Pr_2C_6H_3)_2$(DMF) (**2.5k**) in $CDCl_3$

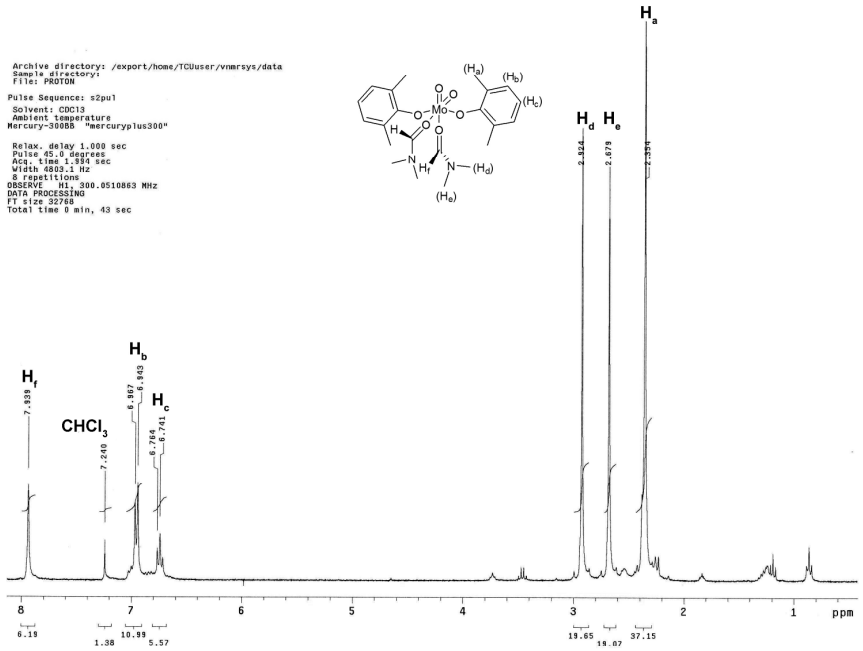

Figure A2.25. ^{1}H NMR of $MoO_2(O\text{-}2,6\text{-}Me_2C_6H_2)_2(DMF)_2$ (**2.5l**) in $CDCl_3$

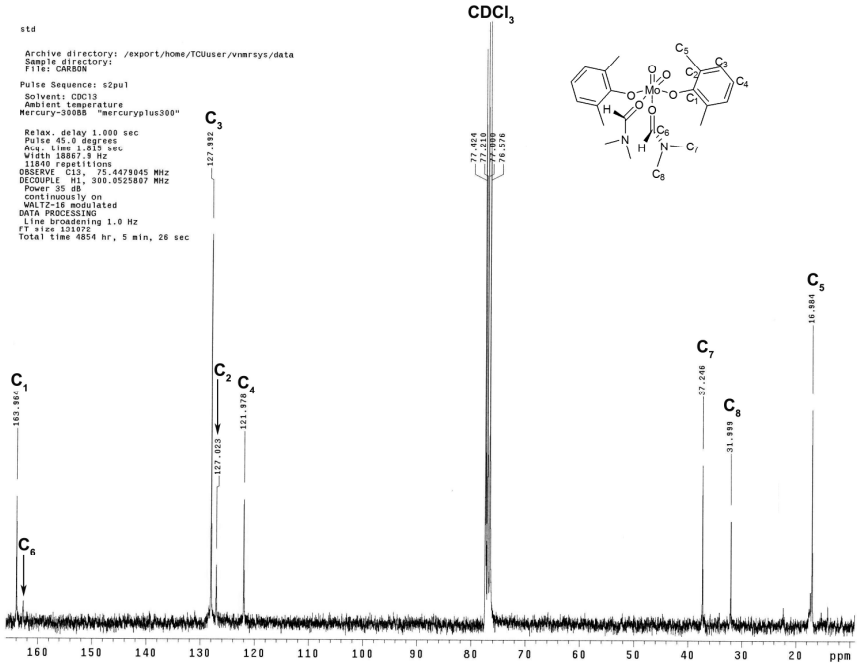

Figure A2.26. ^{13}C NMR of $MoO_2(O\text{-}2,6\text{-}Me_2C_6H_2)_2(DMF)_2$ (**2.5l**) in $CDCl_3$

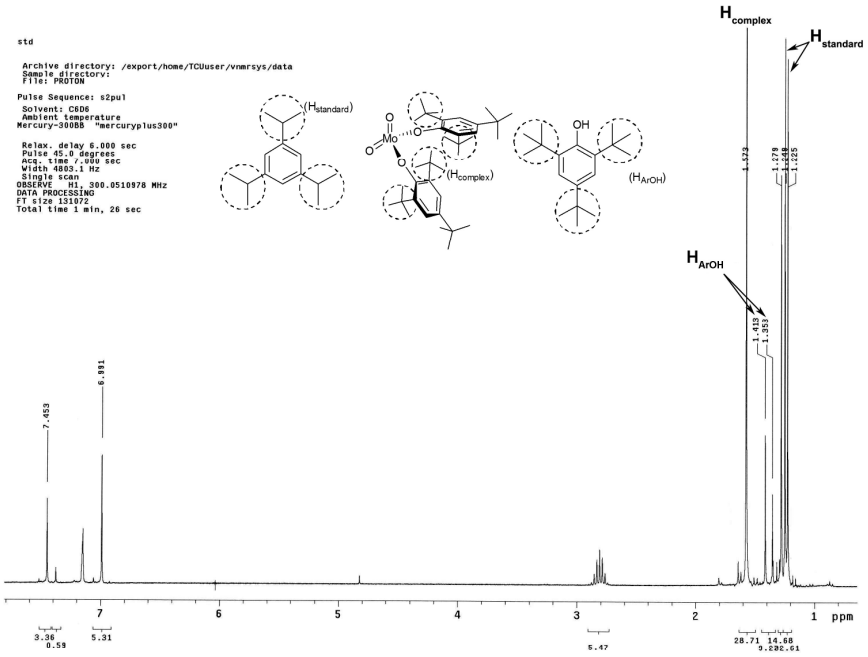

Figure A2.27. Correlation between weighed complex and its NMR spectrum in C_6D_6

^{1}H NMR of 0.70 mL of a 0.040 M solution of 1,3,5-triisopropylbenzene (0.0057 g, 2.8 x 10^{-5} mol) containing 9.6 x 10^{-3} g (1.5 x 10^{-5} mol) of complex MoO_2(O-2,4,6-^{t}Bu$_3$C$_6$H$_2$)$_2$ (**2j**). The ^{1}H NMR spectrum revealed that although 4 recrystallizations from pentane were performed, some parent aryl alcohol remained. A characteristic peak for each compound in the mixture was chosen as shown in this ^{1}H NMR spectrum. Each integral value was divided by the number of protons that it accounts for:

Standard: 32.6/18 = 1.8 per H; complex: 28.7/36 = 0.80 per H; ArOH: 9.3/27 = 0.34 per H.

Normalized with the standard value:

Standard: 1.8/1.8 = 1; Complex: 1.8/0.80 = 2.3; ArOH: 1.8/0.34 = 5.3

With the normalized values the numerical correspondence to each signal was assigned:

Complex: 2.8 x 10^{-5} mol/2.3 = 1.2 x 10^{-5} mol of complex (650.78 g/mol) = 0.0080 g

Phenol: 2.8 x 10^{-5} mol/5.3 = 5.3 x 10^{-6} mol of HOAr (262.43 g/mol) = 0.0014g

The addition of 0.0080 g + 0.0014 g = 0.0094 g calculated from ^{1}H NMR (actual 0.0096 g).

For this experiment the acquisition time was set = 7.00 sec and the relaxation time = 6.00 sec.

UV-vis spectrum

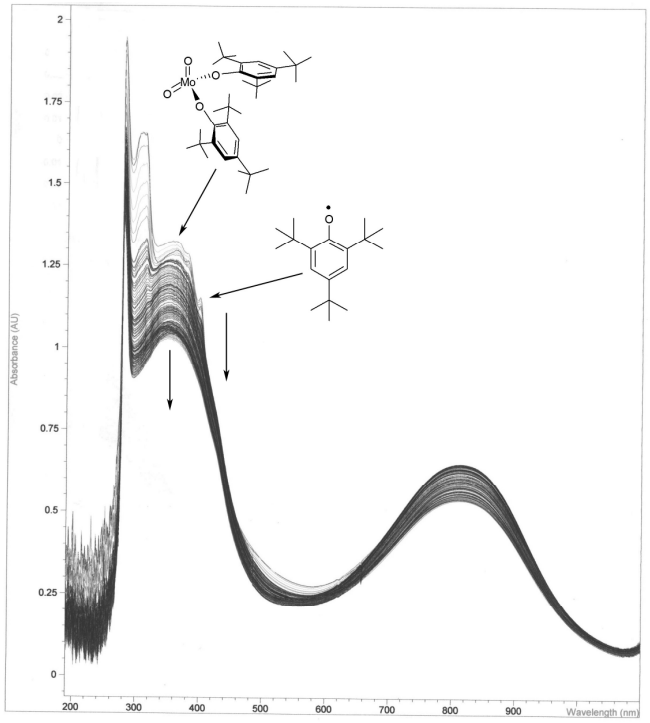

Figure A2.28. UV-vis spectra of the reaction of MoO_2Cl_2 + 2 LiO-2,4,6-^{t}Bu$_3$C$_6$H$_2$ (**2j**) in benzene. When the addition of the reagents was completed, a UV-vis run was set up for 43 200 s spectra with 300 s lapses. Absorbance at specific wavelengths was recorded: 401 nm for ·O-2,4,6-^{t}Bu$_3$-C$_6$H$_2$ (weak) and 357 nm for MoO_2(O-2,4,6-^{t}Bu$_3$C$_6$H$_2$)$_2$) (**2.2j**) (strong). Both wavelengths showed a sudden increase in their absorbance after addition of reagents was completed (within the first 300 s). As the run proceeded, both wavelengths displayed a steady decrease in their absorbance values (*ca*. an overall 10% of the original value). The formation of **2.2j** and ·O-2,4,6-^{t}Bu$_3$C$_6$H$_2$ took place at about the same time. Degradation of the radical is believed to happen as a consequence of the experimental conditions (not completely air-free atmosphere inside of the cell).

EPR spectra

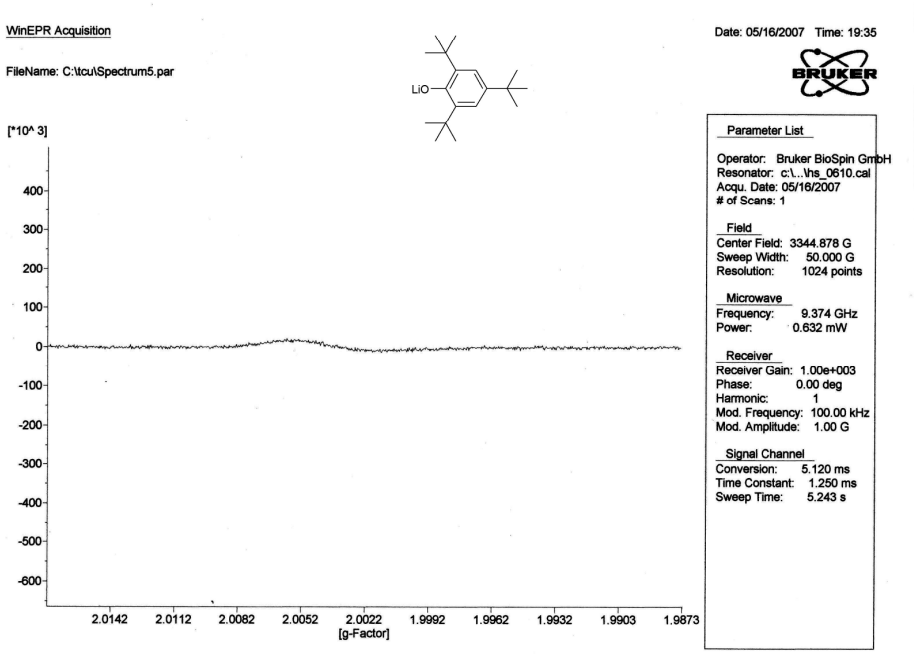

Figure A2.29. Room temperature EPR in solid state of LiO-2,4,6-$^{t}Bu_3C_6H_2$ (**2.1j**).

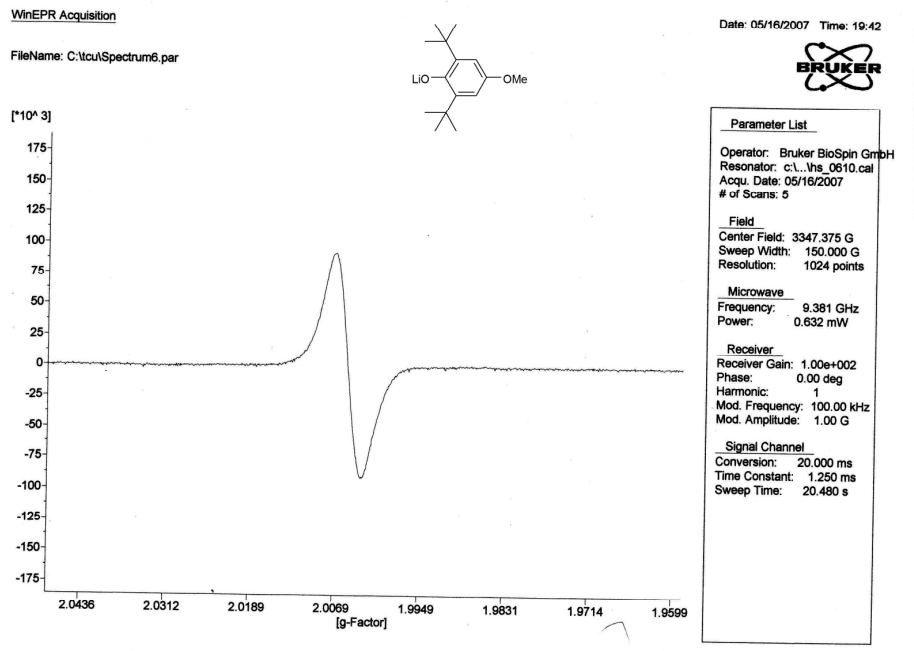

Figure A2.30. Room temperature EPR in solid state of LiO-2,6-$^{t}Bu_2$-4-(OMe)C_6H_2 (**2.1e**).

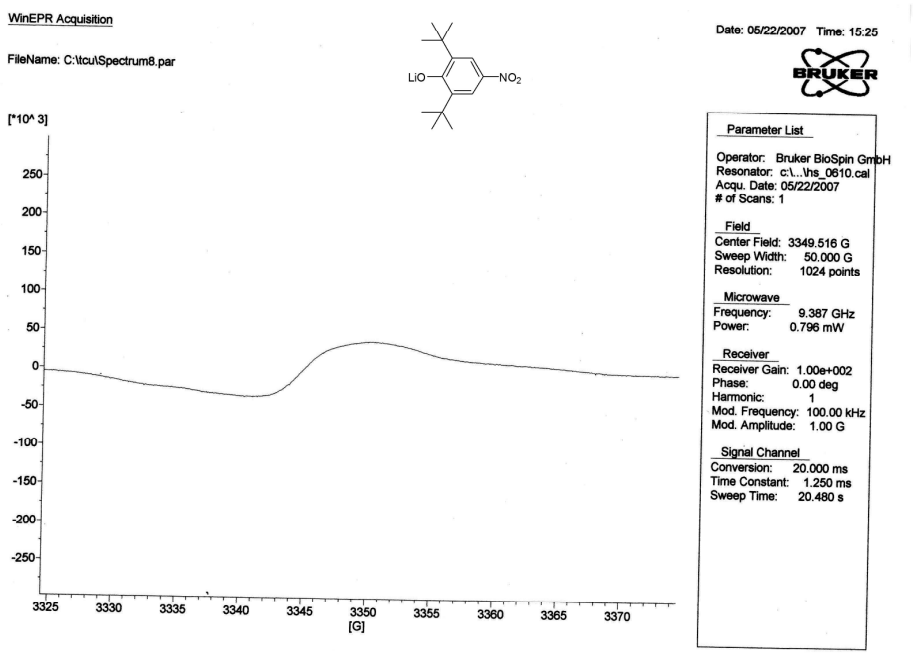

Figure A2.31. Room temperature EPR in solid state of LiO-2,6-^{t}Bu$_2$-4-(NO$_2$)C$_6$H$_2$ (**2.1h**).

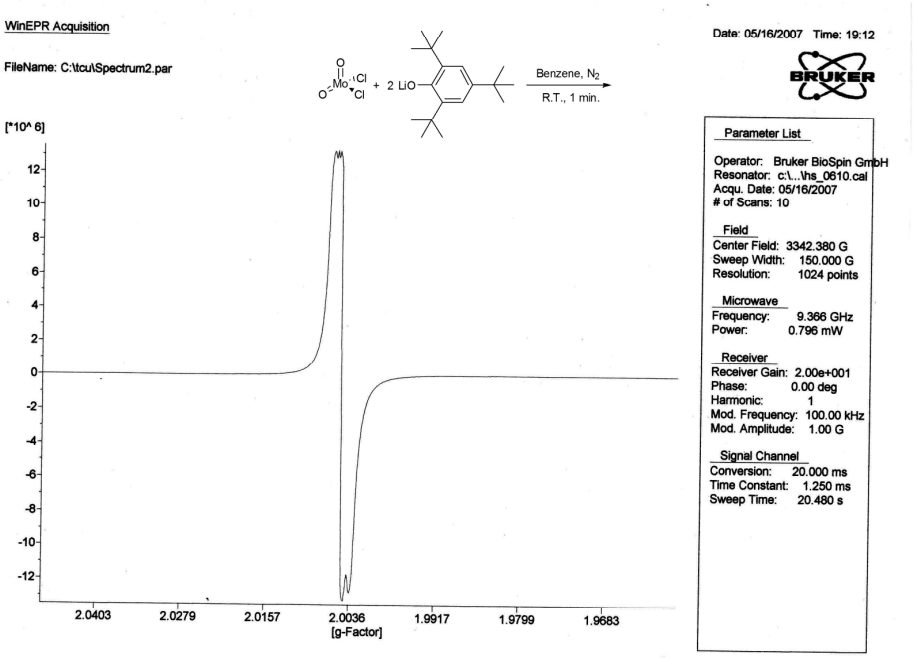

Figure A2.32. Room temperature EPR of MoO_2Cl_2 + 2 LiO-2,4,6-^{t}Bu$_3$C$_6$H$_2$ in benzene.

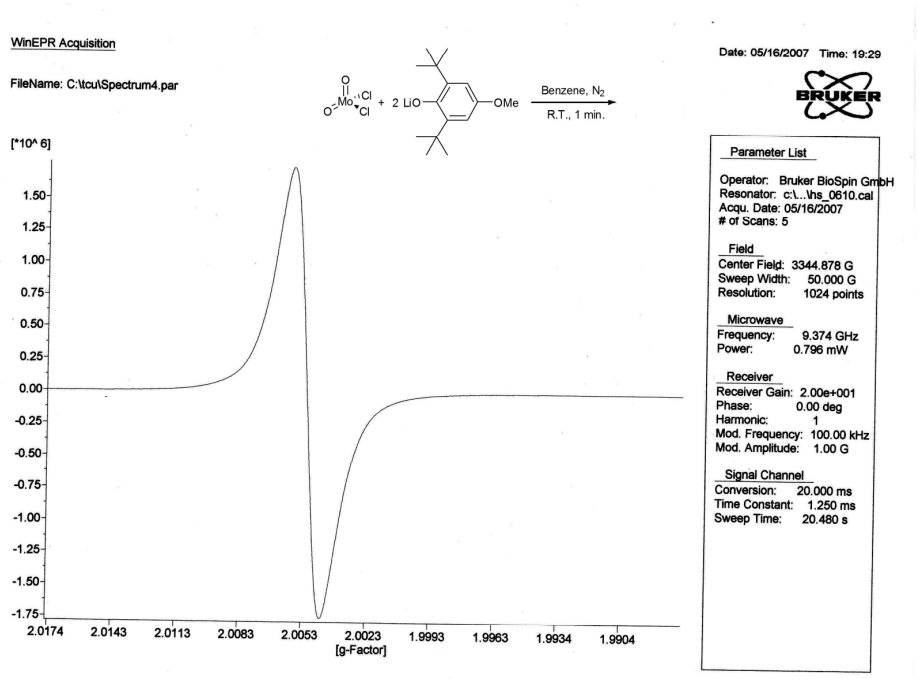

Figure A2.33. Room temperature EPR of MoO_2Cl_2 + 2 LiO-2,6-^{t}Bu$_2$-4-(OMe)C_6H_2 in benzene.

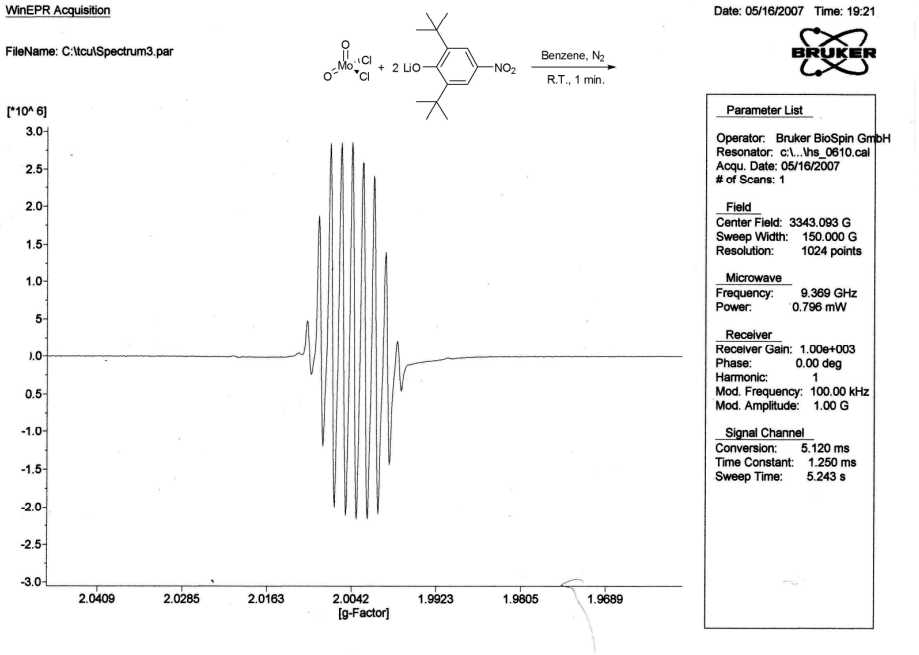

Figure A2.34. Room temperature EPR of MoO_2Cl_2 + 2 LiO-2,6-^{t}Bu$_2$-4-(NO_2)C_6H_2 in benzene.

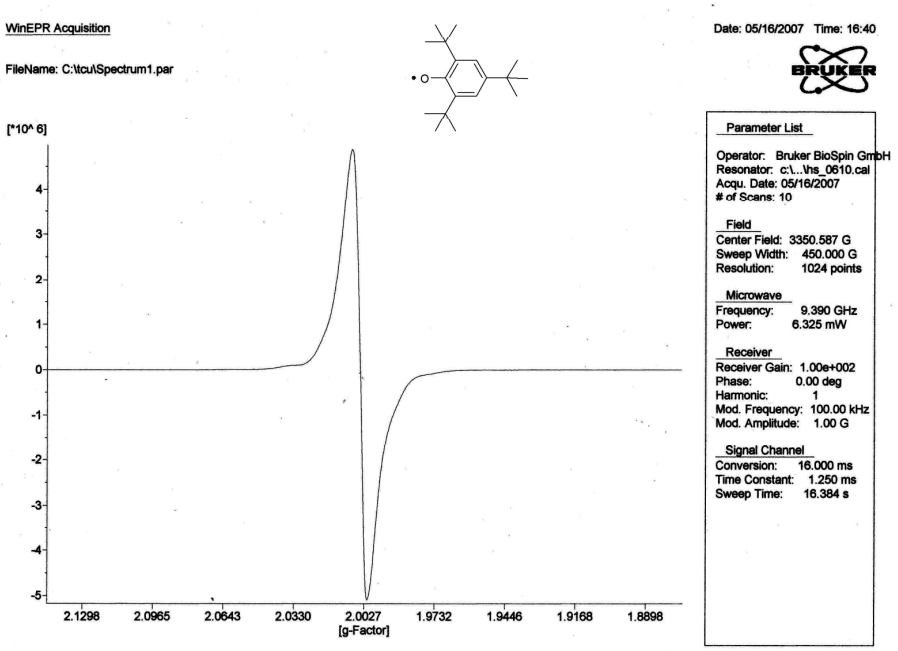

Figure A2.35. Room temperature EPR in solid state of phenoxyl radical •O-2,4,6-$^{t}Bu_3C_6H_2$.

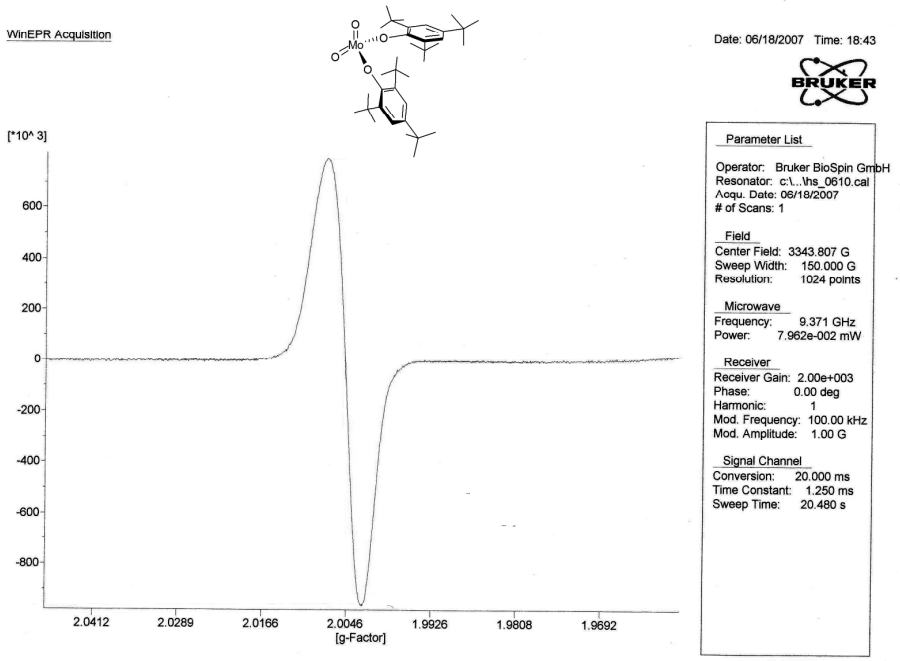

Figure A2.36. Room temperature EPR in solid state of complex MoO_2(O-2,4,6-$^{t}Bu_3C_6H_2)_2$ (**2.2j**).

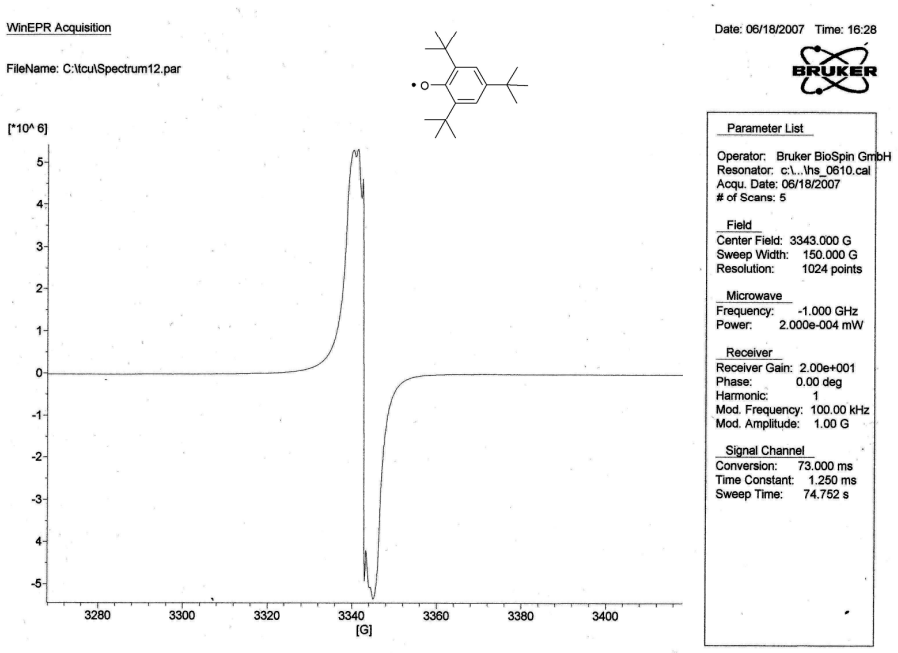

Figure A2.37. Room temperature EPR of phenoxyl radical •O-2,4,6-$^{t}Bu_3C_6H_2$ in benzene.

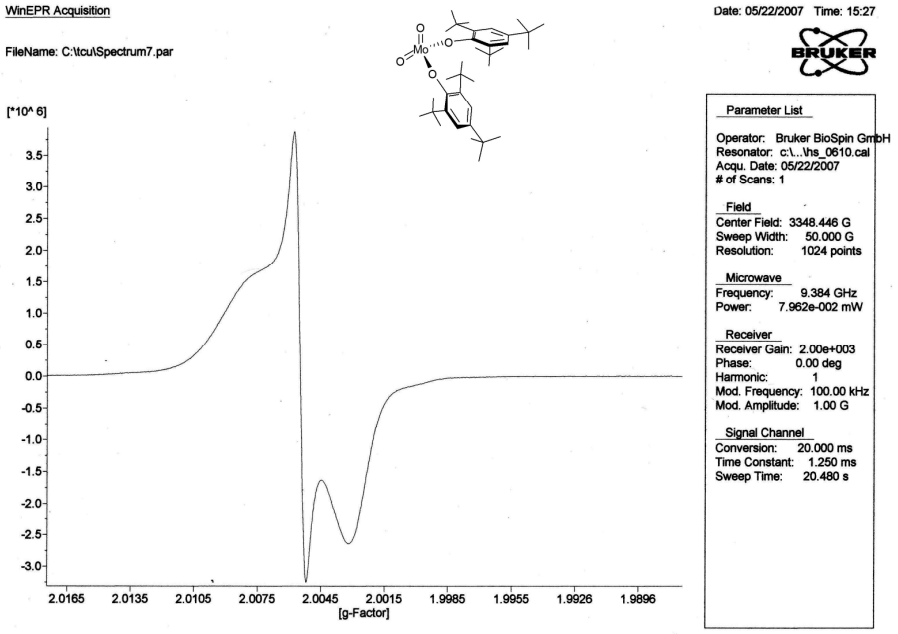

Figure A2.38. Room temperature EPR of complex MoO_2(O-2,4,6-$^{t}Bu_3C_6H_2)_2$ in benzene (**2.2j**).

X-ray structures

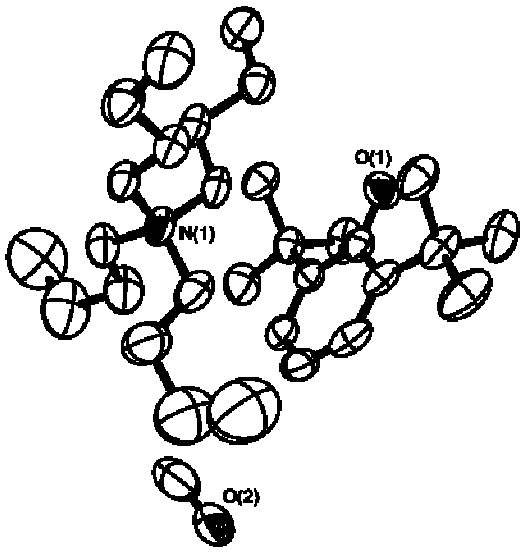

Figure A2.39. X-ray structure of $(Bu_4N)(O\text{-}2,6\text{-}^tBu_2C_6H_3)\cdot MeOH$ (**2.1m**). (50% probability). Hydrogen atoms have been omitted for clarity.

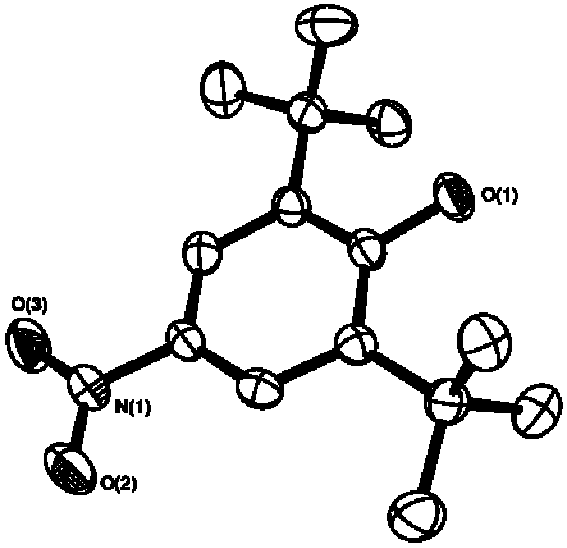

Figure A2.40. X-ray structure of $HO\text{-}2,6\text{-}^tBu_2\text{-}4\text{-}(NO_2)C_6H_2$ (50% probability). Hydrogen atoms have been omitted for clarity.

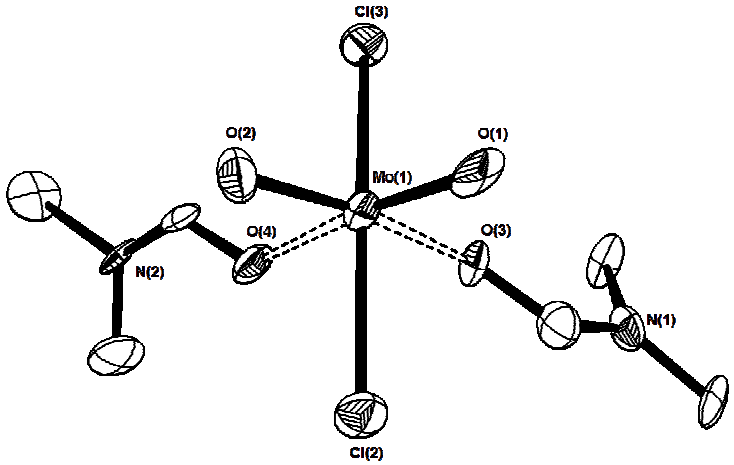

Figure A2.41. X-ray structure of $MoO_2Cl_2(DMF)_2$ (50% probability). Hydrogen atoms have been omitted for clarity.

Appendix for Chapter 3

^{1}H and ^{13}C NMR Spectra

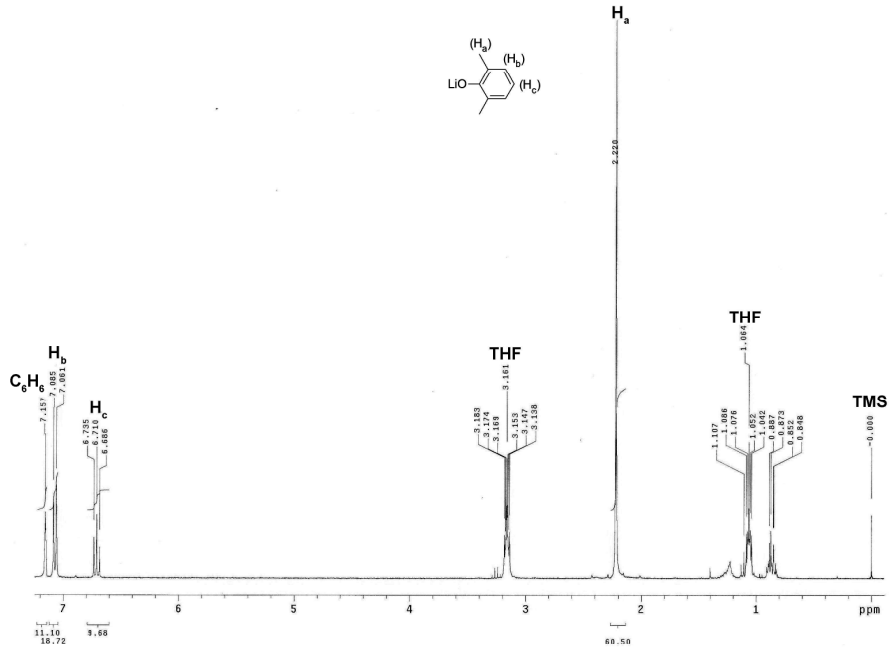

Figure A3.1. ^{1}H NMR of LiO-2,6-$Me_2C_6H_3$ (**3.1a**) in C_6D_6

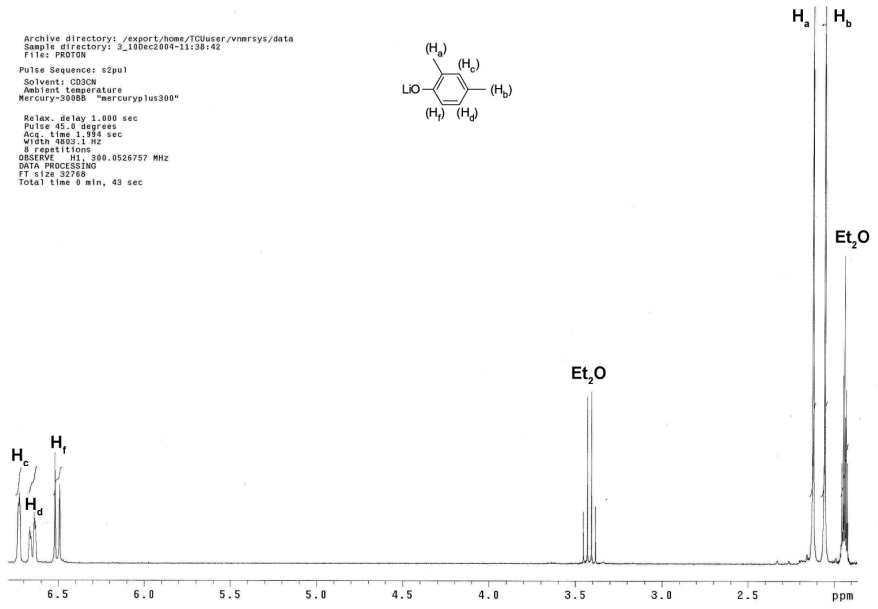

Figure A3.2. ^{1}H NMR of LiO-2,4-$Me_2C_6H_3$ (**3.1b**) in CD_3CN

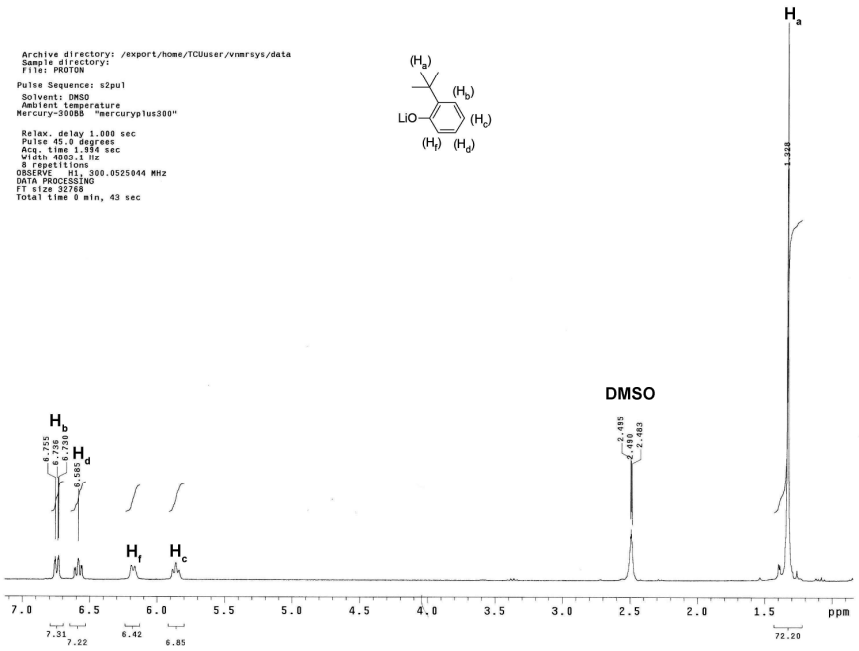

Figure A3.3. ^{1}H NMR of LiO-2-^{t}BuC$_6$H$_4$ (**3.1c**) in DMSO-d$_6$

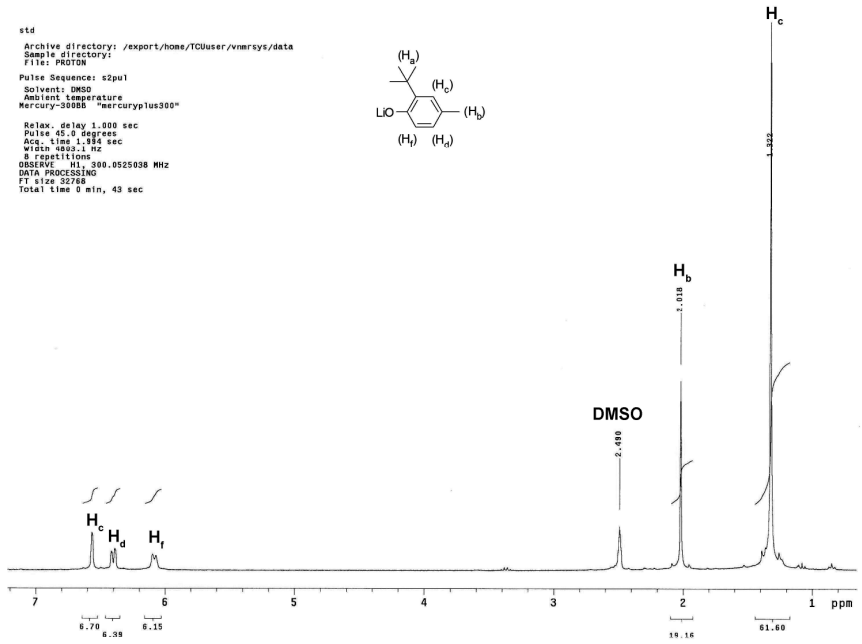

Figure A3.4. ^{1}H NMR of LiO-2-^{t}Bu-4-MeC$_6$H$_3$ (**3.1d**) in DMSO-d$_6$

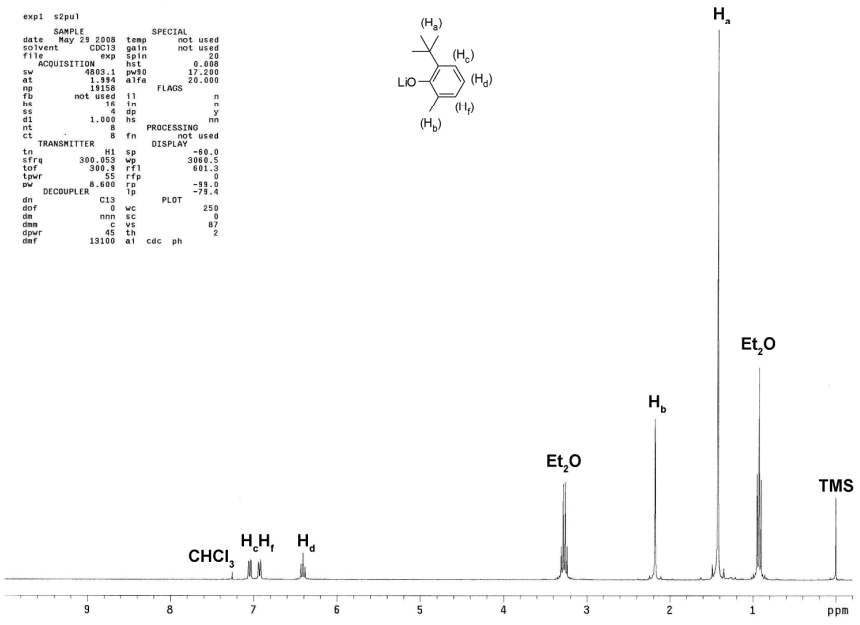

Figure A3.5. ^{1}H NMR of LiO-2-^{t}Bu-6-MeC_6H_3 (**3.1e**) in $CDCl_3$

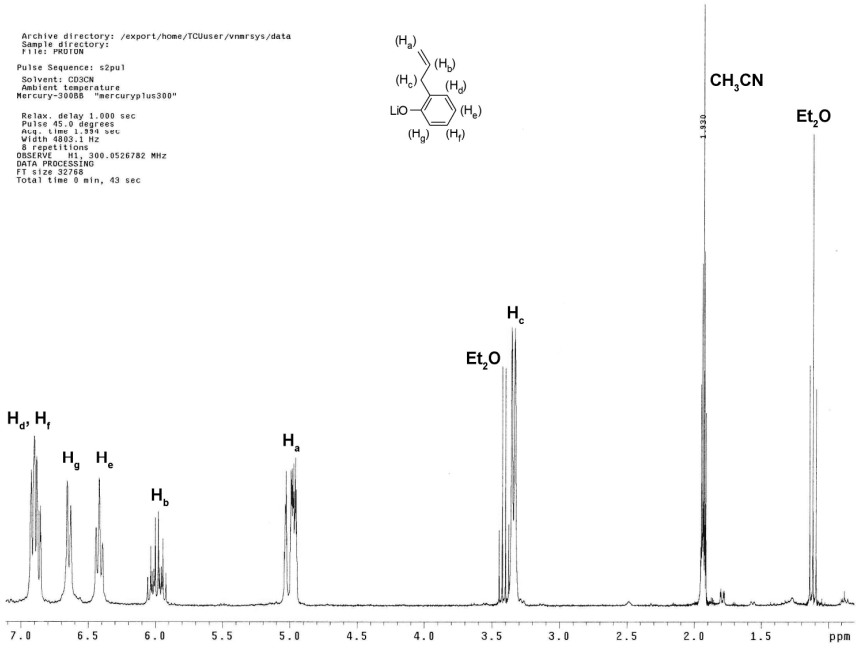

Figure A3.6. ^{1}H NMR of LiO-2-(allyl)C_6H_4 (**3.1f**) in CD_3CN

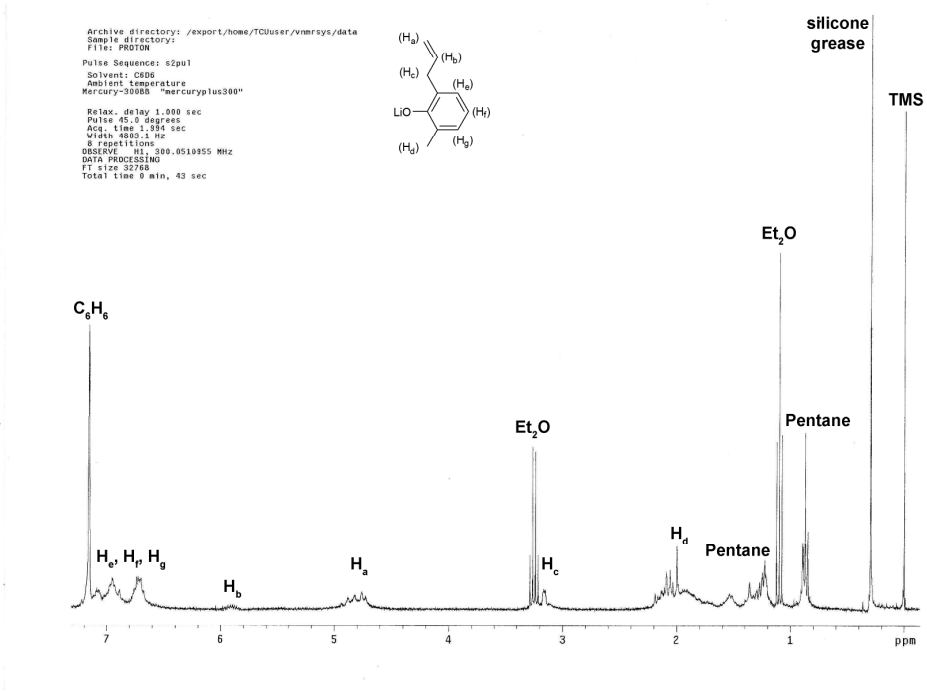

Figure A3.7. ^{1}H NMR of LiO-2-(allyl)-6-MeC_6H_3 (**3.1g**) in C_6D_6

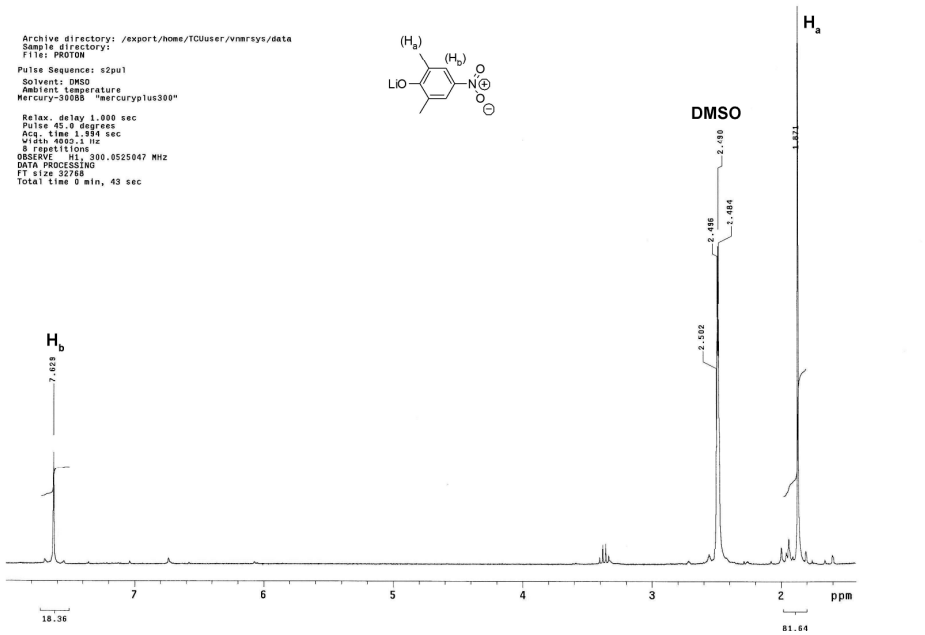

Figure A3.8. ^{1}H NMR of LiO-2,6-Me_2-4-$(NO_2)C_6H_2$ (**3.1k**) in DMSO-d_6

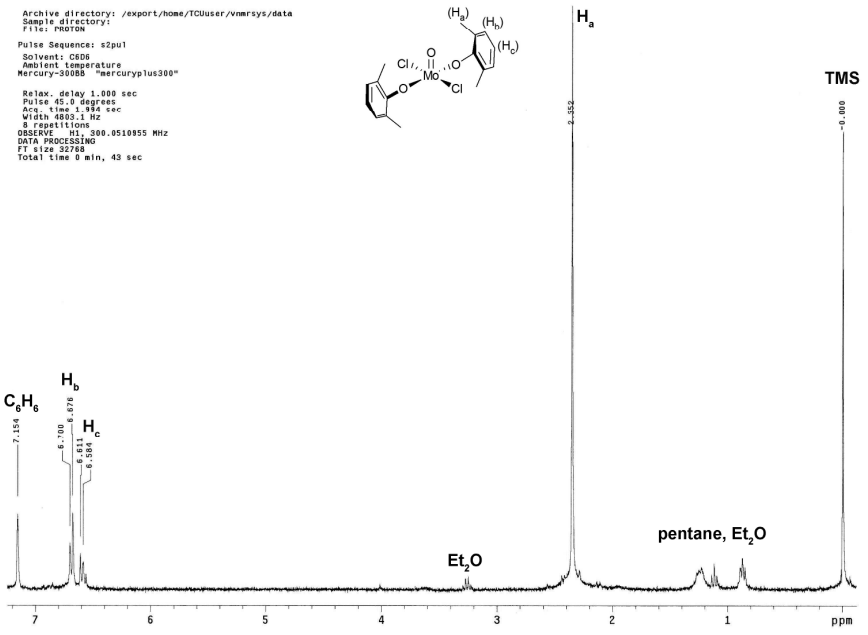

Figure A3.9. ^{1}H NMR of MoO(O-2,6-$Me_2C_6H_3)_2Cl_2$ (**3.2a**) in C_6D_6

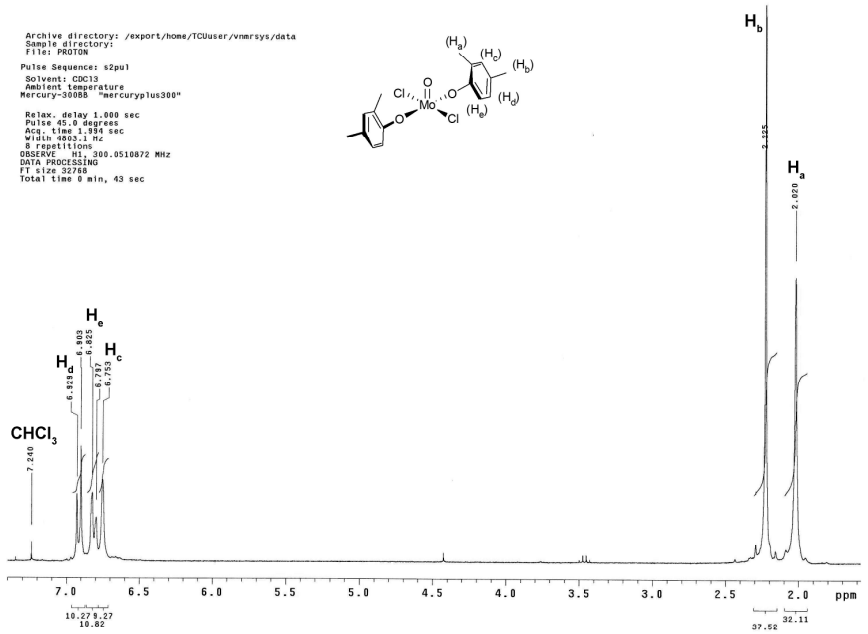

Figure A3.10. ^{1}H NMR of MoO(O-2,4-$Me_2C_6H_3)_2Cl_2$ (**3.2b**) in $CDCl_3$

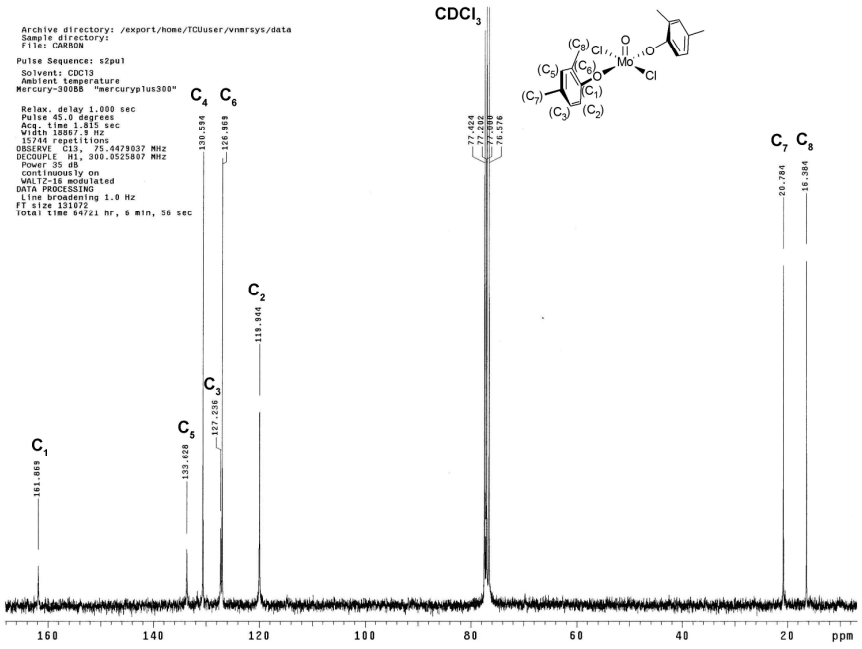

Figure A3.11. ^{13}C NMR of $MoO(O\text{-}2,4\text{-}Me_2C_6H_3)_2Cl_2$ (**3.2b**) in $CDCl_3$

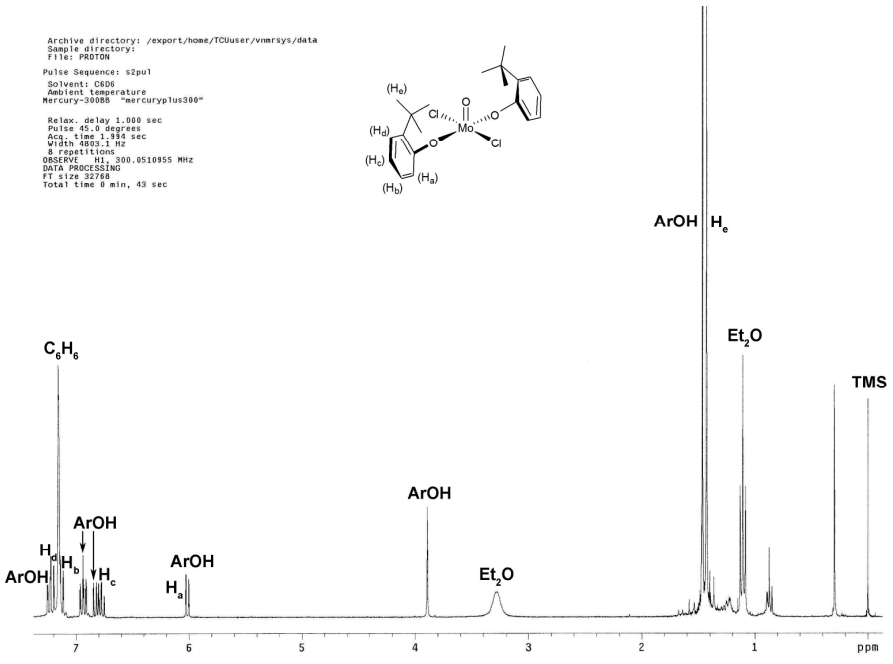

Figure A3.12. ^{1}H NMR of $MoO(O\text{-}2\text{-}^{t}BuC_6H_4)_2Cl_2$ (**3.2c**) in C_6D_6

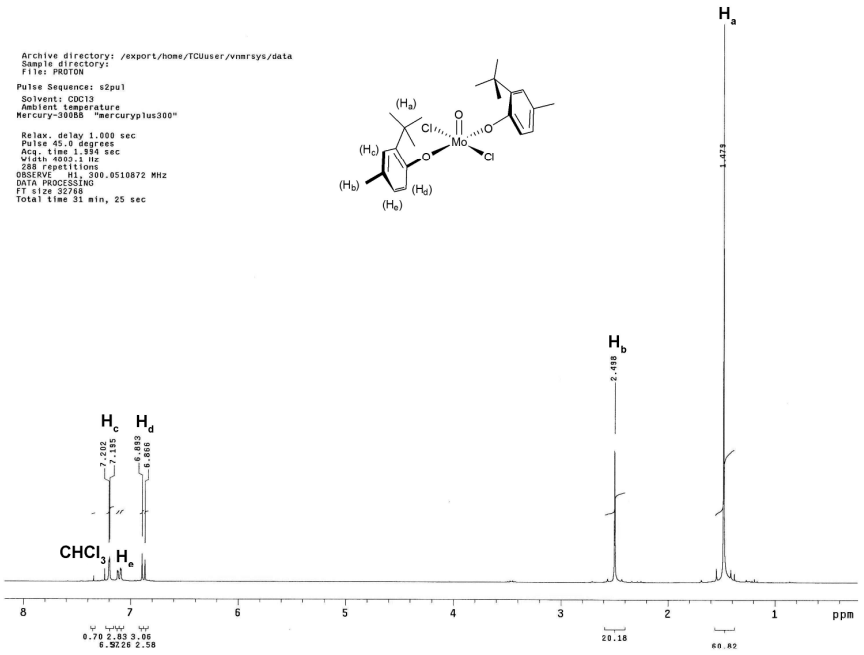

Figure A3.13. ^{1}H NMR of MoO(O-2-^{t}Bu-4-MeC$_6$H$_3$)$_2$Cl$_2$ (**3.2d**) in CDCl$_3$

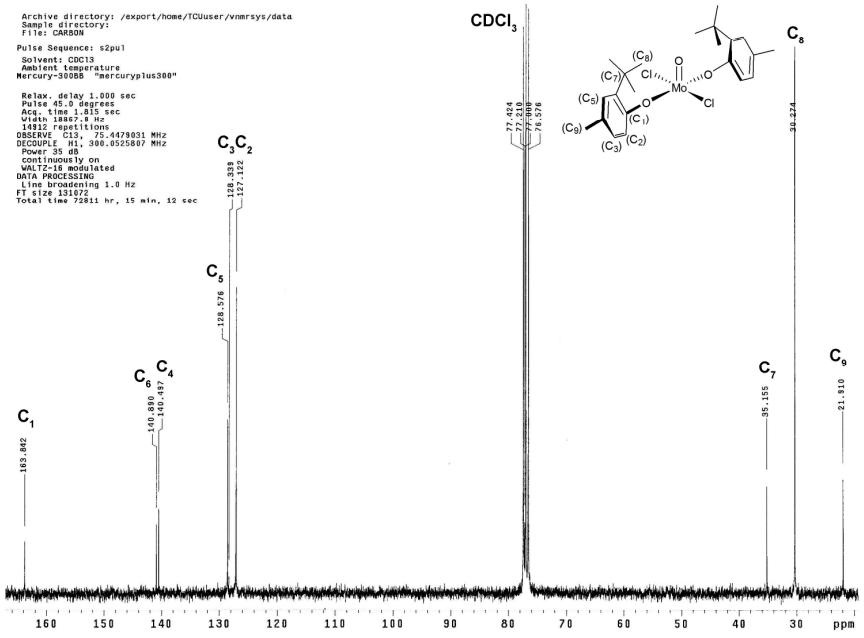

Figure A3.14. ^{13}C NMR of MoO(O-2-^{t}Bu-4-MeC$_6$H$_3$)$_2$Cl$_2$ (**3.2d**) in CDCl$_3$

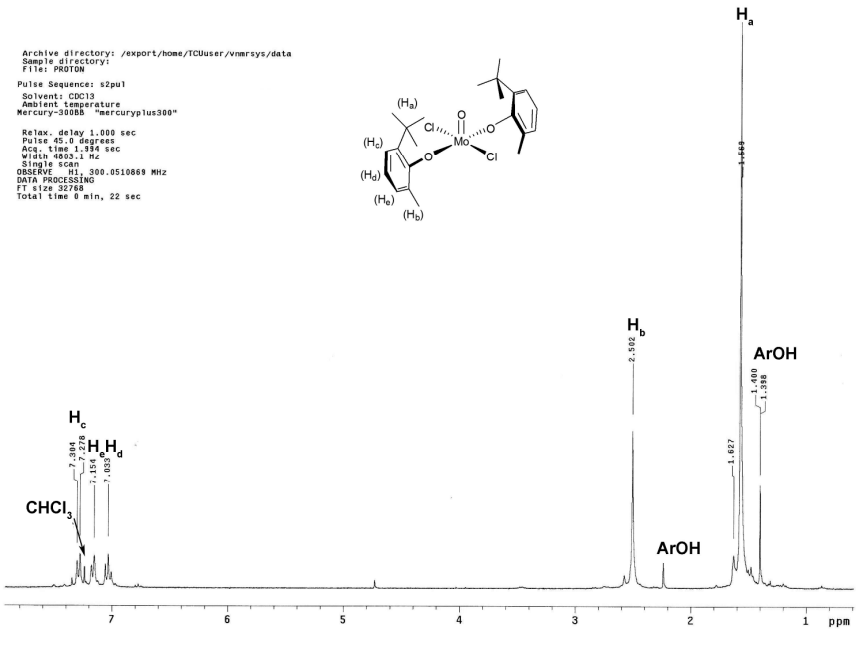

Figure A3.15. ^{1}H NMR of MoO(O-2-^{t}Bu-6-MeC_6H_3)$_2Cl_2$ (**3.2e**) in $CDCl_3$

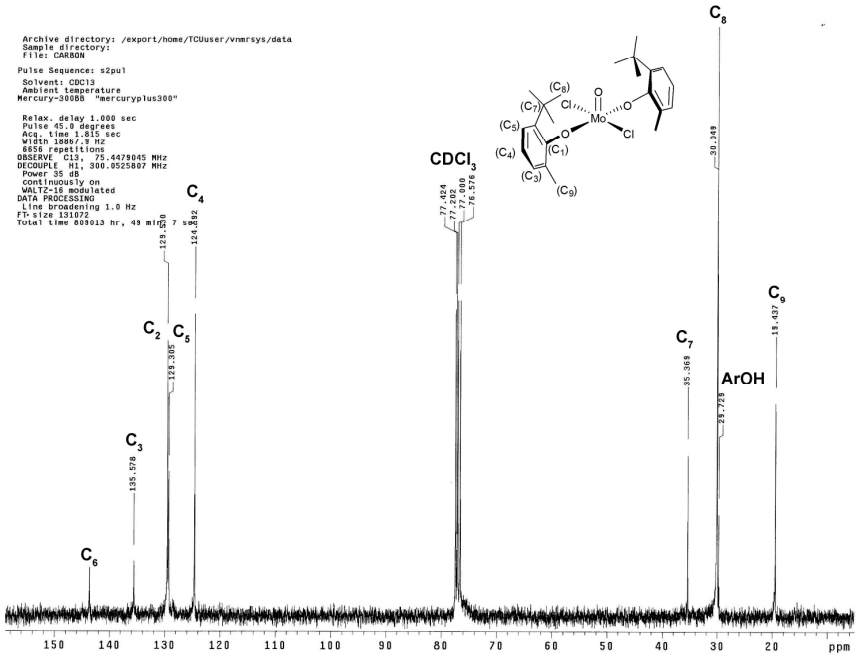

Figure A3.16. ^{13}C NMR of MoO(O-2-^{t}Bu-6-MeC_6H_3)$_2Cl_2$ (**3.2e**) in $CDCl_3$

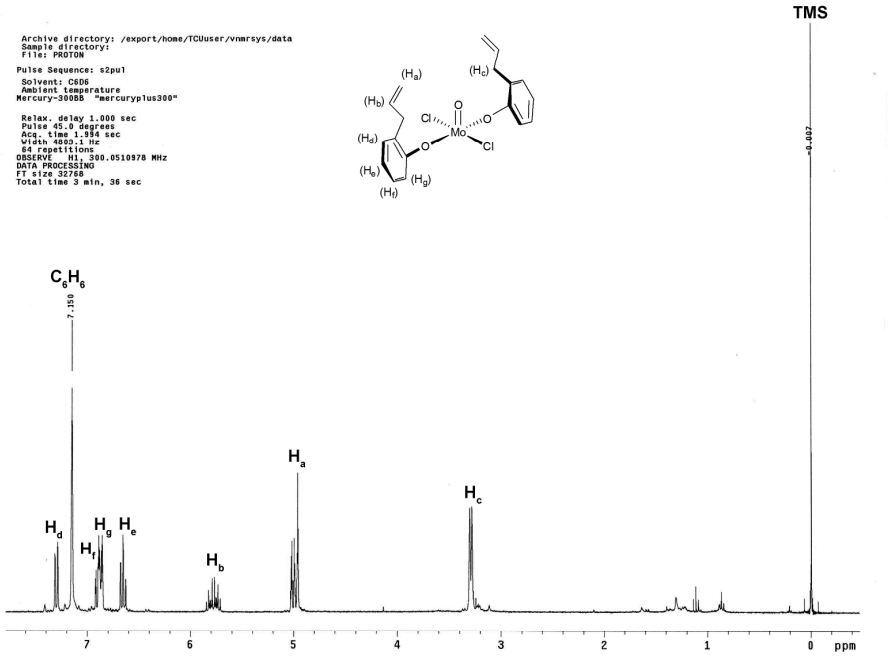

Figure A3.17. ^{1}H NMR of MoO(O-2-(allyl)$C_6H_4)_2Cl_2$ (**3.2f**) in C_6D_6

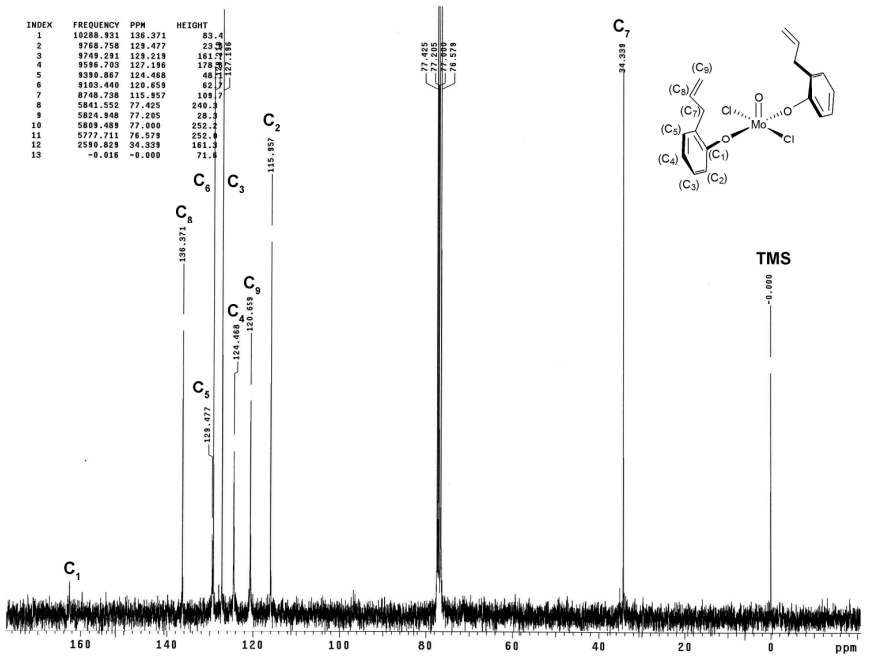

Figure A3.18. ^{13}C NMR of MoO(O-2-(allyl)$C_6H_4)_2Cl_2$ (**3.2f**) in C_6D_6

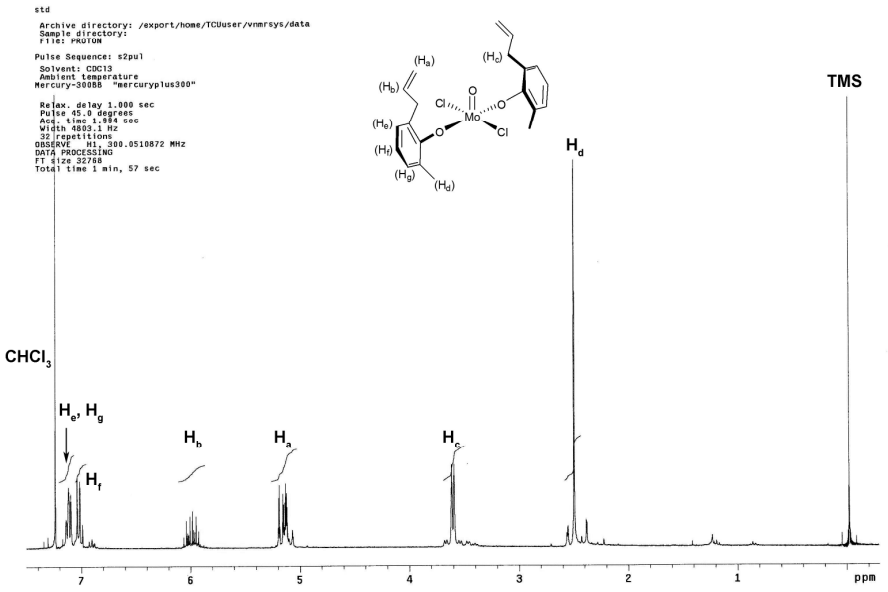

Figure A3.19. ^{1}H NMR of MoO(O-2-(allyl)-6-MeC_6H_3)$_2Cl_2$ (**3.2g**) in C_6D_6

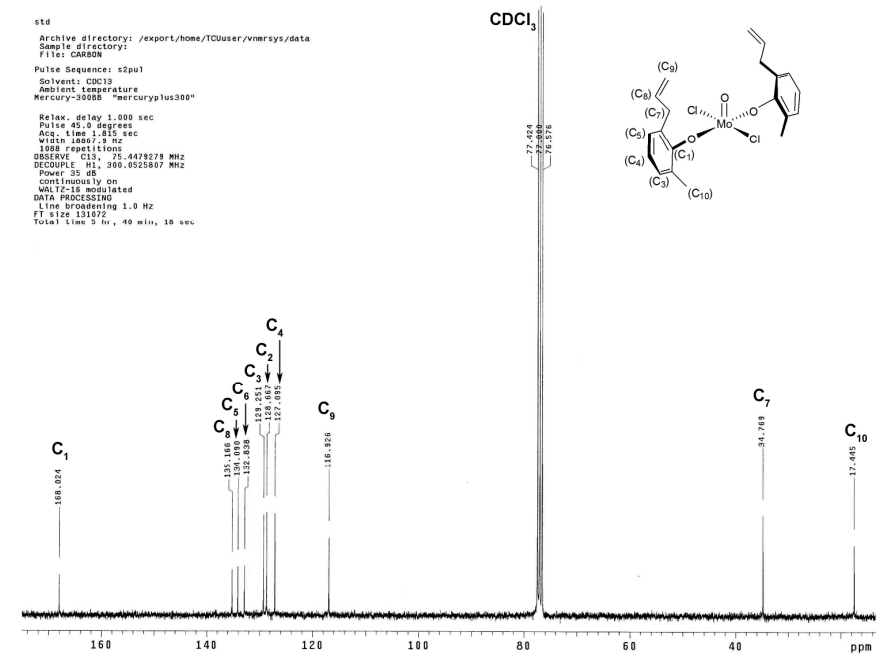

Figure A3.20. ^{13}C NMR of MoO(O-2-(allyl)-6-MeC_6H_3)$_2Cl_2$ (**3.2g**) in C_6D_6

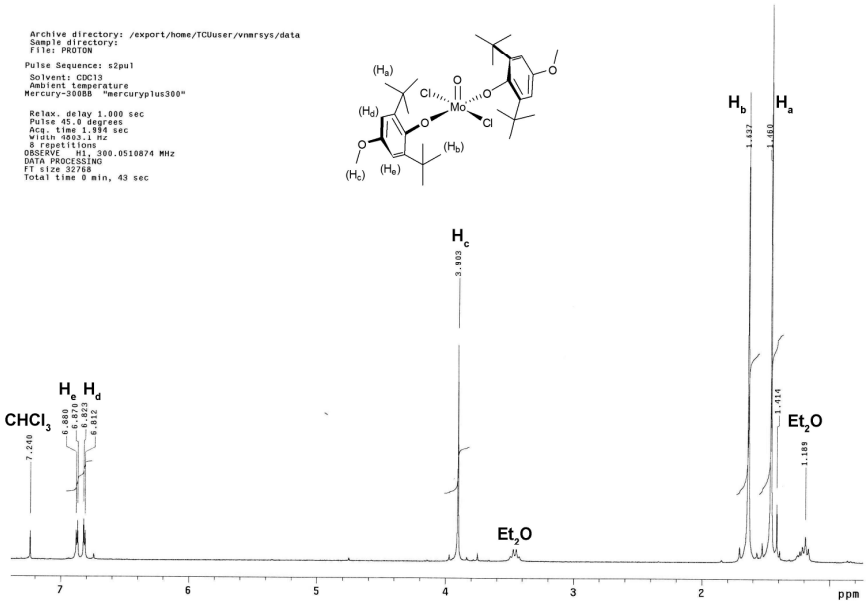

Figure A3.21. ^{1}H NMR of MoO(O-2,6-^{t}Bu$_2$-4-(OMe)C$_6$H$_2$)$_2$Cl$_2$ (**3.2j**) in CDCl$_3$

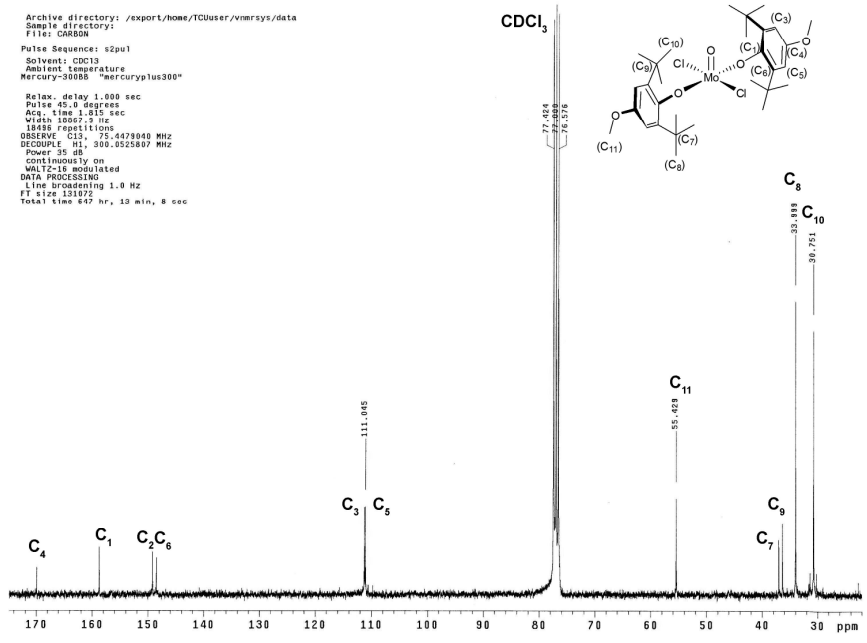

Figure A3.22. ^{13}C NMR of MoO(O-2,6-^{t}Bu$_2$-4-(OMe)C$_6$H$_2$)$_2$Cl$_2$ (**3.2j**) in CDCl$_3$

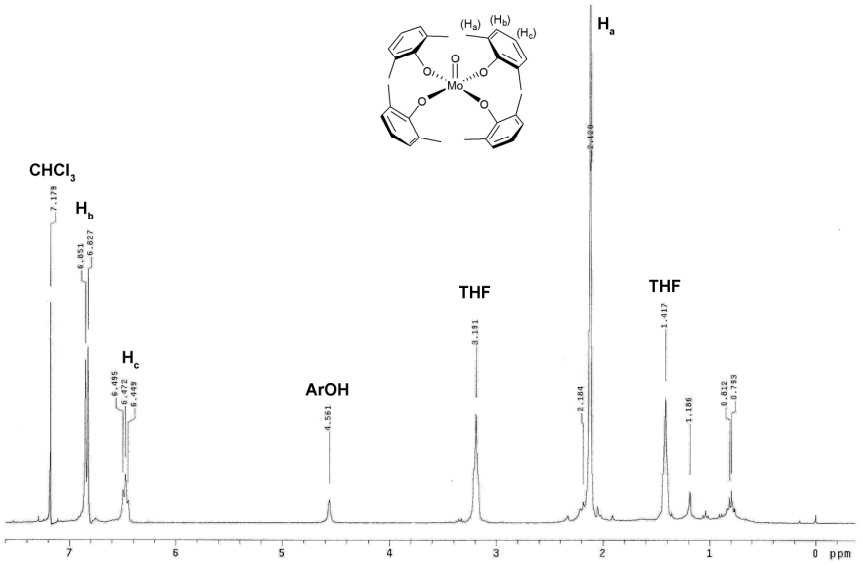

Figure A3.23. ^{1}H NMR of $MoO(O\text{-}2,4\text{-}Me_2C_6H_3)_4$ (**3.4a**) in $CDCl_3$

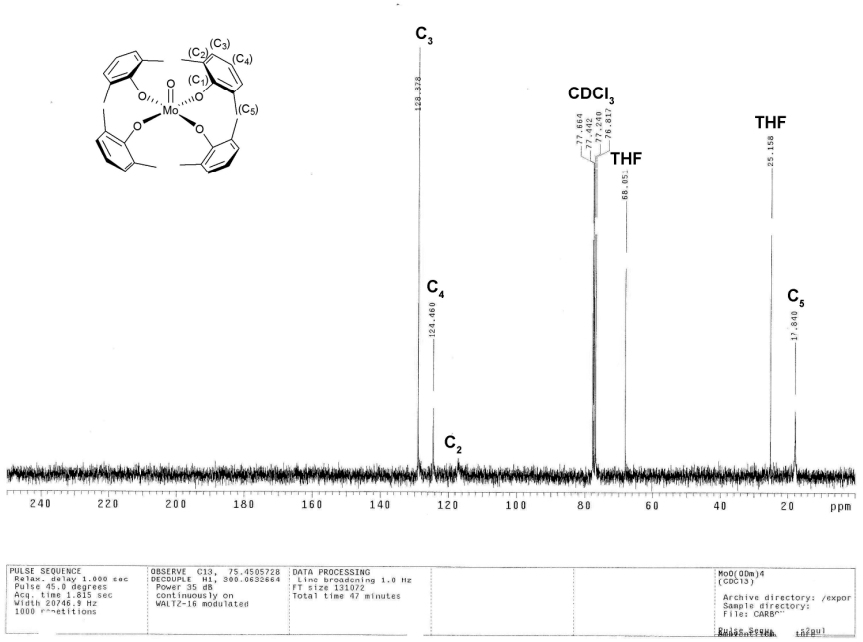

Figure A3.24. ^{13}C NMR of $MoO(O\text{-}2,4\text{-}Me_2C_6H_3)_4$ (**3.4a**) in $CDCl_3$

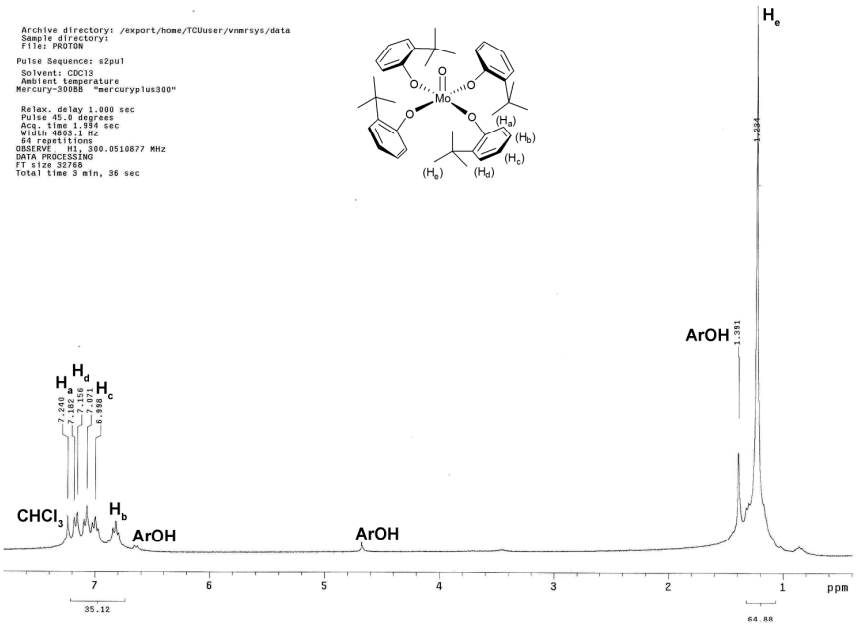

Figure A3.25. ^{1}H NMR of MoO(O-2-^{t}BuC$_6$H$_4$)$_4$ (**3.4c**) in CDCl$_3$

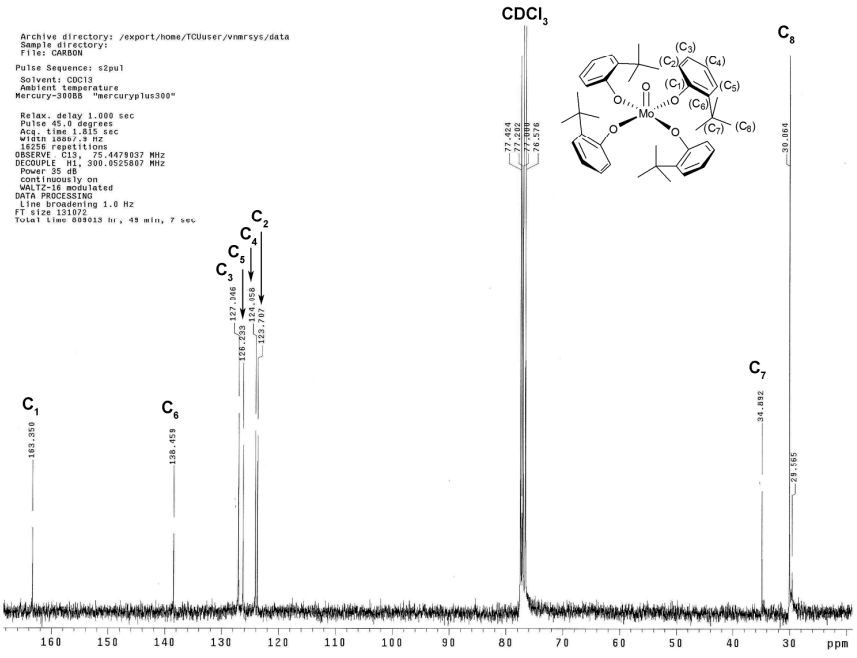

Figure A3.26. ^{13}C NMR of MoO(O-2-^{t}BuC$_6$H$_4$)$_4$ (**3.4c**) in CDCl$_3$

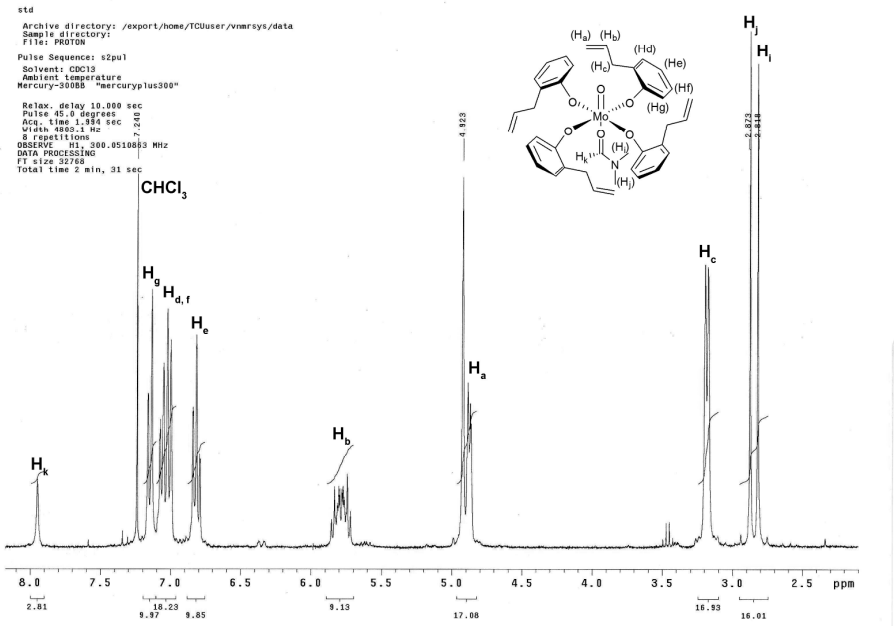

Figure A3.27. ^{1}H NMR of MoO(O-2-(allyl)C_6H_4)$_4$(DMF) (**3.5f**) in $CDCl_3$

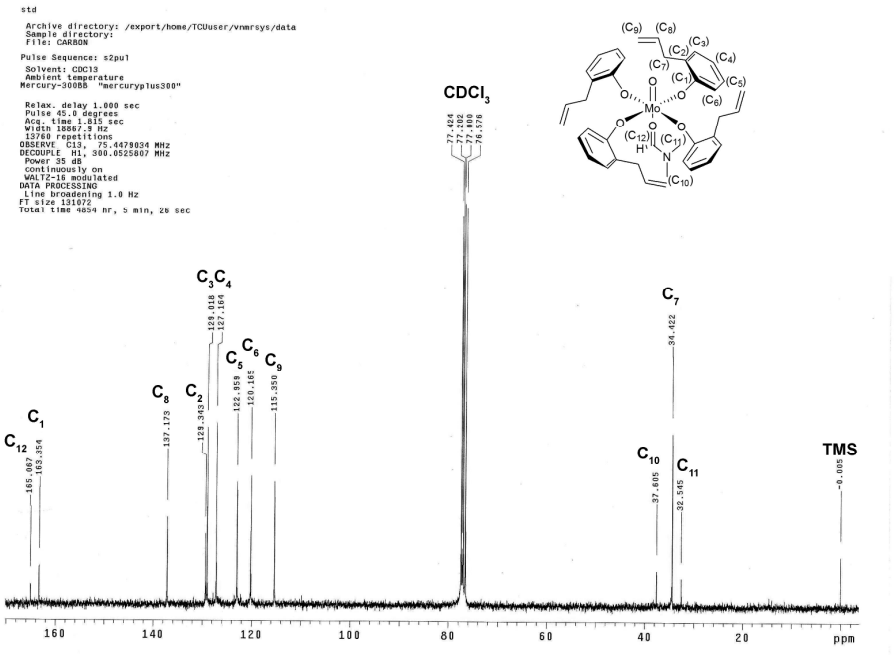

Figure A3.28. ^{13}C NMR of MoO(O-2-(allyl)C_6H_4)$_4$(DMF) (**3.5f**) in $CDCl_3$

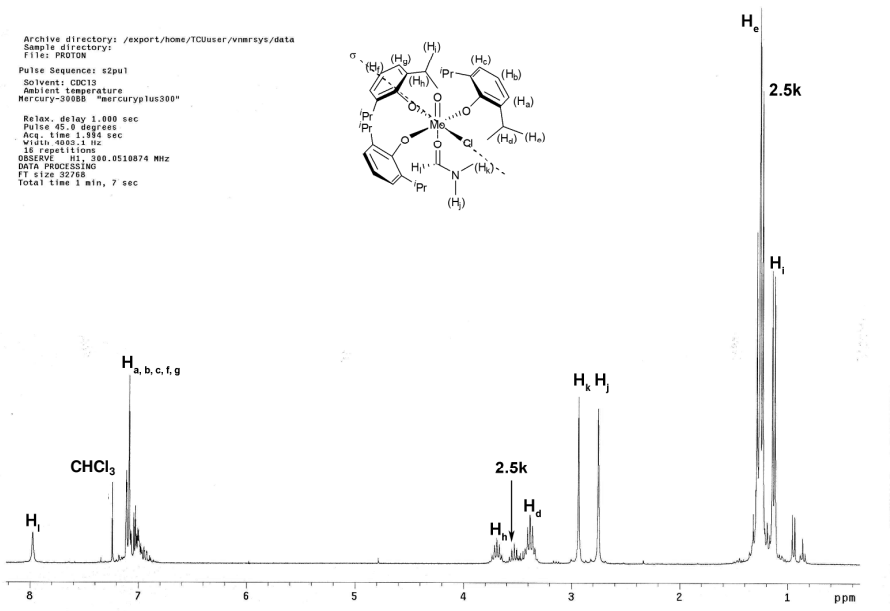

Figure A3.29. ^{1}H NMR of MoO(O-2,6-^{i}Pr$_2$C$_6$H$_3$)$_3$(DMF)Cl (**3.5g**) in $CDCl_3$

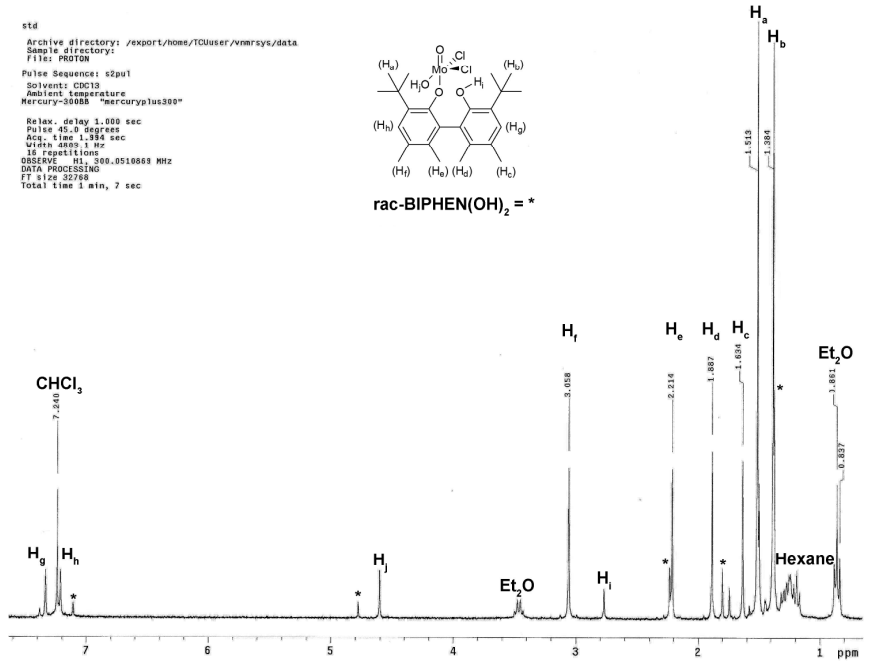

Figure A3.30. ^{1}H NMR of Mo(O)(OH)[rac-BIPHEN(O)(OH)]Cl_2 (**3.6**) in $CDCl_3$

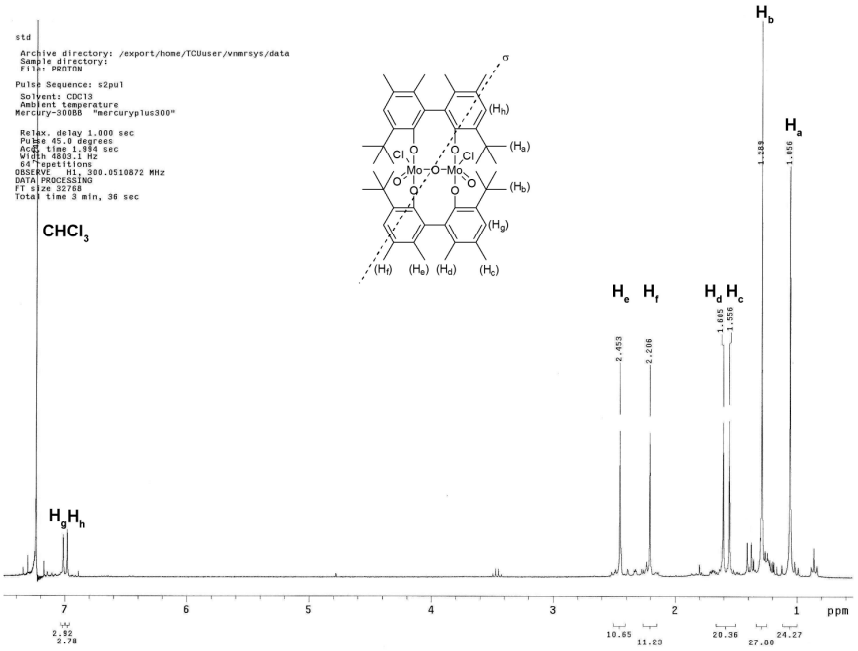

Figure A3.31. ^{1}H NMR of [Mo(O)Cl]$_2${[μ-rac-BIPHEN(O)$_2$-κ^2*O:O'*]$_2$(μ-O)} (**3.7**) in $CDCl_3$

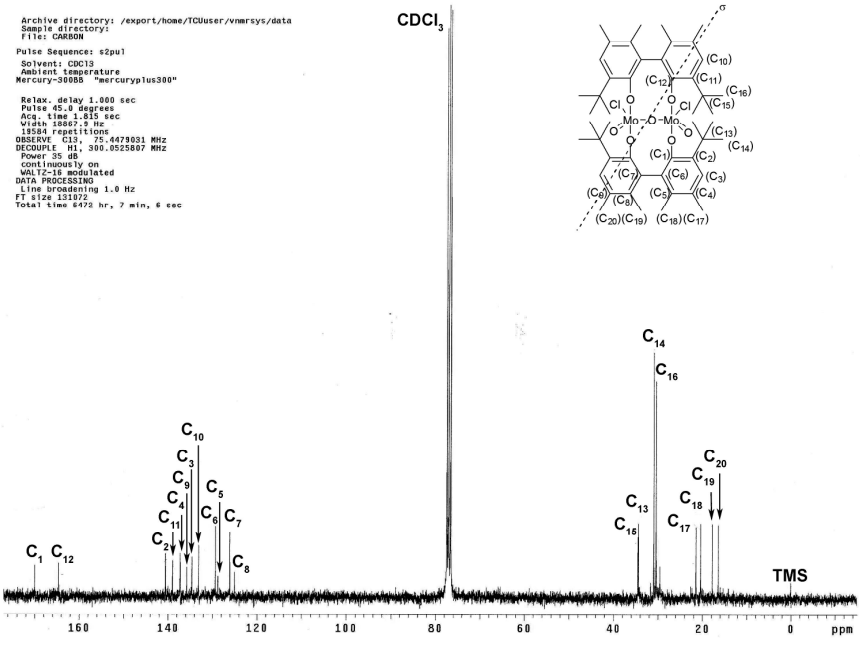

Figure A3.32. ^{13}C NMR of [Mo(O)Cl]$_2${[μ-rac-BIPHEN(O)$_2$-κ^2*O:O'*]$_2$(μ-O)} (**3.7**) in $CDCl_3$

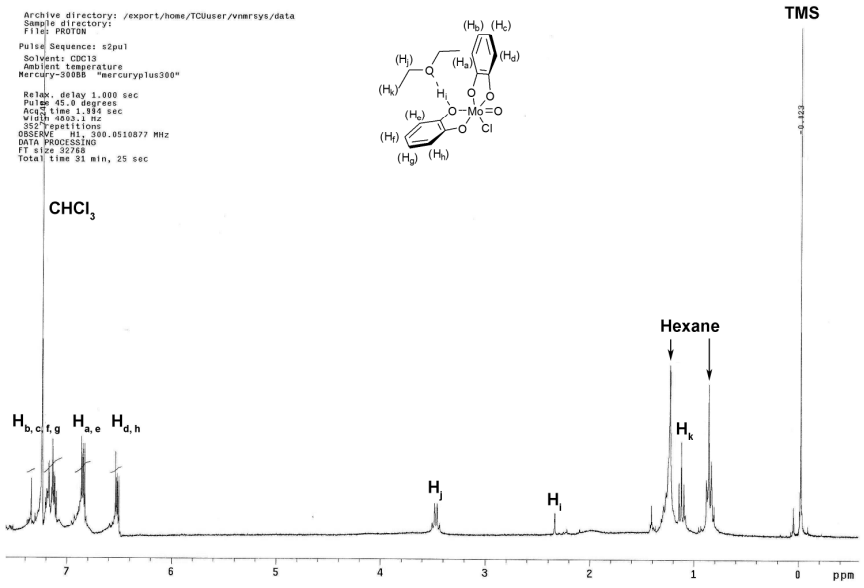

Figure A3.33. ^{1}H NMR of Mo(O)Cl($C_6H_4O_2$-κ^2O,O')(C_6H_4O(OH)-κ^2O,O')·Et_2O (**3.8**) in $CDCl_3$

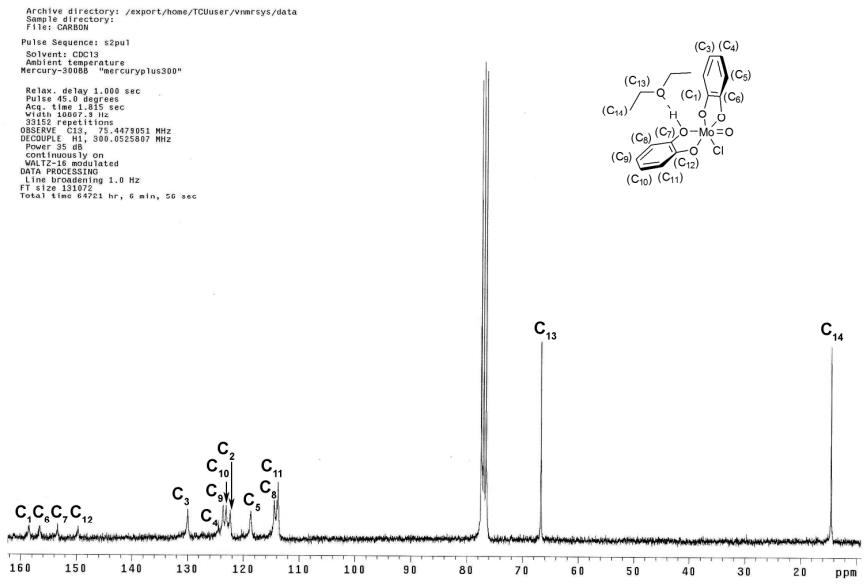

Figure A3.34. ^{13}C NMR of Mo(O)Cl($C_6H_4O_2$-κ^2O,O')(C_6H_4O(OH)-κ^2O,O')·Et_2O (**3.8**) in $CDCl_3$

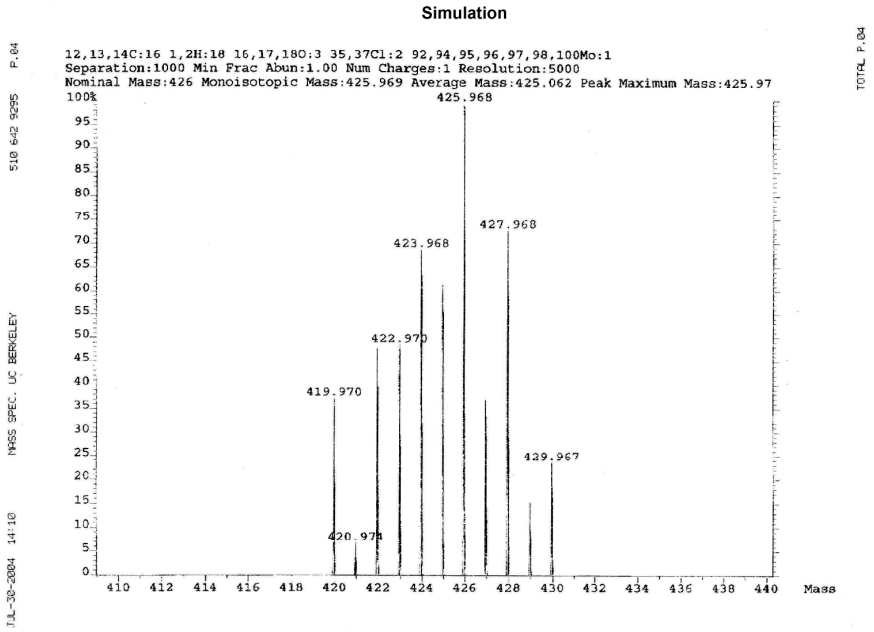

Figure A3.35. Simulated low resolution mass spectrum of $MoO(O\text{-}2,6\text{-}Me_2C_6H_3)_2Cl_2$ (**3.2a**), M.W. = 425.16 g/mol

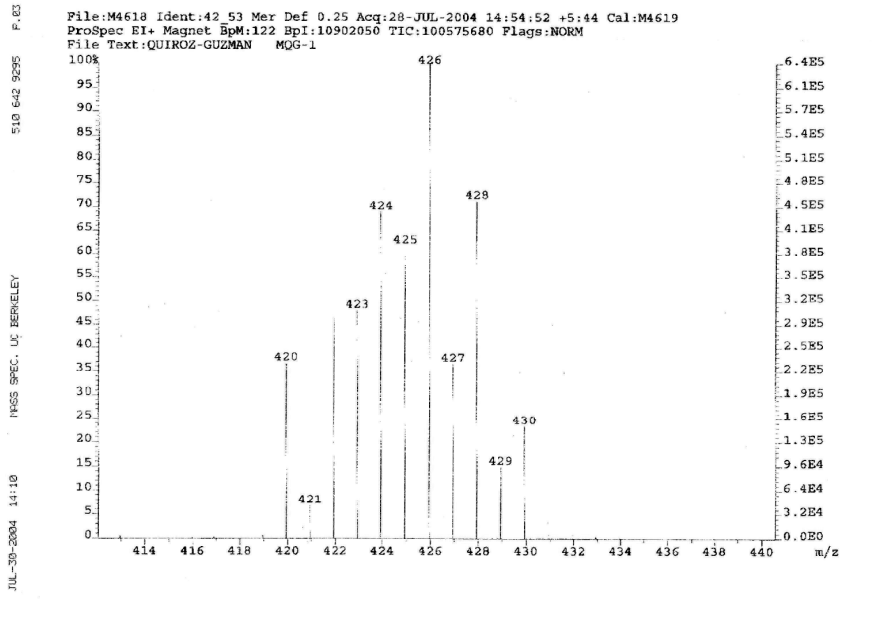

Figure A3.36. Low resolution mass spectrum (EI) of $MoO(O\text{-}2,6\text{-}Me_2C_6H_3)_2Cl_2$ (**3.2a**), M.W. = 425.16 g/mol

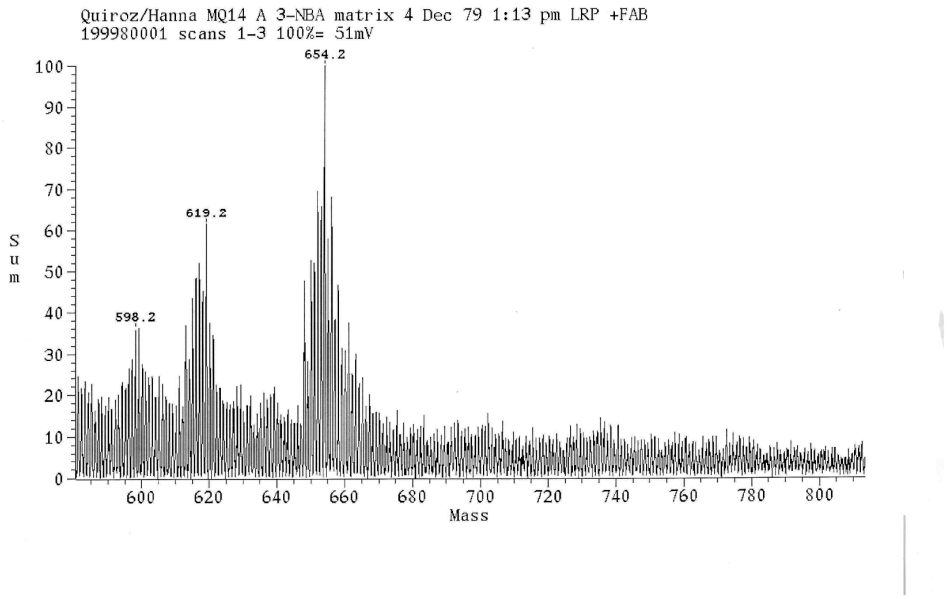

Figure A3.37. Low resolution mass spectrum (FAB) of MoO(O-2,6-$^{t}Bu_2$-4-(OMe)$C_6H_2)_2Cl_2$ (**3.2j**), M.W. = 653.53 g/mol

Appendix for Chapter 4

^{1}H and ^{13}C NMR spectra.

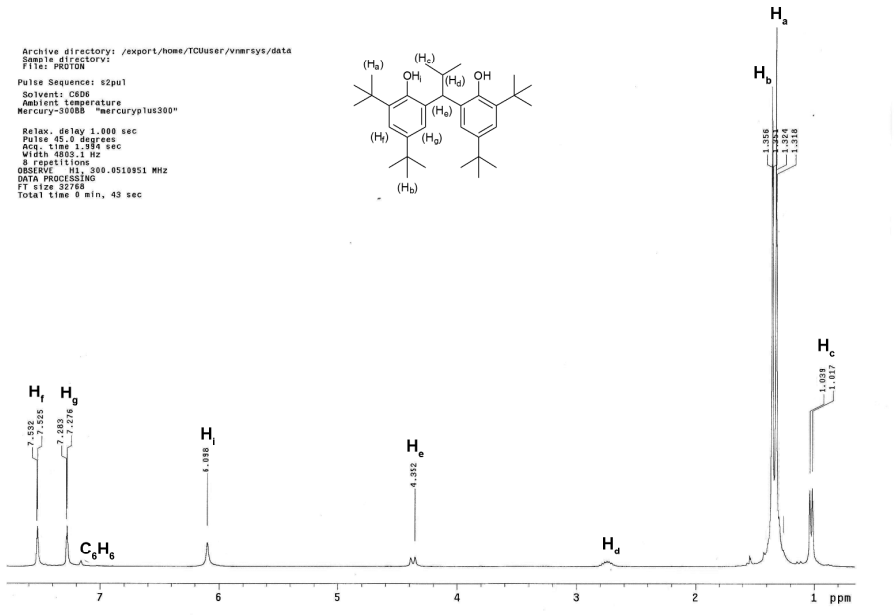

Figure A4.1 ^{1}H NMR of 2,2'-CH(^{i}Pr)(4,6-$^{t}Bu_2C_6H_2OH)_2$ (**4.1b**) in C_6D_6

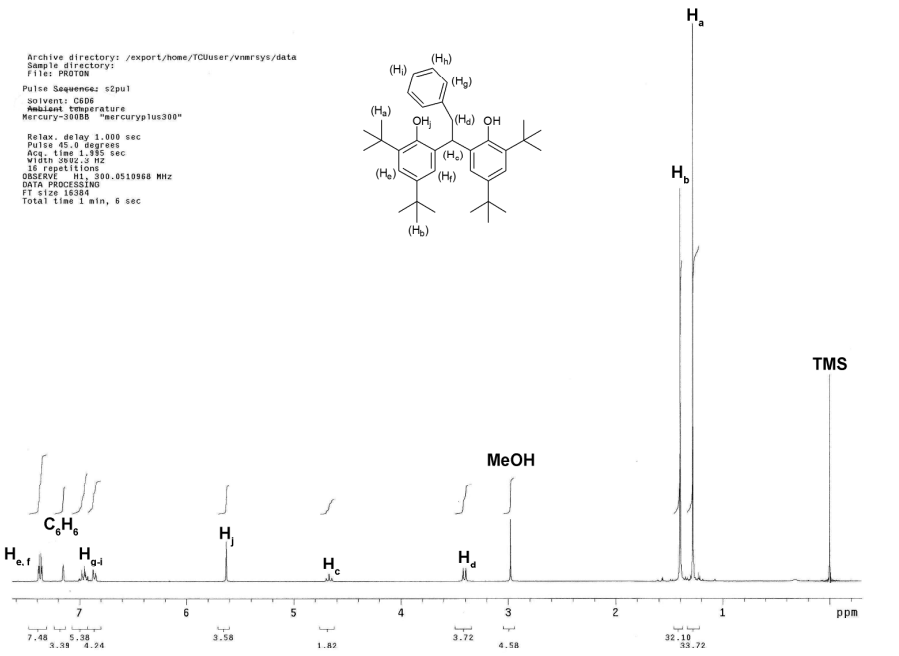

Figure A4.2 ^{1}H NMR of 2,2'-CH(Bn)(4,6-$^{t}Bu_2C_6H_2OH)_2$ (**4.1c**) in C_6D_6

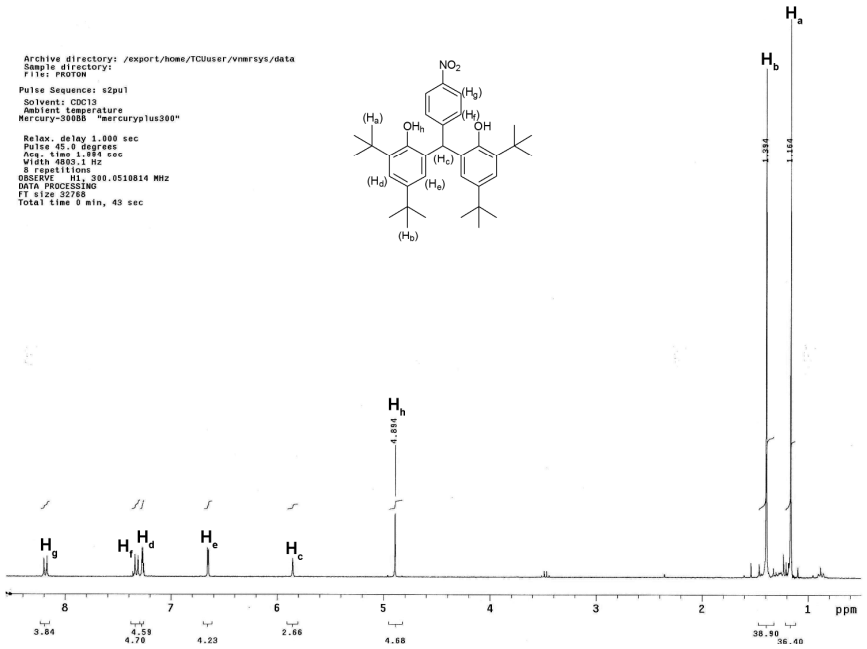

Figure A4.3 ^{1}H NMR of 2,2'-CH[4-(NO_2)C_6H_4](4,6-^{t}Bu$_2C_6H_2OH)_2$ (**4.1d**) in $CDCl_3$

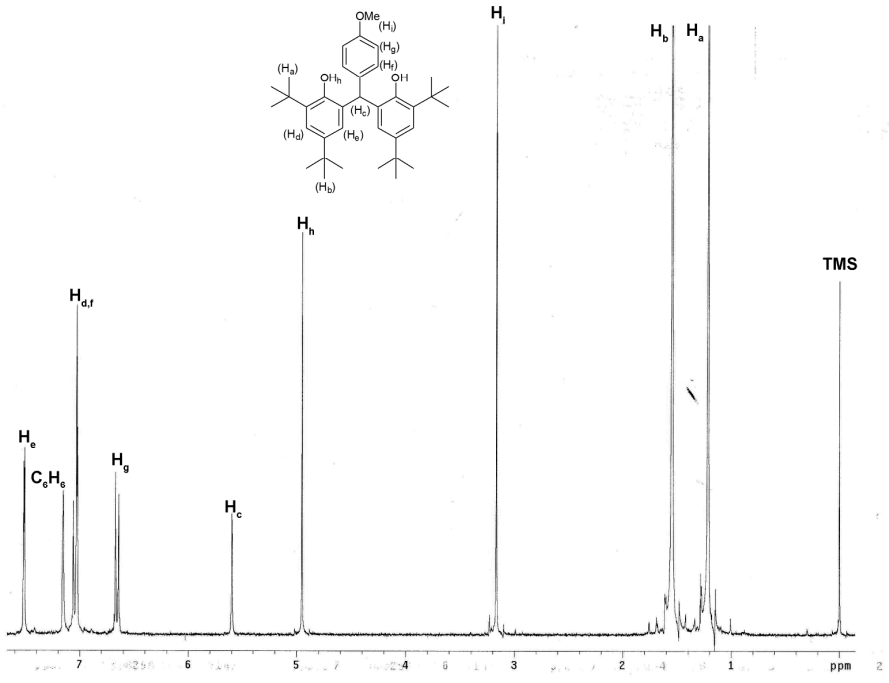

Figure A4.4 ^{1}H NMR of 2,2'-CH[4-(OMe)C_6H_4](4,6-^{t}Bu$_2C_6H_2OH)_2$ (**4.1e**) in C_6D_6

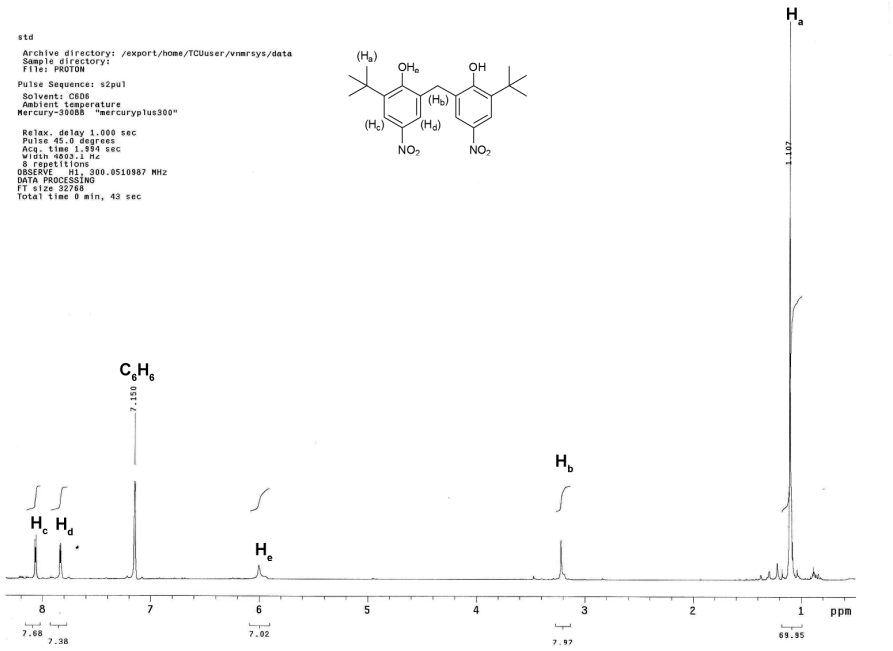

Figure A4.5 ^{1}H NMR of 2,2'-CH_2[4-(NO_2)-6-^{t}Bu$_2$$C_6H_2$OH]$_2$ (**4.1f**) in C_6D_6

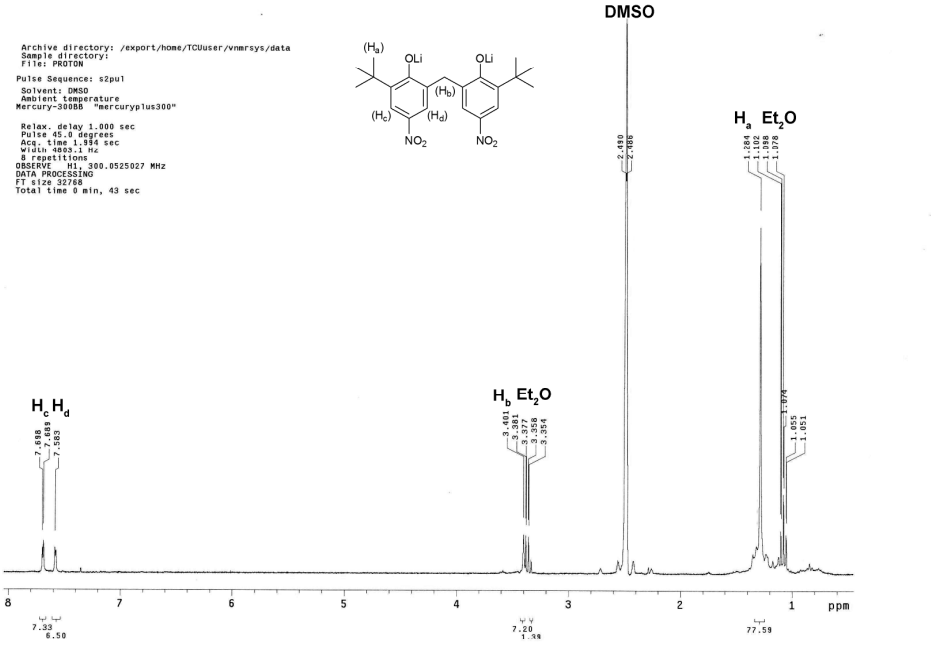

Figure A4.6 ^{1}H NMR of 2,2'-CH_2[LiO-4-(NO_2)-6-^{t}Bu$_2$$C_6H_2$]$_2$ (**4.2f**) in DMSO-d_6

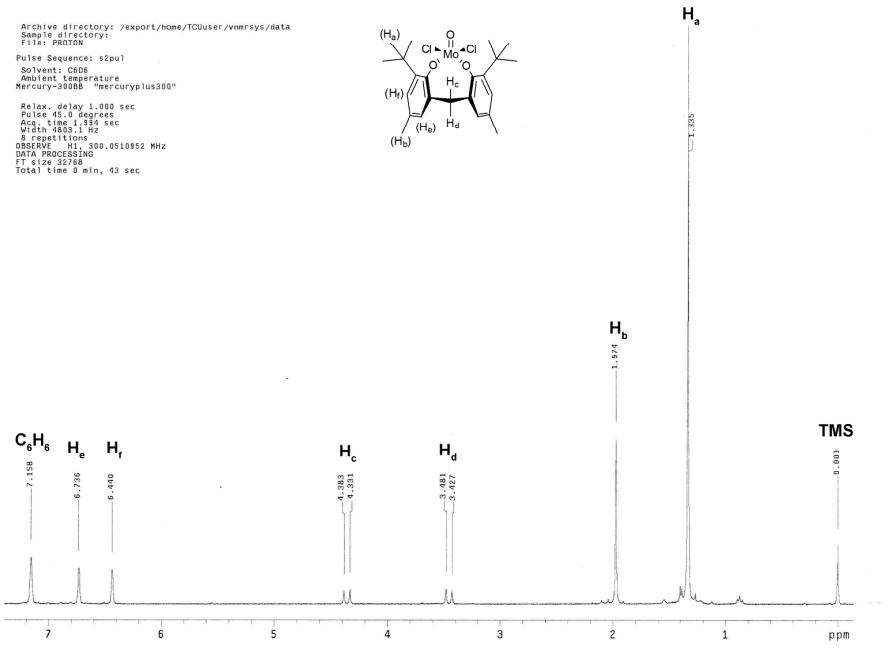

Figure A4.7 ^{1}H NMR of Mo(O)Cl$_2${2,2'-CH$_2$(O-6-^{t}Bu-4-MeC$_6$H$_2$)$_2$-κ^2*O,O*'} (**4.3a**) in C_6D_6

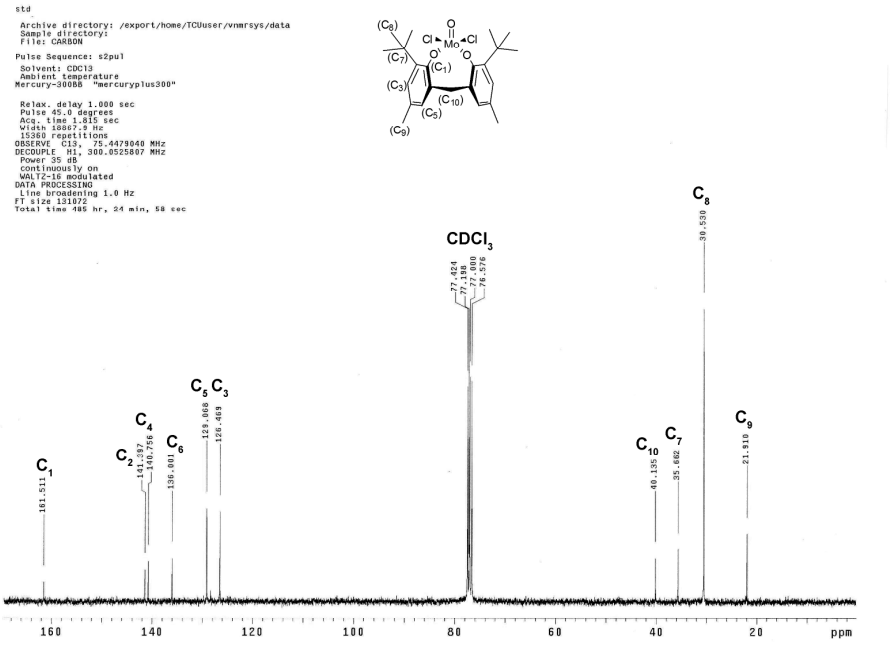

Figure A4.8 ^{13}C NMR of Mo(O)Cl$_2${2,2'-CH$_2$(O-6-^{t}Bu-4-MeC$_6$H$_2$)$_2$-κ^2*O,O*'} (**4.3a**) in C_6D_6

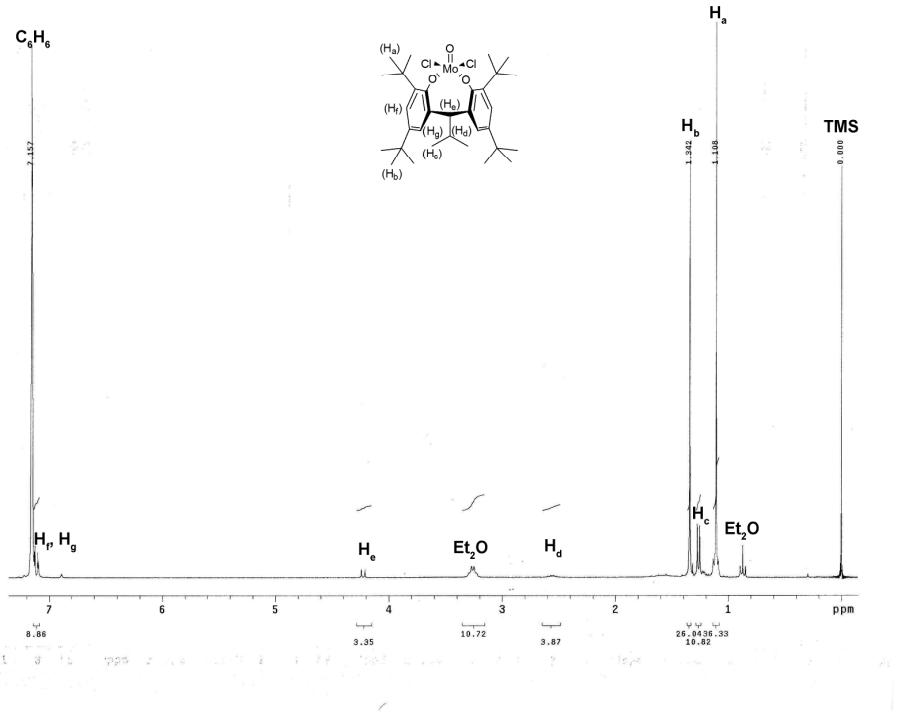

Figure A4.9 ^{1}H NMR of Mo(O)Cl$_2${2,2'-CH(^{i}Pr)(O-4,6-^{t}Bu$_2$C$_6$H$_2$)$_2$-κ^2*O,O'*} (**4.3b**) in C_6D_6

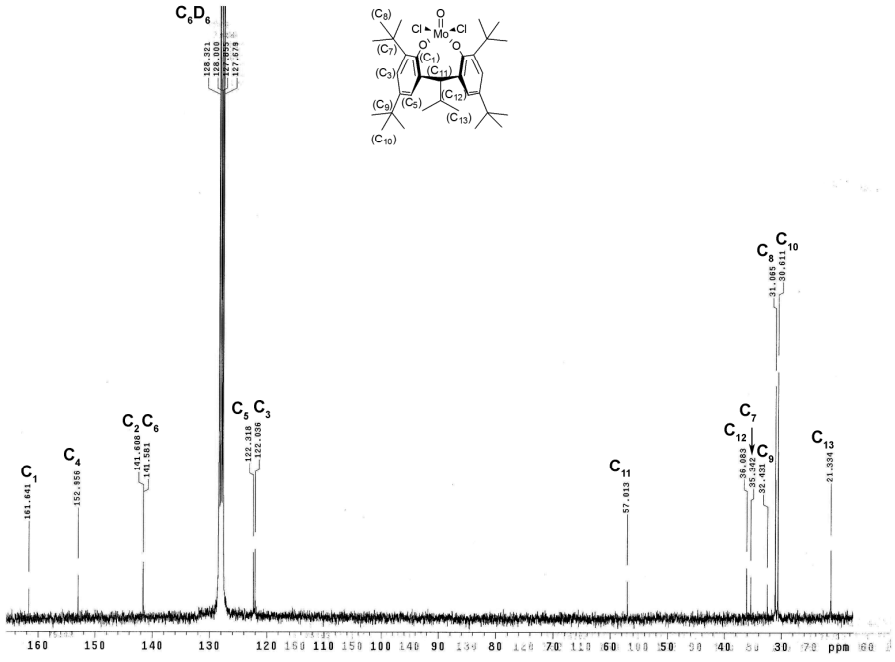

Figure A4.10 ^{13}C NMR of Mo(O)Cl$_2${2,2'-CH(^{i}Pr)(O-4,6-^{t}Bu$_2$C$_6$H$_2$)$_2$-κ^2*O,O'*} (**4.3b**) in C_6D_6

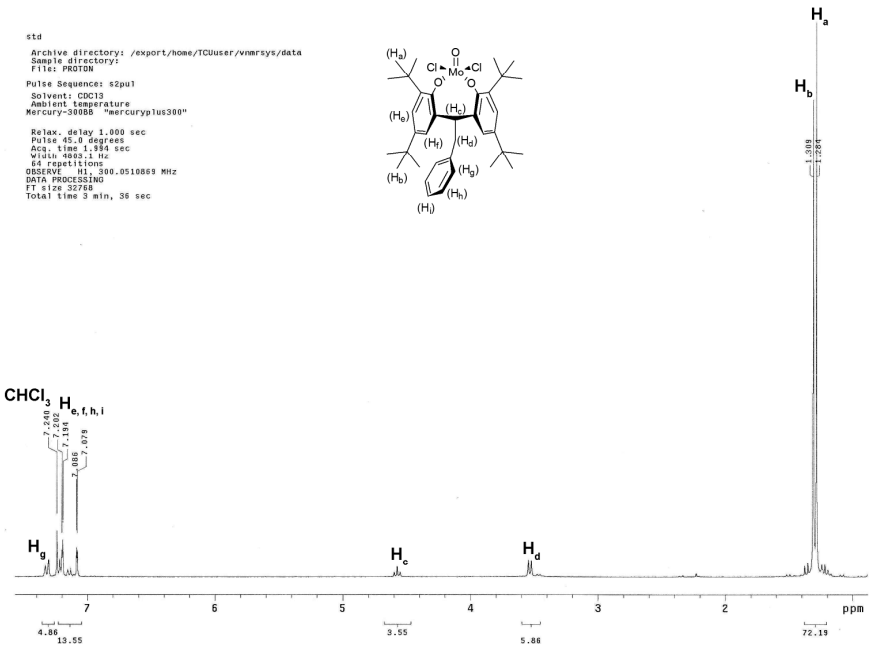

Figure A4.11 ^{1}H NMR of Mo(O)Cl$_2${2,2'-CH(Bn)(O-4,6-^{t}Bu$_2$C$_6$H$_2$)$_2$-κ^2*O,O*'} (**4.3c**) in CDCl$_3$

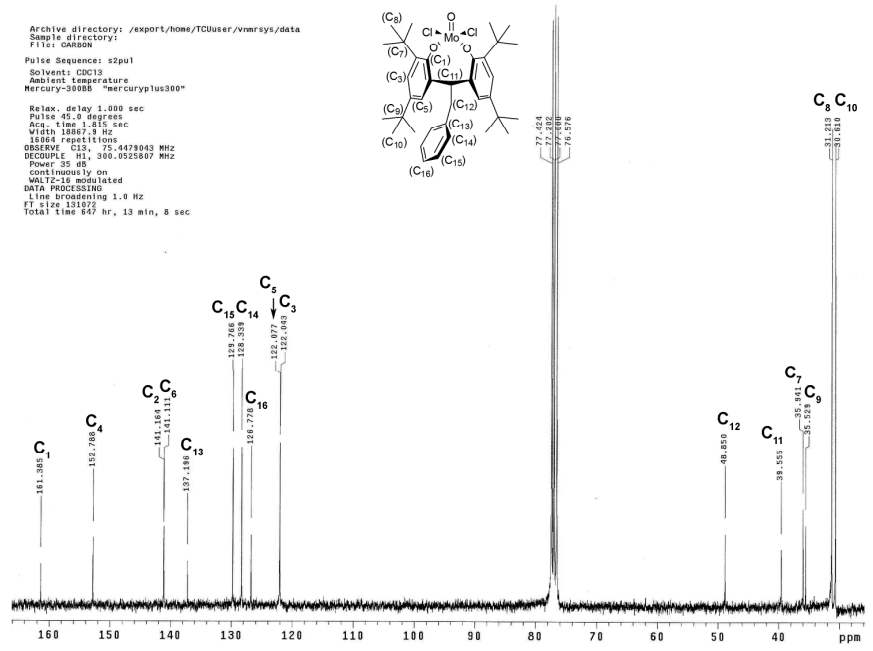

Figure A4.12 ^{13}C NMR of Mo(O)Cl$_2${2,2'-CH(Bn)(O-4,6-^{t}Bu$_2$C$_6$H$_2$)$_2$-κ^2*O,O*'} (**4.3c**) in CDCl$_3$

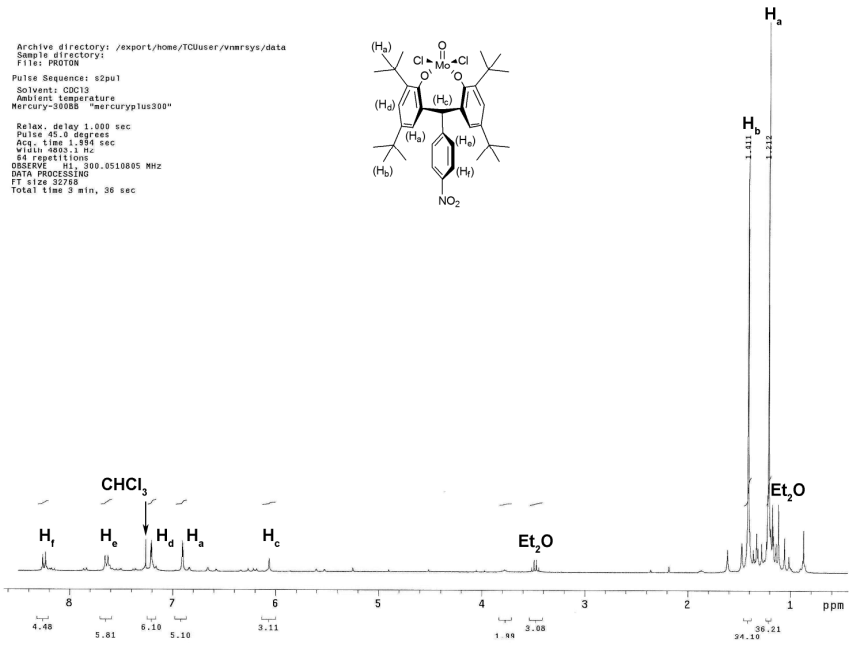

Figure A4.13 ^{1}H NMR of Mo(O)Cl$_2${2,2'-CH[4-(NO$_2$)C$_6$H$_4$](O-4,6-^{t}Bu$_2$C$_6$H$_2$)$_2$-κ^2*O,O*'} (**4.3d**) in $CDCl_3$

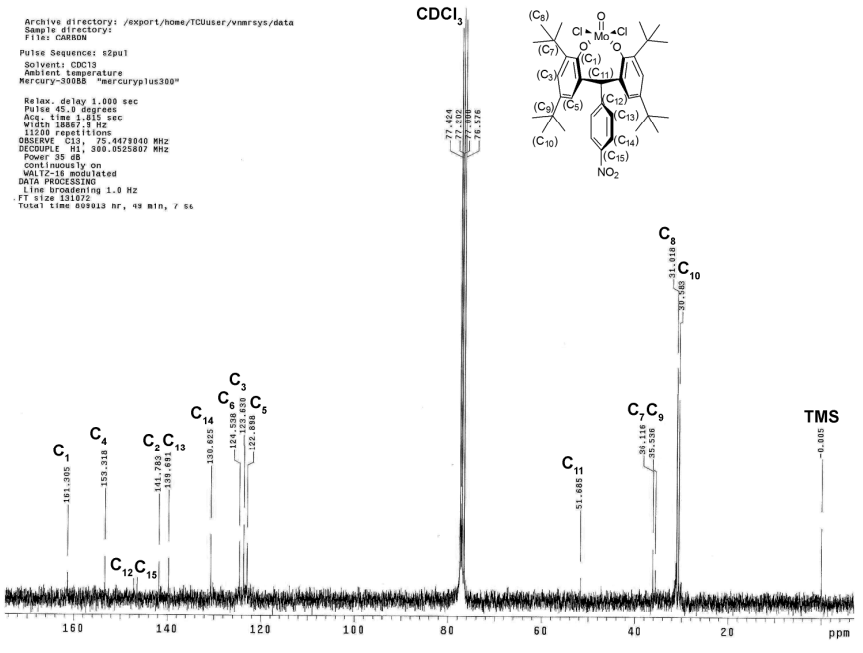

Figure A4.14 ^{13}C NMR of Mo(O)Cl$_2${2,2'-CH[4-(NO$_2$)C$_6$H$_4$](O-4,6-^{t}Bu$_2$C$_6$H$_2$)$_2$-κ^2*O,O*'} (**4.3d**) in $CDCl_3$

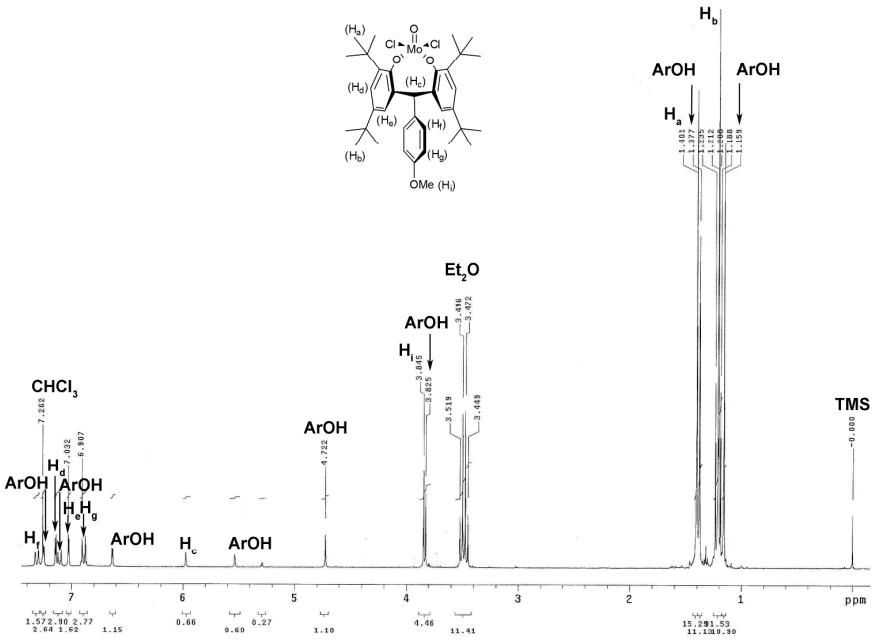

Figure A4.15 ^{1}H NMR of Mo(O)Cl$_2${2,2'-CH[4-(OMe)C$_6$H$_4$](O-4,6-^{t}Bu$_2$C$_6$H$_2$)$_2$-κ^2*O,O'*} (**4.3e**) in $CDCl_3$

References

1. Green, M. L. H. An Introduction to the Chemistry of Molybdenum. In *Molybdenum: An Outline of its Chemistry and Uses*, Braithwaite, E. R., Haber, J., Eds. Elsevier: Amsterdam, The Netherlands, 1994; Vol. 19, pp 94-145.
2. Emsley, J. Molybdenum. In *Nature's Building Blocks, an A-Z Guide to the Elements*, Oxford University Press: New York, 2001; pp 262-266.
3. Emsley, J., *The Elements*; 3rd ed.; Oxford University Press: Oxford, United Kingdom, 1998; pp 130-131.
4. Wieser, M. E. *Pure Appl. Chem.* **2006,** 78, 2051-2066.
5. Bowen, H. J. M.; Donohue, J.; Jenkin, D. G.; Kennard, O.; Wheatley, P. J.; Whiffen, D. H. In *Tables of Interatomic Distances and Configuration in Molecules and Ions*, Sutton, L. E., Jenkin, D. G., Mitchell, A. D., Cross, L. C., Eds. Chemical Society: London, 1958; Vol. 11, pp 80-81.
6. Slater, J. C. *J. Chem. Phys.* **1964,** 41, 3199-3204.
7. Clementi, E.; Raimondi, D. L.; Reinhardt, W. P. *J. Chem. Phys.* **1967,** 47, 1300-1307.
8. Pauling, L. *J. Am. Chem. Soc.* **1947,** 69, 542-553.
9. Greenwood, N. N.; Earnshaw, A. Chromium, Molybdenum and Tungsten. In *Chemistry of the Elements*, Butterworth-Heinemann: Boston, 1997; pp 1002-1039.
10. Winter, M. WebElements. http://www.webelements.com/ (accessed Feb 2008).
11. Pauling, L., *The Chemical Bond*; Cornell University Press: Ithaca, NY, 1967; pp 49-64.
12. Huheey, J. E.; Keiter, E. A.; Keiter, R. L., *Inorganic Chemistry: Principles of Structure and Reactivity*; 4th ed.; HarperCollins: New York, 1993; pp 188-189.
13. Crabtree, R. H., *The Organometallic Chemistry of Transition Metals*; 3rd ed.; John Wiley & Sons Inc.: Ithaca, New York, 2001; pp 45-48.

14. Braithwaite, E. R. Occurrence, Extraction, Production and Uses of Molybdenum. In *Molybdenum: An Outline of its Chemistry and Uses*, Braithwaite, E. R., Haber, J., Eds. Elsevier: Amsterdam, The Netherlands, 1994; Vol. 19, pp 1-87.

15. Gupta, C. K.; Gupta, S.; Gupta, K., *Extractive Metallurgy of Molybdenum*; CRC Press: Boca Raton, Florida, 1992; p 10.

16. Killeffer, D. H.; Linz, A.; Pauling, L., *Molybdenum Compounds: Their Chemistry and Technology*; Interscience Publishers: New York, 1952; pp 13-46.

17. Jani, A. R.; Tripathi, G. S.; Brener, N. E.; Callaway, J. *Phys. Rev. B: Condens. Matter* **1989,** 40, 1593-1602.

18. IMOA International Molybdenum Association. http://www.imoa.info/index.html (accessed May 2008).

19. Rollinson, C. L. Chromium, Molybdenum and Tungsten. In *Comprehensive Inorganic Chemistry*, 1st ed.; Bailar, J. C., Emeleus, H. J., Nyholm, S. R., Trotman-Dickenson, A. F., Eds. Pergamon Press: Oxford 1973; Vol. 2, pp 700-742.

20. Kühn, F. E.; Santos, A. M.; Abrantes, M. *Chem. Rev.* **2006,** 106, 2455-2475.

21. Limberg, C. The SOHIO Process as an Inspiration for Molecular Organometallic Chemistry. In *Organometallic Oxidation Catalysis*, Meyer, F., Limberg, C., Eds. Springer-Verlag: Berlin, 2007; Vol. 22, pp 79-95.

22. Pope, M. T. Molybdenum Oxygen Chemistry: Oxides, Oxo Complexes, and Polyoxoanions. In *Progress in Inorganic Chemistry*, Lippard, S. J., Ed. Interscience Publishers: New York, 1991; Vol. 39, pp 181-257.

23. Thiel, W. R. Molybdenum Peroxo Complexes as Catalysts in Olefin Epoxidation. In *Inorganic Chemistry Highlights*, Meyer, G., Naumann, D., Wesemann, L., Eds. Wiley-VCH Verlag-GmbH: Cologne, Germany, 2002; pp 123-138.

24. Spivack, B.; Dori, Z. *Coord. Chem. Rev.* **1975,** 17, 99-136.

25. Stiefel, E. I. Molybdenum(VI). In *Comprehensive Coordination Chemistry* Wilkinson, G., Gillard, R. D., McCleverty, J. A., Eds. Pergamon Press: Oxford, United Kingdom, 1987; Vol. 3, pp 1375-1420.

26. Müller, A.; Serain, C. *Acc. Chem. Res.* **2000,** 33, 2-10.

27. Müller, A.; Peters, F.; Pope, M. T.; Gatteschi, D. *Chem. Rev.* **1998,** 98, 239-271.

28. Müller, A. *Chem. Comm.* **2003**, 803-806.

29. Mitchell, P. C. H. *Chem. Eng. News* **2003,** 81, 108.

30. Mitchell, P. C. H. *J. Inorg. Biochem.* **1986,** 28, 107-123.

31. Hille, R. *Chem. Rev.* **1996,** 96, 2757-2816.

32. Kisker, C.; Schindelin, H.; Rees, D. C. *Annu. Rev. Biochem.* **1997,** 66, 233-267.

33. Hille, R. *Trends Biochem. Sci.* **2002,** 27, 360-367.

34. Hille, R. *Biochim. Biophys. Acta, Bioenerg.* **1994,** 1184, 143-169.

35. Meyer, O. *J. Biol. Chem.* **1982,** 257, 1333-1341.

36. Kisker, C.; Schindelin, H.; Baas, D.; Retey, J.; Meckenstock, R. U.; Kroneck, P. M. H. *FEMS Microbiol. Rev.* **1999,** 22, 503-521.

37. Polsinelli, G. A. Bacterial Generation of the Anti-Greenhouse Gas Dimethylsulfide: Kinetic, Spectroscopic, and Computational Studies of the DMSO Reductase System. Doctoral Dissertation, Ohio State University, Ohio, 2008.

38. Grasselli, R. K. *Top. Catal.* **2002,** 21, 79-88.

39. ACS American Chemical Society's National Historic Chemical Landmarks Program: The Sohio Acrylonitrile Process. http://portal.acs.org/portal/acs/corg/content?_nfpb=true&_pageLabel=PP_ARTICLEMAIN&node_id=924&content_id=WPCP_007593&use_sec=true&sec_url_var=region1 (accessed April 2008).

40. Haber, J. Molybdenum Compounds in Heterogeneous Catalysis. In *Molybdenum: An Outline of its Chemistry and Uses*, Braithwaite, E. R., Haber, J., Eds. Elsevier: Amsterdam, The Netherlands, 1994; Vol. 19, pp 477-617.

41. Freund, C.; Herrmann, W.; Kuhn, F. E. Organorhenium and Organomolybdenum Oxides as Heterogenised Catalysts. In *Organometallic Oxidation Catalysis*, Meyer, F., Limberg, C., Eds. Springer-Verlag: Berlin, 2007; Vol. 22, pp 39-77.

42. Magomedov, G. K. I.; Morozova, L. V. *Zh. Obshch. Khim.* **1981,** 51, 2266-2270.

43. Schrock, R. R. *Tetrahedron* **1999,** 55, 8141-8153.

44. Cefalo, D. R.; Kiely, A. F.; Wuchrer, M.; Jamieson, J. Y.; Schrock, R. R.; Hoveyda, A., H. *J. Am. Chem. Soc.* **2001,** 123, 3139-3140.

45. McCann, M.; Beaumont, A. J. *J. Mol. Catal. A: Chem.* **1996,** 111, 251-255.

46. Kühn, F. E.; Santos, A. M.; Lopes, A. D.; Gonçalves, I. S.; Herdtweck, E.; Romão, C. C. *J. Mol. Catal. A: Chem.* **2000,** 164, 25-38.

47. Kühn, F. E.; Groarke, M.; Bencze, É.; Herdtweck, E.; Prazeres, A.; Santos, A. M.; Calhorda, M. J.; Romão, C. C.; Gonçalves, I. S.; Lopes, A. D.; Pillinger, M. *Chem. Eur. J.* **2002,** 8, 2370-2383.

48. Kollar, J. Catalytic Epoxidation of an Olefinically Unsaturated Compound Using an Organic Hydroperoxide as an Epoxidizing Agent. U.S. Patent 3,350,422, Oct. 31, 1967.

49. Barlan, A. U.; Basak, A.; Yamamoto, H. *Angew. Chem.* **2006,** 118, 5981-5984.

50. Jain, K. R.; Kühn, F. E. *Dalton Trans.* **2008**, 2221-2227.

51. Herberhold, M.; Razavi, A. *Angew. Chem., Int. Ed. Engl.* **1972,** 11, 1092-1094.

52. Swanson, B. I.; Satija, S. K. *J. Chem. Soc., Chem. Commun.* **1973**, 40-41.

53. Andrews, L.; Zhou, M. *J. Phys. Chem. A* **1999,** 103, 4167-4173.

54. Gatehouse, B. M.; Leverett, P. *J. Chem. Soc. (A)* **1969**, 849-854.

55. Sieber, K.; Kershaw, K.; Dwight, K.; Wold, A. *Inorg. Chem.* **1983,** 22, 2667-2669.

56. Chippindale, A. M.; Cheetham, A. K. The Oxide Chemistry of Molybdenum. In *Molybdenum: An Outline of its Chemistry and Uses*, Braithwaite, E. R., Haber, J., Eds. Elsevier: Amsterdam, The Netherlands, 1994; Vol. 19, pp 146-177.

57. Young, C. G. Molybdenum. In *Comprehensive Coordination Chemistry II: From Biology to Nanotechnology*, 1st ed.; McCleverty, J. A., Meyer, T. J., Eds. Elsevier-Pergamon: Oxford, United Kingdom, 2004; Vol. 4, pp 415-527.

58. Cotton, F. A.; Elder, R. C. *Inorg. Chem.* **1964**, 397-401.

59. Marzluff, W. F. *Inorg. Chem.* **1964,** 3, 395-397.

60. Roy, P. S.; Wieghardt, K. *Inorg. Chem.* **1987,** 26, 1885-1888.

61. Baker, M. V.; North, M. R.; Skelton, B. W.; White, A. H. *Inorg. Chem.* **1999,** 38, 4515-4521.

62. Shustorovich, E. M.; Atovmyan, L. O. *Zh. Strukt. Khim.* **1963,** 4, 273-276.

63. Iorns, T. V.; Stafford, F. E. *J. Am. Chem. Soc.* **1966,** 88, 4819-4822.

64. Huang, M.; DeKock, C. W. *Inorg. Chem.* **1993,** 32, 2287-2291.

65. Berg, J. M.; Holm, R. H. *J. Am. Chem. Soc.* **1985,** 107, 917-925.

66. Wong, Y. L.; Cowley, A. R.; Dilworth, J. R. *Inorg. Chim. Acta* **2004,** 357, 4358-4372.

67. da Costa, A. P.; Reis, P. M.; Gamelas, C.; Romao, C. C.; Royo, B. *Inorg. Chim. Acta* **2008,** 361, 1915-1921.

68. Hanna, T. A.; Incarvito, C. D.; Rheingold, A. L. *Inorg. Chem.* **2000,** 39, 630-631.

69. Hanna, T. A.; Ghosh, A. K.; Ibarra, C.; Mendez-Rojas, M.; Rheingold, A. L.; Watson, W. H. *Inorg. Chem.* **2004,** 43, 1511-1516.

70. Holm, R. H. *Chem. Rev.* **1987,** 87, 1401-1449.

71. Copley, R. C. B.; Dyer, P. W.; Gibson, V. C.; Howard, J. A. K.; Marshall, E. L.; Wang, W.; Whittle, B. *Polyhedron* **1996,** 15, 3001-3008.

72. Chou, C. Y.; Huffman, J. C.; Maatta, E. A. *J. Chem. Soc., Chem. Commun.* **1984**, 1184-1189.

73. Mondal, J. U.; Zamora, J. G.; Merritt, D. K.; Schultz, F. A. *Inorg. Chim. Acta* **2000,** 309, 147-150.

74. Mondal, J. U.; Zamora, J. G.; Siew, S.-C.; Garcia, G. T.; George, E. R.; Kinon, M. D.; Schultz, F. A. *Inorg. Chim. Acta* **2001,** 321, 83-88.

75. Tran, B. L.; Carrano, C. J. *Inorg. Chem.* **2007,** 46, 5429-5438.

76. Enemark, J. H.; Cooney, J. J.; Wang, J.-J.; Holm, R. H. *Chem. Rev.* **2004,** 104, 1175-1200.

77. Bell, A. *J. Mol. Catal.* **1992,** 76, 165-180.

78. Hayano, S.; Tsunogae, Y. *Chem. Lett.* **2005,** 34, 1520-1521.

79. Hayano, S.; Kurakata, H.; Tsunogae, Y.; Nakayama, Y.; Sato, Y.; Yasuda, H. *Macromolecules* **2003,** 36, 7422-7431.

80. Sinclair, L.; Mondal, J. U.; Uhrhammer, D.; Schultz, F. A. *Inorg. Chim. Acta* **1998,** 278, 1-5.

81. Hanna, T. A.; Ghosh, A. K.; Ibarra, C.; Zakharov, L. N.; Rheingold, A. L.; Watson, W. H. *Inorg. Chem.* **2004,** 43, 7567-7569.

82. Idol, J. D. Process for the Manufacture of Acrylonitrile. U.S. Patent 2,904,580, September 15, 1959.

83. Callahan, J. L.; Foreman, R. W.; Veatch, F. Attrition Resistant Oxidation Catalysts. U.S. Patent 3,044,966, July 17, 1962.

84. Hanna, T. A. *Coord. Chem. Rev.* **2004,** 248, 429-440.

85. Grasselli, R. K. Ammoxidation. In *Handbook of Heterogeneous Catalysis*, Ertl, G., Knozinger, H., Weitkamp, J., Eds. VCH-Verlagsgesellshaft mbH: Weinheim, Germany, 1997; pp 2302-2326.

86. Jang, Y. H.; Goddard, W. A., III. *Top. Catal.* **2001,** 15, 273-289.

87. Hall, K. A.; Mayer, J. M. *J. Am. Chem. Soc.* **1992,** 114, 10402-10411.

88. Borgmann, C.; Limberg, C.; Cunskis, S.; Kircher, P. *Eur. J. Inorg. Chem.* **2001**, 349-352.

89. Rodrigues, C. W.; Limberg, C.; Pritzkow, H. *Eur. J. Inorg. Chem.* **2004**, 3644-3650.

90. Rodrigues, C. W.; Antelmann, B.; Limberg, C.; Kaifer, E.; Pritzkow, H. *Organometallics* **2001,** 20, 1825-1831.

91. Limberg, C. *Angew. Chem. Int. Ed.* **2003,** 42, 5932-5954.

92. Green, M. L. H.; Konidaris, P. C.; Mountford, P. *J. Chem. Soc., Dalton Trans.* **1994**, 2975-2982.

93. Radius, U.; Sundermeyer, J.; Peters, K.; Von Schnering, H. G. *Z. Anorg. Allg. Chem.* **2002,** 628, 1226-1235.

94. Siewert, I.; Limberg, C.; Ziemer, B. *Z. Anorg. Allg. Chem.* **2006,** 632, 1078-1082.

95. Hunger, M.; Limberg, C.; Kircher, P. *Angew. Chem. Int. Ed.* **1999,** 38, 1105-1108.

96. Hunger, M.; Limberg, C.; Kircher, P. *Organometallics* **2000,** 19, 1044-1050.

97. Roggan, S.; Schnakenburg, G.; Limberg, C.; Sandhofner, S.; Pritzkow, H.; Ziemer, B. *Chem. Eur. J.* **2005,** 11, 225-234.

98. Hunger, M.; Limberg, C.; Kaifer, E.; Rutsch, P. *J. Organomet. Chem.* **2002,** 641, 9-14.

99. Roggan, S.; Limberg, C.; Ziemer, B. *Angew. Chem. Int. Ed.* **2005,** 44, 5259-5262.

100. Roggan, S.; Limberg, C.; Brandt, M.; Ziemer, B. *J. Organomet. Chem.* **2005,** 690, 5282-5289.

101. Sanchez-Delgado, R. A. In *Organometallic Modelling of the Hydrodesulfurization and Hydrodenitrogenation Reactions*, James, B. R., van Leeuwen, P. W. N. M., Eds. Kluwer Academic Publisher: Hingham, MA, 2002; Vol. 24, pp 3-24.

102. Mitchell, J. M.; Finney, N. S. *J. Am. Chem. Soc.* **2001,** 123, 862-869.

103. Rappé, A. K.; Goddard, W. A., III. *J. Am. Chem. Soc.* **1982,** 104, 448-456.

104. Emsley, J. Molybdenum. In *Nature's Building Blocks, an E-Z Guide to the Elements*, Oxford University Press: New York, 2001; pp 262-266.

105. Selassie, C. D.; Verma, R. P.; Kapur, S.; Shusterman, A. J.; Hansch, C. J. *J. Chem. Soc. Perkin Trans. 2* **2002**, 1112-1117.

106. Khalilzadeh, M. A.; Hosseini, A.; Shokrollahzadeh, M.; Halvagar, M. R.; Ahmadi, D.; Mohannazadeh, F.; Tajbakhsh, M. *Tetrahedron Lett.* **2006,** 47, 3525-3528.

107. Forrester, A. R.; Hay, J. M.; Thomson, R. H. Aroxyl radicals. In *Organic Chemistry of Stable Free Radicals*, Academic Press. Inc: Bristol, Great Britain, 1968; pp 281-341.

108. Krauss, H.-L.; Huber, W. *Chem. Ber.* **1961,** 94, 2864 - 2876.

109. Arnaíz, F. J.; Aguado, R.; Sanz-Aparicio, J.; Martinez-Ripoll, M. *Polyhedron* **1994,** 13, 2745-2749.

110. Arnaíz, F. J.; Aguado, R.; Pedrosa, M. R.; De Cian, A. *Inorg. Chim. Acta* **2003,** 347, 33-40.

111. Arnaíz, F. J.; Aguado, R.; Pedrosa, M. R.; Mahía, J.; Maestro, M. A. *Polyhedron* **2002,** 21, 1635-1642.

112. Butcher, R. J.; Penfold, B. R.; Sinn, E. *J. Chem. Soc., Dalton Trans.* **1979**, 668-675.

113. Butcher, R. J.; Gunz, H. P.; Maclagan, R. G. A. R.; Powell, H. K. J.; Wilkins, C. J.; Hian, Y. S. *J. Chem. Soc., Dalton Trans.* **1975**, 1223-1227.

114. Dreisch, K.; Andersson, C.; Stalhåndske, C. *Polyhedron* **1992,** 11, 2143-2150.

115. Pangborn, A. B.; Giardello, M. A.; Grubbs, R. H.; Rosen, R. K.; Timmers, F. J. *Organometallics* **1996,** 15, 1518-1520.

116. Armarego, W. L. F.; Perrin, D. D., *Purification of Organic Chemicals*; 4th ed.; Butterworth-Heinemann: Oxford, Great Britain, 1998; p 136.

117. Sheldrick, G. M. *SHELXL 97-2: Program for the Solution of Crystal Structures*, University of Göttingen, Germany, 1997.

118. McNeese, T. J. M., T. E.; Wierda, D. A.; Darensbourg, D. J.; Delord, T. J. *Inorg. Chem.* **1985,** 24, 3465-3468.

119. Dyall, L. K.; Winstein, S. *J. Am. Chem. Soc.* **1972,** 94, 2196-2199.

120. Hanna, T. A.; Rieger, A. L.; Rieger, P. H.; Wang, X. *Inorg. Chem.* **2002,** 41, 3590-3592.

121. Chisholm, M. H.; Folting, K.; Huffman, J. C.; Kirkpatrick , C. C. *Inorg. Chem.* **1984,** 23, 1021-1027.

122. Kessler, V. G.; Turova, N. Y.; Korolev, A. V.; Yanovskii, A. I.; Struchkov, Y. T. *Mendeleev Commun.* **1991,** 1, 89-91.

123. Kessler, V. G.; Mironov, A. V.; Turova, N. Y. *Polyhedron* **1993,** 12, 1573-1576.

124. Jolly, W. L., *Modern Inorganic Chemistry*; McGraw-Hill: New York, 1984; p 368.

125. Lehtonen, A.; Kessler, V. G. *Inorg. Chem. Commun.* **2004,** 7, 691-693.

126. Silverstein, R. M.; Bassler, G. C. Ultraviolet Spectrometry. In *Spectrometric Identification of Organic Compounds*, John Wiley and Sons: New York, 1963; pp 90-103.

127. Torrent, M.; Gili, P.; Duran, M.; Solà, M. *Int. J. Quantum Chem.* **1997,** 61, 405-414.

128. 1,2-dimethoxyethane 99.5%, Anhydrous Grade from Aldrich reports water content to be less than 0.003%. In our hands, this solvent does not pass the "ketyl test" (see below) when used as received, turning our visual indicator from purple to pink. Anhydrous DME from Aldrich requires storage over activated molecular sieves for 2 days for the ketyl test to be positive. On the other hand, our freshly distilled DME keeps this visual indicator purple when tested either right away after collection or at the end of a month (this implies < 0.003% water impurities). Maximum dryness is reached (see experimental section) by storing the distilled solvent over activated molecular sieves (they absorb at least half of the moisture present in the solvent, see ref. 129). The final water content is expected to be less than 30 ppm (15 ppm by extrapolation). Recent evidence suggests that organic solvents distilled from solvent stills might have a water content of 10 ppm and an oxygen content of 100 ppb, see ref 130. Ketyl reagent preparation: Benzophenone (0.091 g, 0.449 mmol) was dissolved in freshly distilled THF (20 mL). Finely cut and oil free sodium metal (0.500 g, 21.7 mmol) was added to the benzophenone solution with strong stirring. Stirring was continued until an intense purple color was observed. We consider

a positive ketyl test when 1 drop of ketyl reagent is added to approx. 7 mL of solvent and the purple color does not fade.

129. Burfield, D. R.; Gan, G. H.; Smithers, R. H. *J. Appl. Chem. Biotech.* **1978,** 28, 23-30.

130. Cournoyer, M. E.; Dare, J. H. *Chem. Health Saf.* **2003,** 10, 15-18.

131. Streitwieser, A., Jr.; Scannon, P. J.; Niemeyer, H. M. *J. Am. Chem. Soc.* **1972,** 94, 7936-7937.

132. Matthews, W. S.; Bares, J. E.; Bartmess, J. E.; Bordwell, F. G.; Cornforth, F. J.; Drucker, G. E.; Margolin, Z.; McCallum, R. J.; McCallum, G. J.; Vanier, N. R. *J. Am. Chem. Soc.* **1975,** 97, 7006-7014.

133. Liptak, M. D.; Gross, K. C.; Seybold, P. G.; Feldgus, S.; Shields, G. C. *J. Am. Chem. Soc.* 124, 6421-6427.

134. Xiao, Z.; Young, C. G.; Enemark, J. H.; Wedd, A. G. *J. Am. Chem. Soc.* **1992,** 114, 9194-9195.

135. Arzoumanian, H. *Coord. Chem. Rev.* **1998,** 178-180, 191-202.

136. Hausser, K. H.; Brunner, H.; Jochims, J. C. *Mol. Phys.* **1966,** 10, 253-260.

137. Kessler, V. G.; Panov, A. N.; Turova, N. Y.; Starikova, Z. A.; Yanovsky, A. I.; Dolgushin, F. M.; Pisarevsky, A. P.; Struchkov, Y. T. *J. Chem. Soc., Dalton Trans.* **1998**, 21-29.

138. Seisenbaeva, G. A.; Kloo, L.; Werndrup, P.; Kessler, V. G. *Inorg. Chem.* **2001,** 40, 3815-3818.

139. Malatesta, V.; Ingold, K. U. *J. Am. Chem. Soc.* **1981,** 103, 609-614.

140. Zuckerman, J. J. *J. Chem. Educ.* **1965,** 42, 315-317.

141. Krishamurthy, R.; Shaap, W. B. *J. Chem. Educ.* **1969,** 46, 799-810.

142. Rappé, A. K.; Goddard, W. A., III. *J. Am. Chem. Soc.* **1982,** 104, 3287-3294.

143. Steffey, B. D.; Fanwick, P. E.; Rothwell, I. P. *Polyhedron* **1990**, 963-968.

144. Pope, M. T., *Molybdenum Oxygen Chemistry: Oxides, Oxo Complexes, and Polyoxoanions*; Interscience: New York, United States, 1991; Vol. 39, pp 181-257.

145. Stiefel, E. I. Molybdenum(VI). In *Comprehensive Coordination Chemistry*, Wilkinson, G., Gillard, R. D., McCleverty, J. A., Eds. Pergamon Press: Oxford, United Kingdom, 1987; Vol. 3, pp 1375-1420.

146. Kessler, V. G.; Mironov, A. J.; Turova, N. Y.; Yanovskii, A.; Struchkov, Y. T. *Polyhedron* **1993,** 12, 1573-1576.

147. Kozlova, N. I.; Kessler, V. G.; Turova, N. Y.; Belokon, A. I. *Russ. J. Coord. Chem.* **1989,** 15, 867-876.

148. Turova, N. Y.; Kessler, V. G.; Kucheiko, S. I. *Polyhedron* **1991,** 10, 2617-2628.

149. Kessler, V. G.; Nikitin, K. V.; Belokon, A. I. *Polyhedron* **1998,** 17, 2309-2311.

150. Chisholm, M. H.; Folting, K.; Huffman, J. C.; Kirkpatrick, C. *Inorg. Chem.* **1984,** 23, 1021-1037.

151. Liu, C. M.; Restorp, P.; Nordlander, E.; Pierpont, G. C. *Chem. Commun.* **2001**, 2686-2687.

152. Kaim, W.; Schwederski, B. *Pure Appl. Chem.* **2004,** 76, 351-364.

153. Turova, N. Y.; Turevskaya, E. P.; Kessler, V. G.; Yanokskaya, M. I., *The Chemistry of Metal Alkoxides*; Kluwer Academic Publishers: Norwell, MA, 2002; pp 425-456.

154. Sharma, K. M.; Anand, S. K. *J. Prakt. Chem.* **1975,** 317, 540-544.

155. Schindelin, H.; Kisker, C.; Hilton, J.; Rajagopalan, K. V.; Rees, D. C. *Science* **1996,** 272, 1615-1621.

156. George, G. N.; Hilton, J.; Rajagopalan, K. V. *J. Am. Chem. Soc.* **1996,** 118, 1113-1117.

157. Ivin, K. J.; Mol, J. C., *Olefin Metathesis and Metathesis Polymerization*; Academic Press Inc: New York, 1997; pp 12-34, 224-259.

158. Lefebvre, F.; Leconte, M.; Pagano, S.; Mutch, A.; Basset, J. M. *Polyhedron* **1995,** 14, 3029-3226.

159. Gómez, F. J.; Abboud, K. A.; Wagener, K. B. *J. Mol. Catal. A: Chem.* **1998,** 133, 159-166.

160. van Schalkwyk, C.; Vosloo, H. C. M.; du Plessis, J. A. K. *J. Mol. Catal. A: Chem.* **1998,** 133, 167-173.

161. Kelsey, D. R.; Handlin, D. L., Jr.; Narayana, M.; Scardino, B. M. *J. Polym. Sci., Part A: Polym. Chem.* **1997,** 35, 3027-3047.

162. Glenny, M. W.; Nielson, A. J.; Rickard, C. E. F. *Polyhedron* **1998,** 17, 851-856.

163. Lehtonen, A.; Sillanpää, R. *Polyhedron* **2002,** 21, 349-352.

164. Taylor, J. C.; Waugh, A. B. *J. Chem. Soc., Dalton Trans.* **1980**, 2006-2009.

165. Nielson, A. J.; Andersen, R. A. *Inorg. Synth.* **1990,** 28, 323-326.

166. Larson, M. L.; Moore, F. W. *Inorg. Chem.* **1966,** 5, 801-805.

167. Cross, G. G.; Fisher, A.; Henderson, G. N.; Smyth, T. A. *Can. J. Chem.* **1984,** 62, 1446-1451.

168. Colton, R.; Tomkins, I. B.; Wilson, P. W. *Aust. J. Chem.* **1964,** 17, 496-497.

169. Turova, N. Y.; Kessler, V. G. *Russ. J. General Chem.* **1990,** 60, 99-104.

170. Johnson, D. A.; Taylor, J. C.; Waugh, A. B. *J. Inorg. Nucl. Chem.* **1980,** 42, 1271-1275.

171. Kessler, V. G.; Panov, A. N.; Turova, N. Y.; Starikova, Z. A.; Yanovskii, A. I.; Dolgushin, F. M.; Pisarevsky, A. P.; Struchkov, Y. T. *J. Chem. Soc., Dalton Trans.* **1998**, 21-29.

172. Mondal, J. U.; Almaraz, E.; Bhat, N. G. *Inorg. Chem. Commun.* **2004,** 7, 1195-1197.

173. Nemykin, V. N.; Basu, P. *J. Chem. Soc., Dalton Trans.* **2004**, 1928-1922.

174. Minelli, M.; Young, C. G.; Enemark, J. H. *Inorg. Chem.* **1985,** 24, 1111-1113.

175. Kessler, V. G. *Chem. Commun.* **2003**, 1213-1222.

176. Chisholm, M. H.; Huffman, J. C.; Kirkpatrick, C.; Folting, K.; Leonelli, J. *J. Am. Chem. Soc.* **1981,** 103, 6093-6099.

177. Chisholm, M. H.; Folting, K.; Huffman, J. C.; Rothwell, I. P. *J. Am. Chem. Soc.* **1982,** 104, 4389-4399.

178. Nakayama, Y.; Ikushima, N.; Nakamura, A. *Chem. Lett.* **1997**, 861-862.

179. Groarke, M.; Gonçalves, I. S.; Herrmann, W. A.; Kühn, F. E. *J. Organomet. Chem.* **2002,** 649, 108-112.

180. Bradley, D. C.; Chisholm, M. H.; Extine, M. W.; Stager, M. E. *Inorg. Chem.* **1977,** 16, 1794-1801.

181. Veiros, L. F.; Prazeres, Â.; Costa, P. J.; Romão, C. C.; Künh, F. E. *J. Chem. Soc., Dalton Trans.* **2006**, 1383-1389.

182. Mayer, J. M. *Polyhedron* **1995,** 14, 3273-3292.

183. Liu, L.; Zakharov, L. N.; Golen, J. A.; Rheingold, A. L.; Watson, W. H.; Hanna, T. A. *Inorg. Chem.* **2006,** 45, 4247-4260.

184. Legzdins, P.; Phillips, E. C.; Sánchez, L. *Organometallics* **1989,** 8, 940-949.

185. DeKock, C. W.; McAfee, L. V. *Inorg. Chem.* **1985,** 24, 4293-4298.

186. McCarron, E. M., III; Staley, R. H.; Sleight, A. W. *Inorg. Chem.* **1984,** 23, 1043-1045.

187. Haunschild, R.; Frenking, G. *J. Organomet. Chem.* **2008,** 693, 737-749.

188. Deng, L.; Ziegler, T. *Organometallics* **1996,** 15, 3011-3021.

189. Gibson, V. C.; Graham, A. J.; Ormsby, D. L.; Ward, B. P.; White, A. J. P.; Williams, D. J. *J. Chem. Soc., Dalton Trans.* **2002**, 2597-2598.

190. Mondal, J. U.; Zamora, J. G.; Kinon, M. D.; Schultz, F. A. *Inorg. Chim. Acta* **2000,** 309, 147-150.

191. Gheller, S. F.; Newton, W. E.; Pabon de Majid, L.; Bradbury, J. R. *Inorg. Chem.* **1988,** 27, 359-366.

192. Enemark, J. H.; Cooney, J. J. A.; Wang, J.-J.; Holm, R. H. *Chem. Rev.* **2004,** 104, 1175-1200.

193. Huheey, J. E.; Keiter, E. A.; Keiter, R. L., *Inorganic Chemistry: Principles of Structure and Reactivity*; 4th ed.; HarperCollins: New York, 1993; pp 479-488.

194. Porai-Koshits, M. A.; Sergienko, V. S. *Russ. Chem. Rev.* **1990,** 59, 52-62.

195. Bart, J. C. J. *Inorg. Chim. Acta* **1979,** 36, 261-265.

196. Cotton, F. A.; Morehouse, S. M.; Wood, J. S. *Inorg. Chem.* **1964**, 1603-1608.

197. Eliel, E. L.; Wilen, S. H., *Stereochemistry of Organic Compounds*; John Wiley & Sons, Inc: New York, 1994; pp 1119-1122, 1142-1150.

198. Fisher, K.; Barbier, G. G.; Hecht, H. J.; Mendel, R. R.; Campbell, W. H.; Schwarz, G. *Plant Cell* **2005,** 17, 1167-1179.

199. Jimtaisong, A.; Luck, R. L. *Inorg. Chem.* **2006,** 45, 10391-10402.

200. Yudanov, I. V. *J. Struct. Chem.* **2007,** 48, S111-S124.

201. Schrock, R. R. *Polyhedron* **1995,** 14, 3177-3195.

202. Pilyugina, T. S.; Schrock, R. R.; Müller, P.; Hoveyda, A. H. *Organometallics* **2007,** 26, 831-837.

203. Belgacem, J.; Kress, J.; Osborn, J. A. *J. Am. Chem. Soc.* **1992,** 114, 1501-1502.

204. Listemann, M. L.; Schrock, R. R.; Dewan, J.; Kolodziej, R. M. *Inorg. Chem.* **1988,** 27, 264-271.

205. Mortimer, P. I.; Strong, M. I. *Aust. J. Chem.* **1965,** 18, 1579-1587.

206. Buccella, D.; Tanski, J. M.; Parkin, G. *Organometallics* **2007,** 26, 3275-3278.

207. Zevaco, T. A.; Sypien, J. K.; Janssen, A.; Walter, O.; Dinjus, E. *J. Organomet. Chem.* **2007,** 692, 1963-1973.

208. Ohba, Y.; Ito, K.; Maeda, H.; Ebara, H.; Takaki, S.; Nagasawa, T. *Bull. Chem. Soc. Jpn.* **1998,** 71, 2393-2402.

209. Casiraghi, G.; Casnati, G.; Pochini, A.; Puglia, G.; Ungaro, R.; Sartori, G. *Synthesis* **1981**, 143-146.

210. Kolly, S.; Meier, H.; Rihs, G.; Winkler, T. *Helv. Chim. Acta* **1988,** 71, 1101-1107.

211. Arnáiz, F. J. *J. Chem. Educ.* **1995,** 72, 1139.

212. Liu, L.; Hanna, T. A. *Unpublished results*.

213. Mulford, D. R.; Fanwick, P. E.; Rothwell, I. P. *Polyhedron* **2000,** 19, 35-42.

214. Eilerts, W. N.; Heppert, J. A. *Polyhedron* **1995,** 14, 3255-3271.

215. Laye, R. H.; Bell, Z. R.; Ward, M. D. *New J. Chem.* **2003,** 27, 684-691.

216. Kayal, A.; Lee, S. C. *Inorg. Chem.* **2002,** 41, 321-330.

217. Antelmann, B.; Chisholm, M. H.; Iyer, S. S.; Huffman, J. C.; Simonsick, W. J.; Zhong, W. *Macromolecules* **2001,** 34, 3159-3175.

218. van der Linden, A.; Schaverien, C. J.; Meijboom, N.; Ganter, C.; Orpen, A. G. *J. Am. Chem. Soc.* **1995,** 117, 3008-3021.

219. Sypien, J. K. Structure-Reactivity Relationships in Aluminum Alkoxides-Catalysed Co-Polymerization Reactions: Aluminum 2,2'-Methylenebisphenoxide in the Synthesis of Poly(Ether-Carbonate)s from Cyclohexene Oxide and Carbon Dioxide. Doctoral Dissertation, University of Heidelberg, Heidelberg, Germany, 2006.

220. Nugent, W. A.; Mayer, J. M., *Metal-Ligand Multiple Bonds*; John Wiley & Sons, Inc: New York, 1988; pp 21-51.

221. Mol, J. C. Metathesis. In *Applied Homogeneous Catalysis with Organometallic Compounds*, Cornils, B., Herrmann, W. A., Eds. Wiley-VCH Verlag GmbH: Weinheim, 2002; Vol. 1, pp 328-343.

222. Kiessling, L. L.; Owen, R. M. Syntheses and Applications of Bioactive Polymers Generated by Ring Opening Metathesis Polymerization. In *Handbook of Metathesis*, Grubbs, R. H., Ed. Wiley-VCH Verlag GmbH & Co: Weinheim, Germany, 2003; Vol. 3, pp 180-225.

223. Bielawski, C. W.; Hillmyer, M. A. Telechelic Polymers from Olefin Metathesis Methodologies. In *Handbook of Metathesis*, Grubbs, R. H., Ed. Wiley-VCH Verlag GmbH & Co: Weinheim, 2003; Vol. 3, pp 255-282.

224. Hirama, M.; Oishi, T.; Uehara, H.; Inoue, M.; Maruyama, M.; Oguri, H.; Satake, M. *Science* **2001,** 294, 1904-1907.

225. Truett, W. L.; Johnson, D. R.; Robinson, I. M.; Montague, B. A. *J. Am. Chem. Soc.* **1960,** 82, 2337-2340.

226. Banks, R. L.; Bailey, G. C. *Ind. Eng. Chem. Prod. Res. Dev.* **1964,** 3, 170-173.

227. Calderon, N.; Chen, H. Y.; Scott, K. W. *Tetrahedron Lett.* **1967**, 3327-3329.

228. Slugovc, C. *Macromol. Rapid Commun.* **2004,** 25, 1283-1297.

229. Coalter, J. N., III; Caulton, K. G. *New J. Chem.* **2001,** 25, 679-684.

230. Rouhi, A. M. *Chem. Eng. News* **2005,** 83, 8.

231. Rouhi, A. M. *Chem. Eng. News* **2002,** 80, 29-33.

232. Grubbs, R. H. Alkene and Alkyne Metathesis Reactions. In *Comprehensive Organometallic Chemistry*, Wilkinson, G., Sir, Stone, F. G. A., Abel, E. W., Eds. Pergamon Press Ltd: Oxford, United Kingdom, 1982; Vol. 8, pp 499-551.

233. Nguyen, S. T.; Trnka, T. M. The Discovery and Development of Well-Defined, Ruthenium-Based Olefin Metathesis Catalysts. In *Handbook of Metathesis*, Grubbs, R. H., Ed. Wiley-VCH Verlag GmbH & Co: Weinheim, Germany, 2003; Vol. 1, pp 61-85.

234. Schrock, R. R. The Discovery and Development of High Oxidation State Mo and W Imido Alkylidene Complexes for Alkene Metathesis. In *Handbook of Metathesis*, Grubbs, R. H., Ed. Wiley-VCH Verlag GmbH & Co: Weinheim, Germany, 2003; Vol. 1, pp 8-32.

235. Copéret, C.; Lefebvre, F.; Basset, J.-M. From Ill-Defined to Well-Defined W Alkylidene Complexes. In *Handbook of Metathesis*, Grubbs, R. H., Ed. Wiley-VCH Verlag GmbH & Co: Weinheim, Germany, 2003; Vol. 1, pp 33-46.

236. Nguyen, S. T.; Johnson, L. K.; Grubbs, R. H. *J. Am. Chem. Soc.* **1992,** 114, 3974-3975.

237. Hoveyda, A. H.; Zhugralin, A. R. *Nature* **2007,** 450, 243-251.

238. Screttas, C. G.; Eastham, J. F.; Kamienski, C. W. *Chimia* **1970,** 24, 109-111.

239. Morton, C. *SyntheticPages* **2001**, http://www.syntheticpages.org/pages/120.

240. Black, G.; Maher, D.; Risse, W. Living Ring-Opening Olefin Metathesis Polymerization. In *Handbook of Metathesis*, Grubbs, R. H., Ed. Wiley-VCH Verlag GmbH & Co: Weinheim 2003; Vol. 3, pp 2-71.

241. Hayano, S.; Masuda, T. *Macromolecules* **1998,** 31, 3170-3174.

242. Leconte, M.; Basset, J. M.; Quignard, F.; Larroche, C. Mechanistic Aspects of the Olefin Metathesis Reaction. In *Reactions of Coordinated Ligands*, Braterman, P. S., Ed. Plenum Press: New York, 1986; Vol. 1, pp 371-420.

243. Schrock, R. R. Alkylidene Complexes of the Earlier Transition Metals. In *Reactions of Coordinated Ligands*, Braterman, P. S., Ed. Plenum Press: New York, 1986; Vol. 1, pp 221-283.

244. Schrock, R. R. *J. Am. Chem. Soc.* **1974,** 96, 6796-6797.

245. Hamilton, J. C. Stereochemistry of Ring-Opening Metathesis Polymerization. In *Handbook of Metathesis*, Grubbs, R. H., Ed. Wiley-VCH Verlag GmbH & Co: Weinheim, Germany, 2003; Vol. 3, pp 143-179.

VITA

Personal Background	Mauricio Quiroz-Guzmán
	Born in Xalapa de Enriquez, Veracruz, Mexico
	Son of Roberto Francisco Quiroz-Hernández and
	Evangelina Guzmán-Ochoa
	July 18, 1980
Education	Bachelor of Science, Chemistry, Universidad de las
	Américas-Puebla, Puebla, Mexico, 2002
	Doctor of Philosophy, Inorganic Chemistry,
	Texas Christian University, Fort Worth, Texas, 2008
Experience	Research Assistant, Texas Christian University, Fort
	Worth, Texas, 2002-2008
	Teaching Assistant, Texas Christian University, Fort
	Worth, Texas, 2003-2005

ABSTRACT

SYNTHESIS, CHARACTERIZATION AND CATALYTIC ACTIVITY OF MOLYBDENUM(VI) DI- AND MONOOXO ARYLOXIDES

By Mauricio Quiroz-Guzman, Ph. D., 2008
Department of Chemistry
Texas Christian University

Dissertation Advisor: Dr. Tracy A. Hanna, Associate Professor of Chemistry

The chemistry of molybdenum is immensely rich and diverse. Molybdenum is essential for life, and has many applications in industry.

The first chapter offers a general perspective of the chemistry of molybdenum in high oxidation states dominated by diverse oxo species, such as the MoO_2^{2+} and MoO^{4+} units that are focus of my research. I describe the importance of MoO_2^{2+} complexes as models for the active sites of oxo transfer molybdoenzymes (e.g. DMSO oxidase) and for industrial heterogeneous transformation such as the SOHIO process (one of our ultimate goals). I also outline the importance of MoO^{4+} complexes as procatalysts for metathesis polymerization and as models of deoxygenated active sites of MoO_2^{2+} oxygen catalysts that have triggered our interest.

The second chapter introduces the synthesis and full characterization of 4-, 5- and 6-coordinated $MoO_2(OAr)_2L_{0-1}$ complexes with bulky aryloxide ligands, starting from the MoO_2Cl_2 or $MoO_2Cl_2(DMF)_2$ precursors. Steric and electronic modifications in the aryloxide moieties were performed in order to understand their effect in the final structure and yields of the synthesized complexes. The nature and mechanism of formation of the radical species detected in their synthesis is proposed.

The third chapter presents the facile synthesis of varios $MoO(OAr)_{4-n}Cl_n$ complexes starting from the MoO_2Cl_2 precursor. Their mechanism of formation is proposed and the supporting evidence for this new reaction is provided. Steric and electronic modifications in the aryloxide moieties were used to study their structural and electronic effects in the MoO^{4+} complexes.

The fourth chapter outlines the synthesis of Mo(VI) monooxo bisphenoxides with a characteristic *cis*-chloro *cis*-bisphoxide arrangement around the MoO^{4+} unit. Electronic and steric modifications in the bisphenoxide rings were done to determine their effect in the structure and reactivity of the final complexes.

The fifth chapter introduces the application of the synthesized $MoO(OAr)_{4-n}Cl_n$ and $MoO(bisphenoxides)_2Cl_2$ complexes as procatalysts for olefin metathesis polymerization of norbornene. The correlation between structure and reactivity of the procatalyst is discussed.